GOVERNMENT OF YUKON

Southern Lakes Flood Mapping Study
Final Report

Revision:

Final / Rev 0

KGS Group Project:

22-2708-001

Date:

May 1, 2024

KGS GROUP

PROFESSIONAL
YUKON
A. L. WEISS
TERRITORY
April 29, 2024
ENGINEER

PREPARED BY:

Andrew Weiss, M.Sc., P.Eng.
Water Resources Engineer

APPROVED BY:

David S. Brown, M.Eng., P.Eng.
Principal

TABLE OF CONTENTS

List of Tables

List of Figures

List of Appendices

List of Abbreviations

AEP – Annual Exceedance Probability
CACS – Canadian Active Control System
CGVD2013 – Canadian Geodetic Vertical Datum 2013
CEM – Coastal Engineering Manual
CMIP5 – Coupled Model Intercomparison Project Phase 5
CSRS – Canadian Spatial Reference System
CDF – Cumulative Density Function
DEM – Digital Elevation Model
ECCC – Environment and Climate Change Canada
GEV – Generalized Extreme Value
GPS – Global Positioning System
HEC-RAS – Hydrologic Engineering Center's River Analysis System
KDFN – Kwanlin Dün First Nation
LiDAR – Light Detection and Ranging
NAD83 CSRS – North American Datum of 1983 Canadian Spatial Reference System
NRCan – Natural Resources Canada
POT – Peak-Over-Threshold
PPK – Post Processed Kinematic
RCP – Representative Concentration Pathways
RTK – Real Time Kinematic
SPM – Shore Protection Manual
SWE – Snow Water Equivalent

SSP – Shared Socioeconomic Pathways
TKC – Ta'an Kwäch'än Council
CTFN – Tagish First Nation
UHF – Ultra-High Frequency
USACE – United States Army Corps of Engineers
WSC – Water Survey of Canada
YG – Government of Yukon

STATEMENT OF LIMITATIONS AND CONDITIONS

Limitations

This report has been prepared for the Government of Yukon in accordance with the agreement between KGS Group and the Yukon Government. This report represents KGS Group's professional judgment and exercising due care consistent with the preparation of similar reports. The information, data, recommendations and conclusions in this report are subject to the constraints and limitations in the Agreement and the qualifications in this report. This report must be read as a whole, and sections or parts should not be read out of context.

This report is based on information made available to KGS Group by the Government of Yukon. Unless stated otherwise, KGS Group has not verified the accuracy, completeness or validity of such information, makes no representation regarding its accuracy and hereby disclaims any liability in connection therewith. KGS Group shall not be responsible for conditions/issues it was not authorized or able to investigate or which were beyond the scope of its work. The information and conclusions provided in this report apply only as they existed at the time of KGS Group's work.

Third Party Use of Report

Any use a third party makes of this report or any reliance on or decisions made based on it, are the responsibility of such third parties. KGS Group accepts no responsibility for damages, if any, suffered by any third party as a result of decisions made or actions undertaken based on this report.

1.0 INTRODUCTION

1.1 Background

In 2021, sustained major flooding occurred throughout the headwaters of the Yukon River Basin from July to September, resulting in an estimated flood response cost for the Government of Yukon (YG) of over $8 million. Emergency works were constructed during a critical one-month period along an estimated 10 km of combined shoreline. The magnitude and logistics of the response required a variety of diking systems be employed, to provide increased protection against the forecasted flood levels and wave action. This flooding was extensive throughout the Southern Lakes area, which comprises Bennett Lake, Nares Lake, Tagish Lake, Marsh Lake, and Lake Laberge, as shown on Figure 1.

FIGURE 1: SOUTHERN LAKES

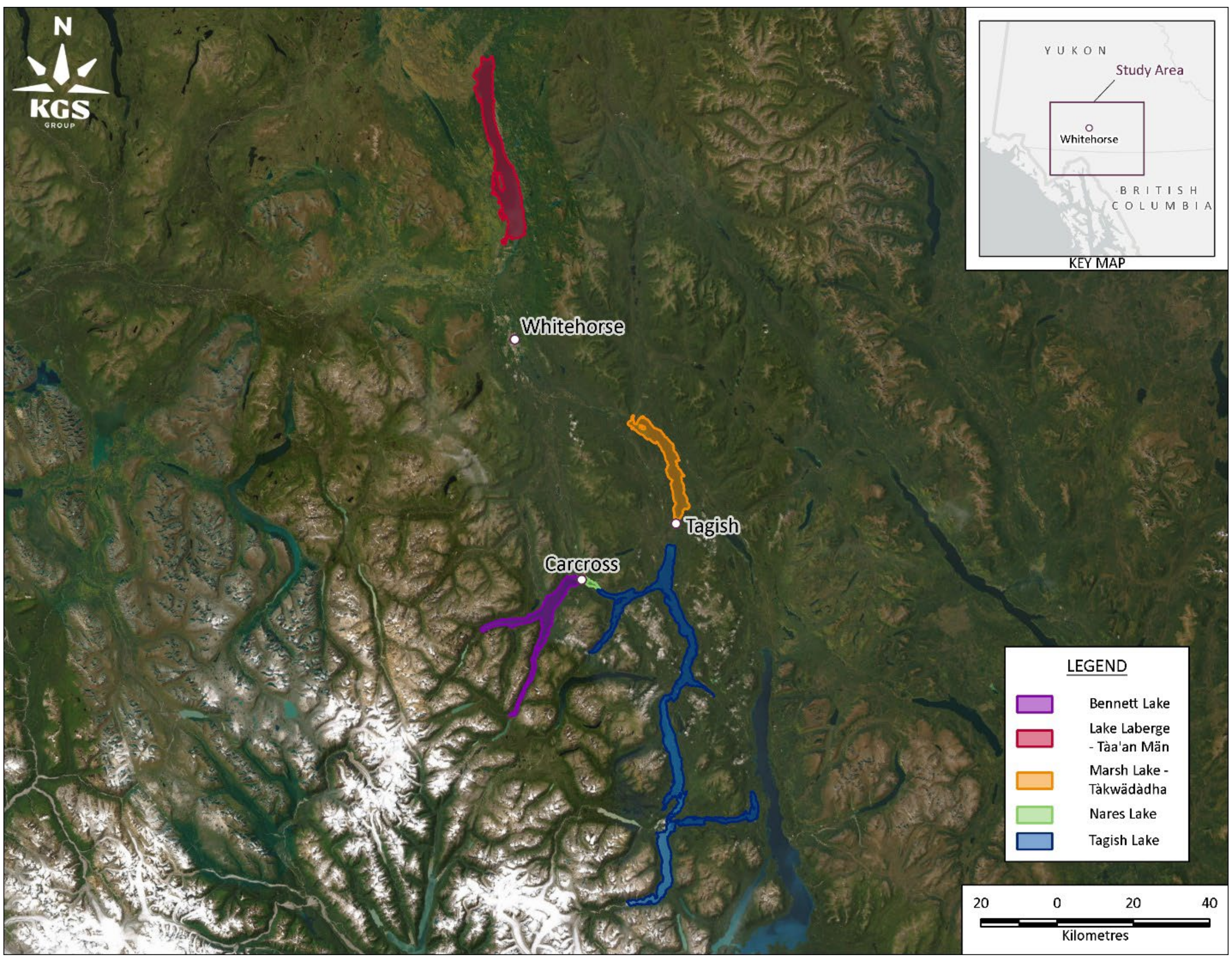

The significant flooding that occurred during 2021 affected over 100 properties, with personal losses due to the flooding unknown. Historic snowfall amounts, combined with warmer than normal summer temperatures, lead to inflows to the Southern Lakes up to 76% higher, as reported by Yukon Energy Corporation (YEC) to YG, than the historic maximum inflows to the lakes prior to the 2021 flood, resulting in historic flood levels on the lakes. The 2021 flood followed extensive flooding that occurred throughout the region 14 years earlier during 2007, which flooded many of the same areas.

As climate change impacts result in more extreme seasonal weather, the timing and magnitude of peak water levels in the Southern Lakes are likely to change. Flood mapping has been increasingly highlighted as a key tool, both in support of emergency preparation and response, and development planning to reduce community vulnerability to flooding in the face of the Yukon's changing climate. Completing flood mapping for all Yukon communities at risk of flooding is a key commitment defined in YG's *Our Clean Future: A Yukon Strategy for Climate Change, Energy, and a Green Economy* (https://our-clean-future.yukon.ca/), as well as YG's *2021 Yukon Flood Recovery Plan* (Government of Yukon – Emergency Measures Organization, 2021) and *2022 Yukon Flood Recovery Plan* (Government of Yukon – Emergency Measures Organization, 2022). The Southern Lakes Flood Mapping Study will serve to advance YG's goals of enhancing public safety, better understanding flood hazards, and reducing future flood vulnerability through the identification and mapping of flood hazards.

To complete flood hazard mapping for the Southern Lakes, KGS Group was retained by YG to complete analyses to define flood levels on Bennett Lake, Nares Lake, Tagish Lake, Marsh Lake, and Lake Laberge, and to prepare flood maps for the communities along those lakes. The study area is shown on Figure 2, with the areas where flood maps were developed shown in red. Specific communities and subdivisions that were considered in the study included:

- Carcross,
- Tagish,
- Judas Creek,
- Army Beach,
- South M'Clintock,
- North M'Clintock,
- Other residential areas along the lakeshore of Marsh Lake,
- Shallow Bay,
- Jackfish Bay, and
- Deep Creek.

FIGURE 2: SOUTHERN LAKES STUDY AREA

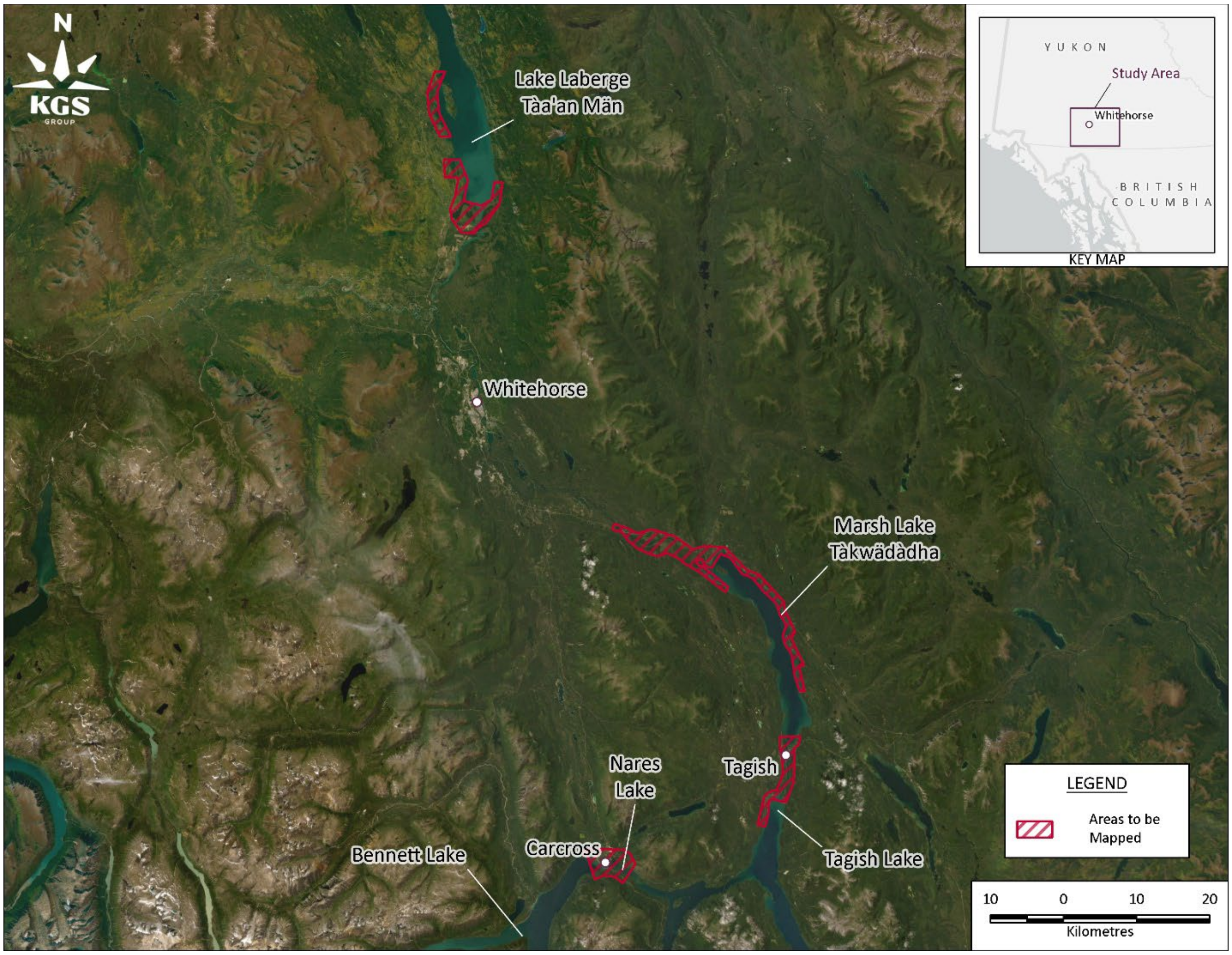

1.2 Objectives

The primary objectives of this study included:

- The completion of bathymetric and topographic surveys to understand shoreline geometry in representative locations, and in support of the development of a digital elevation model (DEM).
- The completion of statistical analyses to define flood levels that will be integrated into the flood hazard maps associated with the 5%, 1%, and 0.5% Annual Exceedance Probability (AEP) flood events.
- Completion of climate change analyses to estimate flood levels considering the potential impacts of climate change.
- The development of flood hazard maps throughout the study area representing flood hazards for a number of AEP conditions under current climate and climate change conditions.

The flood hazard maps developed as part of this study will serve to enhance the understanding of the potential for flooding on Bennett Lake, Nares Lake, Tagish Lake, Marsh Lake, and Lake Laberge considering both current climate conditions, as well as potential future conditions impacted by climate change.

1.3 Scope of Work

The scope of work of the study included:

- A review of available background information, and the attendance of a site visit with representatives from KGS Group, YG, Kwanlin Dün First Nation (KDFN) and Carcross / Tagish First Nation (CTFN). Representatives from the Ta'an Kwäch'än Council (TKC) were unable to attend the site visit.
- The planning and execution of a field survey, including topographic and bathymetric surveys, surveys of high water marks, and the development of a georeferenced photographic inventory.
- The documentation of historical floods throughout the study area.
- An assessment of the impacts associated with regulation of Marsh Lake.
- An analysis of static lake levels, wind setup, and wave runup.
- An evaluation of the joint probability of peak lake water levels, wind setup, and wave runup.
- Definition of flood levels associated with high static lake levels, wind setup, and wave runup. Through discussions with YG, it was agreed that a Monte Carlo analysis was the most appropriate approach to evaluating the joint flooding associated with the three causes.
- A review of anticipated climate change and future land use impacts, and how those impacts could affect future flooding.
- The development of flood hazard maps for the communities and subdivisions within the study area.
- Providing support to YG in the engagement of First Nations and the general public in the presentation of the flood hazard maps.

This report documents the scope of work completed by KGS Group, including the review of background information, details of the field survey program, a high-level assessment of the estimated impacts associated with lake level regulation, the methodology that was implemented for the development of flood hazard maps, key takeaways from stakeholder engagement, and key conclusions and recommendations resulting from this study.

2.0 BACKGROUND REVIEW

2.1 Overview

A thorough review of available background information was completed as part of this study to provide the Project Team with key context and understanding of the history of flooding in the Southern Lakes area. This provided a basis for the various analyses completed for the study and for the development and calibration of the hydrologic and hydraulic models.

The background data acquired and reviewed for this project included aerial imagery, satellite imagery, water level and flow data, meteorological data, and reports documenting the previously completed flood risk mapping studies for the communities. This data was collected from a variety of sources, including the Government of Yukon and Environment, Climate Change Canada (ECCC), and YEC.

As part of the background information review, a review of previous flood events in the Southern Lakes area was completed for inclusion in a Historical Flood Event Inventory. The review identified four significant historical flood events in the communities that were added to the Flood Event Inventory, specifically flood events in 1981, 2007, 2021, and 2022.

2.2 Site Visit

Key Project Team Members from KGS Group met with representatives from YG, KDFN, and CTFN on May 24 and 25, 2023, to visit the various communities considered in the flood mapping study. Representatives from TKC were invited to attend the site visits, however were unavailable to attend. The objectives of the site visit included:

- Providing an opportunity for the Project Team to have a clear understanding of the study area, as well as the magnitude of the 2021 flood.
- Evaluate typical shoreline conditions, as well as the level of exposure of buildings located near the shoreline.
- Understand areas that were at-risk during the 2021 flood, as well as the YG's response to the 2021 flood.
- To identify any readily identifiable high water marks that could be surveyed as part of the field survey program.

Key findings from the site visits throughout the study area included:

- ***Carcross***
  - Sand dunes located along the west side of Carcross provide protection from flooding on Bennett Lake.
  - A large amount of sand was eroded from the shoreline on Bennett Lake during the 2021 flood.
  - A berm was constructed along Waterfront Drive along Nares River. The berm was initially approximately 1.2 m (i.e. 4') above the road elevation, but since water levels were near the top of the berm, it was raised to approximately 1.6 m (i.e. 6') above the road crest.

  - A topographic low point was identified near the Carcross Airstrip that frequently experiences flood issues.
  - Waves are generally not an issue on the east side of Carcross on Nares Lake, as there is a very gently sloped shoreline. Typical annual peak water levels reach the edge of the grassy areas near the CTFN office, although it was considerably higher during the 2021 flood. The peak water level during 2022 was roughly 0.3 to 0.6 m (i.e. 1 to 2') higher than the edge of the grassy areas near the CTFN office.
  - The peak water level during the 2021 flood came up to the underside of the rail bridge and pedestrian bridge. Water levels were splashing onto the deck at the northern extent of the pedestrian bridge.
- ***Tagish***
  - The shoreline along Tagish Lake during the site visit was very flat, with steep sand banks near the typical high water level.
  - The extent of debris along the shoreline was indicative of the high water level from the 2021 flood.
  - There are issues with flooding in the campground, as well as nearby private properties, which were assumed to be flooded due to groundwater conditions.
- ***Marsh Lake***
  - Peak water levels during the 2021 flood extended up to the extent of the debris along the shoreline at the Judas Creek Subdivision.
  - Portions of the temporary flood protection that were constructed along sections of shoreline in the Judas Creek Subdivision were still in place.
  - Considerable flood and wave protection was noted along Army Beach, including extensive rock armoring.
  - The shoreline at Army Beach was very mild and sandy up to the armored banks.
  - Shoreline conditions near Swan Haven during the site visit consisted of a mild, sandy slope up to a steep bank.
  - It was noted that the 2021 flood level extended as high as the bottom of the sandbags along the shoreline near Swan Haven.
- ***Lake Laberge***
  - Temporary flood protection was still visible at select locations throughout Deep Creek.
  - A high water mark from the 2021 flood was visible on the fence of the northeastern-most residence on Deep Creek Rd.
  - Two high water marks were apparent on the rock faces north of the confluence of Deep Creek with Lake Laberge, likely from the 2021 and 2022 high water levels.
  - It was noted that a portion of Jackfish Bay Rd. was reconstructed following the 2021 flood and was raised by approximately 0.5 m (i.e. 18").
  - KGS Group and YG personnel discussed the 2021 flood with a resident of Jackfish Bay. The resident indicated the approximate height of the 2021 flood levels, and also noted that his property was susceptible to waves from north winds.

A number of photographs from the Site Visit are included in Appendix A.

2.3 Background Information

Key background information acquired and reviewed as part of this project included:

- Hydrometric records on Bennett Lake, Tagish Lake, Marsh Lake, and Lake Laberge from WSC.
- Flow records for numerous waterways in the Southern Lakes region from WSC.
- Meteorological data from ECCC for the Whitehorse A and Carcross meteorological stations.
- Meteorological data from YG for the Mount Sima and Jakes Corner meteorological stations.
- Light Detection and Ranging (LiDAR) data and orthoimagery collected for the Yukon Government, which included:
  - Carcross (Captured in October 2019),
  - Lake Laberge, Deep Creek Area (Captured in June 2022),
  - Lake Laberge, Jackfish Bay Area (Captured in June 2022),
  - Marsh Lake (Captured in June 2022), and
  - Tagish (Captured in June 2022).
- Orthoimagery captured via drone during the 2021 flood. Capture locations and dates included:
  - Carcross – July 10, 2021,
  - Lake Laberge, Jackfish Bay – July 9, 2021,
  - Lake Laberge, Jackfish Bay – July 11, 2021,
  - Lake Laberge, Shallow Bay – July 15, 2021,
  - Marsh Lake – July 8, 2021,
  - Marsh Lake – July 9, 2021, and
  - Tagish – July 10, 2021.
- Various background reports provided by YG, including:
  - A 1974 flood study completed for Yukon by the Foundation of Canada Engineering Corporation Limited (FENCO) (FENCO, 1974).
  - A 1983 flood risk study for the Yukon River Basin completed by Underwood McLellan Ltd. (Underwood McLellan Ltd., 1983).
  - A 2010 study completed by KGS Group for Yukon Energy evaluating the hydraulic regime of the Yukon River between Marsh Lake and Schwatka Lake (KGS Group, 2010).
  - A 2015 study completed by Environmental Dynamics Inc. evaluating flood frequency relationships for Yukon floodplain communities (Environmental Dynamics Inc., 2015).
  - A 2021 memo prepared by Morrison Hershfield reviewing available historical hydrometric information, and preliminary reviews of LiDAR for various Yukon communities. (Morrison Hershfield, 2021)
  - A 2022 memo prepared by Morrison Hershfield defining updated AEP flood levels for Bennett Lake, Tagish Lake, Marsh Lake, and Lake Laberge (Morrison Hershfield, 2022).
  - A 2022 report prepared by Stantec reviewing dike conditions following the 2022 spring melt, as well as the level of flood preparedness for various Yukon communities (Stantec, 2022).

Following the thorough review of the available background data, the Project Team completed an assessment of any potential data gaps, and to identify if any errors were present in the background information. One key finding related to the vertical datum defined by WSC for the gauges on Bennett Lake and Tagish Lake, as there is an apparent discrepancy between the two reference datums. This discrepancy is discussed further in Section 5.2.1.

2.4 Review of Historical Flooding

A thorough review of available information relating to flooding in the Southern Lakes region was completed to identify significant flood events that have occurred for inclusion in a digital Flood Event Inventory. It is envisioned that the Flood Event Inventory can serve as a living document that can be updated to include additional historical flood events, should further information or research become available to identify those floods, as well as future flood events. This document can be used to track causal mechanisms of flood events, as well as the impacts associated with those floods, throughout the Yukon.

Four significant flood events were identified as part of the review of historical flooding:

- ***Summer 2021*** – The highest levels on record occurred on Bennett Lake, Tagish Lake, Marsh Lake, and Lake Laberge during summer 2021, with peak water levels occurring on July 11 (Bennett Lake, Tagish Lake, and Marsh Lake) and July 16 (Lake Laberge). The flooding was a product of record snowpack, a cold spring leading to a delayed melt, then very high temperatures in mid-June to early July associated with a heat dome in British Columbia. These factors resulted in inflows to the lakes up to 76% higher than the previous historical maximum inflows.
- ***Summer 2007*** – The second highest water levels on record occurred during summer 2007, with peak water levels occurring on August 12 (Bennett Lake and Tagish Lake), August 14 (Marsh Lake) and August 15 (Lake Laberge). The flooding resulted from a high snowpack, augmented by substantial rain in mid-July, as well as high glacial melt.
- ***Summer 2022*** – Significant snowpack depths across the upper Yukon River basin in 2022 created a widespread risk of summer lake flooding. A cold spring led to a delayed melt. This resulted in the latest peak level timing on record for Bennett Lake, Tagish Lake, and Marsh Lake. This late peak was primarily driven by heavy precipitation in the basin in September and early October, after the typical mid-August peak driven by glacial melt and precipitation. The 2022 flood was the 3rd highest flood event on record for Tagish Lake, Marsh Lake, and Lake Laberge.
- ***August 1981*** – Limited information is available regarding the 1981 flood; however, it was noted to have had the highest water levels in the lakes in at least the preceding 10 years (i.e. prior to 1981). Available information notes that the flood impacted Marsh Lake, where the 1981 flood is the 4th highest level on record. The available hydrometric records also indicate that 1981 was the 3rd highest flood on record on Bennett Lake.

The Flood Event Inventory was provided to YG as a separate document from this report.

3.0 FIELD SURVEY PROGRAM

3.1 Overview

An extensive field survey program was completed for this project to measure the ground level of the lake shore at representative locations throughout the study area, to collect measurements to develop an approximate representation of the lakebed elevations for Bennett Lake, Nares Lake, Tagish Lake, Marsh Lake, and Lake Laberge, and to collect ground elevation measurements to serve as an independent check on the LiDAR data provided by YG. Specifically, the field program included:

- Survey of 72 km of lake bottom elevations along Bennett Lake;
- Survey of 5 km of lake bottom elevations along Nares Lake;
- Survey of 153 km of lake bottom elevations along Tagish Lake;
- Survey of 18 km of lake bottom elevations along Marsh Lake;
- Survey of 30 km of lake bottom elevations along Lake Laberge;
- Survey of 9 representative shoreline cross sections in Carcross;
- Survey of 8 representative shoreline cross sections in Tagish;
- Survey of 17 representative shoreline cross sections along Marsh Lake;
- Survey of 5 representative shoreline cross sections along Lake Laberge;
- Survey of 10 high water marks throughout the study area;
- Measurement of ground elevations throughout the study area.

The information gathered from the field survey was used to develop a representation of the lake bottom elevations throughout the study area, and to support the estimation of wind setup and wave runup heights for a range of meteorological conditions. Surveyed ground elevations were also used as an independent validation of the LiDAR data provided by YG.

3.2 Topographic and Bathymetric Surveys

Bathymetric surveys were completed using a Real Time Kinematic (RTK) dual frequency Global Positioning System (GPS) in combination with hydrographic survey grade sounding equipment (i.e. a Sonarmite TM) that interfaced with the RTK GPS. A GPS base station was set up along the project route and broadcasted corrected strings for navigation and data recordings. In areas where the lake shoreline was too shallow, surveyors completed manual GPS shots along cross sections until a depth of 1.2 m was encountered using a Topcon HiPer VR unit.

Survey data was collected using the NAD83 CSRS (North American Datum of 1983 Canadian Spatial Reference System), Yukon Albers projection for horizontal reference. The CGVD2013 (Canadian Geodetic Vertical Datum of 2013), GEOID2013 projection was used for the determination of all the orthometric heights.

Existing federal and provincial monuments were used as primary control to support the bathymetric and ground survey activities. Additionally, federal vertical monuments were tied dependent on the current condition of the monument. Independent confirmation was completed using data from the Canadian Active Control System (CACS) available on the CSRS website.

Stop and go kinematics occupations (RTK or Post Processed Kinematic (PPK)) of three or more epochs was used for the collection of topographic and shallow shoreline survey data. Positions were collected using real time correction with Ultra-High Frequency (UHF) radio links that communicate between the rover and the base. The relative accuracy of the topographic points was within +/- 1.0 cm in the horizontal and +/- 2.0 cm in the vertical.

The survey data collected throughout the study area is shown on Figure 3 to Figure 5, with bathymetric survey points shown in purple, shoreline points shown in orange, and control points shown in red.

FIGURE 3: SURVEY DATA COLLECTED ON BENNETT LAKE, NARES LAKE, AND TAGISH LAKE

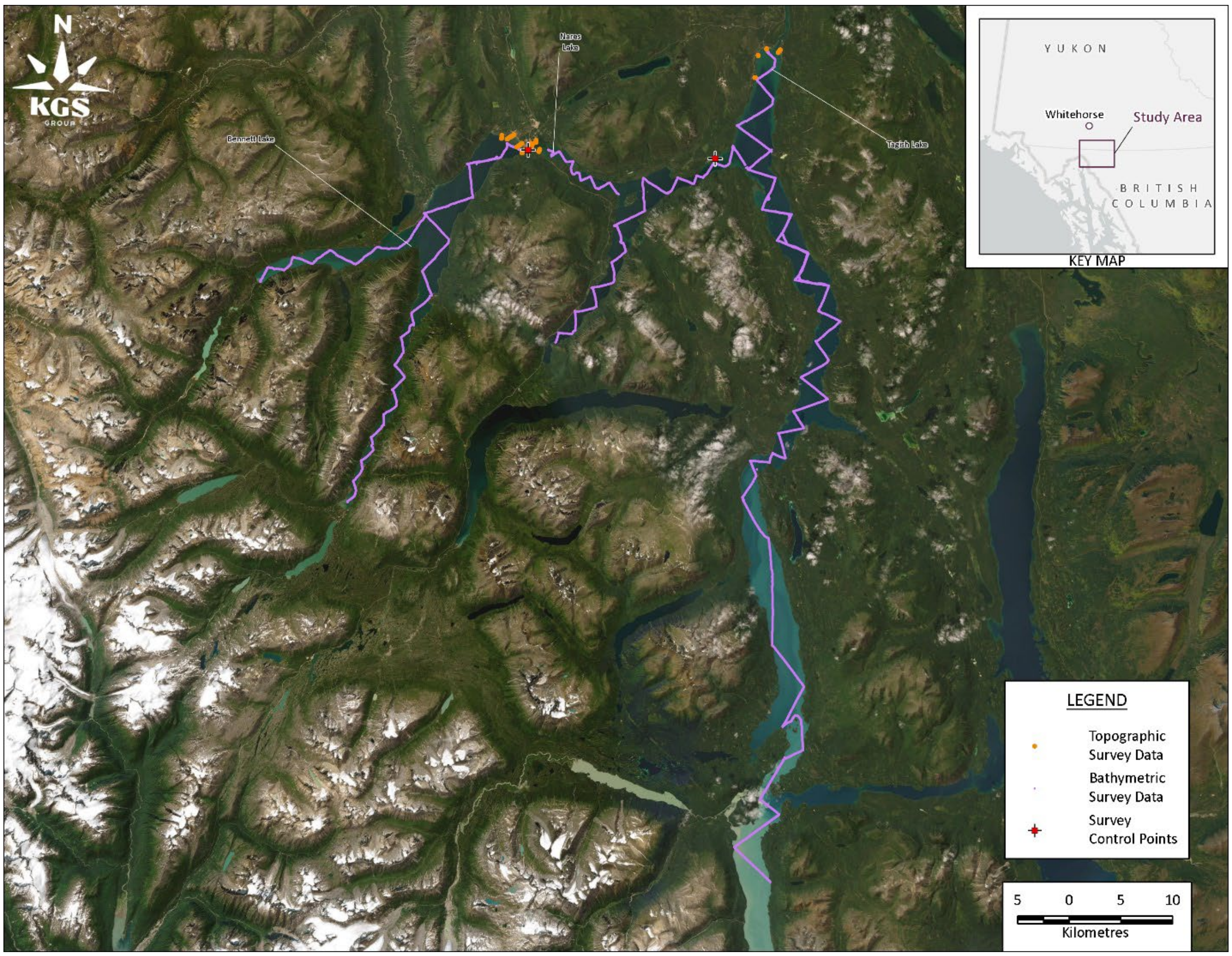

FIGURE 4: SURVEY DATA COLLECTED ON MARSH LAKE

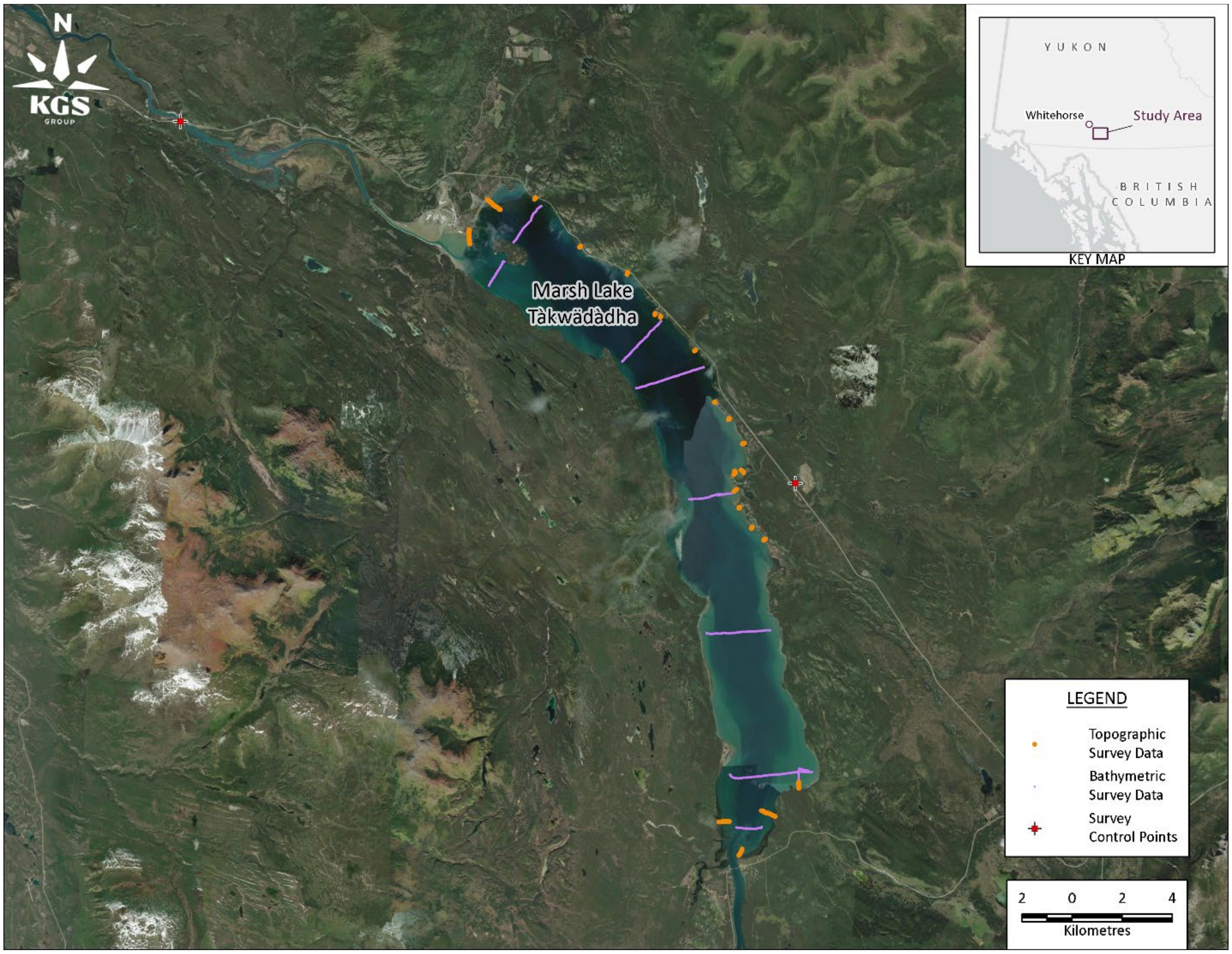

FIGURE 5: SURVEY DATA COLLECTED ON LAKE LABERGE

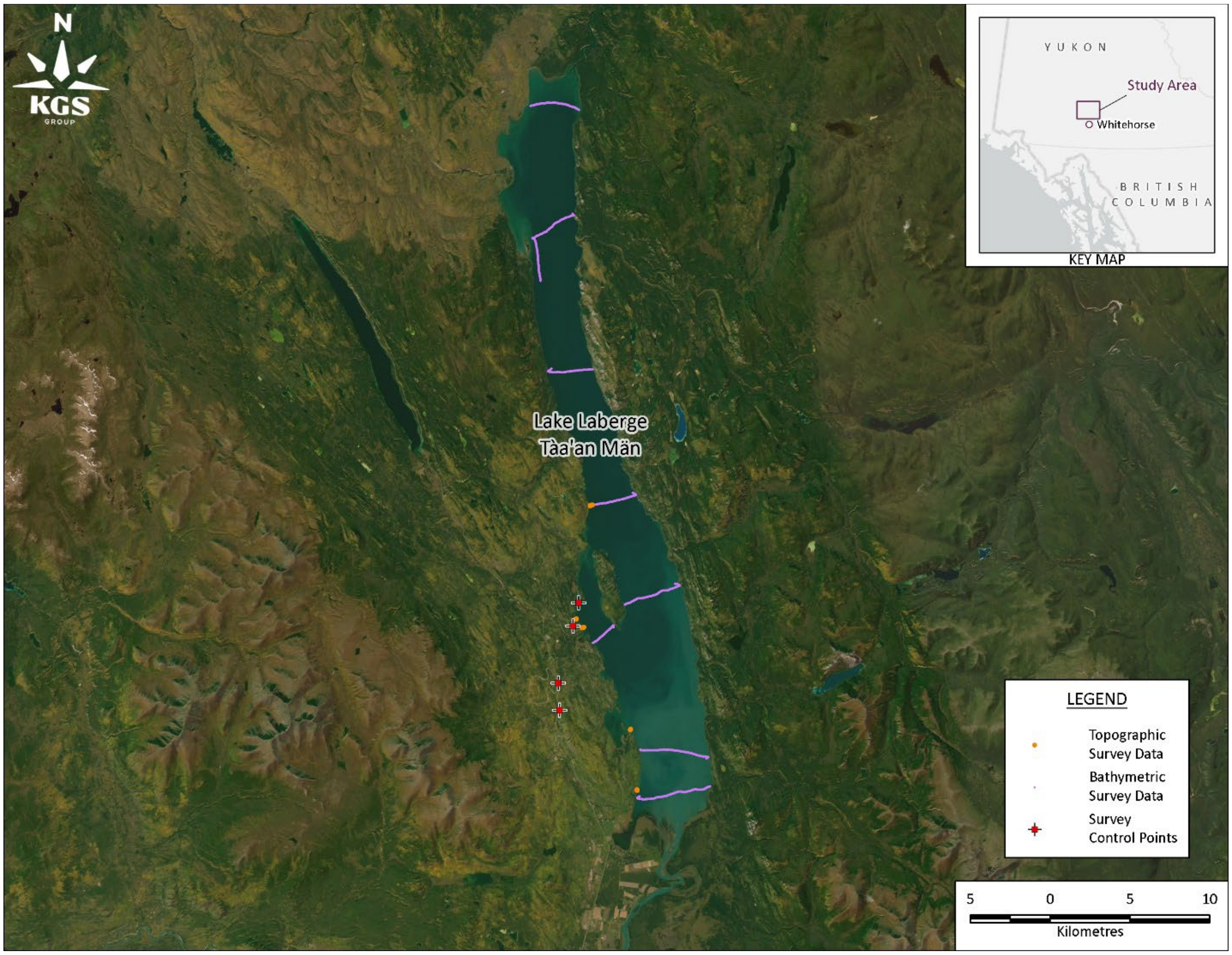

Water levels were regularly surveyed throughout the execution of the field survey program, as well as high water marks at a number of locations throughout the study area. Measured high water marks were in generally good agreement with the hydrometric records associated with the 2021 and 2022 flood events, four high water marks associated with the 2021 flood, and six high water marks associated with the 2022 flood.

During the field survey, surveyors collected georeferenced photographs to characterize shoreline conditions throughout the study area.

3.3 LiDAR Validation

KGS Group reviewed the bare earth digital elevation models (DEM) that were provided for Tagish, Marsh Lake, and Lake Laberge as part of the background data for the study area. The DEMs were provided as 1 m grid datasets and served as the primary data source for all topography data. GPS/RTK survey data was used to confirm the accuracy of the DEM. This survey data was compared to the DEMs at the same location to ascertain the vertical accuracy of the DEMs.

In addition to the DEMs that were provided for Tagish, Marsh Lake, and Lake Laberge, KGS Group developed a bare earth DEM for Carcross based on the LAS LiDAR tiles provided as part of the background information. Similar to the bare earth DEMs for Tagish, Marsh Lake, and Lake Laberge, the resulting DEM was generated as a 1 m grid dataset, and was compared to GPS/RTK survey data collected by KGS Group to confirm the accuracy of the DEM.

Comparisons were made at 17 locations in Carcross, 49 locations in Tagish, 13 locations on Marsh Lake, and 14 locations on Lake Laberge. The number of comparison locations were limited to areas where the surveyed ground elevations were above the water level on the lakes during the LiDAR captures. It should also be noted that many of the survey locations were along shoreline slopes and in vegetated areas. The results are summarized in Table 1.

TABLE 1: LIDAR VALIDATION

Location	Number of Points	Average Difference (m)	Median Difference (m)
Carcross	17	0.115	0.018
Tagish	49	0.178	0.181
Marsh Lake	22	0.182	0.143
Lake Laberge	14	0.067	0.092

The calculated differences between surveyed points and the DEM surface were found to be acceptable.

3.4 Bathymetric DEM Development

Bathymetric DEMs were developed for Bennett Lake, Nares Lake, Tagish Lake, Marsh Lake, and Lake Laberge based on a combination of LiDAR data, bathymetric survey data, and existing nautical mapping data. The DEM was developed at a resolution of 5 m in the CGVD 2013 vertical datum and NAD83 CSRS (North American Datum of 1983), Yukon Albers horizontal projection. The bathymetric DEM was primarily used to develop stage-storage curves for each of the lakes, but was also used in combination with LiDAR data to estimate shoreline transects in areas where survey data was not captured.

4.0 ASSESSMENT OF LAKE LEVEL REGULATION

4.1 Overview

Water levels on Bennett Lake, Nares Lake, Tagish Lake, and Marsh Lake are affected by water level regulation by the Lewes Dam. Similarly, water levels on Lake Laberge are influenced by the storage of water in the lakes upstream of the Lewes Dam. While the Lewes Dam is located downstream of the outlet of Marsh Lake, the small difference in water levels between Bennett Lake, Nares Lake, Tagish Lake, and Marsh Lake during high water level conditions means that any impacts to Marsh Lake water levels influence water levels on the upstream lakes. During low water level conditions, there are greater differences in lake levels between Marsh Lake and Tagish Lake, reducing the impact of Marsh Lake water levels.

Water level regulation on Marsh Lake is defined by Yukon Energy Corporation's Water Use License HY99-010. In that license, operating conditions are defined for the Lewes Dam depending on water levels on Marsh Lake, and key seasonal timelines. In particular, it is noted that all gates on Lewes Dam are to remain fully open between May 15 and August 15 of each year, unless water levels are below minimum thresholds. The license also specifies controlled minimum and maximum allowable water levels.

To assess the potential impacts on flood levels associated with the Lewes Dam, a high-level analysis was completed by developing a model of Bennett Lake, Nares Lake, Tagish Lake, Marsh Lake and Lake Laberge to represent the changes in lake levels that occur due to the varying inflows into and outflows out of the lakes over time. The model was originally developed to represent existing conditions with Lewes Dam in place, and then modified to represent a condition without the Lewes Dam in place. A comparison of the resulting water levels for these two conditions was completed to estimate the impact that the Lewes Dam has on peak flood levels.

4.2 Estimation of Impacts Associated with Lake Level Regulation

Volume routing models were developed for Bennett Lake, Nares and Tagish Lake, Marsh Lake, and Lake Laberge in Microsoft Excel. The intent of the models was to develop representative historical water levels with the Lewes Dam in place, and then modifying the Marsh Lake outflow rating curve, and in turn, outflows from Marsh Lake, in the models to be representative of a natural condition (i.e. with the Lewes Dam removed). The simulated historical flood levels could then be compared with and without the Lewes Dam in place to estimate the impacts associated with the dam. It should be noted that this assessment was a high-level desktop exercise to estimate the potential impacts associated with the Lewes Dam, and as such the impacts described herein should be treated as a preliminary estimate. Further analyses should be completed to better refine the estimated impacts of the Lewes Dam on flood levels.

The models were based on a combination of recorded and estimated data, which included:

- Recorded water levels on Bennett Lake, Tagish Lake, Marsh Lake, and Lake Laberge.
- Recorded flows on Wheaton River (i.e. WSC gauge 09AA012), Tutshi River (i.e. WSC gauge 09AA013), Atlin River (i.e. WSC gauge 09AA006), M'Clintock River (i.e. WSC gauge 09AB008), and Takhini River (i.e. WSC gauge 09AC001).

- Ungauged inflows, which were estimated based on inflows on the Wheaton River, Atlin River, Sidney Creek (i.e. WSC gauge 09AD002), and Morley River (i.e. 09AE006).
- River flows on the Yukon River in Whitehorse (i.e. WSC gauge 09AB001).
- River flows on the Yukon River downstream of Lake Laberge (i.e. WSC gauge 09AB009).
- Outflow rating curves for each lake.
- Stage-storage curves that were estimated for Bennett Lake, Nares and Tagish Lake, Marsh Lake, and Lake Laberge based on the bathymetric dem described in Section 3.4, and are shown on Figure 6 to Figure 9.

FIGURE 6: STAGE-STORAGE CURVE FOR BENNETT LAKE

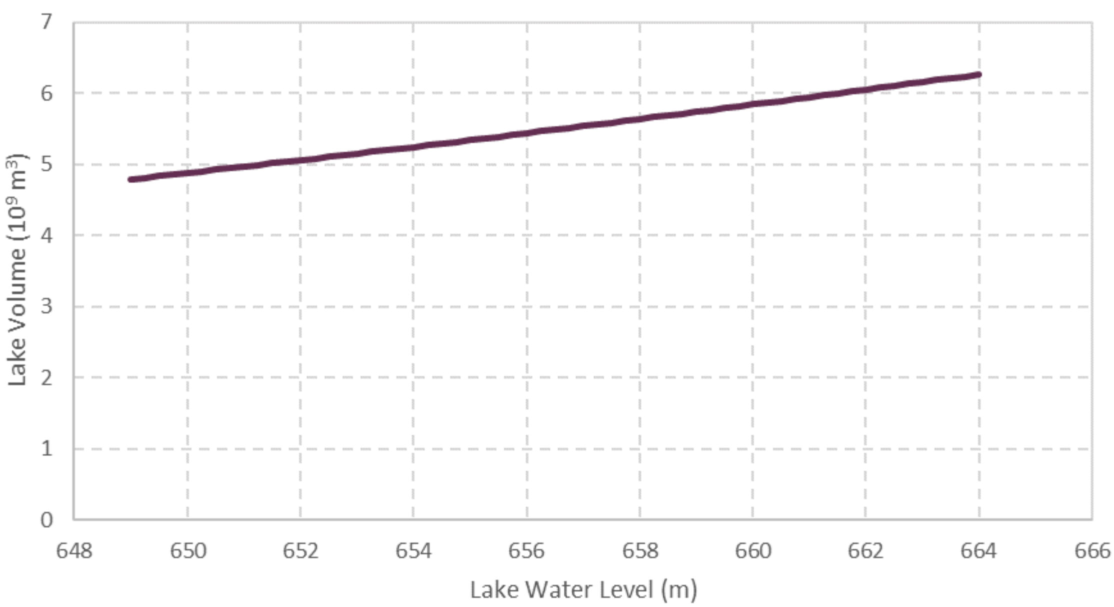

FIGURE 7: STAGE STORAGE CURVE FOR NARES AND TAGISH LAKE

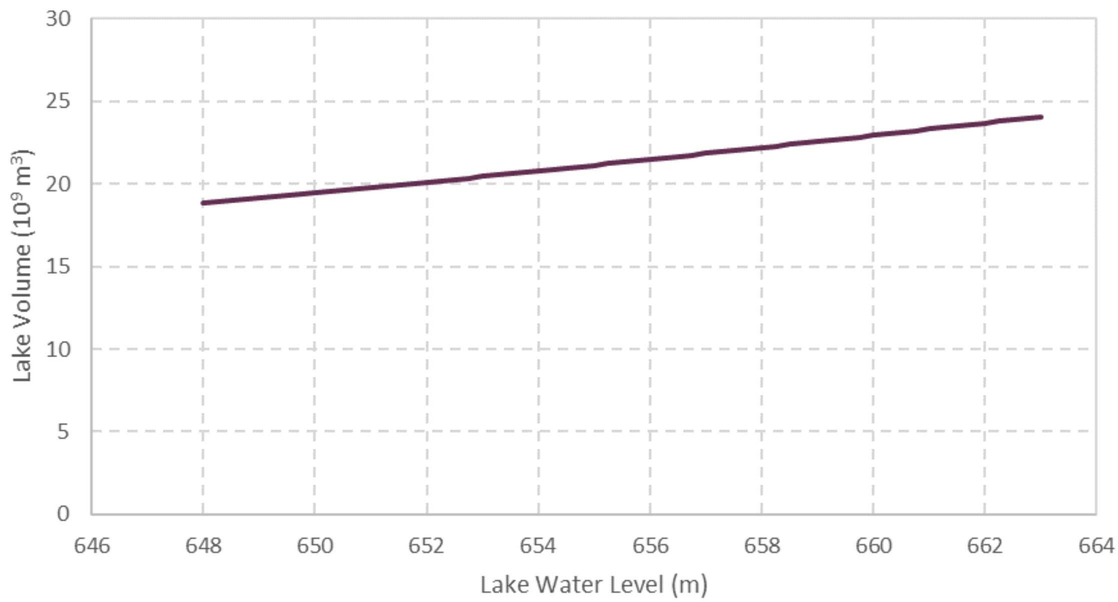

FIGURE 8: STAGE-STORAGE CURVE FOR MARSH LAKE

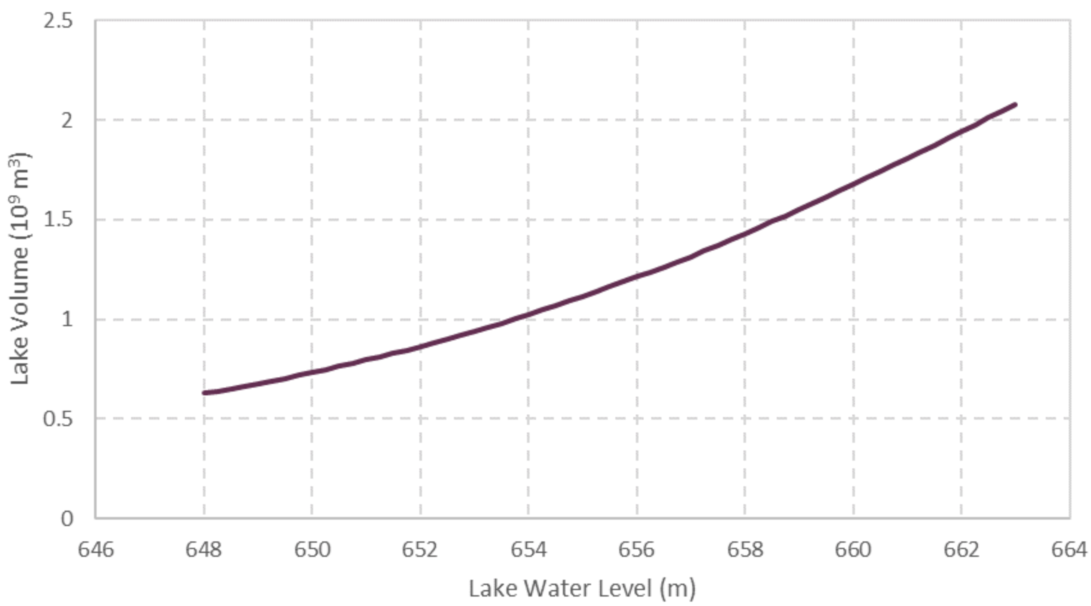

FIGURE 9: STAGE-STORAGE CURVE FOR LAKE LABERGE

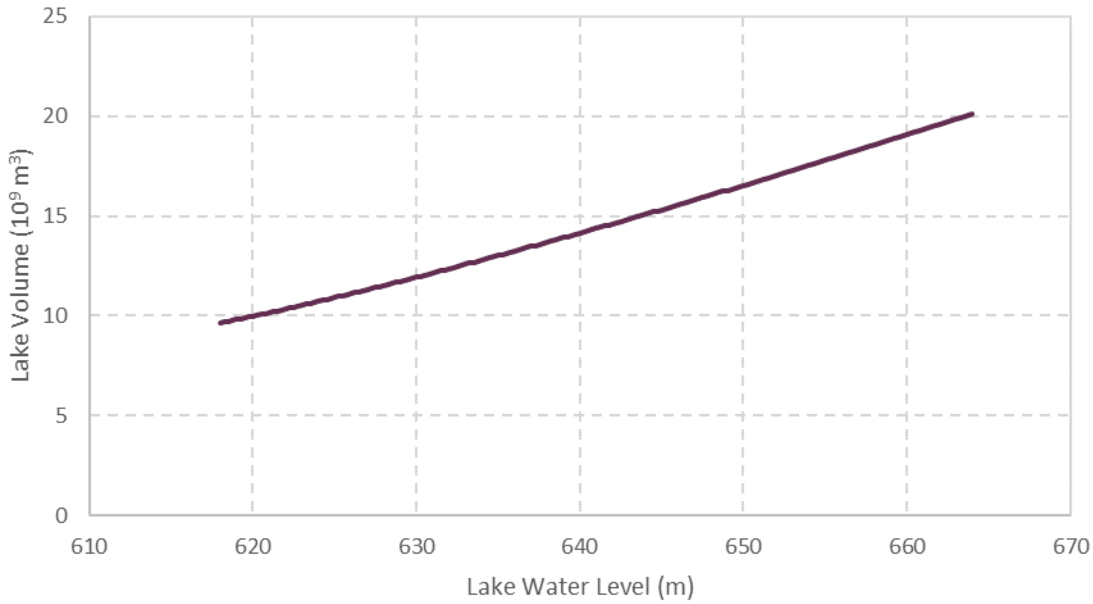

Two outflow rating curves were estimated for Marsh Lake based on recorded water levels on the lake and flows on the Yukon River in Whitehorse, with the first curve representing the fully opened gates at Lewes Dam between May 15 and August 15, while the second curve represented restricted outflow at Lewes Dam to store water, as allowed by the water use license. It should be noted that the restricted outflow rating curve where Lewes Dam is partially open is bound by the controlled water levels defined in the water use license, specifically between a controlled minimum of 654.111 m in the CGVD 2013 vertical datum (i.e. 653.796 m in the vertical datum referenced in the water use license) and a controlled maximum of 656.549 m in the CGVD 2013 vertical datum (i.e. 656.234 m in the vertical datum referenced in the water use license). Amendments to the water use license were issued in 2021 and 2022 allowing for a lower controlled minimum elevation of 654.011 m in the CGVD 2013 vertical datum (i.e. 653.696 m in the vertical datum referenced in the water use license). The Marsh Lake outlet rating curves are shown on Figure 10, with water levels shown in the CGVD 2013 vertical datum.

FIGURE 10: MARSH LAKE OUTFLOW RATING CURVE

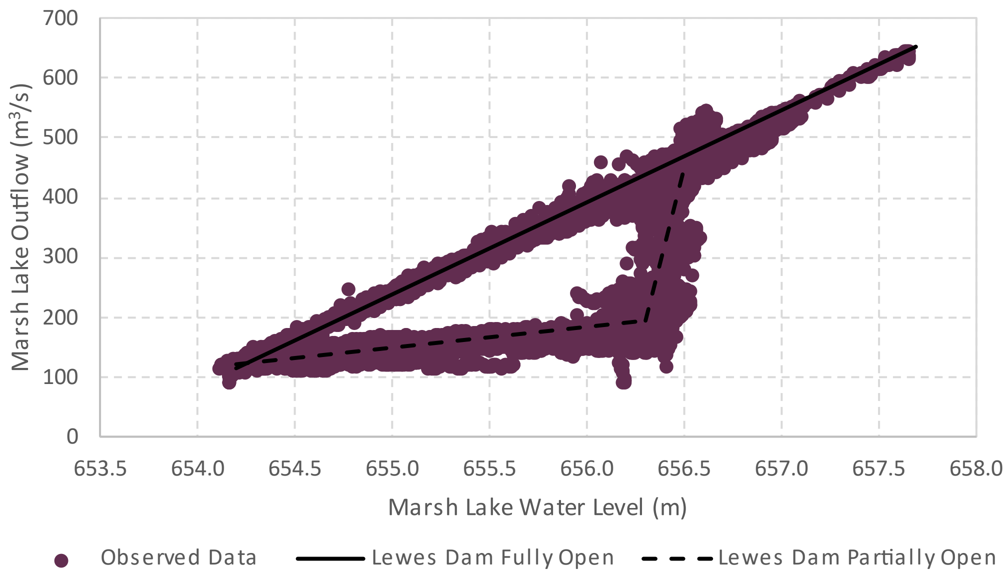

The Lake Laberge outflow rating curve was estimated based on recorded water levels on the lake and Yukon River flows downstream of the lake, as shown on Figure 11.

FIGURE 11: LAKE LABERGE OUTFLOW RATING CURVE

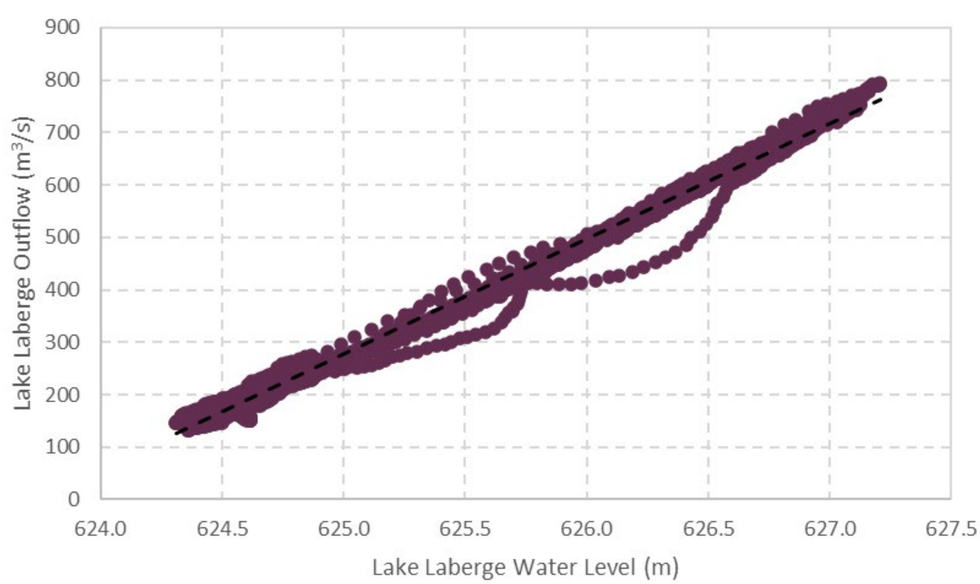

Outflow rating curves for Tagish Lake and Bennett Lake were developed using the *Stage-Fall-Discharge* method as described in Open Channel Hydraulics (Chow, 1959), which relates discharge that has been normalized by the square root of the head between two locations (i.e. Root F) relative to the water level at one of the locations. Historical outflows from Bennett Lake were calculated based on the gauged and estimated ungauged inflows to the lake, and changes to the lake storage volume given by the stage-storage curve and historical water levels on the lake. Similarly, outflows from Tagish Lake were calculated as the inflows to Marsh Lake based on the gauged and estimated ungauged inflows to Marsh Lake, as well as changes to the lake storage volume defined by the stage-storage curve and historical water levels on Marsh Lake.

The Bennett Lake outflow rating curve is shown on Figure 12, while the Tagish Lake outflow rating curve is shown on Figure 13. It should be noted that only considering water levels from 2007 to 2023 resulted in a much better representation of simulated water levels on Bennett Lake and Tagish Lake, and thus water levels and outflows prior to 2007 were not included in the outflow rating curves. It should also be noted that a better relationship was defined for Bennett Lake outflows considering the water level on Tagish Lake, and was thus adopted for defining the outflow rating curve.

FIGURE 12: BENNETT LAKE OUTFLOW RATING CURVE

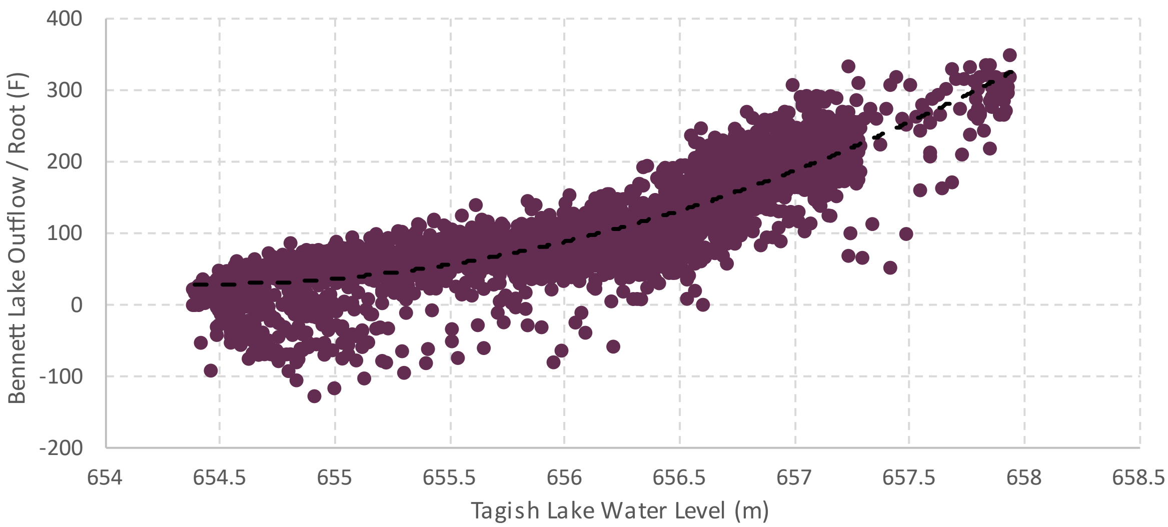

FIGURE 13: TAGISH LAKE OUTFLOW RATING CURVE

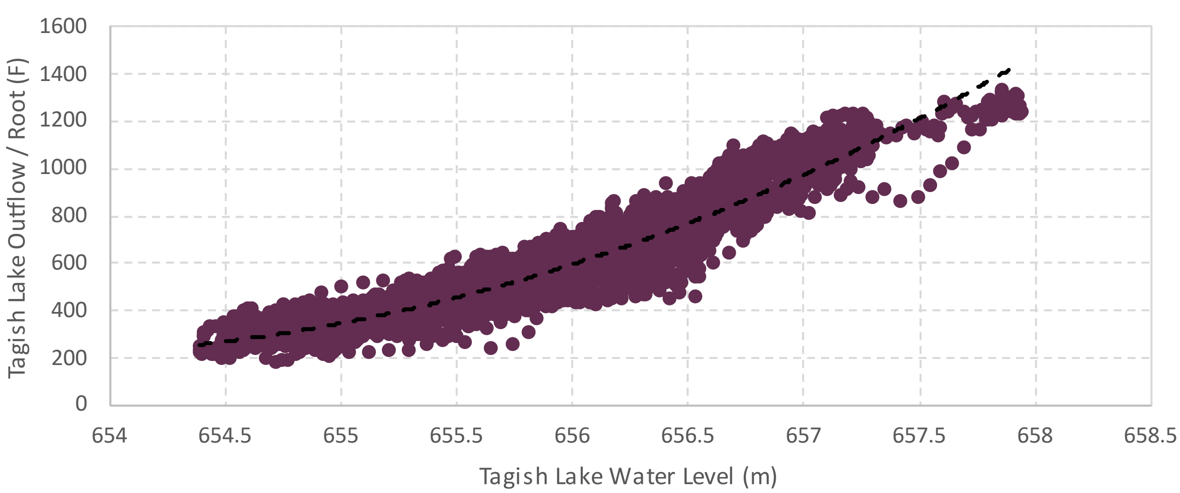

Historical water levels on Bennett Lake, Nares and Tagish Lake, Marsh Lake, and Lake Laberge were simulated between January 1, 1986, and December 31, 2022, as shown on Figure 14 to Figure 17, by developing a volume routing model for each lake. Flows were routed on a daily basis, with inflows defined by gauged and estimated ungauged inflows, outflows were defined based on the outflow rating curves for each lake given the water level on the previous day. Changes to the stored volume on each lake were calculated on a daily basis, with increases in stored water occurring when daily inflows exceed daily outflows, and reductions in stored water occurring when daily outflows exceed daily inflows. The resulting daily water levels were calculated considering the resulting volume of stored water based on the stage storage curves defined for the lakes.

FIGURE 14: COMPARISON OF SIMULATED AND OBSERVED WATER LEVELS ON BENNETT LAKE

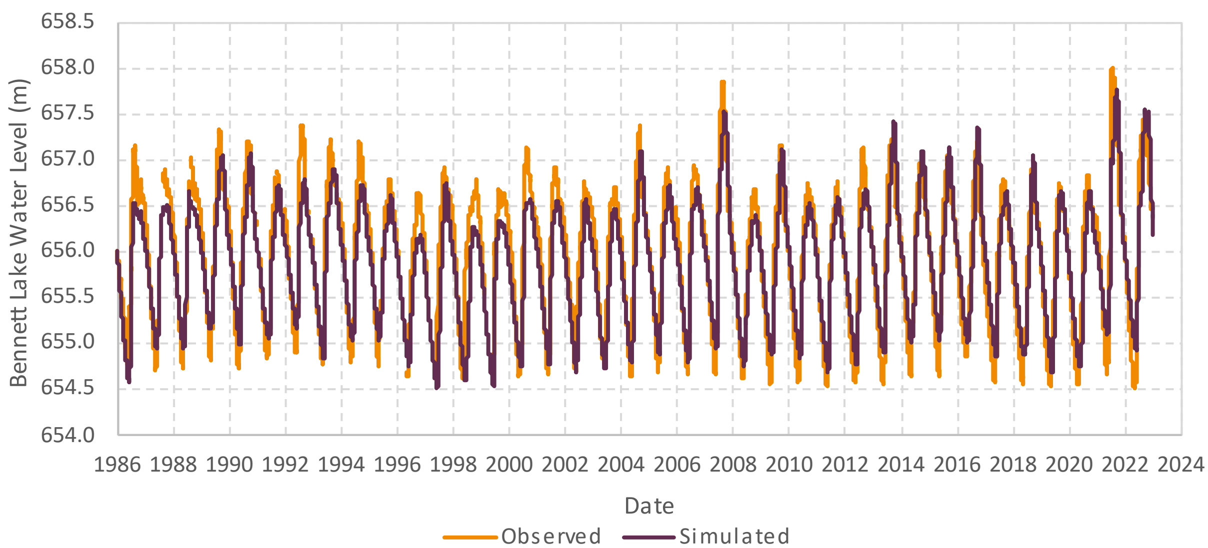

FIGURE 15: COMPARISON OF SIMULATED AND OBSERVED WATER LEVELS ON TAGISH LAKE

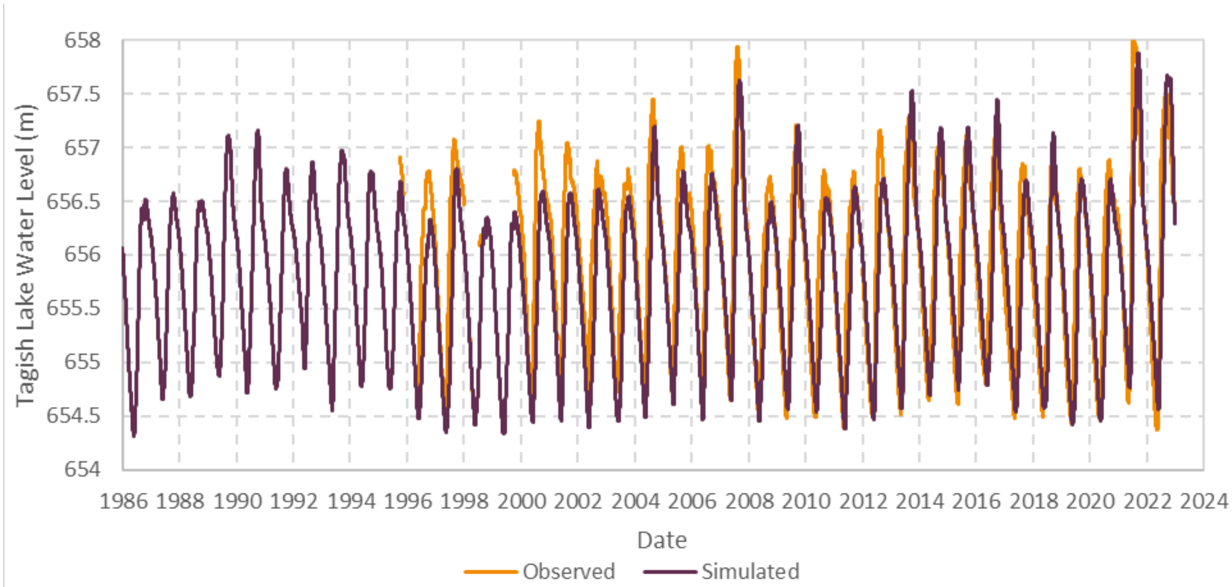

FIGURE 16: COMPARISON OF SIMULATED AND OBSERVED WATER LEVELS ON MARSH LAKE

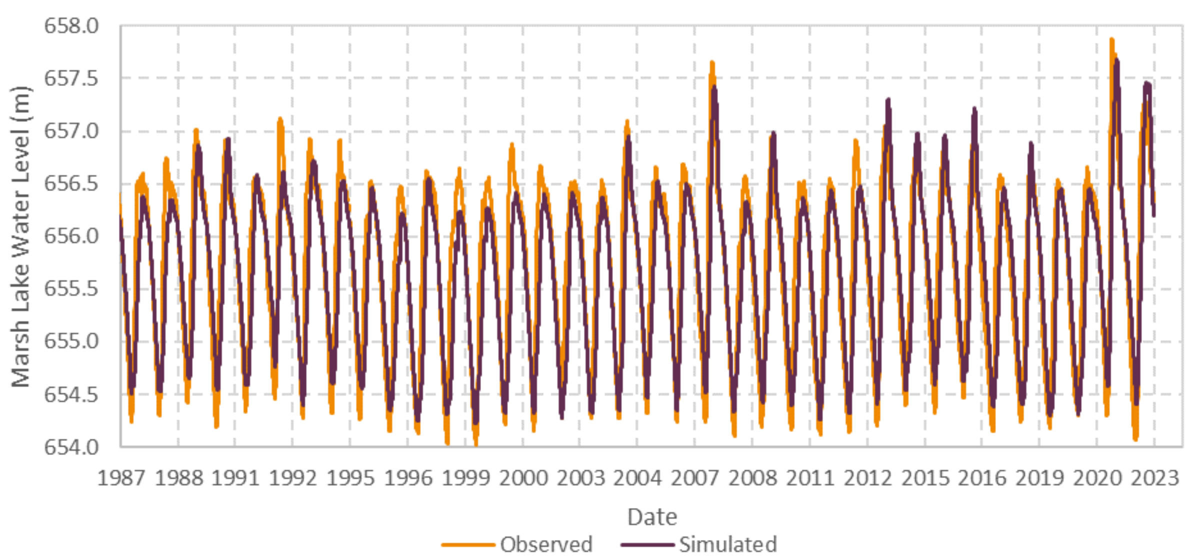

FIGURE 17: COMPARISON OF SIMULATED AND OBSERVED WATER LEVELS ON LAKE LABERGE

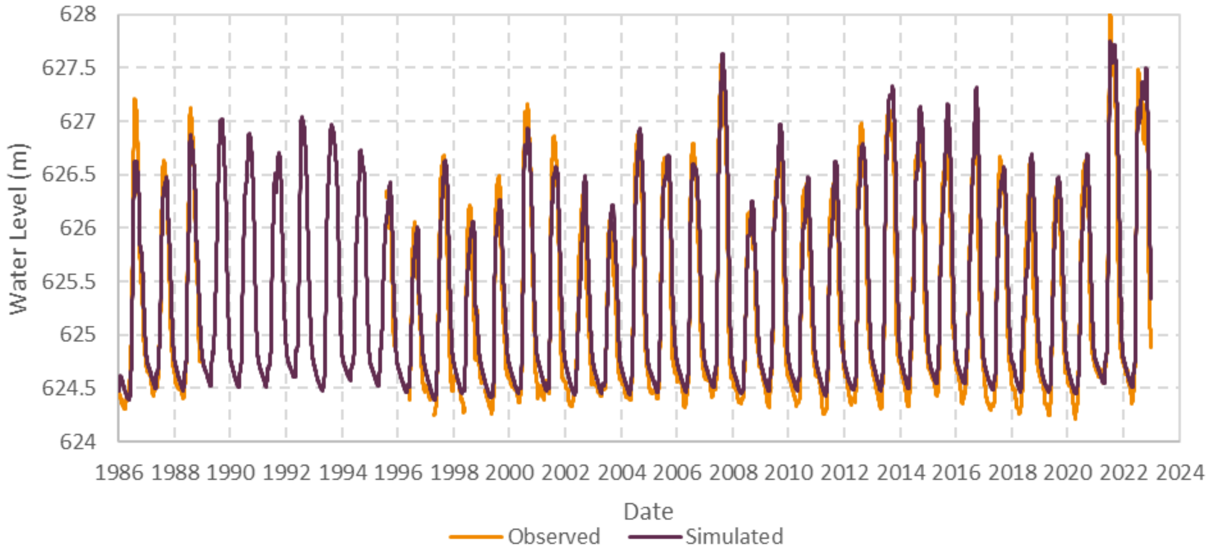

Nash-Sutcliff Efficiency (NSE) and percent bias (PBIAS) were calculated for the model representation of observed water levels on each of the lakes, as summarized in Table 2.

TABLE 2: MODEL PERFORMANCE STATISTICS

Lake	NSE	PBIAS (%)
Bennett Lake	0.84	0.02
Tagish Lake	0.67	0.03
Marsh Lake	0.71	0.02
Lake Laberge	0.91	-0.02

Based on the performance evaluation criteria described in Moriasi et al. (2015), the calculated NSE for the model representation of observed water levels on Bennett Lake and Lake Laberge is considered very good, while the NSE for Tagish Lake considered is satisfactory and the NSE for Marsh Lake is considered good. The calculated PBIAS for all lakes was considered to be very good. However, it should be noted that the very good PBIAS calculated for the model is likely due to the model overpredicting water levels to the same degree that it underpredicts water levels. Given the performance of the model based on both the NSE and PBIAS, it was considered to provide a reasonable representation of historical water levels, including the representation of the relative magnitude of flood events, although annual maxima and minima were over- or underestimated for a number of floods. Further hydrological analyses could improve the estimation of ungauged inflows to the lakes, thus enhancing the model representation of observed water levels. It should be noted that a perfect representation of the historical water levels is not necessarily required to estimate the impacts associated with the Lewes Dam, as the same sources of error associated with estimated inflows, estimated outflows, and stage-storage relationships will be consistent between simulated historical records with or without Lewes Dam in place, with the exception of the Marsh Lake outflow rating curve and associated outflows.

Water levels on Bennett Lake, Nares and Tagish Lake, Marsh Lake, and Lake Laberge without the Lewes Dam in place were simulated using the same gauged and estimated ungauged inflows, stage-storage relationships, and outflow rating curves for Bennett Lake, Tagish Lake, and Lake Laberge. The outflow rating curve for Marsh Lake without the Lewes Dam in place was defined using an existing United States Army Corps of Engineers (USACE) Hydrologic Engineering Center's River Analysis System (HEC-RAS) model extending from Marsh Lake to Schwatka Lake that was modified to remove Lewes Dam from the model. A range of flow conditions were then simulated in the model to determine the corresponding water level on Marsh Lake. The outflow rating curve defined by the HEC-RAS model is shown on Figure 18. It should be noted that the rating curve assumes that water levels are maintained at the maximum allowable level for Schwatka Lake as defined in the water use license.

FIGURE 18: MARSH LAKE OUTFLOW RATING CURVE WITHOUT LEWES DAM IN PLACE

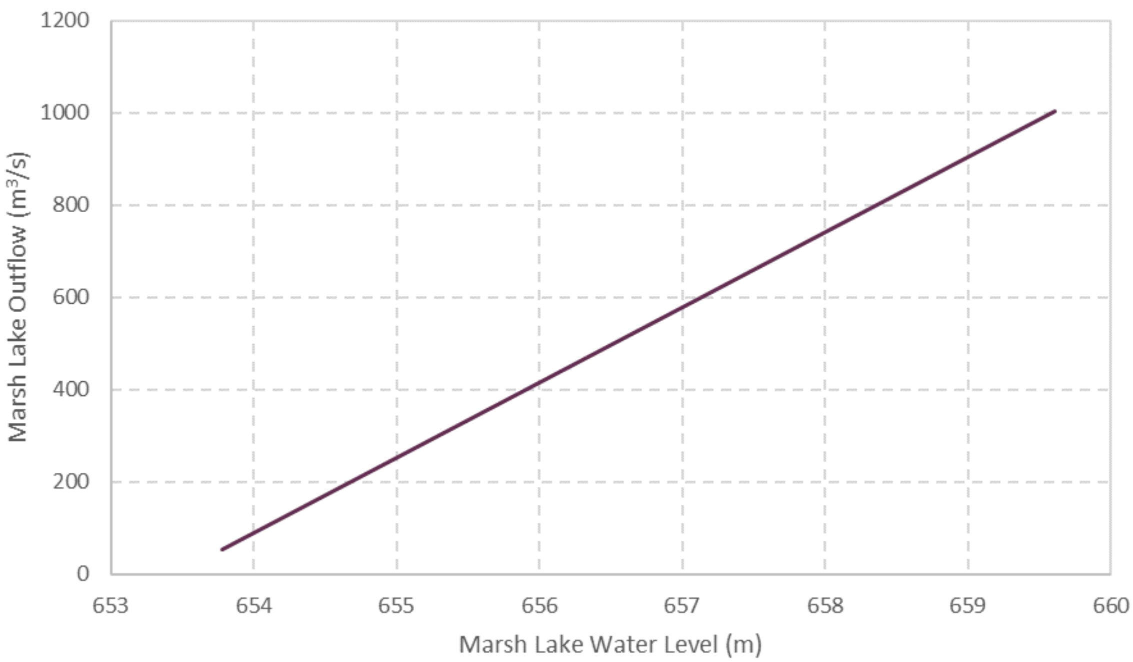

A comparison of the simulated water levels with and without Lewes Dam in place are shown for Bennett Lake, Nares and Tagish Lake, Marsh Lake, and Lake Laberge on Figure 19 to Figure 22.

FIGURE 19: COMPARISON OF BENNETT LAKE WATER LEVELS WITH AND WITHOUT LEWES DAM

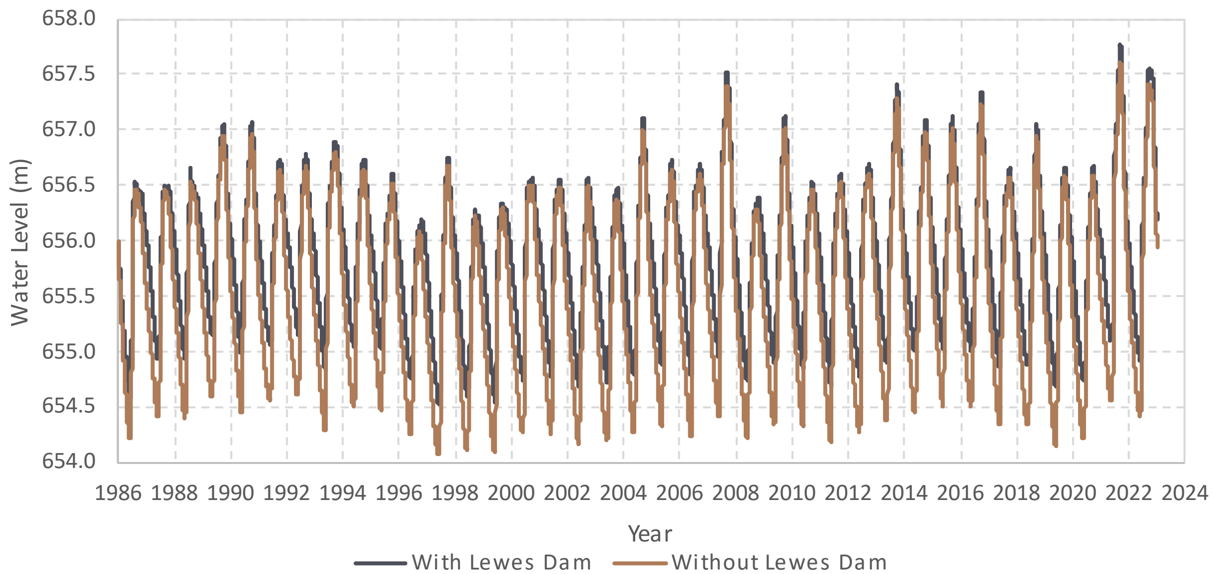

FIGURE 20: COMPARISON OF TAGISH LAKE WATER LEVELS WITH AND WITHOUT LEWES DAM

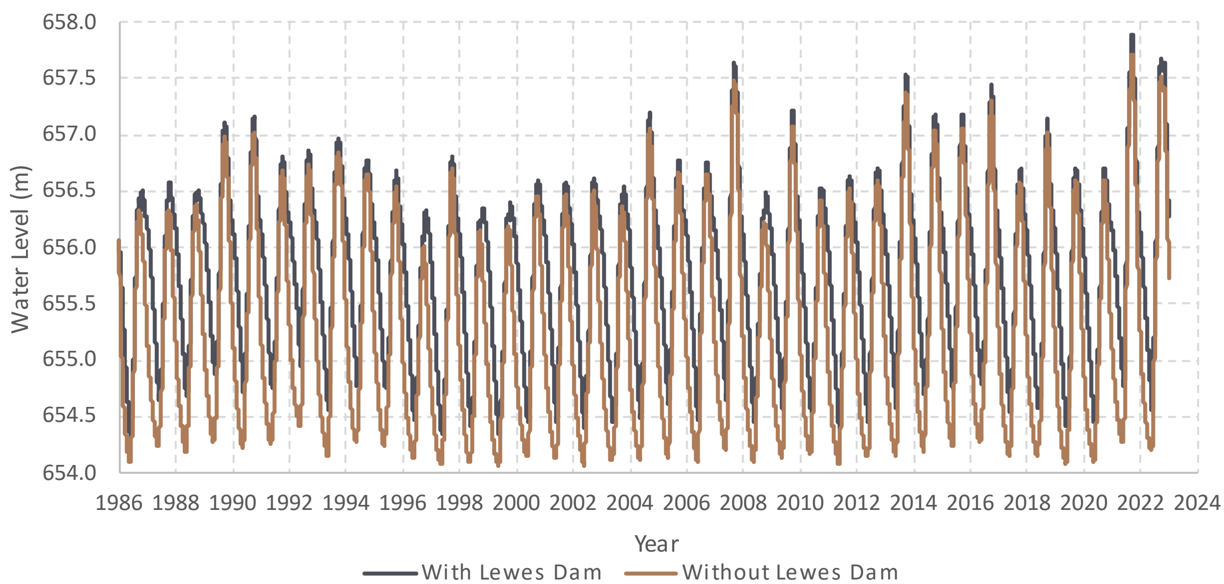

FIGURE 21: COMPARISON OF MARSH LAKE WATER LEVELS WITH AND WITHOUT LEWES DAM

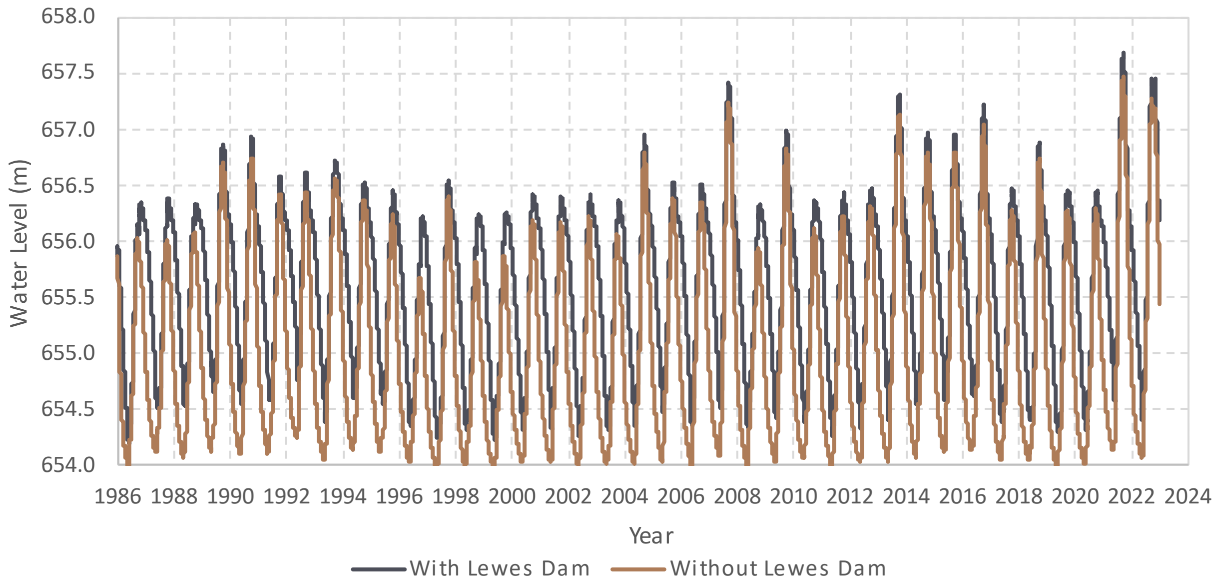

FIGURE 22: COMPARISON OF LAKE LABERGE WATER LEVELS WITH AND WITHOUT LEWES DAM

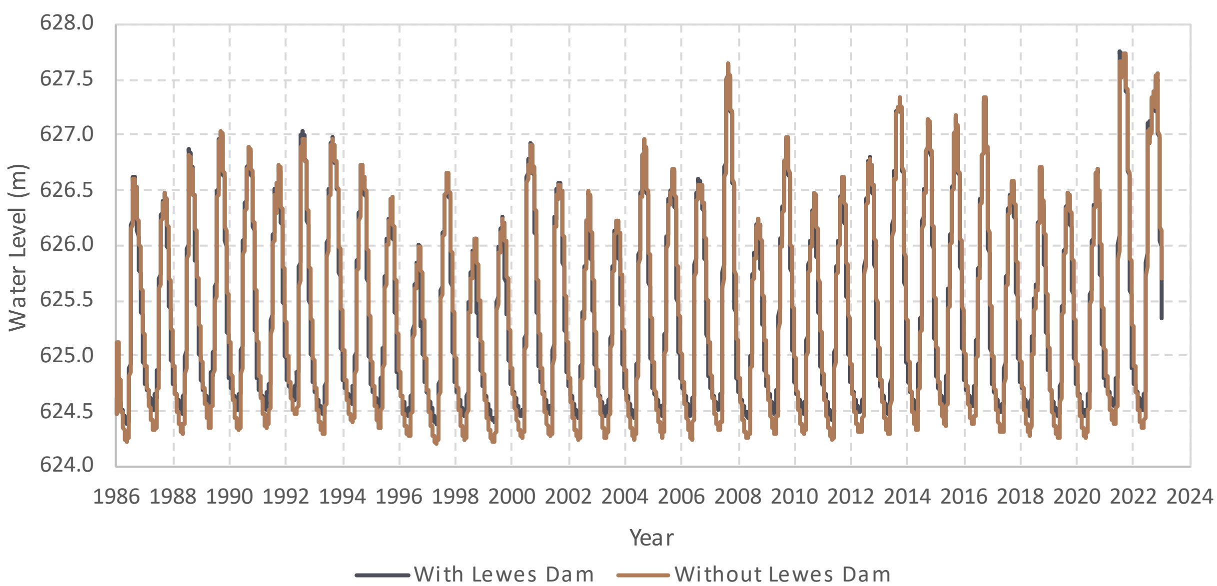

As shown on Figure 19 to Figure 22, annual peak water levels were compared between the simulated water levels with and without Lewes Dam in place. On Bennett Lake, peak flood levels are on average 0.10 m higher with Lewes Dam in place than without, with the 2007 and 2021 floods approximately 0.14 m and 0.17 m higher than if Lewes Dam were not in place. On Nares and Tagish Lake, annual peak water levels are on average 0.15 m higher with Lewes Dam in place than without, with the 2007 and 2021 floods approximately 0.15 and 0.17 m higher than if the Lewes Dam were not in place. On Marsh Lake, the average annual peak water levels with Lewes Dam in place are 0.22 m higher than without the dam in place, while the 2007 and 2021 floods were approximately 0.19 and 0.21 m higher than if the dam were not in place. On Lake Laberge, the difference between annual peak water levels with and without Lewes Dam in place is 0.00 m (i.e. no change). The 2007 flood would have been approximately 0.01 m higher, while the 2021 flood would have been 0.02 m lower if Lewes Dam were not in place.

As a check of the model sensitivity to the outflow rating curve on Marsh Lake, a separate set of water levels on Bennett Lake, Tagish Lake, Marsh Lake, and Lake Laberge were calculated using the outflow rating curve from Marsh Lake defined by the HEC-RAS model considering Lewes Dam in place. On average, annual peak water levels on Bennett Lake, Nares Lake and Tagish Lake, and Marsh Lake were 0.03 m, 0.05 m, 0.07 m higher considering the HEC-RAS outlet rating curve than the curve calculated based on historical data, while Lake Laberge annual peak water levels were 0.01 m lower. Accordingly, the model is somewhat sensitive to the adopted outflow rating curve. Further assessments of the outlet rating curve from Marsh Lake should be completed to better understand the implications of Marsh Lake outflows on the historical levels on the Southern Lakes.

To further understand the potential impacts of Lewes Dam on flood levels, frequency curves were fit to the annual peak water levels defined by the simulated water level records with and without Lewes Dam in place. The frequency curves were fit to the annual peak water level data following the methodology described in Section 5.2.1, although it was found that 3-Parameter Lognormal distributions were found to best represent the simulated annual peak water level data. The difference between the AEP water levels with and without Lewes Dam in place are summarized in Table 3.

TABLE 3: ESTIMATED AEP FLOOD LEVEL DIFFERENCES

Annual Exceedance Probability (%)	Water Level Difference (m)			
	Bennett Lake	Tagish Lake	Marsh Lake	Lake Laberge
0.5	0.22	0.20	0.24	-0.03
1	0.20	0.18	0.20	-0.02
2	0.17	0.16	0.18	-0.02
5	0.14	0.14	0.15	-0.01
10	0.12	0.13	0.15	-0.01
50	0.08	0.13	0.20	0.00

Based on the analysis described above, Lewes Dam in place results in higher flood levels on Bennett Lake, Nares Lake and Tagish Lake, and Marsh Lake, with a more pronounced effect for more severe floods. Flood levels on Lake Laberge are slightly lower with Lewes Dam in place than without the dam in place.

5.0 STATISTICAL ANALYSES

5.1 Overview

A number of statistical analyses were completed to understand the magnitude and timing of extreme water levels on the various lakes, as well as extreme wind speeds and wind directions in the Southern Lakes areas. The results of the statistical analyses were subsequently used in the Monte Carlo analysis of lake levels, wind setup, and wave runup, described further in Section 6.0, to define the flood levels ultimately to be considered in the development of the flood hazard maps.

Statistical analyses of annual peak water levels were completed for static lake levels on Bennett Lake, Tagish Lake, Marsh Lake, and Lake Laberge to understand the overall range of flood levels. Statistical analyses were also completed for the peak daily water level data on a monthly basis on those lakes to understand the variability in timing of peak lake levels. A statistical analysis of monthly and direction peak hourly wind speeds was completed to understand the seasonal and directional variability of the wind speeds. Similarly, an evaluation of historical wind directions was completed to understand the nature of prevailing winds throughout the study area. These analyses are described in the following sections of this report.

5.2 Static Lake Level Frequency Analysis

5.2.1 ANNUAL PEAK WATER LEVELS

As requested in the terms of reference for the project, frequency analyses were completed on Bennett Lake, Tagish Lake, Marsh Lake, and Lake Laberge to define static AEP flood levels on those lakes. While this method may be appropriate for estimating flood levels associated with more frequent flood events, extrapolating the frequency relationships can result in some uncertainty in the estimated flood level, depending on the data available to develop the frequency relationships.

As noted in the *Federal Hydrologic and Hydraulic Procedures for Flood Hazard Delineation Version 2.0* (Natural Resources Canada (NRCan), 2023), while there is no standard guidance on the required period of record to estimate frequency relationships, it is ideal to avoid extrapolating frequency relationships to AEP flood events more than double the length of the available record, although this is not always practical in a Canadian context. As noted in Table 4, the hydrometric records available on the Southern Lakes range from 25 years (i.e. Tagish Lake) to 69 years (i.e. Bennett Lake), suggesting that the estimation of floods up to the 1% AEP is reasonable, although there may be increased uncertainty with the 0.5% AEP flood event. Given the consistent water level response between Bennett Lake, Tagish Lake, Marsh Lake, and Lake Laberge, as well as the consistency between the resulting frequency curves, this statistical approach is considered to be reasonable for the estimation of flood levels up to the 0.5% AEP event, although future studies should consider different approaches to validate the results of this statistical approach.

More deterministic methods can be used to estimate low-probability flood levels by developing frequency curves of inflows available for the lakes, and then route the volume through a flood routing model that considers stage-storage relationships, as well as stage-discharge relationships at the outlet of the lakes. Future studies should consider the development of flood routing models and the estimation of inflow volume frequency curves to estimate flood levels on the lakes for low-frequency flood events to validate the flood levels estimated via statistical analyses. This deterministic approach could also facilitate applying anticipated climate change impacts to the hydrological processes that drive flooding on the lakes, as those impacts become better understood over time.

Available historical hydrometric data was acquired from WSC on Bennett Lake, Tagish Lake, Marsh Lake, and Lake Laberge. Where possible, instantaneous peak water level data was used in the analysis, with peak mean daily data used where instantaneous peak water level data was unavailable. A comparison of the instantaneous peak and mean daily data found that differences between the two water levels was generally on the order of 0.01 m or less.

The historical instantaneous peak and peak daily water level data was supplemented with real-time data to ensure that the historic levels observed during summer 2021, as well as the high levels observed that occurred during the summer and fall of 2022, were included in the analysis. Water level data from WSC were acquired in the CGVD2013 vertical datum, according to WSC metadata for each station. The historical hydrometric data that was used for the frequency analysis of static lake levels is summarized in Table 4. The locations of the hydrometric stations are shown on Figure 23 in blue.

TABLE 4: GAUGE STATIONS USED FOR FREQUENCY ANALYSIS

Station Number	Station Name	Period of Record	Number of Years Used in Analysis
09AB010	LABERGE LAKE AT WHITEHORSE	1980-2022	34
09AA004	BENNETT LAKE AT CARCROSS	1947-2022	69
09AB004	MARSH LAKE NEAR WHITEHORSE	1950-2022	61
09AA017	TAGISH LAKE AT 10 MILE ROAD	1995-2022	25

FIGURE 23: SOUTHERN LAKES HYDROMETRIC STATIONS

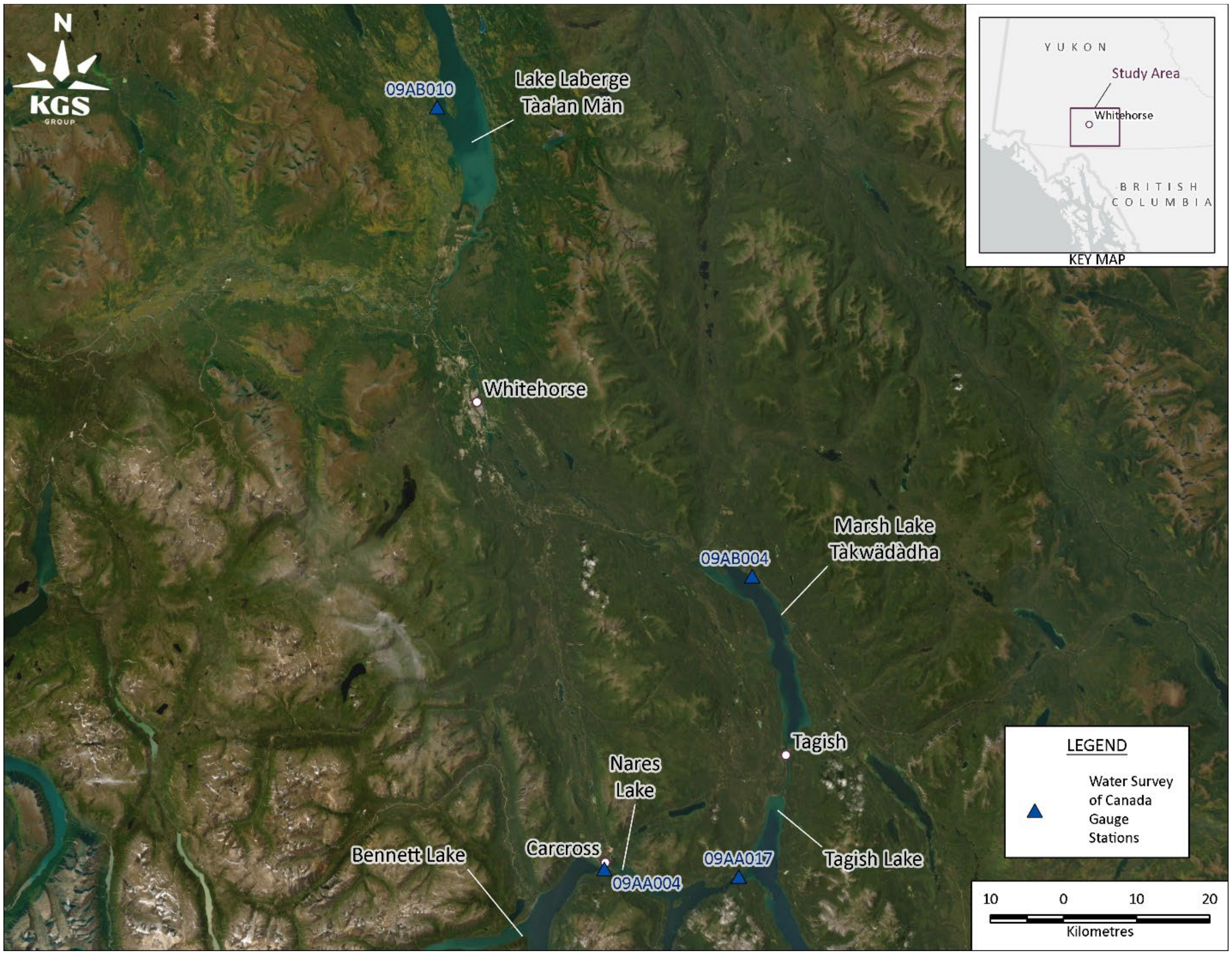

Frequency curves were fit to the annual peak water level data for each gauge station using the statistical hydrology software HYFRAN. A number of statistical distributions (e.g. Weibull, Log-Normal, Log-Pearson Type III, etc.) were fit to the annual peak lake level data to determine which distribution best represented the data. Annual peak water levels were considered in the analysis, as a review of the historical data showed that there is generally only one water level peak per year on each lake. As a result, conducting a peak-over-threshold (POT) analysis with this data was not considered appropriate.

The Gumbel frequency distribution was found to best fit the annual peak water level data based on combination of the results of the Chi-Squared statistical test and a visual inspection of the distribution, and was therefore selected as the frequency distribution for the historical annual peak water level data. The distributions fit to the data are shown on Figure 24, with the resulting AEP water levels summarized in Table 5.

FIGURE 24: ANNUAL FREQUENCY DISTRIBUTIONS

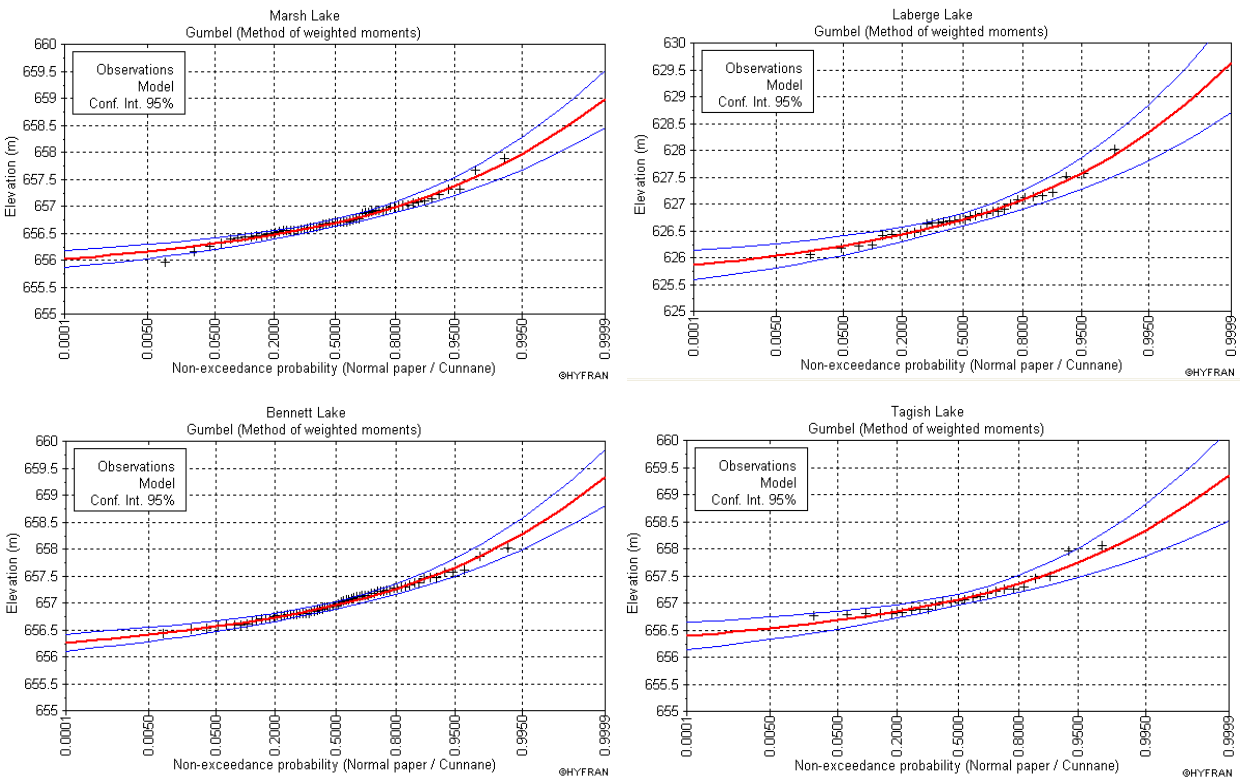

TABLE 5: ANNUAL FLOOD FREQUENCY LEVELS

Lake	AEP Water Level (m)								
	50%	20%	10%	5%	2%	1%	0.5%	0.33%	0.2%
Lake Laberge	626.71	627.08	627.33	627.56	627.87	628.10	628.33	628.46	628.63
Marsh Lake	656.69	656.98	657.18	657.36	657.61	657.79	657.97	658.07	658.21
Tagish Lake	657.06	657.36	657.55	657.74	657.98	658.16	658.34	658.45	658.58
Bennett Lake*	656.96	657.26	657.46	657.65	657.90	658.09	658.28	658.39	658.52

*Note: Due to uncertainty in Bennett Lake hydrometric records, water levels from Tagish Lake are proposed to define flood levels on Bennett Lake.

It should be noted that the frequency levels shown in Table 5 on Bennett Lake are lower than those defined for Tagish Lake, which is in contradiction to anticipated water level gradients. While some discrepancy between the two sets of AEP water levels would be expected due to the difference in the periods of record for each gauge, a review of both historical and near-real time water levels has shown conflicting patterns in the water levels on each lake that vary depending on season. The annual minimum water level on Tagish Lake is generally lower than the level on Bennett Lake, which would result in Bennett Lake draining into Tagish Lake, as expected. However, the annual maximum recorded water level on Tagish Lake is generally higher than the level on Bennett Lake, which would result in Tagish Lake flowing back into Bennett Lake. Examples of this discrepancy between WSC gauges are shown on Figure 25 (i.e. historical) and Figure 26 (i.e. near-real time). Water levels that were surveyed as part of KGS Group's field survey program are also shown on Figure 26, and were found to be in reasonable agreement with WSC's recorded water levels. Discussions with YG and NRCan have suggested that there may be issues with the geoid used in the CGVD2013 vertical datum, as the area near Carcross is experiencing significant crustal rebound. While local residents have noted that flow can reverse on Nares River, water levels on Tagish Lake were conservatively used for further analyses to represent Bennett Lake water levels. Monitoring of the flow direction on Nares River and the relative difference in water levels between Bennett Lake and Nares Lake should be completed to better understand the potential uncertainty in recorded water levels collected by WSC.

FIGURE 25: COMPARISON OF TAGISH AND BENNETT LAKE WATER LEVELS (HISTORICAL)

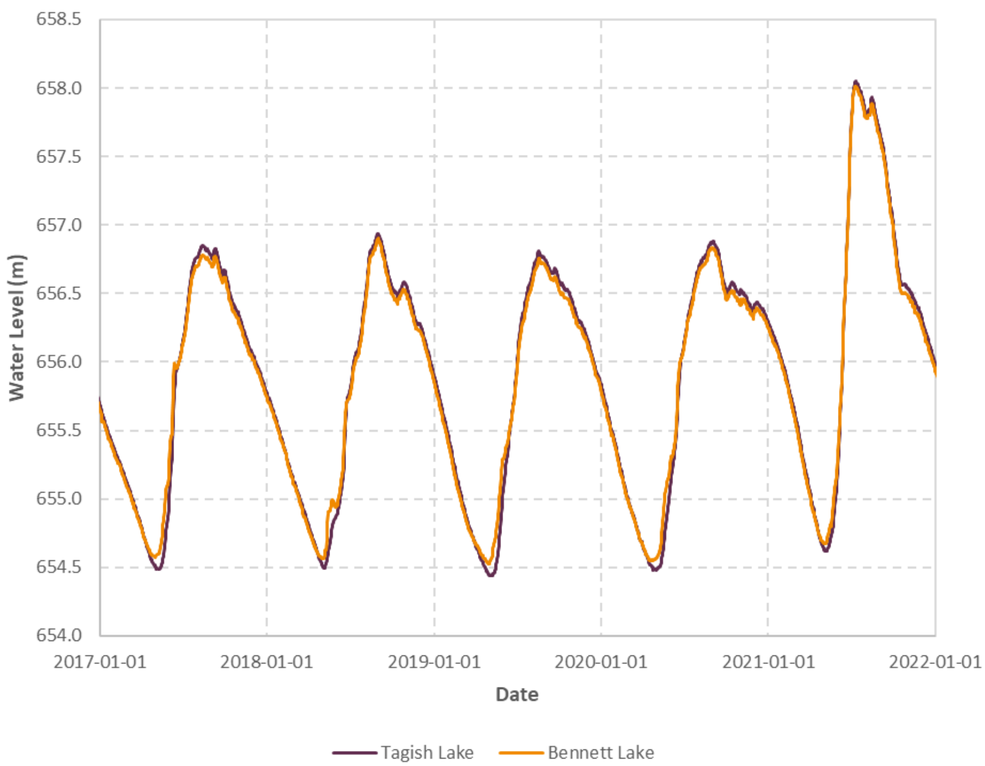

FIGURE 26: COMPARISON OF TAGISH AND BENNETT LAKE WATER LEVELS IN SUMMER, 2023 (REAL-TIME)

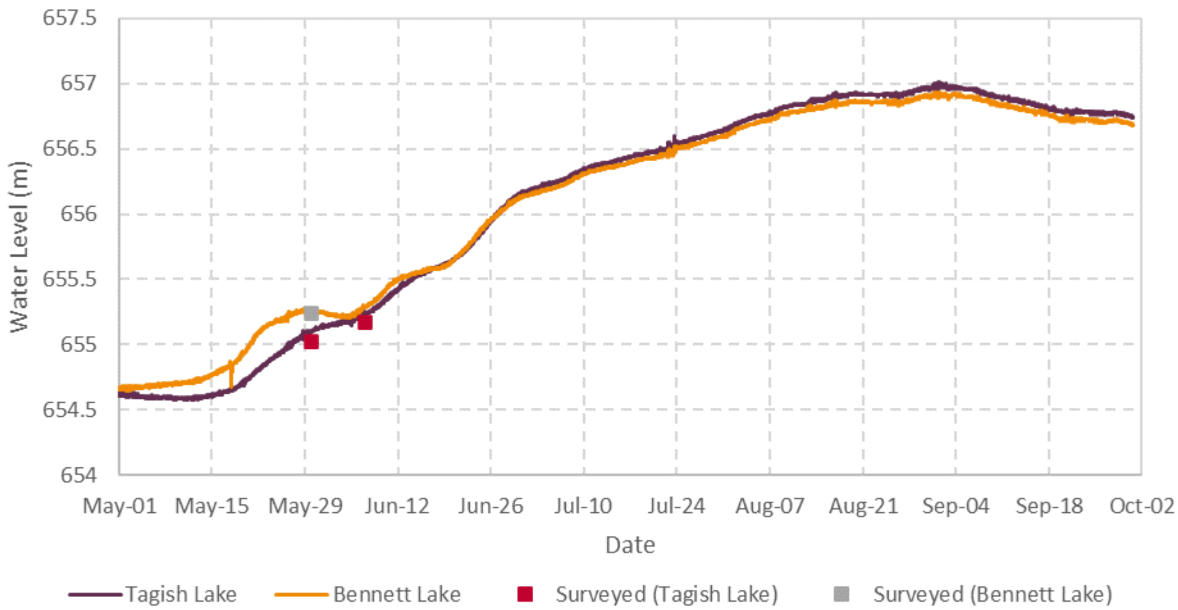

5.2.2 MONTHLY PEAK WATER LEVELS

Frequency analyses were completed on a monthly basis using mean daily peak water level data on Bennett Lake, Tagish Lake, Marsh Lake and Lake Laberge. Instantaneous data were not used, as they are only reported by WSC on an annual basis, and thus could not be used beyond annual analyses. The analyses were based on the available historical recorded water level data on each of the lakes, as summarized in Table 4. A review of timing of peak water levels on the lakes found that floods have historically only occurred between July and October. While many peak water levels occur in July, no peak flood levels have occurred in June, as the rising limbs of the historical flood hydrographs occur in June. This is shown on Figure 27, which shows the mean daily water levels between May 1 and November 1 on Marsh Lake, and is consistent with the hydrometric records for Tagish Lake, Bennett Lake, and Lake Laberge.

FIGURE 27: HISTORICAL WATER LEVELS ON MARSH LAKE

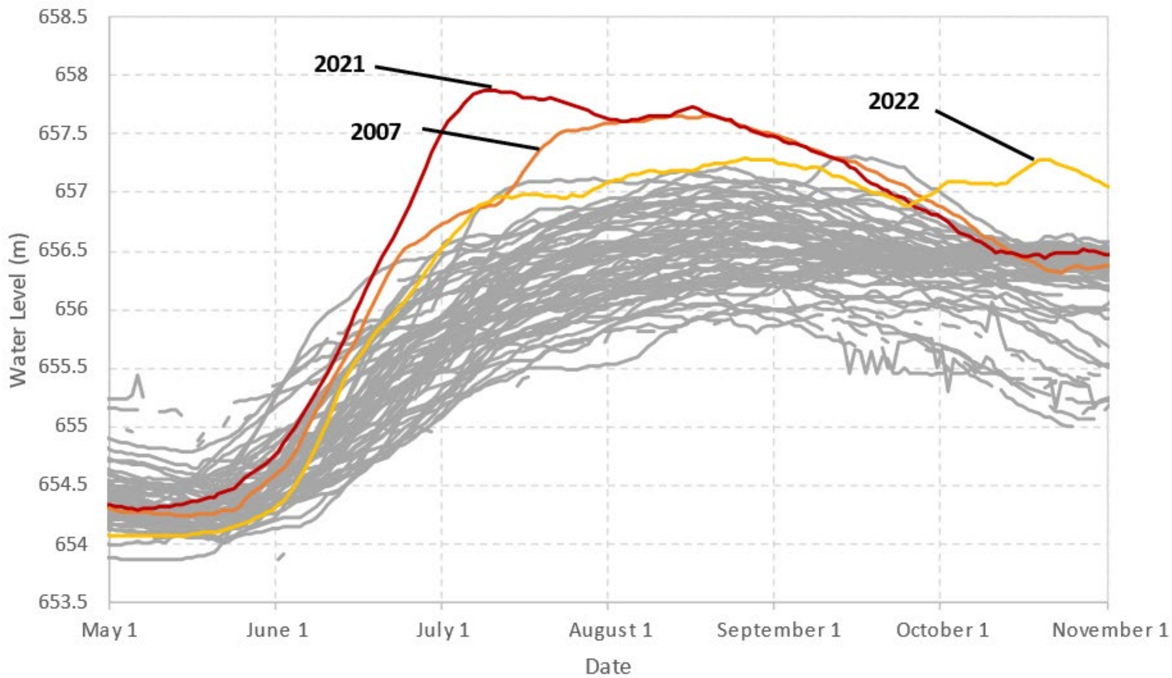

Mean daily peak daily water levels were extracted from the historical water level records on a monthly basis during the flood season (i.e. July to October), and frequency distributions were fit to those peak daily levels for each month following the same methodology as described in Section 5.2.1. A Gumbel distribution was found to best represent the peak water level data for all of the months and all of the gauges. The resulting monthly frequency levels are summarized in Table 6 to Table 9, with the frequency curves included in Appendix B for reference.

TABLE 6: BENNETT LAKE MONTHLY AEP WATER LEVELS

Annual Exceedance Probability (%)	AEP Water Level (m)			
	July	August	September	October
0.2	658.49	658.55	658.35	657.94
0.3	658.33	658.41	658.22	657.83
0.5	658.20	658.29	658.12	657.74
1.0	657.99	658.10	657.94	657.58
2.0	657.78	657.90	657.76	657.42
5.0	657.49	657.64	657.53	657.22
10.0	657.27	657.44	657.35	657.05
20.0	657.04	657.23	657.16	656.89
33.3	656.85	657.06	657.01	656.75
50.0	656.69	656.91	656.87	656.63

Note: AEP water levels from Tagish Lake adopted to define flood levels on Bennett Lake

TABLE 7: TAGISH LAKE MONTHLY AEP WATER LEVELS

Annual Exceedance Probability (%)	AEP Water Level (m)			
	July	August	September	October
0.2	658.74	658.63	658.37	657.74
0.3	658.57	658.49	658.25	657.65
0.5	658.43	658.38	658.15	657.59
1.0	658.20	658.19	657.99	657.48
2.0	657.96	657.99	657.83	657.36
5.0	657.65	657.74	657.61	657.21
10.0	657.40	657.54	657.44	657.09
20.0	657.15	657.33	657.26	656.97
33.3	656.95	657.16	657.12	656.87
50.0	656.77	657.01	657.00	656.79

TABLE 8: MARSH LAKE MONTHLY AEP WATER LEVELS

Annual Exceedance Probability (%)	AEP Water Level (m)			
	July	August	September	October
0.2	658.35	658.37	658.39	657.43
0.3	658.18	658.21	658.27	657.35
0.5	658.04	658.09	658.18	657.28
1.0	657.81	657.89	658.01	657.17
2.0	657.57	657.68	657.85	657.06
5.0	657.26	657.40	657.62	656.92
10.0	657.01	657.18	657.45	656.80
20.0	656.76	656.96	657.28	656.68
33.3	656.56	656.78	657.13	656.59
50.0	656.38	656.62	657.01	656.50

TABLE 9: LAKE LABERGE MONTHLY AEP WATER LEVELS

Annual Exceedance Probability (%)	AEP Water Level (m)			
	July	August	September	October
0.2	628.72	628.50	628.32	628.52
0.3	628.53	628.34	628.17	628.31
0.5	628.38	628.21	628.05	628.14
1.0	628.12	628.00	627.84	627.86
2.0	627.86	627.78	627.64	627.57
5.0	627.51	627.49	627.36	627.18
10.0	627.25	627.26	627.15	626.88
20.0	626.97	627.03	626.93	626.57
33.3	626.75	626.84	626.76	626.32
50.0	626.55	626.67	626.60	626.10

The difference in monthly AEP water levels between Tagish Lake and Bennett Lake is generally consistent with the differences noted for the annual AEP levels. In July to October, the 0.5% period water levels on Tagish Lake range from 0.23 m higher in July to 0.15 m lower in October than those on Bennett Lake. Similar to the analysis for the annual frequency curves, some discrepancy in the frequency water levels would be expected due to differences in the period of record available for each gauge. However, as previously noted, it is suspected that there is an issue with the datum of the gauges due to crustal rebound affecting the geoid used in the CGVD2013 vertical datum. Given the uncertainty in the cause of the discrepancy between the Bennett Lake and Tagish Lake WSC gauges, the AEP water levels on Tagish Lake were conservatively adopted to define static lake levels on Bennett Lake.

The timing of the historical annual peak water levels was used to define the probability that a flood would occur in any given month. These probabilities were calculated for Bennett Lake, Nares Lake and Tagish Lake, Marsh Lake, and Lake Laberge based on the hydrometric records on each lake, with the likelihood of a flood occurring in any given month being defined by the number of peak water levels occurred during that month relative to the total number of flood events within the historical record. The probabilities of floods occurring between July and October are summarized for each lake in Table 10.

TABLE 10: FLOOD TIMING PROBABILITIES

Month	Bennett Lake	Tagish Lake	Marsh Lake	Lake Laberge
July	6%	4%	5%	15%
August	59%	56%	50%	55%
September	27%	28%	23%	30%
October	9%	12%	21%	0%

5.3 Monthly Wind Speed Frequency Analysis

Frequency analyses were completed on the monthly peak hourly wind speed data for the Environment and Climate Change Canada (ECCC) stations 2100200 (i.e. Carcross) and 2101300 / 2101303 (i.e. Whitehorse A), as well as data from the Yukon Wildland Fire Weather Data Portal for Mount Sima and Jake's Corner. The historical meteorological data used for the frequency analyses is summarized in Table 11, while the locations of the meteorological stations are shown in orange relative to the study area on Figure 28.

TABLE 11: METEOROLOGICAL STATIONS USED FOR FREQUENCY ANALYSIS

Station Number	Station Name	Period of Record	Number of Years Used in Analysis
15	Carcross	2005 - 2022	16
2101300 / 2101303	Whitehorse A	1953 - 2022	69
22	Jake's Corner	2005 - 2022	16
50	Mount Sima	2004 - 2022	17

FIGURE 28: SOUTHERN LAKES CLIMATE STATIONS

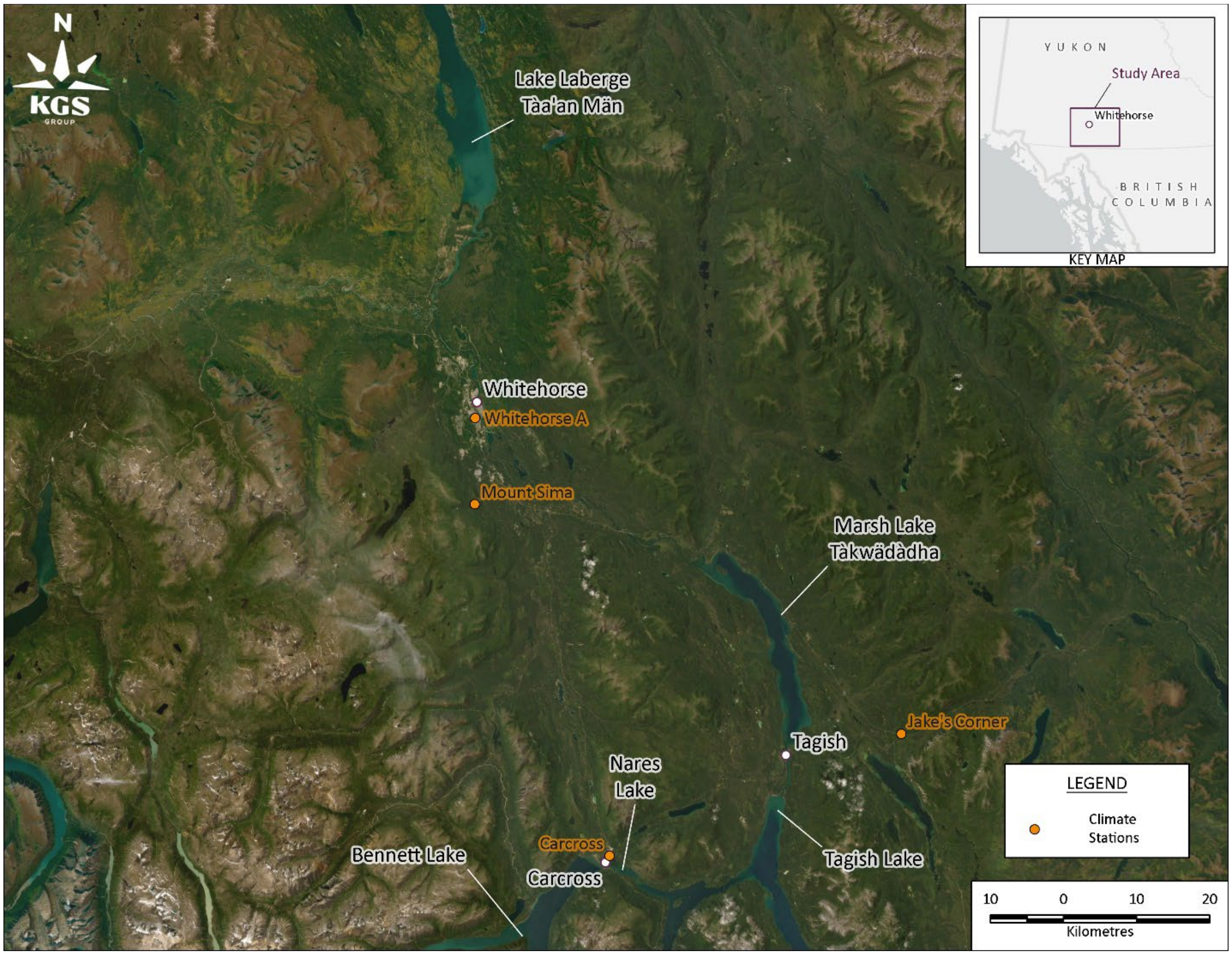

Monthly peak hourly wind speeds were extracted from the historical wind speed records for each year in each of the North, Northeast, East, Southeast, South, Southwest, West and Northwest Directions during the flood season (i.e. July to October). Frequency distributions were then fit to the monthly and directional peak hourly wind speed datasets following the same methodology as described in Section 5.2.1. A Generalized Extreme Value (GEV) distribution was found to best represent the daily peak hourly wind speed data for each month and wind direction. The resulting monthly and directional AEP hourly wind speeds are summarized in Table 12 to Table 15, with the frequency curves included in Appendix C for reference.

TABLE 12: MONTHLY AND DIRECTIONAL AEP HOURLY WIND SPEEDS AT CARCROSS

Month	AEP (%)	AEP Wind Speed (km) For Given Direction							
		N	NE	E	SE	S	SW	W	NW
July	0.2	25.9	24.9	28.4	36.6	28.8	25.6	25.4	25.0
	0.3	25.9	24.9	28.2	34.9	28.6	25.4	25.3	24.9
	0.5	25.8	24.9	28.0	33.6	28.4	25.3	25.2	24.9
	0.1	25.6	24.8	27.6	31.4	27.9	25.0	25.1	24.7
	2.0	25.3	24.8	27.0	29.2	27.4	24.6	24.8	24.5
	5.0	24.8	24.5	25.8	26.2	26.2	23.9	24.4	24.1
	10.0	24.1	24.2	24.5	24.0	25.0	23.1	24.0	23.6
	20.0	23.1	23.4	22.5	21.6	23.2	22.1	23.3	22.7
	33.0	21.9	22.3	20.4	19.8	21.2	21.0	22.7	21.8
	50.0	20.5	20.6	17.9	18.1	19.0	19.9	21.9	20.6
August	0.2	31.5	23.1	27.2	25.2	27.8	34.1	41.7	55.2
	0.3	31.1	22.9	27.1	25.0	27.6	33.3	38.7	48.9
	0.5	30.8	22.8	26.9	24.9	27.4	32.7	36.6	44.6
	0.1	30.0	22.4	26.5	24.5	26.9	31.5	33.4	38.4
	2.0	29.1	22.0	25.9	24.0	26.3	30.1	30.5	33.4
	5.0	27.6	21.0	24.7	23.1	25.2	28.1	27.2	28.2
	10.0	26.1	20.0	23.4	22.2	24.0	26.3	25.1	25.1
	20.0	24.1	18.5	21.5	21.0	22.2	24.3	23.2	22.6
	33.0	22.1	16.9	19.3	19.8	20.3	22.5	21.8	20.9
	50.0	20.0	15.0	16.8	18.4	18.2	20.8	20.7	19.7
September	0.2	37.2	27.8	31.5	27.4	27.0	32.3	27.0	34.1
	0.3	36.4	27.3	30.9	27.3	26.9	31.6	26.9	33.5
	0.5	35.6	26.9	30.4	27.1	26.8	31.0	26.8	33.0
	0.1	34.2	26.2	29.4	26.7	26.5	29.9	26.6	32.0
	2.0	32.6	25.2	28.2	26.2	26.2	28.6	26.3	30.9
	5.0	30.1	23.6	26.3	25.3	25.5	26.6	25.7	29.1
	10.0	27.9	22.1	24.5	24.3	24.6	24.9	25.0	27.5
	20.0	25.2	20.1	22.2	22.9	23.2	22.8	23.9	25.5
	33.0	22.8	18.3	20.0	21.5	21.6	20.9	22.8	23.8
	50.0	20.4	16.3	17.8	19.9	19.6	19.0	21.4	22.0
October	0.2	33.7	38.6	33.4	31.8	30.8	35.1	32.5	37.1
	0.3	33.2	37.3	33.0	31.6	30.4	34.8	32.2	36.7
	0.5	32.8	36.2	32.6	31.4	30.1	34.4	31.9	36.3
	0.1	31.9	34.1	31.8	30.9	29.5	33.6	31.3	35.5
	2.0	30.9	32.0	30.8	30.4	28.7	32.7	30.4	34.5
	5.0	29.1	28.8	29.0	29.2	27.3	30.9	29.0	32.7
	10.0	27.4	26.1	27.2	28.0	25.9	29.2	27.6	30.9
	20.0	25.2	23.1	24.8	26.2	24.0	26.7	25.7	28.5
	33.0	23.0	20.5	22.4	24.3	22.1	24.3	23.7	26.1
	50.0	20.8	18.0	19.8	22.2	20.1	21.6	21.6	23.5

TABLE 13: MONTHLY AND DIRECTIONAL AEP HOURLY WIND SPEEDS AT WHITEHORSE A

Month	AEP (%)	AEP Wind Speed (km) For Given Direction							
		N	NE	E	SE	S	SW	W	NW
July	0.2	45.6	43.9	56.2	43.7	49.2	43.2	35.0	42.1
	0.3	44.0	40.9	52.2	43.2	48.3	42.7	34.7	40.9
	0.5	42.7	38.5	49.1	42.7	47.6	42.3	34.4	39.9
	0.1	40.4	34.5	44.0	41.8	46.1	41.3	33.8	38.1
	2.0	37.9	30.6	39.1	40.7	44.5	40.2	33.0	36.0
	5.0	34.5	25.6	32.7	38.9	41.9	38.2	31.5	32.8
	10.0	31.6	21.9	28.0	37.2	39.7	36.1	29.9	30.0
	20.0	28.5	18.1	23.4	35.1	37.0	33.5	27.8	26.8
	33.0	25.8	15.2	19.8	33.1	34.6	30.9	25.6	23.9
	50.0	23.3	12.6	16.6	31.1	32.3	28.0	23.1	21.0
August	0.2	42.5	41.1	81.8	49.6	55.5	44.2	39.4	37.4
	0.3	41.4	37.7	72.4	48.7	54.5	44.0	38.7	37.0
	0.5	40.5	35.1	65.5	48.0	53.6	43.7	38.1	36.5
	0.1	38.7	30.9	54.9	46.6	51.9	43.1	36.8	35.5
	2.0	36.8	27.0	45.6	45.0	49.9	42.3	35.3	34.3
	5.0	33.9	22.0	35.0	42.4	46.8	40.7	32.8	32.2
	10.0	31.3	18.5	28.0	40.2	44.0	38.8	30.4	30.0
	20.0	28.3	15.0	21.7	37.4	40.6	36.1	27.4	27.2
	33.0	25.6	12.4	17.3	35.0	37.5	33.2	24.5	24.3
	50.0	23.0	10.1	13.8	32.5	34.3	29.7	21.5	21.1
September	0.2	56.6	25.1	65.9	51.7	73.1	47.6	51.6	36.6
	0.3	53.5	23.8	60.7	50.8	70.0	47.2	49.5	36.0
	0.5	51.0	22.8	56.6	50.1	67.6	46.7	47.7	35.5
	0.1	46.8	21.0	49.8	48.7	63.5	45.8	44.4	34.4
	2.0	42.5	19.1	43.1	47.1	59.4	44.5	41.0	33.0
	5.0	36.8	16.5	34.6	44.7	53.9	42.2	36.0	30.7
	10.0	32.4	14.4	28.2	42.6	49.7	39.8	31.9	28.4
	20.0	27.7	12.2	21.8	40.1	45.2	36.4	27.3	25.4
	33.0	24.0	10.3	16.8	37.8	41.7	32.9	23.5	22.5
	50.0	20.6	8.6	12.4	35.6	38.6	29.0	19.8	19.4
October	0.2	38.1	35.3	60.8	57.4	58.8	52.4	44.5	47.0
	0.3	38.0	32.5	57.1	56.5	58.3	50.9	42.9	45.5
	0.5	37.8	30.3	54.0	55.8	57.7	49.5	41.5	44.2
	0.1	37.5	26.7	48.7	54.3	56.7	47.0	38.9	41.7
	2.0	37.0	23.2	43.3	52.6	55.4	44.2	36.0	39.0
	5.0	35.8	18.7	35.8	49.8	53.1	39.9	31.8	34.9
	10.0	34.4	15.5	29.9	47.3	50.9	36.3	28.2	31.3
	20.0	32.1	12.2	23.6	44.2	48.1	32.0	24.0	27.2
	33.0	29.4	9.7	18.5	41.4	45.3	28.2	20.4	23.6
	50.0	26.0	7.6	13.8	38.5	42.3	24.5	16.8	20.0

TABLE 14: MONTHLY AND DIRECTIONAL AEP HOURLY WIND SPEEDS AT JAKE'S CORNER

Month	AEP (%)	AEP Wind Speed (km) For Given Direction							
		N	NE	E	SE	S	SW	W	NW
July	0.2	28.7	19.2	15.8	20.5	35.9	24.7	33.9	26.3
	0.3	27.1	18.1	15.6	20.0	34.0	24.5	31.5	25.7
	0.5	25.9	17.3	15.4	19.7	32.6	24.3	29.7	25.2
	0.1	23.9	15.9	15.1	18.9	30.3	23.9	26.9	24.3
	2.0	22.0	14.6	14.6	18.1	28.2	23.4	24.4	23.3
	5.0	19.5	13.0	13.7	16.7	25.7	22.5	21.5	21.8
	10.0	17.7	11.8	12.9	15.5	24.0	21.5	19.5	20.5
	20.0	15.9	10.6	11.6	14.1	22.4	20.2	17.7	19.1
	33.0	14.5	9.7	10.4	12.8	21.1	18.8	16.4	17.8
	50.0	13.3	9.0	9.0	11.5	20.1	17.4	15.4	16.6
August	0.2	33.5	14.0	17.5	25.6	39.2	21.6	21.4	22.5
	0.3	30.4	13.9	16.8	24.9	37.4	21.5	21.0	22.4
	0.5	28.1	13.7	16.3	24.3	36.0	21.4	20.7	22.2
	0.1	24.7	13.5	15.4	23.2	33.6	21.2	20.2	21.9
	2.0	21.7	13.1	14.4	22.0	31.4	20.9	19.5	21.5
	5.0	18.4	12.5	12.9	20.1	28.4	20.4	18.6	20.7
	10.0	16.3	11.8	11.7	18.3	26.3	19.7	17.7	19.8
	20.0	14.3	10.9	10.3	16.3	24.1	18.8	16.6	18.6
	33.0	13.0	9.9	9.1	14.4	22.4	17.7	15.7	17.4
	50.0	12.0	8.8	7.9	12.5	20.9	16.5	14.7	16.0
September	0.2	66.5	19.7	26.5	25.0	27.9	30.2	28.0	28.8
	0.3	56.7	18.8	25.7	24.9	27.9	29.5	26.3	28.1
	0.5	50.0	18.1	25.0	24.7	27.8	28.9	25.0	27.5
	0.1	40.5	16.9	23.7	24.4	27.7	27.8	23.0	26.3
	2.0	32.9	15.7	22.3	24.0	27.5	26.5	21.1	25.1
	5.0	25.1	14.2	20.1	23.1	27.0	24.5	18.8	23.2
	10.0	20.6	13.0	18.3	22.2	26.6	22.7	17.2	21.5
	20.0	16.8	11.8	16.1	20.8	25.8	20.6	15.7	19.5
	33.0	14.5	10.8	14.2	19.3	24.9	18.6	14.5	17.8
	50.0	12.7	10.0	12.3	17.5	23.8	16.7	13.6	16.1
October	0.2	25.4	20.7	26.5	32.7	32.4	24.4	36.2	26.1
	0.3	23.3	20.0	26.1	32.3	32.3	24.2	33.8	25.7
	0.5	21.8	19.4	25.7	32.0	32.2	24.0	31.9	25.3
	0.1	19.4	18.3	24.9	31.3	31.9	23.5	28.9	24.5
	2.0	17.4	17.1	24.0	30.4	31.4	22.9	26.0	23.6
	5.0	15.1	15.5	22.5	28.7	30.6	21.7	22.4	22.0
	10.0	13.6	14.1	21.0	27.0	29.5	20.5	19.8	20.5
	20.0	12.2	12.6	19.1	24.6	27.9	18.8	17.3	18.6
	33.0	11.3	11.4	17.3	22.1	26.0	16.9	15.4	16.8
	50.0	10.6	10.2	15.4	19.3	23.7	14.9	13.7	15.0

TABLE 15: MONTHLY AND DIRECTIONAL AEP HOURLY WIND SPEEDS AT MOUNT SIMA

Month	AEP (%)	AEP Wind Speed (km) For Given Direction							
		N	NE	E	SE	S	SW	W	NW
July	0.2	47.4	27.5	28.5	40.1	29.3	48.0	39.3	32.4
	0.3	43.4	25.8	27.7	38.5	28.8	47.0	39.1	31.7
	0.5	40.3	24.5	27.0	37.2	28.4	46.1	38.8	31.1
	0.1	35.3	22.3	25.8	34.9	27.5	44.3	38.3	29.9
	2.0	30.6	20.1	24.4	32.6	26.5	42.3	37.7	28.5
	5.0	24.9	17.2	22.3	29.3	24.7	39.2	36.6	26.2
	10.0	20.8	15.0	20.5	26.6	23.0	36.3	35.6	24.1
	20.0	16.9	12.7	18.3	23.8	20.8	32.8	34.2	21.6
	33.0	14.0	10.9	16.3	21.5	18.7	29.7	32.8	19.2
	50.0	11.5	9.2	14.4	19.3	16.5	26.5	31.4	16.8
August	0.2	57.5	19.5	24.5	30.7	28.5	48.6	64.8	29.0
	0.3	51.9	19.0	24.0	30.2	28.1	47.5	61.5	28.9
	0.5	47.8	18.5	23.6	29.7	27.8	46.6	58.9	28.8
	0.1	41.2	17.7	22.7	28.7	27.1	44.8	54.5	28.5
	2.0	35.1	16.7	21.8	27.6	26.3	42.7	50.4	28.1
	5.0	27.8	15.1	20.3	25.9	24.8	39.3	45.1	27.2
	10.0	22.7	13.6	18.9	24.2	23.3	36.2	41.3	26.2
	20.0	17.9	11.9	17.2	22.2	21.4	32.3	37.4	24.4
	33.0	14.3	10.3	15.6	20.3	19.5	28.7	34.5	22.4
	50.0	11.4	8.8	14.1	18.4	17.4	25.0	31.9	19.9
September	0.2	43.7	14.5	29.8	46.6	30.1	64.0	71.0	38.2
	0.3	40.9	14.2	28.4	45.1	29.8	61.8	68.7	37.5
	0.5	38.6	13.9	27.3	43.8	29.6	60.0	66.8	36.9
	0.1	34.7	13.4	25.5	41.4	29.1	56.6	63.5	35.6
	2.0	30.8	12.7	23.6	38.8	28.4	52.9	59.8	34.1
	5.0	25.6	11.7	21.1	35.0	27.1	47.5	54.4	31.4
	10.0	21.5	10.7	19.1	31.8	25.6	42.9	49.9	28.8
	20.0	17.2	9.6	17.1	28.2	23.5	37.6	44.9	25.3
	33.0	13.8	8.5	15.5	25.1	21.3	33.1	40.5	22.0
	50.0	10.7	7.4	14.0	22.1	18.8	28.7	36.4	18.5
October	0.2	75.3	18.7	31.9	73.8	43.9	93.6	51.3	37.2
	0.3	63.1	17.8	30.8	67.0	41.1	87.3	51.2	36.2
	0.5	54.8	17.0	29.8	62.0	38.9	82.3	51.1	35.3
	0.1	42.8	15.7	28.1	54.1	35.4	74.1	50.9	33.6
	2.0	33.3	14.3	26.3	46.9	32.0	66.0	50.5	31.7
	5.0	23.6	12.5	23.6	38.5	27.6	55.6	49.5	28.8
	10.0	17.9	11.0	21.3	32.8	24.4	47.9	48.1	26.1
	20.0	13.2	9.3	18.7	27.5	21.3	40.0	45.6	23.0
	33.0	10.2	8.0	16.4	23.6	18.8	34.0	42.3	20.2
	50.0	8.0	6.8	14.3	20.5	16.8	28.7	37.7	17.3

5.4 Monthly Wind Direction

Monthly wind direction probability plots were developed for ECCC stations 2100200 (i.e. Carcross) and 2101300 / 2101303 (i.e. Whitehorse A), as well as data from the Yukon Wildland Fire Weather Data Portal for Mount Sima and Jake's Corner. These probability plots were developed based on the available hourly wind direction data from those stations during the flood season (i.e. July to October) to understand the nature of prevailing winds in the study area. The resulting monthly wind direction probability plots for each weather station are represented schematically on Figure 29 to Figure 32.

FIGURE 29: MONTHLY WIND DIRECTIONS AT CARCROSS

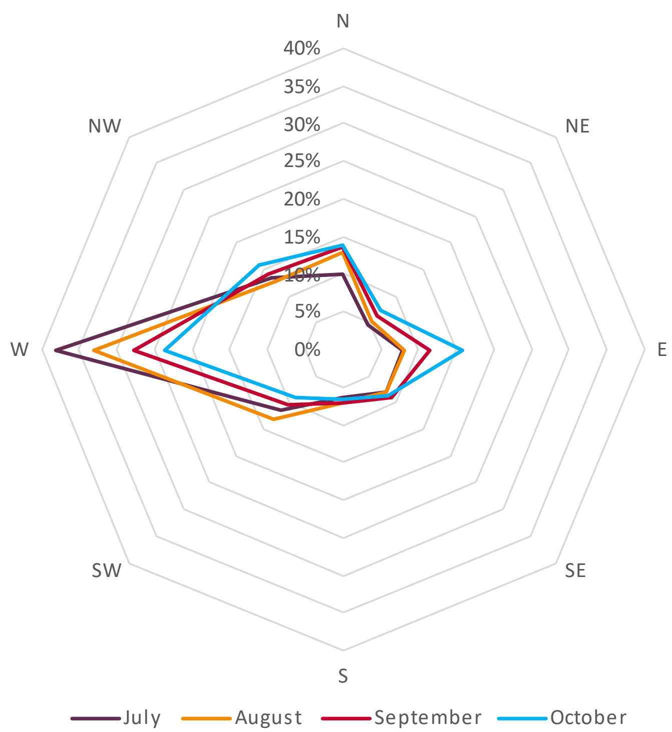

FIGURE 30: MONTHLY WIND DIRECTIONS AT WHITEHORSE A

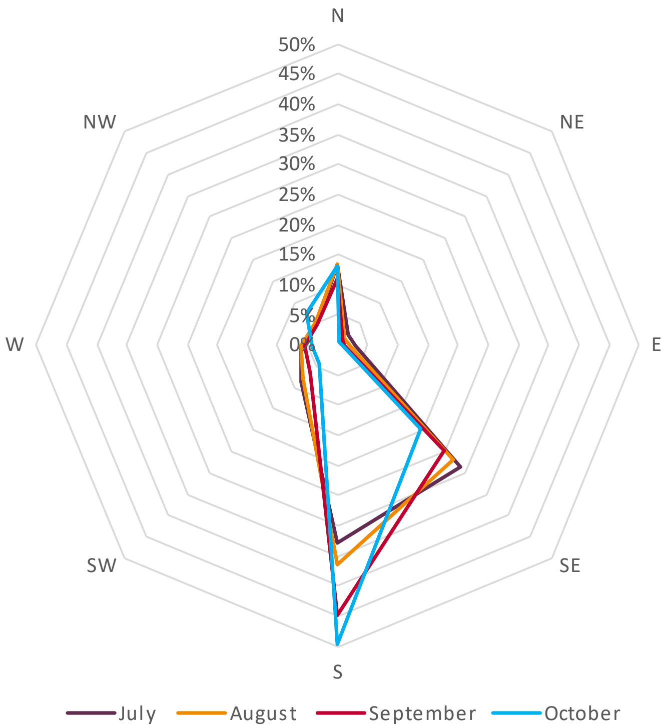

FIGURE 31: MONTHLY WIND DIRECTIONS AT JAKE'S CORNER

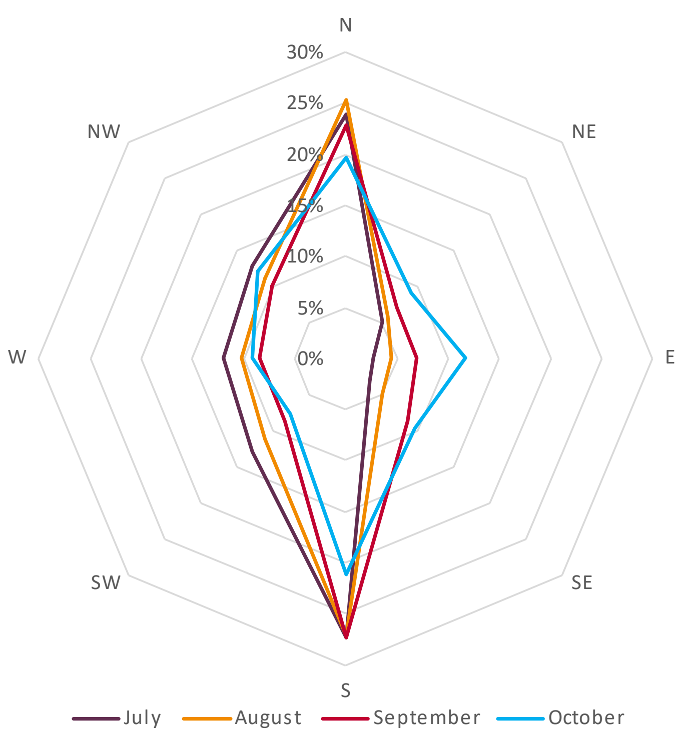

FIGURE 32: MONTHLY WIND DIRECTIONS AT MOUNT SIMA

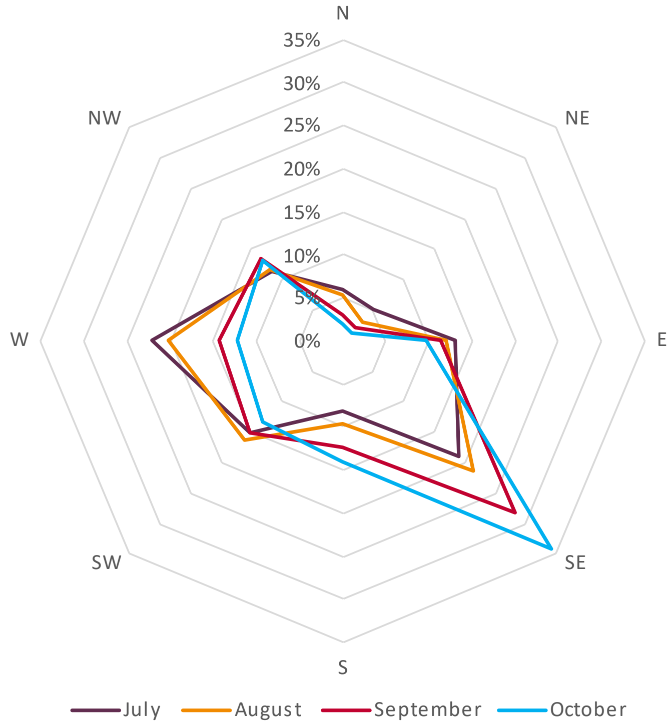

5.5 Joint Probability Analysis

A review of the potential statistical interdependence between static water level and wind setup and wave runup was completed, in accordance with the requirements of the project Terms of Reference. To evaluate the potential relationship between static lake levels, which occur during the spring season, and wave setup, which can occur at any time during the open water season, relationships between the highest monthly observations of wind speed and water levels on each lake were reviewed to determine if there are any seasonal trends that affect either wind speed or wind direction.

Table 16 summarizes the WSC gauging and ECCC climate stations used for this analysis. Each month in the open water season (i.e. April to October) was considered in this analysis. Months with fewer than 70% of daily observations were removed.

TABLE 16: WSC AND CLIMATE STATIONS CONSIDERED IN THE JOINT PROBABILITY ANALYSIS

Lake	WSC Station	Climate Station
Bennett Lake	09AA004 (1947-2022)	Carcross (2006-2022)
Tagish Lake	09AA017 (1995-2022)	Carcross (2006-2022)
Marsh Lake	09AB004 (1950-2022)	Jake's Corner (2006-2022)
Lake Laberge	09AB010 (1981-2022)	Whitehorse A (2101300) (1981-2012) Whitehorse A (2101303) (2013-2022)

For each daily water level, the maximum wind speed on that date was determined from sub-daily wind speed data. The average wind direction at the maximum wind speed on that date was also determined. Four subsets of water level, wind speed, and wind direction data were assessed on a monthly basis for the open water season, including:

- Water levels equal to or greater than the 10th percentile water level for each year in a given month.
- Water levels equal to the maximum water level for each year in a given month.
- Wind speeds equal to or greater than the 10th percentile wind speed for each year in a given month.
- Wind speed equal to the maximum wind speed for each year in a given month.

Within each subset, the Pearson correlation coefficient was determined using the *stat_cor* function of the *ggpubr* package in R (Kassambara, 2023).

In general, most correlations had a p-value greater than 0.05 and the R^2 values were generally low, indicating statistical independence of the two variables. This is consistent with expectations, as the physical processes that drive wind speed and lake levels are fundamentally different.

Figures showing the correlations between water level, wind speed, and wind direction data for each subset of data for each lake are provided in Appendix D. Based on discussions with representatives from YG, ECCC, and NRCan, and given that flood levels on the lakes are sustained for long durations, it was agreed that a range of wind setup and wave runup conditions should be evaluated for the static lake level.

6.0 MONTE CARLO ANALYSIS OF FLOOD LEVELS

6.1 Overview

To evaluate flood levels on Bennett Lake, Tagish Lake, Marsh Lake, and Lake Laberge, a Monte Carlo statistical modelling approach was implemented to evaluate the combination of high water level and wind / wave events. Monte Carlo modelling relies on the repeated random simulation of statistical events, and for this study was used to generate large, artificial records of flood events on the Southern Lakes.

A Monte Carlo model was developed in Microsoft Excel to evaluate the combined flood levels associated with static peak water levels, wind setup and wave runup at multiple locations on each of the lakes. While Microsoft Excel has limitations on the complexity of processes that can be modelled, potential for high computational demands, and uses a pseudo-random approach to random number generation, these limitations were not anticipated to impact the results of the analyses, and ultimately Microsoft Excel was found to be well suited to the modelling methods that were implemented for the estimation of flood levels and wind / wave processes.

A Monte Carlo approach was determined to be the most suitable methodology to evaluate the combined influence of statistically independent water level and wind events. The Monte Carlo model developed for this project produced a synthetic record of maximum water levels caused by a combination of static flood levels and wind effects, from which probabilities of combined events can be estimated. This approach provides a more realistic estimate of the combined probabilities than strictly adding together AEP water levels, wind setup, and wave runup, which would significantly overstate the flood risk for a given AEP.

The Monte Carlo analysis has been configured to simulate a large number of flood events, with key parameters for each event randomly sampled from representative statistical distributions for those parameters. The number of flood events considered in the model (i.e. 5,000 flood events) was selected as a sufficiently large number of simulated flood events to reliably predict the 0.5% AEP flood event, as the analysis would expect to yield approximately twenty five 0.5% AEP flood events, each consisting of different combinations of flood levels and wind effects.

Randomly selected parameters are used in the model to calculate wind setup, wave runup, and stable (i.e. combined static lake level and setup) and dynamic (i.e. combined static lake level, setup, and wave runup) total water levels. Percentile water levels corresponding to AEPs of interest are then calculated for the resulting set of stable and dynamic water levels. Conventionally, frequency analyses are completed on the results of the Monte Carlo analysis to define water levels at AEPs of interest. The use of calculated percentiles was implemented as a simplifying assumption, but through testing was found to define flood levels at a comparable level of accuracy to those defined via frequency analyses.

For this model, the key parameters that were randomly defined included:

- The month during which a flood will occur;
- Static lake levels;
- Wind speeds.

It should be noted that for each static lake level, unique wind speeds are evaluated for each of the wind directions considered for wind setup and wave runup calculations (i.e. North, Northeast, East, Southeast, South, Southwest, West, and Northwest). In reality, and as demonstrated in Section 5.4, there are prevailing winds during the open water season. However, the nature of the prevailing winds is implicitly accounted for in the monthly peak hourly wind frequency curves that have been developed on a direction basis, as previously described in Section 5.3, as there would be fewer data points available to develop those frequency curves for infrequent wind directions. Simulating wind events in each direction for each static lake level accounts for the fact that a wind event could occur in each direction during the sustained flood levels on Bennett Lake, Nares Lake, Tagish Lake, Marsh Lake, and Lake Laberge.

The methodology for defining the above randomized parameters, as well as how they are used in the Monte Carlo model, are summarized in the following sections of this report.

6.2 Monte Carlo Model Methodology

To calculate stable (i.e. combined static water level and wind setup) and dynamic (i.e. combined static water level, wind setup, and wave runup) flood levels, a number of steps are completed in the Monte Carlo model, as described at a high-level below and as shown on Figure 33. Most of these steps are repeated for the 5,000 simulated flood events, and unless otherwise stated, each step outlined below can be assumed to be completed for each simulated flood event (i.e. 5,000 times). The steps of the Monte Carlo model include:

- ***Step 1: Definition of Random Numbers*** – This step initializes the random numbers that are to be used to define each of the model parameters.
- ***Step 2***: ***Definition of the Flood Month*** – This step defines the month during which the flood will occur based on the historical probability of flood timing.
- ***Step 3***: ***Definition of the Static Lake Level*** – This step defines the static lake level based on the frequency curve corresponding to the randomly selected month.
- ***Step 4***: ***Definition of Wind Speeds (x8)*** – This step defines the wind speed based on the randomly selected month. One unique wind speed is generated for each wind direction evaluated for wind setup and wave runup. It should be noted that the eight sets of randomly selected wind speeds are defined for each static lake level to account for the likely occurrence of a wind event from all directions during the sustained flooding on Bennett Lake, Nares Lake, Tagish Lake, Marsh Lake, and Lake Laberge.
- ***Step 5***: ***Calculation of Wind Setup and Wave Runup (x8)*** – This step calculates wind setup and wave runup for the randomly selected static lake level and each unique set of wind speeds for each direction. Wind setup and wave runup are calculated using the Shore Protection Manual (SPM) (USACE, 1984) and Coastal Engineering Manual (CEM) (USACE, 2001) methods.
- ***Step 6***: ***Calculation of Maximum Wave Runup and Wind Setup*** – This step calculates the maximum wind setup, and the maximum combined wind setup and wave runup for the CEM and SPM methods based on the eight unique sets of wind speeds for each direction.
- ***Step 7***: ***Calculation of the Stable and Dynamic Water Level*** – This step combines the maximum wind setup with the static lake level to define the stable water level, and combines the maximum combined wind setup and wave runup with the static lake level to define the dynamic water level.

- ***Step 8: Calculation of the AEP Stable and Dynamic Water Levels*** – This step calculates AEP stable water levels and AEP dynamic water levels for the SPM and CEM methods from the sets of stable and dynamic water levels by calculating the percentiles associated with each simulated flood event, and matching those percentiles to AEPs of interest. **This step only occurs once.** The contribution of wind setup and wave runup can then be back calculated from calculated AEP static lake levels and the AEP stable and dynamic water levels.

FIGURE 33: CONCEPTUAL REPRESENTATION OF THE MONTE CARLO MODEL

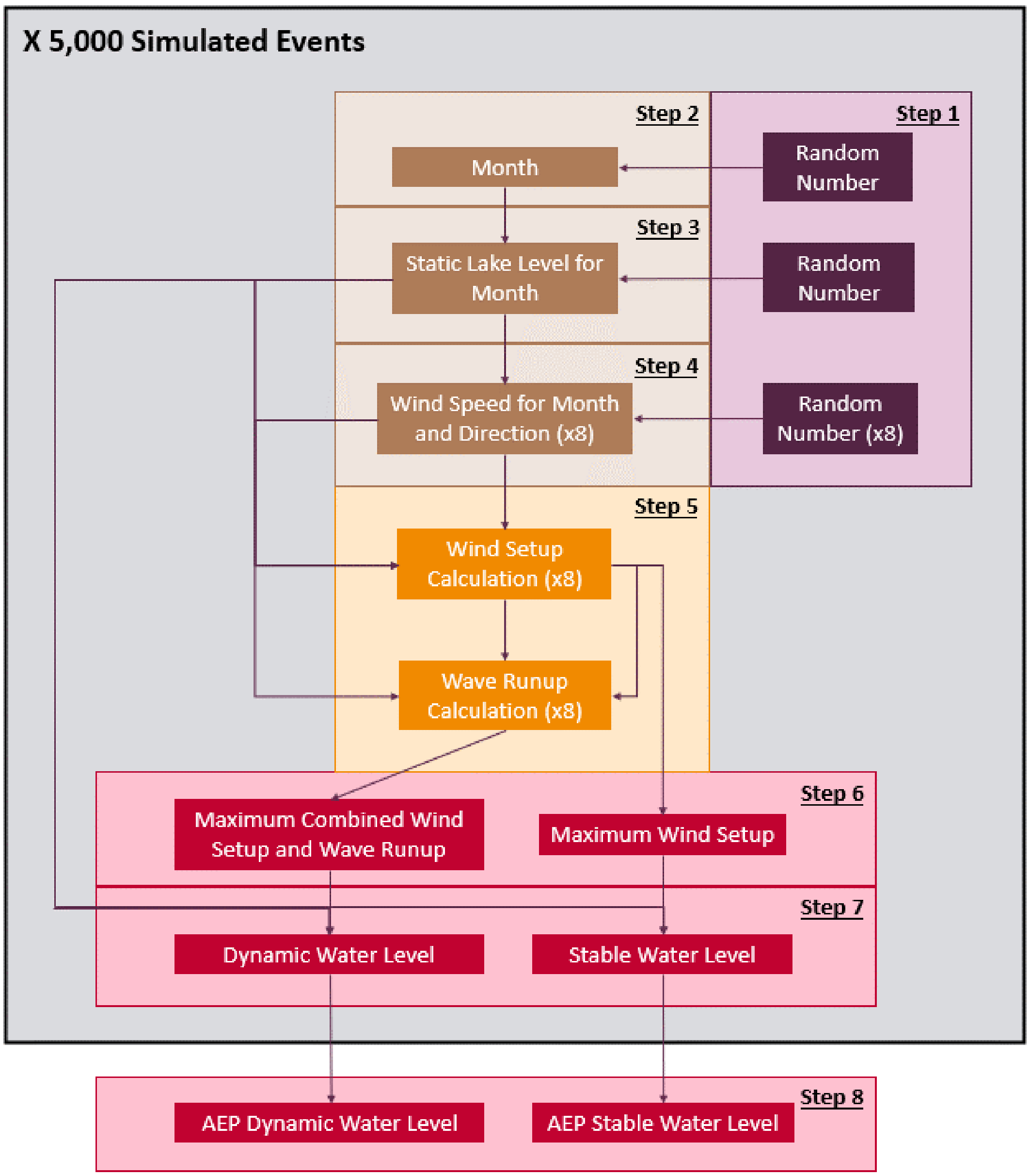

Each step of the Monte Carlo analysis is described in further detail in Section 6.2.1 to 6.2.8. An example calculation is carried out across these report sections for clarity. Within this section, specific examples of the variables and formulae included in the Monte Carlo model are referenced.

6.2.1 STEP 1 – RANDOM NUMBER GENERATION

Random numbers for each of the model parameters are defined using the Excel *rand* function, which generates random numbers using a uniform distribution between 0 and 1. A sample set of random numbers are summarized in Table 17 of an example of the process. It should be noted that the same random numbers were used for multiple analysis locations on each lake (ex. Marsh Lake), but new sets of random numbers were generated for each lake.

TABLE 17: SAMPLE RANDOM NUMBERS

Parameter	Random Number
Month	0.620
Lake Level	0.977
Wind Speed – N	0.036
Wind Speed – NE	0.241
Wind Speed – E	0.411
Wind Speed – SE	0.400
Wind Speed – S	0.060
Wind Speed – SW	0.591
Wind Speed – W	0.741
Wind Speed – NW	0.093

6.2.2 STEP 2 – DEFINITION OF THE FLOOD MONTH

The flood month is defined based on the random number defined for the ***Month*** variable, as well as the historical probability that a flood could occur in any month in the flood season, as described in Section 5.2.2. As an example, the random number assigned to the ***Month*** variable corresponds to 0.620. The random number is then input as a probability into the historical peak water level timing probability plot, with the month being defined by the intersection of the probability with the plot. The definition of the flood month is shown conceptually on Figure 34.

FIGURE 34: DETERMINATION OF FLOOD MONTH

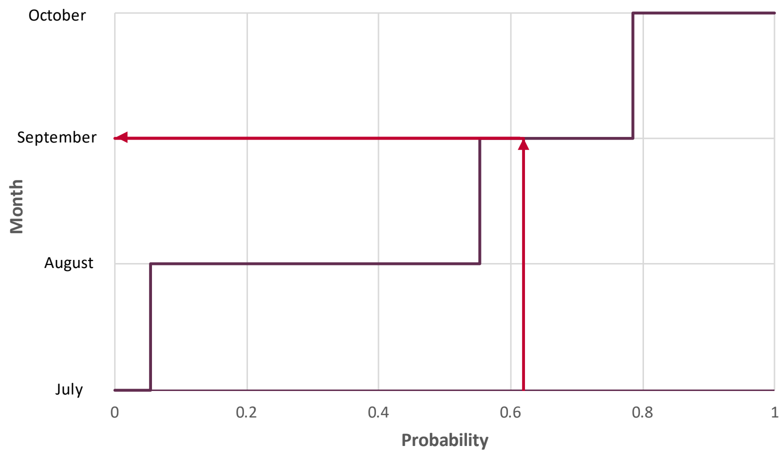

In this example calculation, the random value of 0.620 for ***Month*** results in the flood month being set to ***September.***

6.2.3 STEP 3 – DEFINITION OF THE STATIC LAKE LEVEL

The static water level is defined based on the random number defined for the ***Lake Level*** variable in the Monte Carlo model. In the sample calculation, this value corresponds to 0.977. The random number is then input as a non-exceedance probability into the inverse cumulative density function (CDF) of the static level frequency curve for the given flood month (i.e. ***September*** in the example calculation). The monthly static lake level frequency curve coefficients that represent the static lake level frequency curves, as previously described in Section 5.2.2, are used in the inverse CDF formula to calculate the static lake level given the random number (i.e. non-exceedance probability) defined for ***Lake Level*** variable.

It should be noted that defining the static lake levels using a frequency curve defined based on peak daily water levels may introduce some bias in the Monte Carlo model towards overall higher water levels. Given that floods are sustained for long durations under which a range of wind conditions could occur, a less conservative approach could consider defining the static lake levels using a frequency curve defined based on mean monthly water levels. In reality, wind events would likely occur at a flood level between that defined by the frequency curves based on peak daily and mean monthly water levels. KGS Group evaluated the sensitivity of the Monte Carlo analysis to using frequency curves defined based on either the peak daily water levels or mean monthly water levels. The comparison found that the 1% AEP flood levels estimated using both frequency curves were within 0.1 m of each other, with the water level defined by the peak daily frequency curve being higher. KGS Group thus defined static lake levels using the frequency that were curves defined based on the peak daily water levels, as this approach represents a minor conservative (i.e. biased to higher water levels) assumption.

The calculation of the static lake level is shown conceptually on Figure 35. It should be noted that the frequency curve represented on Figure 35 is merely a simplified representation of the frequency relationship. In reality, water levels would exceed the maximum water level shown on the y-axis as the non-exceedance probabilities asymptotically approach a value of 1.

FIGURE 35: CALCULATION OF STATIC LAKE LEVEL

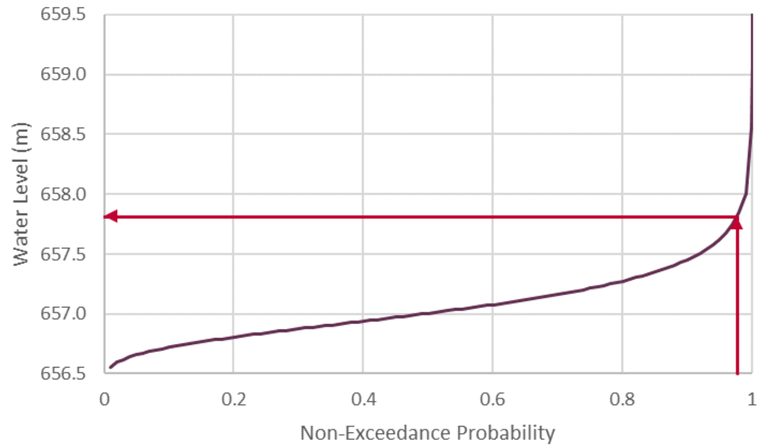

In this example calculation, the random value of 0.977 for the ***Water Level*** variable results in the static lake level being set to ***657.81 m*** based on the frequency curve equation associated with the ***September*** variable.

6.2.4 STEP 4 – DEFINITION OF THE WIND SPEED

As previously noted, eight sets of random numbers are generated to define one unique wind speed in each wind direction, corresponding to the ***Wind Speed N, Wind Speed NE, Wind Speed E, Wind Speed SE, Wind Speed S, Wind Speed SW, Wind Speed W,*** and ***Wind Speed NW*** variables. As an example, the value for the ***Wind Speed N*** variable corresponds to 0.036. The random number is then input as a non-exceedance probability into the inverse CDF equation for the wind speed frequency curve for the given flood month (i.e. ***September*** in the example calculation) and direction (i.e. ***N*** for ***Wind Speed N***) to generate the corresponding wind speed. The inverse CDF equation coefficients represent the monthly and directional wind speed frequency curves, as previously described in Section 5.3. The calculation of the wind speed is shown conceptually on Figure 36. It should be noted that the frequency curve represented on Figure 36 is merely a simplified representation of the frequency relationship. In reality, wind speeds could exceed the maximum wind speed shown on the y-axis as non-exceedance probabilities asymptotically approach a value of 1.

FIGURE 36: DEFINITION OF WIND SPEED

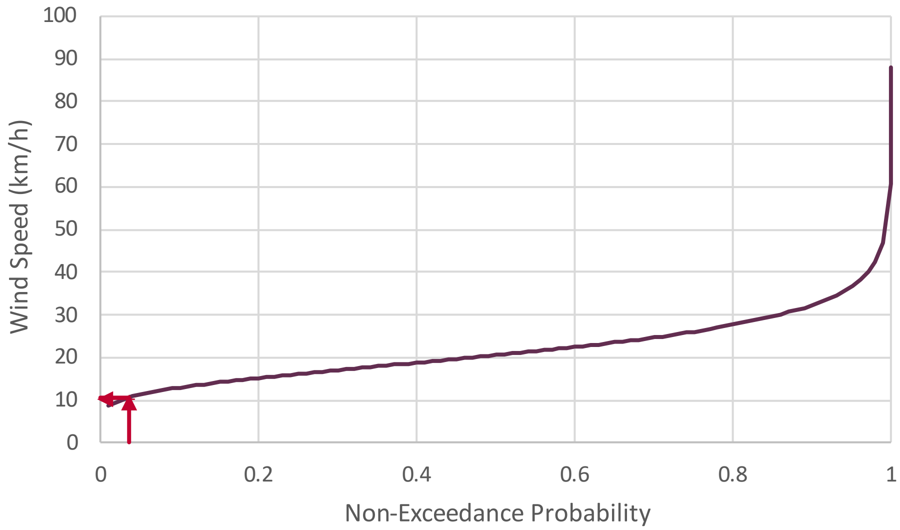

In this example calculation, the random value of 0.036 for the ***Wind Speed*** variable results in the wind speed being set to ***10.7 km/h*** based on the wind speed curve for the month of ***September*** and a wind direction of ***N.*** The wind speeds for all eight directions in the sample calculation are summarized in Table 18.

TABLE 18: DEFINITION OF WIND SPEED

Parameter	Random Number	Wind Direction	Wind Speed (km/h)
Wind Speed – N	0.036	N	10.7
Wind Speed – NE	0.241	NE	4.8
Wind Speed – E	0.411	E	11.6
Wind Speed – SE	0.400	SE	36.8
Wind Speed – S	0.060	S	31.9
Wind Speed – SW	0.591	SW	26.4
Wind Speed – W	0.741	W	22.2
Wind Speed – NW	0.093	NW	10.8

6.2.5 STEP 6 – CALCULATION OF THE WIND SETUP AND WAVE RUNUP

The methods that are used in the Monte Carlo model to calculate wind setup and wave runup are based on the widely accepted methodologies developed by the USACE as presented in the Shore Protection Manual (SPM) (1984) and the Coastal Engineering Manual (CEM) (2002). Further details of the wind setup and wave runup calculations using the SPM and CEM methods in the Monte Carlo analysis are provided in Section 6.3 to 6.5.

Wave runup and wind setup are calculated for each random static lake level and associated set of eight wind directions and wind speeds. Wind setup and wave runup are calculated given a number of key transect characteristics at a given transect location, including:

- Key elevations and slopes of the shoreline, as well as elevations and slopes associated with any berms along the transect,
- Reduction coefficients for CEM and SPM associated with surface roughness along the transect,
- The orientation of the transect in degrees from north,
- Correction factors to reduce wave runup depending on the angle of the approaching waves relative to the orientation of the shoreline. As noted in Kuiper (1965), wave runup calculations assume that waves are approaching perpendicular to the shoreline. However, if the waves are approaching the shoreline under an angle, the uprush becomes less. Kuiper (1965) recommends reducing the calculated wave runup with a factor equal to the sine of the angle between the shoreline and the direction of wave travel. This has been implemented in the wave runup calculation.
- The maximum fetch in each direction is available to generate wind setup, as well as the average elevation of the lake bottom over that fetch.
- The distance from the transect to the centroid of the lake, as well as the maximum distance from all transects to the centroid of the lake. For Marsh Lake and Lake Laberge, wind setup in any given direction is assumed to hinge about the centroid of the lake, with zero wind setup at the centroid. These parameters are used to linearly interpolate wind setup between the centroid (i.e. 0.0 m) and the maximum wind setup at the location with maximum fetch.
- Effective fetch lengths for wave calculations using the CEM and SPM methods. These are calculated based on radial length lines that were generated for each transect location.

Some simplifying assumptions have been made in the Monte Carlo model regarding wind setup and wave runup, and generally bias the model to slightly higher water levels. These assumptions include:

- For wind setup calculations, it was assumed that the wind speed defined in the model, which is sampled from a frequency curve of peak hourly wind levels, can be sustained sufficiently long to generate maximum setup. In reality, the wind would need to be sustained for up to 3 hours to generate maximum setup.
- The Monte Carlo model does not consider wind set-down (i.e. negative setup) for offshore winds. Instead, set-down is assumed to be 0.0 m for offshore winds.
- Lake outlets that convey flow downstream to another lake (i.e. Bennett Lake to Tagish Lake and Tagish Lake to Marsh Lake), conditions could occur where wind setup would result in raised water levels at the outlet of the upstream lake due to wind setup and lowered levels at the inlet to the downstream lake due to set-down. In reality, this would increase outflow from the upstream lake and could moderate the wind setup in the upstream lake. However, this outflow would need to be sustained over an extended period of time to affect the wind setup, and as such has been excluded from the Monte Carlo analysis.

Wind setup and wave runup heights are calculated given the static lake level and set of wind speeds and directions using the SPM and CEM methods. The wind setup and wave runup heights for the sample calculation are summarized in Table 19.

TABLE 19: CALCULATED WIND SETUP AND WAVE RUNUP

Calculation	Static Lake Level (m)	Wind Direction	Wind Speed (km/h)	SPM84		CEM	
				Setup (m)	Runup (m)	Setup (m)	Runup (m)
1	657.81	N	10.7	0.00	0.00	0.00	0.00
2	657.81	NE	4.8	0.00	0.00	0.00	0.00
3	657.81	E	11.6	0.00	0.06	0.00	0.05
4	657.81	SE	36.8	0.02	0.36	0.02	0.33
5	657.81	S	31.9	0.02	0.17	0.02	0.22
6	657.81	SW	26.4	0.02	0.00	0.02	0.00
7	657.81	W	22.2	0.00	0.00	0.00	0.00
8	657.81	NW	10.8	0.00	0.00	0.00	0.00

6.2.6 STEP 7 – CALCULATION OF MAXIMUM WAVE RUNUP AND WIND SETUP

The maximum wind setup and maximum combined wind setup and wave runup defined by the random wind speeds in each direction are calculated for each of the SPM and CEM methods. In the example calculation, the maximum SPM wind setup is **0.02 m**, while the maximum SPM combined wind setup and wave runup is **0.38 m**. The maximum CEM wind setup is **0.02 m,** and the maximum CEM combined wind setup and wave runup is **0.35 m.** The maximum wind setup is calculated separately from the combined maximum wind setup and wave runup, as there may be a different direction that generates the maximum wind setup than the wind direction that generates the maximum combined wind setup and wave runup.

6.2.7 STEP 8 – CALCULATION OF THE STABLE AND DYNAMIC WATER LEVELS

The stable water level is calculated by combining the calculated static lake level and the maximum wind setup, while the dynamic water level is calculated by combining the static lake level with the maximum combined wind setup, and wave runup. The stable water level in the example calculation is **657.84 m** using the SPM method, and **657.84 m** using the CEM method. The dynamic water level in the example calculation is **658.22 m** using the SPM method and **658.19 m** using the CEM method.

6.2.8 STEP 9 – CALCULATION OF THE AEP STABLE AND DYNAMIC WATER LEVELS

AEP water levels are calculated using Excel's *Percentile* function given the array of stable and dynamic water levels defined by the Monte Carlo model and the desired AEP, defined as a non-exceedance value. As previously noted, this represents a simplification relative to the conventional approach of completing frequency analyses on the sets of resulting water levels. However, testing has found that the impact on the estimated water levels associated with this assumption are negligible.

Water levels for the 5%, 1%, and 0.5% AEP floods are calculated for:

- The static water level.
- The stable water level (i.e. static lake level and maximum directional wind setup).

- The dynamic water level (i.e. static lake level and maximum directional combination of wind setup and wave runup).

The calculation of the above percentile water levels can be used to back-calculate the relative contribution of wind setup and wave runup to the stable and dynamic flood levels for the AEPs of interest.

The calculation of the 1% AEP dynamic water level using the CEM method is represented graphically based on the sample set of total water levels included in the sample model on Figure 37.

FIGURE 37: CALCULATION OF THE 1% AEP DYNAMIC WATER LEVEL

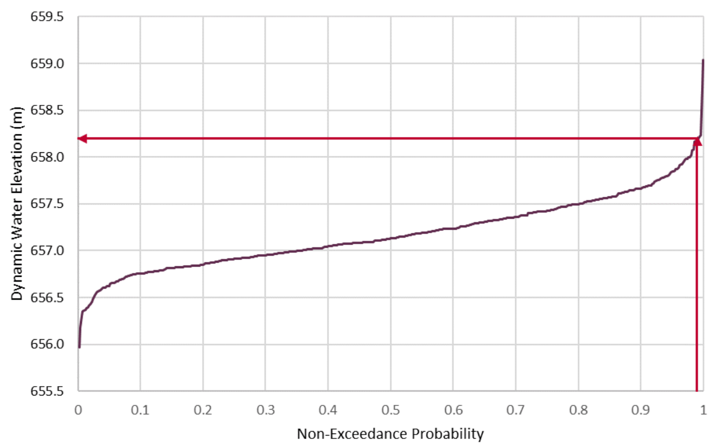

6.3 Definition of Wind Setup

When sustained winds pass over a water surface, a horizontal friction force is exerted on the water. These forces drive the water in the direction of the wind, which results in a "piling up" of the water at the downward end of a water body, and a corresponding lowering of the water level at the upwind end. This total effect is called wind tide, while the "piling up" at the downwind end is referred to as wind set-up.

Wind setup can be calculated according to the classical Zuider Zee equation (USACE, 1984):

$$S = 1.6 \times 10^{-5} \frac{{U_w}^2 F_s}{d} \qquad 1$$

where:

S = wind setup above still water level (m)
U_w = overwater wind velocity (km/hr)
F_s = direct fetch length (km)
d = average depth of the lake over the fetch distance (m)

Overwater wind velocities are almost always greater than the overland wind velocities measured at nearby, land-based climate stations. This is known as the *wind over water effect* and is due to the topographical relief over a lake. The overland to overwater wind speed corrections recommended in the SPM and CEM were applied to the land-based wind data described in Sections 5.3 and 5.4.

The direct fetch, or wind setup fetch, is the maximum overwater distance for a wind blowing over the lake area towards the point of interest distance. At each defined point of interest along the lake shoreline, the direct fetch was estimated for each cardinal/inter-cardinal direction as the straight-line distance between the point of interest and the opposite shore. Since wind setup can accumulate around bends, this estimate took into consideration that the line of direct fetch does not need to be continuously over water.

The average depth of the lake over the direct fetch distance was estimated for each point of interest based on the bathymetry surveyed by KGS Group.

6.4 Definition of Wave Characteristics

Wind is the driving force behind wave formation. The speed of the wind plays a critical role in determining the size and strength of the waves, and higher wind speeds typically produce larger and more powerful waves. Wind-generated waves are not uniform in height, but consist of spectrums of waves ranging in height. Available methods for forecasting waves correspond to irregular waves and are represented by statistical and spectral methods. Both SPM and CEM methods are based on the significant wave height (H_s), which is the average of the highest one-third of the waves in a wave train, and the significant wave period (T_p), which is the average time interval between successive crests or troughs of groups of the highest waves.

The fetch used in wave calculations is not the same as the fetch used in wind tide calculations, since wave effects cannot be transferred around bends, past islands, and may also be reduced by frictional effects on the sides of a narrow lake. The effective fetch, or wave fetch, is the unobstructed overwater distance in which the wind generates waves. The longer the effective fetch, the more time and space waves have to accumulate energy, which generally leads to higher wave heights and consequently, increased wave runup at the shore.

Although the SPM and CEM recommend different equations to calculate the effective fetch, both methods utilize radials that extend from the point of interest on the shoreline out to where the radial intersects the nearest shore or obstacle. At each defined point of interest along the lake shoreline, radials were constructed at 1-degree intervals from the point of interest and extended until the radial intersected the shoreline. The effective fetch length was calculated according to both SPM and CEM methods for each cardinal/inter-cardinal direction.

6.4.1 SPM WAVE FORECASTING

The SPM method presents a series of equations and nomograms to calculate the significant wave and period of the spectral peak for a given windspeed and fetch or duration. Overwater wind speed is first converted to a wind-stress factor for use in the wave growth equations:

$$U_A = 0.71 {U_w}^{1.23} \quad (2)$$

where:

U_A = wind-stress factor (m/s)

U_W = overwater wind speed (m/s)

The SPM equations for predicting waves in deep water are presented in Equations 3 to 5.

$$H_s = 1.616 \times 10^{-2} (U_A F)^{\frac{1}{2}} \quad (3)$$

$$T_P = 6.238 \times 10^{-1} (U_A F)^{\frac{1}{3}} \quad (4)$$

$$t = 8.93 \times 10^{-1} \left(\frac{F^2}{U_A}\right)^{\frac{1}{3}} \quad (5)$$

where:

H_s = significant wave height (m)
T_P = significant wave period (m)
t = time required for waves crossing a fetch length under the given wind velocity to become fetch limited (hr)
U_A = wind-stress factor (m/s)
F = effective fetch length (km)

For a given set of wind and fetch conditions, wave heights will be smaller and wave periods shorter in shallow water as compared to in deep water, due to the effect of frictional dissipation of energy at the bottom of shallow water bodies. The SPM equations for predicting waves in shallow water are presented in Equations 6 to 8.

$$H_s = \frac{{U_A}^2}{g} 0.283 \tanh\left[0.530 \left(\frac{gd}{{U_A}^2}\right)^{\frac{3}{4}}\right] \tanh\left[\frac{0.00565 \left(\frac{gF}{{U_A}^2}\right)^{\frac{1}{2}}}{\tanh\left[0.530 \left(\frac{gd}{{U_A}^2}\right)^{\frac{3}{4}}\right]}\right] \quad (6)$$

$$T_P = \frac{U_A}{g} 7.54\, tanh\left[0.833 \left(\frac{gd}{{U_A}^2}\right)^{\frac{3}{8}}\right] tanh\left[\frac{0.0379 \left(\frac{gF}{{U_A}^2}\right)^{\frac{1}{3}}}{tanh\left[0.833 \left(\frac{gd}{{U_A}^2}\right)^{\frac{3}{8}}\right]}\right] \quad (7)$$

$$t = \frac{U_A}{g} 5.37 \times 10^2 \left(\frac{gT}{U_A}\right)^{\frac{7}{3}} \quad (8)$$

where:

H_s = significant wave height (m)
T_P = significant wave period (m)
t = time required for waves crossing a fetch length under the given wind velocity to become fetch limited (s)
U_A = wind-stress factor (m/s)

F = effective fetch length (m)
g = acceleration due to gravity (9.81 m/s^2)
d = average depth of the lake (m)

To check if deep or shallow water waves apply, the depth to wavelength ratio must be determined. The wavelength (*L*) can be found as a function of the significant wave period, as follows:

$$L = \frac{gT_P{}^2}{2\pi} \tag{9}$$

where:

L = wavelength (m)
T_P = wave period (m)
g = acceleration due to gravity (9.81 m/s^2)

The deepwater wave height and period will be adopted if the depth to wavelength ratio (*d*/*L*) is found to be greater than 0.5.

The SPM wave height and period equations assume the wave conditions are fetch limited, or that winds have blown constantly long enough for wave heights at the end of the fetch length to reach equilibrium. It is essential that the fetch-limited wave calculations be checked to see if conditions are duration-limited, in which case the wave heights are actually limited by the length of time the wind has blown. If the required wind duration to reach the fetch-limited wave conditions is greater than the duration over which the available wind speed data was averaged (1 hr), then an equivalent fetch length can be calculated by rearranging Equations 5 and 8 and setting the duration to 1 hr. This equivalent fetch can then be substituted into the fetch-limited equations to obtain duration-limited estimates for wave height and period.

6.4.2 CEM WAVE FORECASTING

The CEM wave growth formulas are expressed in terms of a friction velocity (U_*), which is calculated from the overwater wind speed as follows:

$$U_* = U_W[0.001(1.1 + 0.035\, U_W)]^{\frac{1}{2}} \tag{10}$$

where:

U_* = friction velocity (m/s)
U_W = overwater wind speed (m/s)

The CEM equations for predicting waves in deep water are presented in Equations 11 to 13.

$$H_S = \frac{U_*{}^2}{g} 4.13 \times 10^{-2} \left[\frac{gF}{U_*{}^2}\right]^{\frac{1}{2}} \tag{11}$$

$$T_P = \frac{U_*}{g} 0.751 \left[\frac{gF}{U_*^{\,2}}\right]^{\frac{1}{3}} \qquad 12$$

$$t = 77.23 \frac{F^{0.67}}{U_W^{0.34} g^{0.33}} \qquad 13$$

where:

H_s = significant wave height (m)

T_P = significant wave period (m)

t = time required for waves crossing a fetch length under the given wind velocity to become fetch limited (s)

U_* = friction velocity (m/s)

U_W = overwater wind speed (m/s)

F = effective fetch length (m)

g = acceleration due to gravity (9.81 m/s^2)

Similar to the SPM method, the equations governing wave growth with wind duration can be obtained by converting duration into an equivalent fetch, given by:

$$F = \frac{U_*^{\,2}}{g} 5.23 \times 10^{-3} \left[\frac{gt}{U_*}\right]^{\frac{3}{2}} \qquad 14$$

where:

F = equivalent fetch length (m)

t = wind duration (s)

U_* = friction velocity (m/s)

g = acceleration due to gravity (9.81 m/s^2)

The fetch estimated from this equation can then be substituted into the fetch-limited equations to obtain duration-limited estimates for wave height and period.

The CEM suggests that wave growth in shallow water appears to follow growth laws that are quite close to deep water wave growth for the same wind speeds. Therefore, the CEM method uses the deepwater wave growth equations for all depths, with the constraint that no wave period can grow past a limiting value. The limiting wave period can be approximated by:

$$T_{p\ (shallow\ limit)} = 9.78 \left(\frac{d}{g}\right)^{\frac{1}{2}} \qquad 15$$

where:

$T_{P\ (shallow\ limit)}$ = limiting wave period (m)

d = average depth of the lake (m)

g = acceleration due to gravity (9.81 m/s^2)

If the wave period found using the deepwater equations is greater than the limiting value, then shallow water conditions apply, and the limiting wave period is adopted. An equivalent fetch associated with the limited wave period can be calculated by rearranging Equation 12 and setting the deepwater wave period to the limiting wave period. This fetch is then substituted in the deepwater wave growth calculation to estimate the shallow water wave height.

6.5 Definition of Wave Runup

6.5.1 OVERVIEW

When a deepwater wave reaches the lake shoreline without major modifications in characteristics, the wave will ultimately break on the beach face and run up the slope to an elevation governed by the slope, the water depth at the toe of the beach face, the surface roughness, and the incident wave characteristics.

Transect characteristics were identified at each point of interest include the following information, as determined from completed transect surveys, lake bathymetry, and available LiDAR:

- Elevation of the shoreline toe (i.e., beach face);
- Slope of the shoreline (above the average water level, most waves will run up this slope);
- Elevation of the berm/backshore (if applicable);
- Width of the berm (if applicable);
- Slope of the shoreline above the berm (if applicable);
- Bottom elevation of the nearshore (applicable if there is a shelf in front of the transect);
- Nearshore slope (aka fronting slope, impacts whether wave will break before it reaches the shoreline).

Wave runup was calculated in the Monte Carlo model using the SPM and CEM methods, as described further in the following sections.

6.5.2 SPM WAVE RUNUP

The SPM method is used in the Monte Carlo model to calculate wave runup for given design wave conditions. The model checks if the wave height at the site is controlled by water depth. If H_s is greater than the breaker height, H_b (i.e. the maximum wave height for the given depth at the toe of the shoreline), the wave will break before reaching the shoreline. The design wave height is then adjusted using relationships defined in the SPM guidance documents (i.e. Figures 7-4 and 7-5 in SPM) to determine the equivalent deepwater wave height.

The SPM method also provides dimensionless wave runup relationship curves for smooth impermeable slopes (i.e. Figure 7-8 through 7-12 in SPM) to determine the relative wave runup (i.e. the ratio of vertical wave runup to the design wave height) as a function of the deep-water wave steepness and the shoreline slope.

Since the wave runup curves are based on equations that were developed from small-scale laboratory tests, the wave runup predicted by Figures 7-8 through 7-12 in SPM are likely smaller than would actually occur, as roughness effects cannot easily be scaled between laboratory and real-world conditions. A correction for scale effects was applied using a wave runup correction factor, as determined from Figure 7-13 in SPM as a function of the shoreline slope.

A roughness and porosity correction factor was also applied to adjust the smooth-slope wave runup curves to other slope characteristics. This was completed on a site-by site basis, using the recommended correction factors for various slope characteristics provided in Table 7-2 in the SPM guidance documents.

At sites where a berm was present, an additional check was completed to determine if the combined height of the still water elevation, setup, and wave runup would overtop the berm. If the berm was found to be overtopped, the wave runup was recalculated using a hypothetical, uniform slope representative of the average slope face.

6.5.3 CEM WAVE RUNUP

The CEM Method (USACE, 2001) uses the surf-similarity parameter (i.e. the Irribarren Number) to define the type of wave breaking that will occur on the beach. This parameter is the ratio between the bank slope and the wave steepness, as calculated by:

$$\xi = \frac{\tan(\theta)}{\sqrt{\frac{H_S}{L}}}$$

where:

ξ = surf similarity parameter
tan(θ)= wave runup slope (V:1H)
H_s = significant wave height (m)
L = wavelength

The relative wave runup (R_u/H) is calculated directly as a function of the surf-similarity parameter (and therefore as a function of the slope geometry), the significant wave height, and up to four reduction factors:

$$R_{u2\%} = \begin{cases} (1.6\xi)H_s\gamma_r\gamma_b\gamma_h\gamma_\beta & \text{for} \quad \xi \le 2.5 \\ (4.5 - 0.2\xi)H_s\gamma_r\gamma_b\gamma_h\gamma_\beta & \quad\quad 2.5 < \xi < 9 \end{cases}$$

where: γ_r = the reduction factor for influence of surface roughness
γ_b = the reduction factor for influence of a berm
γ_h = the reduction factor for influence of shallow-water conditions
γ_β = the factor for influence of angle of incidence β of the waves

For milder beach slopes (i.e. ξ > 9), the Monte Carlo uses the empirical wave runup formula developed by Stockdon et al. (2006) for natural beaches. This approach takes into consideration both the wave setup caused by the presence of breaking waves which push the water toward the shoreline, and the wave runup up the beach after a wave breaks.

An additional wave runup calculation is completed in the Monte Carlo model using the method described in the Coastal and Hydraulics Engineering Notes (Hughes 2003a, 2003b, 2005), based on the wave momentum flux parameter. Wave momentum flux is the property of progressive waves that is most closely related to force loads on coastal structures/any solid object placed in the wave field. This calculation can be used to improve the characterization of the structure/bank response to wave loading, and is given by the empirical equation for the momentum flux parameter:

$$\left(\frac{M_F}{\rho g h^2}\right)_{max} = A_0 \left(\frac{h}{gT^2}\right)^{-A_1}$$

where:

h = surf similarity parameter
H = wave runup slope (V:1H)
ρ = significant wave height (m)
$A_0 = 0.639 \left(\frac{H}{h}\right)^{2.026}$
$A_1 = 0.180 \left(\frac{H}{h}\right)^{-0.391}$

The CEM method leverages three different equations to calculate wave runup, depending on the wave steepness and characteristics of the shoreline (slope, roughness). For cases where there are non-breaking (i.e. surging or collapsing) waves on smooth slopes (i.e. H/L < 0.0225), wave runup is given by:

$$\frac{R_{u2\%}}{h} = 1.75\left[1 - e^{-(1.3 \cot\theta)}\right]\left(\frac{M_F}{\rho g h^2}\right)^{\frac{1}{2}} \qquad \text{for} \qquad 1.0 \leq \cot(\theta) \leq 4.0$$

For breaking (i.e. plunging or spilling) waves on smooth slopes (i.e. H/L > 0.0225), wave runup is given by:

$$\frac{R_{u2\%}}{h} = 4.4(\tan\theta)^{0.7}\left(\frac{M_F}{\rho g h^2}\right)^{\frac{1}{2}} \qquad \text{for} \qquad 1.0 \leq \cot(\theta) \leq 30$$

And in cases where no significant difference exists between breaking and nonbreaking waves on rough slopes, a single equation is used for both cases, with wave runup given by:

$$\frac{R_{u2\%}}{h} = 4.4(\tan\theta)^{0.7}\left(\frac{M_F}{\rho g h^2}\right)^{\frac{1}{2}}(0.505) \qquad \text{for} \qquad 2.0 \leq \cot(\theta) \leq 4.0$$

At sites where a berm was present, an additional check is completed in the Monte Carlo model to determine if the still water elevation, setup, and wave runup would overtop the berm height defined for the given transect. If the berm is anticipated to be overtopped, the wave runup is recalculated using a hypothetical, uniform slope representative of the equivalent slope face.

6.6 AEP Flood Levels

The Monte Carlo modelling approach to estimating flood levels was implemented at 70 shoreline locations throughout the study area to define representative flood levels, specifically:

- Five locations along Bennett Lake near Carcross,
- Eight locations along Nares Lake near Carcross,
- Six locations along Tagish Lake near Tagish,
- Four locations along Marsh Lake near Tagish,
- Thirty locations along the remainder of Marsh Lake, and

- Fifteen locations along Lake Laberge.

The locations of the Monte Carlo analysis locations are shown on Figure 38 to Figure 43. The resulting AEP flood levels for stable and dynamic conditions are summarized in Table 20 to Table 23.

FIGURE 38: ANALYSIS LOCATIONS IN CARCROSS

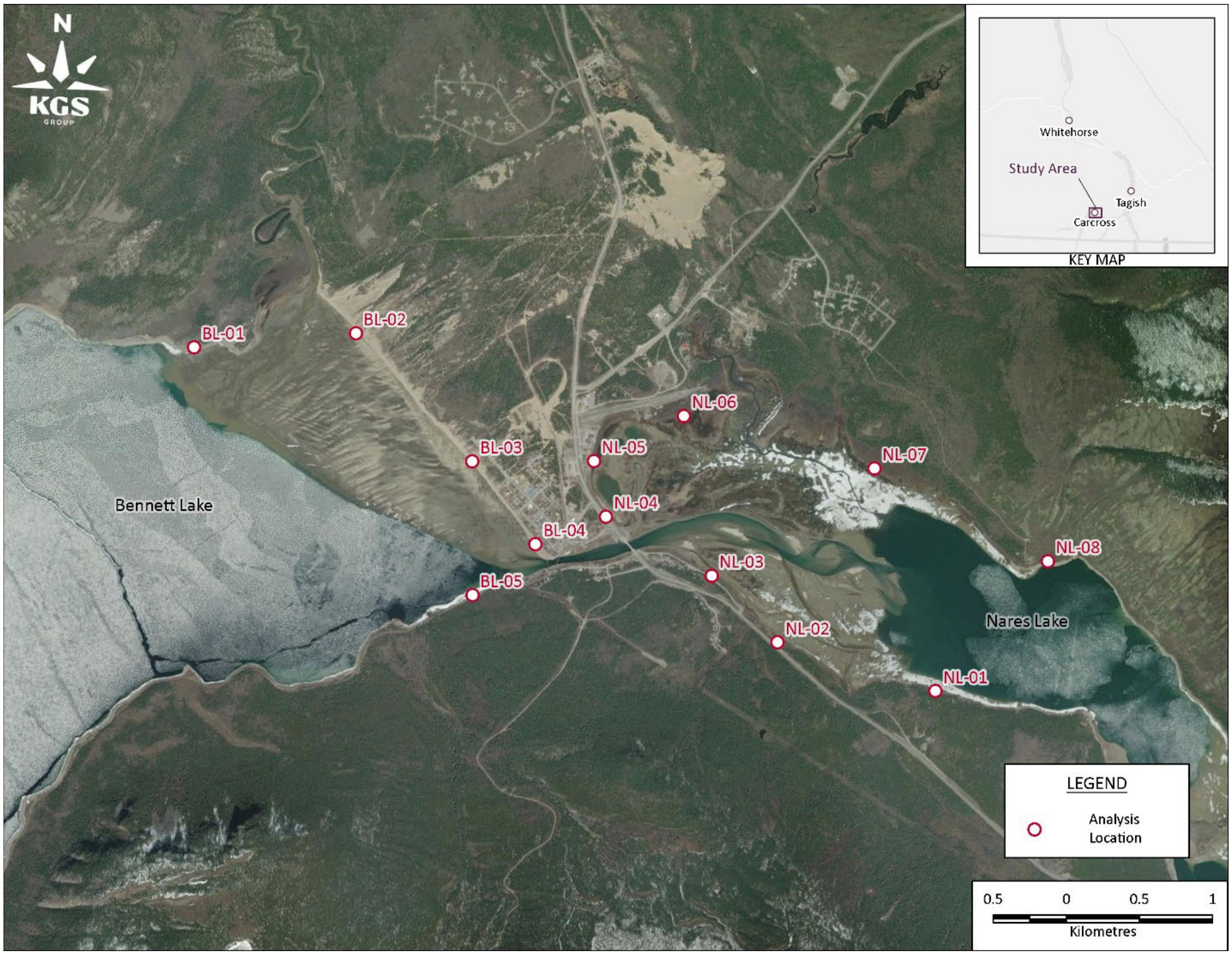

FIGURE 39: ANALYSIS LOCATIONS ON TAGISH LAKE

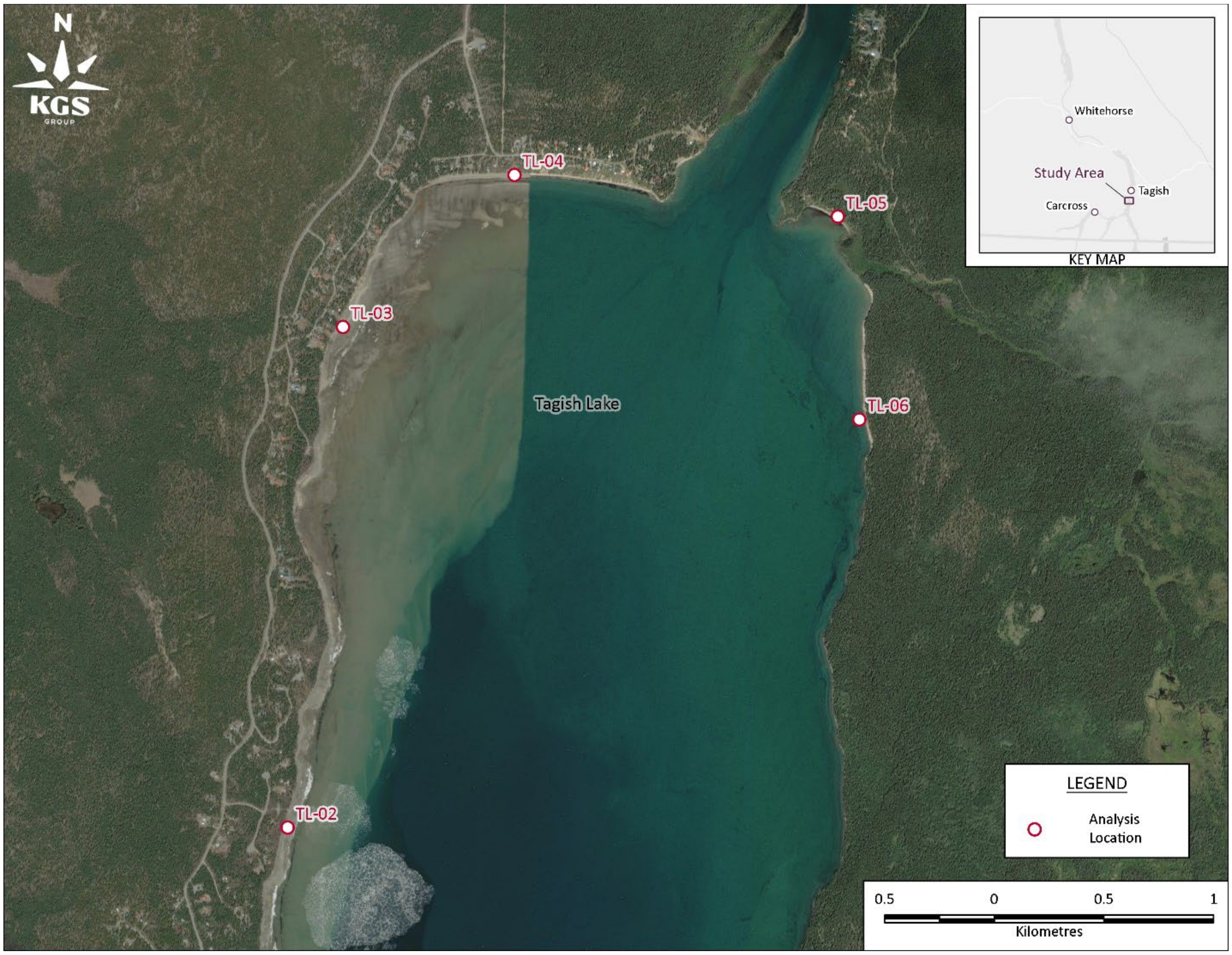

FIGURE 40: ANALYSIS LOCATIONS ON MARSH LAKE (1 OF 3)

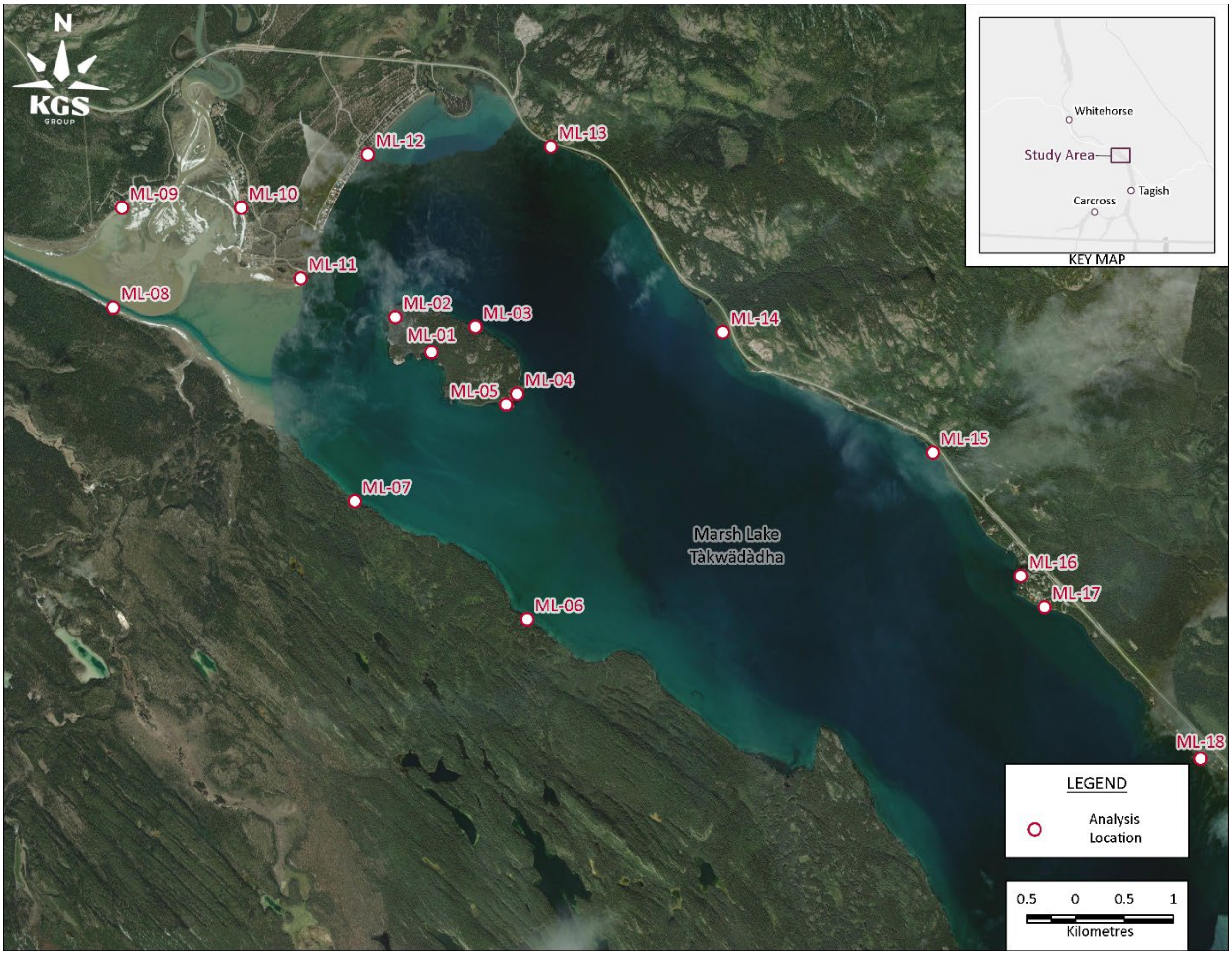

FIGURE 41 ANALYSIS LOCATIONS ON MARSH LAKE (2 OF 3)

FIGURE 42: ANALYSIS LOCATIONS ON MARSH LAKE (3 OF 3)

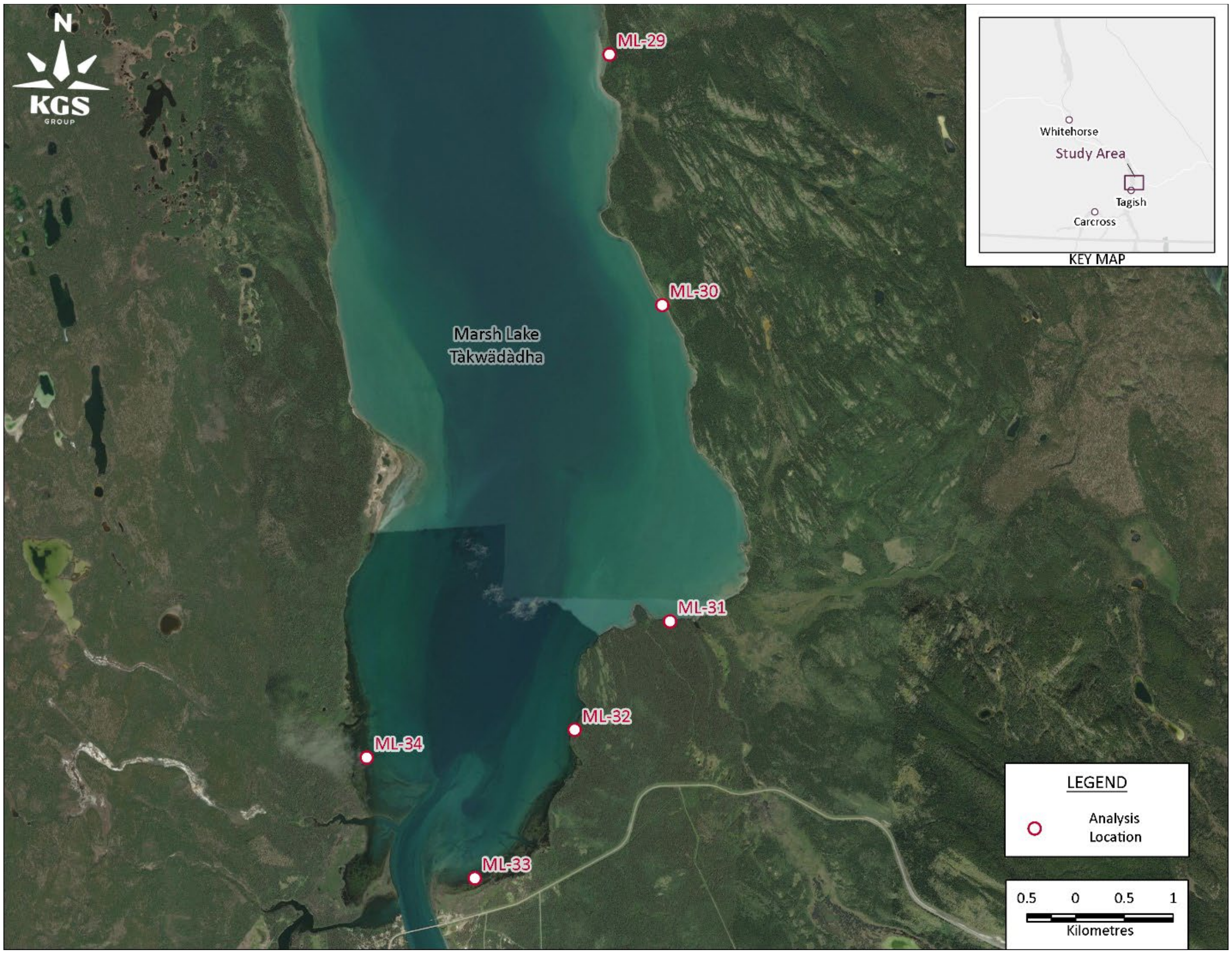

FIGURE 43: ANALYSIS LOCATIONS ON LAKE LABERGE

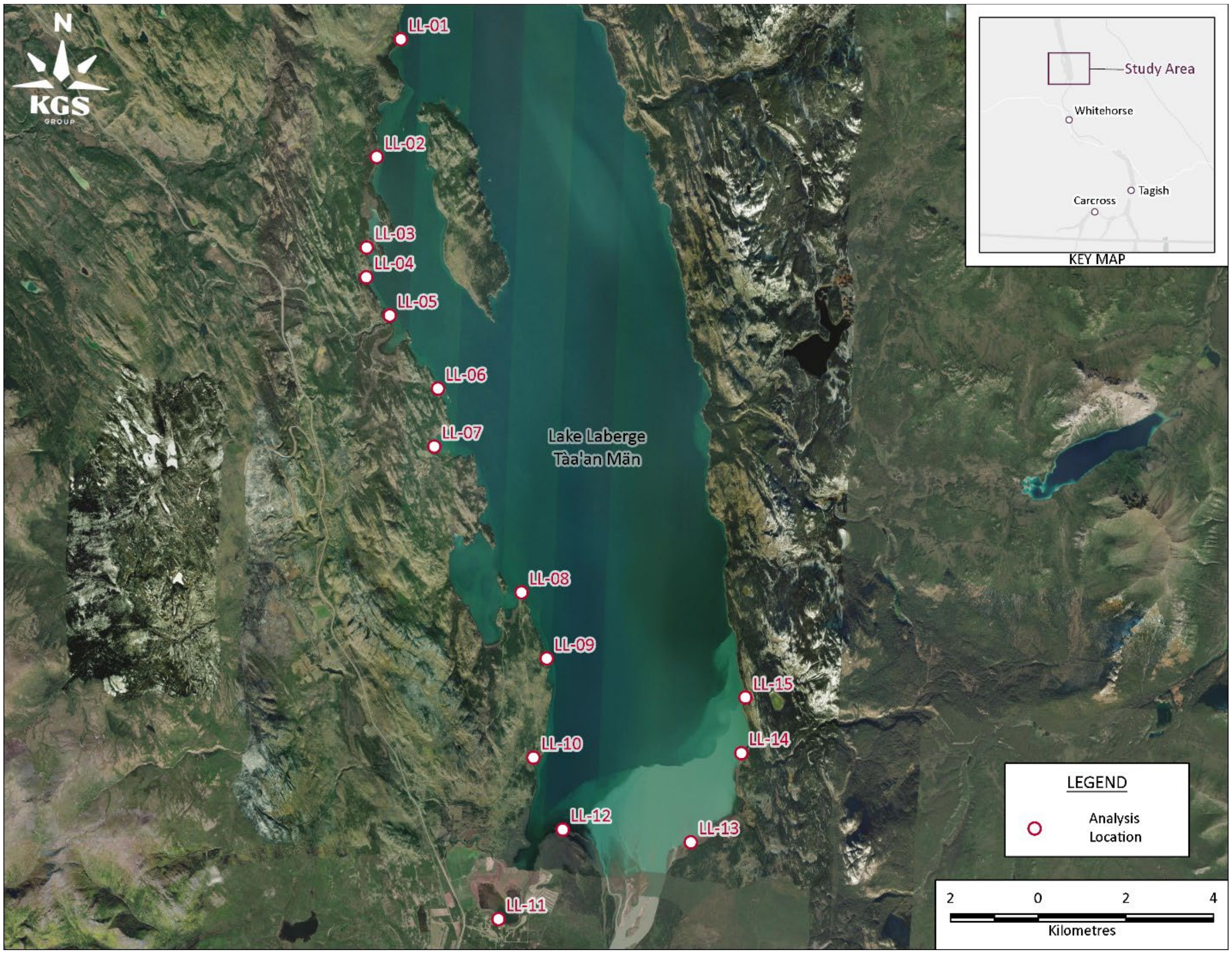

TABLE 20: AEP FLOOD LEVELS IN CARCROSS

Location	Stable AEP Water Levels (m)			Dynamic AEP Water Levels (m)		
	5%	1%	0.50%	5%	1%	0.50%
BL-01	657.68	658.12	658.25	658.23	658.62	658.80
BL-02	657.68	658.12	658.25	657.84	658.26	658.42
BL-03	657.68	658.12	658.25	657.82	658.24	658.40
BL-04	657.68	658.12	658.25	657.81	658.24	658.39
BL-05	657.68	658.12	658.25	657.90	658.34	658.44
NL-01	657.65	658.07	658.28	657.79	658.24	658.40
NL-02	657.65	658.07	658.28	657.71	658.13	658.33
NL-03	657.65	658.07	658.28	657.71	658.12	658.35
NL-04	657.65	658.07	658.28	657.76	658.18	658.40
NL-05	657.65	658.07	658.28	657.73	658.15	658.38
NL-06	657.65	658.07	658.28	657.67	658.09	658.29
NL-07	657.65	658.07	658.28	657.67	658.08	658.29
NL-08	657.65	658.07	658.28	658.04	658.45	658.66

TABLE 21: AEP FLOOD LEVELS IN TAGISH

Location	Stable AEP Water Levels (m)			Dynamic AEP Water Levels (m)		
	5%	1%	0.50%	5%	1%	0.50%
TL-01	657.71	658.13	658.32	658.01	658.41	658.63
TL-02	657.71	658.13	658.32	658.19	658.62	658.83
TL-03	657.71	658.13	658.32	658.24	658.66	658.87
TL-04	657.72	658.14	658.33	658.38	658.87	659.01
TL-05	657.72	658.14	658.33	657.95	658.40	658.56
TL-06	657.72	658.14	658.33	658.49	658.92	659.13
ML-31	657.44	657.89	658.09	657.52	657.98	658.15
ML-32	657.43	657.89	658.09	657.53	658.00	658.20
ML-33	657.44	657.89	658.09	657.46	657.92	658.11
ML-34	657.43	657.89	658.09	657.44	657.90	658.09

TABLE 22: AEP FLOOD LEVELS ON MARSH LAKE (EXCLUDING TAGISH)

	Stable AEP Water Levels (m)			Dynamic AEP Water Levels (m)		
Location	5%	1%	0.50%	5%	1%	0.50%
ML-01	657.46	657.91	658.11	657.50	657.95	658.15
ML-02	657.46	657.91	658.11	657.49	657.95	658.19
ML-03	657.46	657.91	658.11	657.60	657.99	658.18
ML-04	657.46	657.91	658.11	657.58	658.04	658.24
ML-05	657.46	657.91	658.11	658.48	658.88	659.06
ML-06	657.45	657.91	658.10	657.48	657.96	658.11
ML-07	657.46	657.91	658.11	657.55	658.06	658.21
ML-08	657.47	657.92	658.12	657.49	657.97	658.12
ML-09	657.47	657.92	658.12	657.72	658.23	658.42
ML-10	657.47	657.92	658.12	657.48	657.93	658.13
ML-11	657.47	657.92	658.12	657.63	657.99	658.26
ML-12	657.47	657.92	658.12	657.80	658.25	658.46
ML-13	657.47	657.92	658.12	658.66	659.13	659.32
ML-14	657.45	657.90	658.11	658.02	658.53	658.73
ML-15	657.45	657.90	658.11	657.86	658.30	658.46
ML-16	657.45	657.90	658.10	657.72	658.22	658.40
ML-17	657.44	657.90	658.10	658.21	658.61	658.84
ML-18	657.43	657.89	658.09	658.02	658.46	658.64
ML-19	657.42	657.89	658.09	657.65	658.11	658.31
ML-20	657.42	657.88	658.08	657.97	658.45	658.62
ML-21	657.42	657.88	658.08	657.83	658.30	658.47
ML-22	657.42	657.88	658.08	657.45	657.91	658.10
ML-23	657.42	657.87	658.08	657.62	658.10	658.27
ML-24	657.42	657.87	658.08	657.75	658.20	658.39
ML-25	657.42	657.88	658.08	657.63	658.08	658.26
ML-26	657.42	657.88	658.08	657.62	658.09	658.25
ML-27	657.42	657.88	658.08	657.47	657.93	658.12
ML-28	657.42	657.88	658.08	657.77	658.24	658.42
ML-29	657.42	657.88	658.08	657.46	657.92	658.11
ML-30	657.43	657.88	658.09	658.20	658.68	658.82

TABLE 23: AEP FLOOD LEVELS ON LAKE LABERGE

Location	Stable AEP Water Levels (m)			Dynamic AEP Water Levels (m)		
	5%	1%	0.50%	5%	1%	0.50%
LL-01	627.43	627.91	628.09	627.87	628.37	628.63
LL-02	627.43	627.91	628.10	627.72	628.20	628.35
LL-03	627.43	627.91	628.10	627.55	628.06	628.23
LL-04	627.43	627.91	628.10	628.22	628.76	629.01
LL-05	627.43	627.91	628.10	627.70	628.18	628.52
LL-06	627.43	627.91	628.09	627.78	628.27	628.57
LL-07	627.43	627.92	628.10	627.70	628.19	628.52
LL-08	627.43	627.92	628.10	627.56	628.06	628.21
LL-09	627.43	627.92	628.10	627.63	628.14	628.41
LL-10	627.43	627.92	628.10	627.70	628.21	628.40
LL-11	627.43	627.92	628.10	627.61	627.99	628.12
LL-12	627.43	627.92	628.10	627.46	627.95	628.13
LL-13	627.44	627.92	628.10	627.46	627.95	628.13
LL-14	627.43	627.92	628.10	627.81	628.26	628.45
LL-15	627.43	627.92	628.10	627.91	628.44	628.61

Flood levels between Bennett Lake and Nares Lake, as well as between Tagish Lake and Marsh Lake, were defined via linear interpolation for each AEP. For water levels on the Yukon River downstream of Marsh Lake, those levels were defined using an existing HEC-RAS model of the Yukon River extending from Schwatka Lake to Marsh Lake. In the model, it was assumed that all gates on Lewes Dam would be fully open, and water levels on Schwatka Lake would be at the maximum allowable level as defined by the water use license.

Recorded water levels that were measured during the 2021 flood were compared to AEP stable flood levels on Bennett Lake, Tagish Lake, Marsh Lake, and Lake Laberge to understand how the AEP flood levels compared to the historical flood of record on each lake, as shown on Figure 44 to Figure 47, and to facilitate the comparison of the inundated areas defined for each AEP with those recorded by YG during the 2021 flood, as discussed further in Section 8.3. It should be noted that while the frequency levels for Tagish Lake were conservatively used to define those on Bennett Lake, as described in Section 5.2.2, the resulting stable AEP flood levels on Tagish Lake are higher than those on Bennett Lake due to substantially higher wind setup on Tagish Lake than Bennett Lake and Nares Lake. As well, while the stable AEP flood levels for Bennett Lake and Tagish shown in Figure 44 and Figure 45 are slightly lower than the annual flood frequency levels described in Table 5, this can be attributed to the assessment of flood levels on a monthly basis to properly account for variations in the monthly wind speeds and prevailing winds, and the impact of those wind speeds on wind setup and wave runup.

FIGURE 44: COMPARISON OF 2021 FLOOD TO AEP LEVELS ON BENNETT LAKE

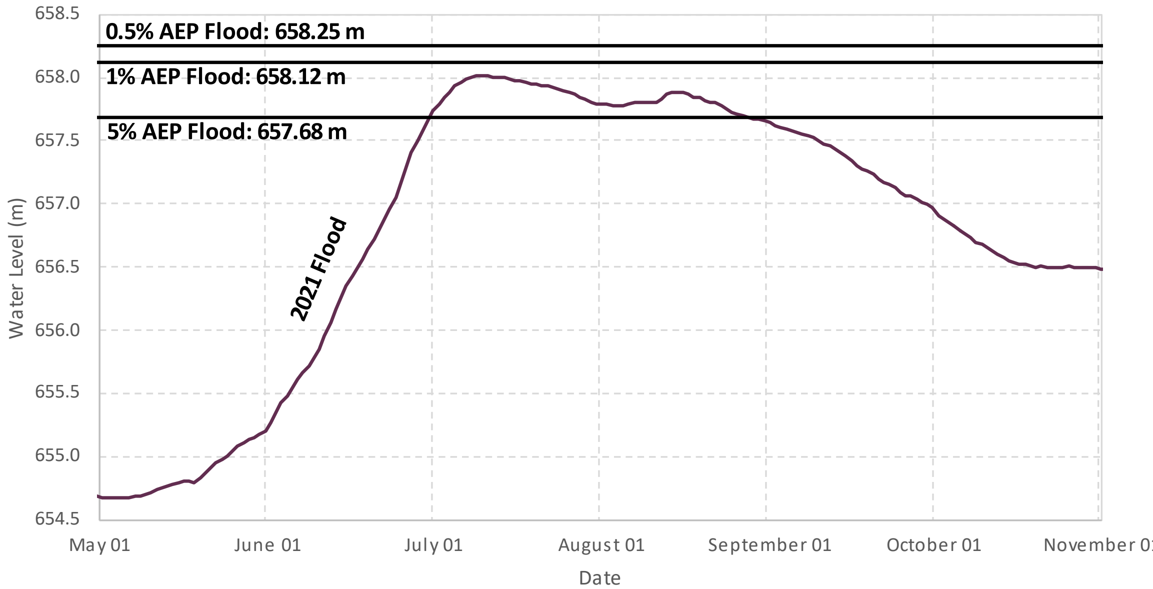

FIGURE 45: COMPARISON OF 2021 FLOOD TO AEP LEVELS ON TAGISH LAKE

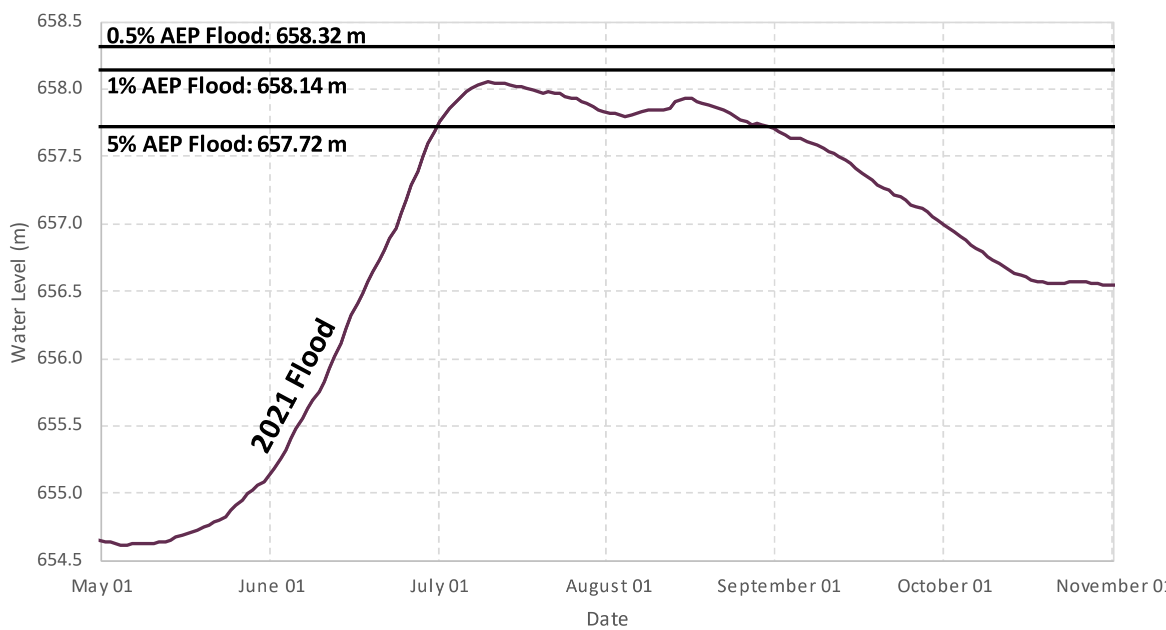

FIGURE 46: COMPARISON OF 2021 FLOOD TO AEP LEVELS ON MARSH LAKE

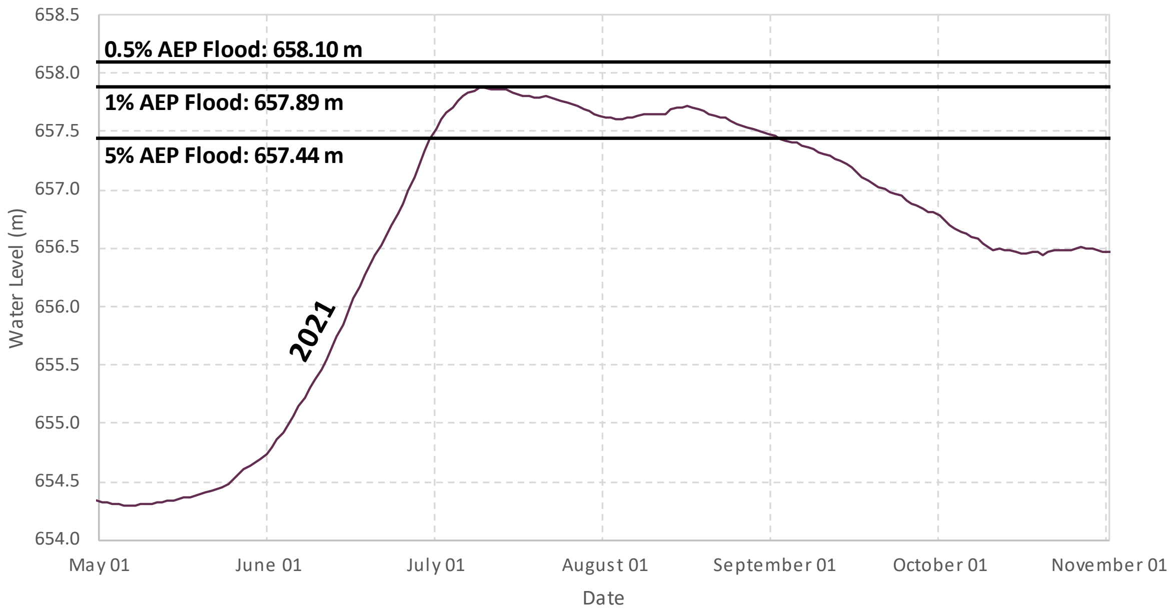

FIGURE 47: COMPARISON OF 2021 FLOOD TO AEP LEVELS ON LAKE LABERGE

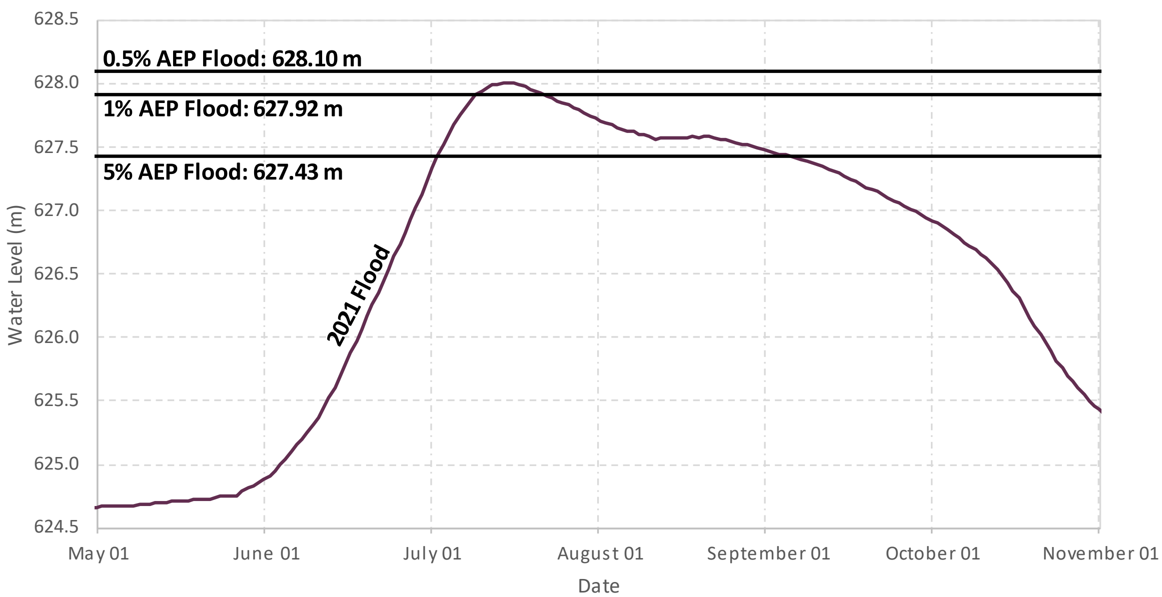

The 2021 flood was somewhat lower than a 1% AEP flood on Bennett Lake and Tagish Lake, and matched very closely with the 1% AEP flood on Marsh Lake. On Lake Laberge, the 2021 flood was between a 1% and 0.5% AEP flood.

7.0 CLIMATE AND LAND USE CHANGE ASSESSMENT

Temperatures in northern Canada are projected to increase faster than the global rate, with greater increases in the winter. Precipitation is also projected to increase in all seasons, including an increase in daily extreme precipitation (Cohen et al., 2019) (Zhang et al., 2019).

Anticipated climate change data from an ensemble of global climate models simulated under a moderate (i.e. Shared Socioeconomic Pathways (SSP 4.5) and high greenhouse gas emission scenario (i.e. SSP 8.5) was obtained from ClimateData.ca (ClimateData.ca, 2023) for the headwaters of the Yukon River – Lake Laberge watershed to indicate projected future changes in 2041-2070. Projected climate change impacts associated with the SSP 4.5 and SSP 8.5 conditions are summarized in Table 24.

TABLE 24: PROJECTED FUTURE CHANGES IN CLIMATE PARAMETERS FOR THE HEADWATERS OF THE YUKON - LAKE LABERGE WATERSHED

Climate Variable	2041-70 Change from 1971-2000 (SSP 4.5)	2041-70 Change from 1971-2000 (SSP 8.5)
Minimum Winter Temperature (°C)	+3.3 (+2.0 to +5.5)	+4.5 (+2.3 to +7.5)
Minimum Summer Temperature (°C)	+2.8 (+1.9 to +4.1)	+3.7 (+2.6 to +5.0)
Total Winter Precipitation (mm)	+11 (+1 to +16)	+12 (+7 to +20)
Total Summer Precipitation (mm)	+19 (+10 to +30)	+25 (+10 to +34)
Maximum Annual 1-Day Precipitation (mm)	+3 (+1 to +4)	+3 (+2 to +6)
Ice Days (days with maximum temperature below 0°C)	-19 (-34 to -15)	-24 (-40 to -19)

Note: Changes are expressed as absolute changes relative to a 1971-2000 baseline. Data is adapted from ClimateData.ca (ClimateData.ca, 2023)

Climate models indicate that a greater fraction of total precipitation will fall as rain in summer months, snow cover duration will decline, and snowmelt rates may increase under warmer temperatures (Cohen et al., 2019) (McKenney et al., 2011) (Rasouli et al., 2019a). The combined effect of increased precipitation and a shorter snow accumulation season is expected to result in minimal changes in the maximum snow water equivalent (SWE) for northern Canada (Derksen et al., 2019). Shrub growth expansion into higher elevations due to warmer temperatures may also promote snow accumulation, which was shown to offset the impact of climate change on SWE in one study that considered both impacts (Rasouli et al., 2019a) (Derksen et al., 2019).

Studies which modelled glacier loss and climate change in the Yukon River Basin have found net losses of glacier area volume, and higher glacier wastage and melt across all scenarios, driven by higher temperatures

(Northern Climate Exchange, 2016). A combination of higher temperatures and precipitation, leading to greater snow accumulation, was found to result in increased glacial melt (Northern Climate Exchange, 2016). Another study found an increase in snowpack accumulation for the Upper Yukon River basin under warmer and wetter climate scenarios, combined with earlier and faster melt rates (Northern Climate Exchange, 2012).

Hydrological modelling of regional climate model projections in Wolf Creek, Yukon found that the timing of peak SWE advanced about three weeks earlier, with a shorter snow cover period overall, 9 to 16 days shorter for all scenarios that included climate changes. The results indicated that higher precipitation partially offset the impacts of warmer temperatures, with a modelled decrease in peak SWE of 11% on average (-45% to +15%), a shift in earlier timing, a greater proportion of precipitation as rainfall, and a higher evapotranspiration rate (Rasouli et al., 2019b).

Net glacier mass loss has been occurring in the Upper Yukon River basin over recent decades (Northern Climate Exchange, 2012). Glaciers, particularly small glaciers, are projected to lose the majority of their mass by the end of the 21st century due to a longer and hotter summer melt (Derksen et al., 2019), with the majority of losses occurring at lower elevations (Northern Climate Exchange, 2016). While glacier volume and area are expected to continue to decline in the Upper Yukon River basin, net glacier loss by 2050 was modelled to be -12% relative to 2010, indicating that larger glaciers, such as the Llewellyn Glacier in the Upper Yukon River Basin, will persist longer than small glaciers and continue to supplement flows (Northern Climate Exchange, 2012).

Regional reviews have indicated that annual streamflow in northern Canada is likely to increase due to higher precipitation, with an earlier shift in the timing of peak streamflow, and higher winter streamflow. A trend analysis of unregulated streams found decreasing and insignificant trends in the one-day maximum streamflow in the southern Yukon, near the Southern Lakes (Bonsal et al., 2019). Permafrost thaw in northwestern Canada could lead to rapid lake drainage as land thaws, however limited studies have been completed regarding this potential process. One study found increased subsurface flows, particularly between April and December. The net effect of climate change was a modelled 15% to 26% increase in annual streamflow, with greater increases occurring during winter and spring and a slightly earlier (zero to four days) date of peak streamflow (Northern Climate Exchange, 2016). Another study which applied climate change scenarios to a hydrologic model also found higher annual streamflow, with increased streamflow in early spring and late fall resulting from the warmer and wetter climate scenarios projected for the region (Northern Climate Exchange, 2012). A modelling study of Wolf Creek, Yukon found statistically higher annual runoff rates under climate change in the alpine and forest biomes and insignificant changes in the shrub tundra biome (Rasouli et al., 2019b).

To estimate potential climate change impacts on flood levels on Bennett Lake, Nares Lake, Tagish Lake, Marsh Lake, and Lake Laberge, a separate set of Monte Carlo analyses were completed using modified statistical relationships that considered approximated climate change impacts. Specifically, the analyses considered:

- Projected increases to flood levels;
- Increases in wind speed;
- Changes to timing of flood events.

To estimate the climate change impacts on flood levels, annual peak water levels on Bennett Lake and Marsh Lake between 1977 and 2023 were evaluated to identify any trends in the data that may be associated with ongoing climate change processes. Data prior to 1977 was excluded from the analysis as the Lewes Dam was rebuilt in 1976, which could skew any trends in the analysis, were that data to be considered. Annual peak water level data on Lake Laberge and Tagish Lake were similarly excluded from the analysis due to their shorter periods of record.

The annual peak water level data from 1977 to 2023 for each lake was subdivided into two sets of data, one extending from 1977 to 2000, and the other extending from 2001 to 2023. Frequency curves were fit to each set of data following the same methodology as described in Section 5.2, with Gumbel distributions being found to be most representative of the datasets. Differences between AEP flood events were then calculated, representing the increases in return period flood levels over a period of nearly 25 years. These changes were then projected to the year 2100 by assuming that these changes would progress at the same rate. The climate change impacts estimated for Bennett Lake and Marsh Lake are summarized in Table 25.

TABLE 25: CLIMATE CHANGE IMPACTS TO FLOOD LEVELS

Lake	AEP	Water Level (1977 - 2000) (m)	Water Level (2001 - 2023) (m)	Water Level Change (m)	Projected Change to 2100 (m)
Bennett Lake	0.5%	658.22	658.40	0.18	0.54
	1.0%	658.04	658.20	0.16	0.48
	2.0%	657.87	658.00	0.13	0.39
	5.0%	657.63	657.73	0.10	0.30
	10.0%	657.45	657.52	0.07	0.21
	20.0%	657.26	657.31	0.05	0.15
	33.3%	657.11	657.13	0.02	0.06
	50.0%	656.98	656.98	0.00	0.00
Marsh Lake	0.5%	657.69	657.90	0.21	0.63
	1.0%	657.55	657.74	0.19	0.57
	2.0%	657.42	657.59	0.17	0.51
	5.0%	657.23	657.38	0.15	0.45
	10.0%	657.09	657.22	0.13	0.39
	20.0%	656.94	657.05	0.11	0.33
	33.3%	656.82	656.92	0.10	0.30
	50.0%	656.72	656.80	0.08	0.24

As a separate check, a linear regression was fit to the annual instantaneous peak water levels on Bennett Lake and Marsh Lake from 1977 to 2023. The linear regressions on both Bennett Lake and Marsh Lake had positive slopes, which if projected to 2100 corresponded to peak flood level increases of 0.14 m on Bennett Lake and 0.36 m on Marsh Lake. While these increases are smaller than those estimated via frequency analysis for severe floods, they do agree well with more moderate flooding, particularly the 20% AEP. The trends in annual peak water levels on Bennett Lake and Marsh Lake are shown on Figure 48 and Figure 49.

FIGURE 48: TREND IN ANNUAL PEAK WATER LEVELS ON BENNETT LAKE

FIGURE 49: TREND IN ANNUAL PEAK WATER LEVELS ON MARSH LAKE

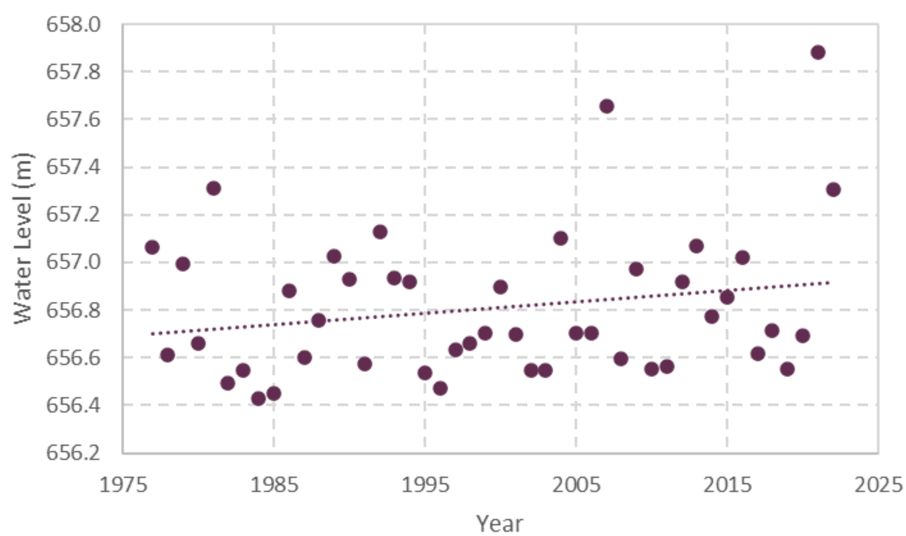

Given that climate change impacts are expected to be more pronounced for severe flood events, the anticipated flood impacts defined via the frequency analysis were adopted in the Monte Carlo model. The anticipated water level increases on Marsh Lake were conservatively adopted for all lakes. It should be noted that the projected increases in flood levels are likely due to a combination of dynamic and complex processes that are sensitive to climate change impacts, such as increased glacial melt, faster spring melts, increased rainfall, and increases in streamflow. As noted in Section 5.1, future flood mapping studies in the Southern Lakes area should leverage volume routing models and the estimation of AEP inflows to the lakes. This would facilitate a more direct representation of climate change impacts on flood levels, as the hydrological inputs to the model could be modified to represent anticipated climate change impacts to stream flows.

Wind speeds were adjusted in the Monte Carlo model to reflect the projected increases in surface wind speeds. Projected impacts to surface wind speeds were estimated based on the Coupled Model Intercomparison Project Phase 5 (CMIP5) dataset made available by the Government of Canada (Canadian Centre for Climate Services, 2023), which provides climate change data from multi-model ensembles. For this study, the projected climate change impacts to surface wind speeds were extracted for the median ensemble results for Carcross, Jake's Corner, Mount Sima, and Whitehorse considering the Representative Concentration Pathway (RCP) 8.5 emissions scenario on a monthly basis, which were then used to increase the AEP wind speeds considered in the Monte Carlo analyses. The projected climate change impacts to wind speeds are summarized in Table 26.

TABLE 26: CLIMATE CHANGE IMPACTS TO WIND SPEEDS

	Projected Change in Wind Speed				
Climate Station	June	July	August	September	October
Whitehorse A	2.2%	2.2%	2.3%	3.0%	3.3%
Mount Sima	2.2%	2.2%	2.3%	3.0%	3.3%
Jake's Corner	2.2%	2.1%	2.2%	2.8%	3.2%
Carcross	2.2%	2.2%	2.3%	2.9%	3.3%

The projected earlier shift in the timing of peak flood water levels due to climate change was accounted for in the Monte Carlo analyses by shifting the timing of the frequency relationships flood events to occur one month earlier (e.g. floods that occur in July under current climate conditions would occur in June). The timing of AEP wind speeds was not adjusted.

Flood levels were defined using the Monte Carlo models to define the 5% and 0.5% AEP flood levels throughout the study area under climate change conditions. Those flood levels are summarized in Table 27 to Table 30.

TABLE 27: CLIMATE CHANGE AEP FLOOD LEVELS IN CARCROSS

	Stable AEP Water Levels (m)		Dynamic AEP Water Levels (m)	
Location	5%	0.50%	5%	0.50%
BL-01	658.07	658.92	658.71	659.51
BL-02	658.07	658.92	658.23	659.04
BL-03	658.07	658.92	658.21	659.03
BL-04	658.07	658.92	658.20	659.00
BL-05	658.07	658.92	658.28	659.10
NL-01	658.07	658.76	658.24	658.93
NL-02	658.07	658.77	658.17	658.87
NL-03	658.07	658.77	658.17	658.87
NL-04	658.07	658.77	658.20	658.91
NL-05	658.07	658.77	658.17	658.87
NL-06	658.07	658.77	658.09	658.79
NL-07	658.07	658.76	658.09	658.78
NL-08	658.07	658.76	658.52	659.21

TABLE 28: CLIMATE CHANGE AEP FLOOD LEVELS IN TAGISH

	Stable AEP Water Levels (m)		Dynamic AEP Water Levels (m)	
Location	5%	0.50%	5%	0.50%
TL-01	658.14	658.86	658.42	659.15
TL-02	658.15	658.86	658.61	659.33
TL-03	658.15	658.86	658.64	659.37
TL-04	658.15	658.87	658.77	659.45
TL-05	658.15	658.87	658.35	659.05
TL-06	658.15	658.87	658.83	659.58
ML-31	657.87	658.72	657.99	658.84
ML-32	657.88	658.72	657.98	658.84
ML-33	657.87	658.72	657.91	658.76
ML-34	657.87	658.72	657.88	658.72

TABLE 29: CLIMATE CHANGE AEP FLOOD LEVELS ON MARSH LAKE

	Stable AEP Water Levels (m)		Dynamic AEP Water Levels (m)	
Location	5%	0.50%	5%	0.50%
ML-01	657.89	658.73	657.93	658.76
ML-02	657.89	658.73	657.93	658.87
ML-03	657.89	658.73	657.98	658.95
ML-04	657.89	658.73	658.04	658.90
ML-05	657.89	658.73	658.91	659.63
ML-06	657.88	658.72	657.92	658.77
ML-07	657.88	658.73	658.00	658.86
ML-08	657.89	658.73	657.93	658.77
ML-09	657.90	658.74	658.20	659.03
ML-10	657.90	658.74	657.94	658.80
ML-11	657.89	658.73	657.96	658.98
ML-12	657.90	658.74	658.21	659.02
ML-13	657.90	658.74	658.93	659.73
ML-14	657.88	658.72	658.46	659.36
ML-15	657.88	658.72	658.24	659.10
ML-16	657.88	658.72	658.17	659.05
ML-17	657.88	658.72	658.56	659.35
ML-18	657.87	658.71	658.46	659.27
ML-19	657.86	658.71	658.08	658.93
ML-20	657.86	658.70	658.44	659.26
ML-21	657.85	658.70	658.25	659.11
ML-22	657.85	658.70	657.89	658.75
ML-23	657.85	658.70	658.05	658.93
ML-24	657.85	658.70	658.20	659.03
ML-25	657.85	658.70	658.07	658.91
ML-26	657.85	658.70	658.03	658.90
ML-27	657.86	658.71	657.94	658.80
ML-28	657.86	658.71	658.20	659.05
ML-29	657.86	658.71	657.90	658.76
ML-30	657.87	658.72	658.71	659.53

TABLE 30: CLIMATE CHANGE AEP FLOOD LEVELS IN LAKE LABERGE

Location	Stable AEP Water Levels (m)		Dynamic AEP Water Levels (m)	
	5%	0.50%	5%	0.50%
LL-01	627.90	628.74	628.36	629.28
LL-02	627.90	628.74	628.21	629.07
LL-03	627.90	628.74	628.12	628.96
LL-04	627.90	628.74	628.73	629.74
LL-05	627.90	628.74	628.24	629.20
LL-06	627.90	628.74	628.35	629.30
LL-07	627.90	628.75	628.25	629.17
LL-08	627.90	628.75	628.05	628.89
LL-09	627.90	628.75	628.10	628.99
LL-10	627.90	628.75	628.15	629.02
LL-11	627.91	628.75	627.99	628.79
LL-12	627.91	628.75	627.94	628.79
LL-13	627.91	628.75	627.94	628.78
LL-14	627.91	628.75	628.32	629.20
LL-15	627.90	628.75	628.45	629.34

8.0 FLOOD HAZARD MAP DEVELOPMENT

8.1 Overview

Once flood levels on Bennett Lake, Nares Lake, Tagish Lake, Marsh Lake, and Lake Laberge were estimated for the 5%, 1% and 0.5% AEP floods under current climate and climate change conditions, the simulated flood levels were used in combination with the LiDAR ground elevations to develop flood hazard maps. The flood hazard maps, which show the flood extent for each AEP flood condition, were developed by overlaying the simulated water levels on top of the ground elevation model. Areas where the modelled water level was higher than the ground elevation were shown as flooded, while areas where the ground elevation was higher than the modelled water level were shown as dry. The flooded areas were carefully reviewed to identify any disconnected areas. Since the flooded areas need to be connected for the flooding to actually occur, any disconnected areas were removed from the maps.

8.2 Flood Hazard Maps

The Monte Carlo models, as described in Section 6.0 for current climate conditions, and Section 7.0 for climate change conditions, were used to define the 5%, 1%, and 0.5% AEP flood levels under current climate conditions, and the 5% and 0.5% flood levels under climate change conditions. For each AEP condition, two sets of flood extents were defined based on the stable flood levels (i.e. the combination of static lake levels and wind setup) and dynamic flood levels (i.e. the combination of static lake levels, wind setup, and wave runup). It should be noted that the stable flood levels represent areas that would be expected to be flooded for a given AEP event, while the dynamic flood levels represent additional areas that are at risk of additional flooding due to wave effects.

To map the flood extents, continuous water level surfaces were generated based on the AEP flood levels. These water level surfaces were then overlain onto the LiDAR-based DEM representation of the ground surface, with the intersection of the water level surfaces with the LiDAR ground surface defining the extents of flooding. These initially generated flood extents were carefully reviewed to identify any areas that are shown as flooded but hydraulically disconnected from the main flooded area. Any hydraulically disconnected areas were removed from the mapping. The flood zones for the current climate and climate change conditions were then overlain on top of the detailed orthoimagery provided by YG, with the exception of a portion of Marsh Lake, where the orthoimagery was offset from the LiDAR. In that area, the flood extents were overlain on satellite imagery acquired from Esri. The draft flood hazard maps were reviewed with community members within the study area, as described further in Section 9.0.

Subsequent to the review of the maps by YG and the community representatives, the maps were updated based on comments received from YG and as part of the stakeholder engagement. These updates included adjustments to the labelling and naming of communities, the inclusion of the 50% AEP flood level, which is representative of average flood conditions, adjustment to symbology for clarity, and the modification and enhancement of the notes that were included in each mapsheet. Each set of flood hazard maps showed both the stable and dynamic flood zones, and consisted of 12 map sheets in Carcross, 27 map sheets in Tagish, 56 map sheets on Marsh Lake, excluding those near Tagish, and 34 map sheets on Lake Laberge. The flood hazard maps are included in Appendix E.

8.3 Comparison of Inundation Boundaries to the 2021 Flood

As part of the background information, YG provided orthoimagery that was collected via drone during the 2021 flood, which shows the flood extents during the 2021 flood. The flood extents shown in the orthoimagery were compared to the most similar AEP flood extent to confirm that the flood extents shown in the flood hazard maps were representative of actual flood conditions. These comparisons are shown on Figure 50 to Figure 55, with the 2021 flood orthoimagery and AEP flood extents overlaying the orthoimagery that was collected during the LiDAR capture. Approximate flood extents that were estimated visually from the 2021 orthoimagery are shown on the figures via dashed red lines. However, there is a high degree of uncertainty in the flood extents in areas with a thick vegetative cover. It should also be noted that the AEP flood extents do not consider any temporary flood protection infrastructure that was constructed during the 2021 flood, which can result in substantial differences between the 2021 and AEP flood extents. An illustrative example of this is shown on Figure 52, where temporary flood protection installed on S. M'Clintock Rd. and along the shoreline for residences along Bay View Rd. prevented significant inland flooding from occurring in the area northwest of Army Beach. It should also be noted that some of the flood extents shown in the 2021 orthoimages are obscured by vegetation.

Overall, the 2021 flood extents were in good agreement with the flood extents for the AEP floods closest in magnitude to the 2021 flood, with the exception of where temporary flood protection works were installed, such as along S. M'Clintock Rd.

FIGURE 50: COMPARISON OF 2021 (TOP) AND 1% AEP (BOTTOM) FLOOD EXTENTS IN CARCROSS

FIGURE 51: COMPARISON OF 2021 (TOP) AND 1% AEP (BOTTOM) FLOOD EXTENTS IN TAGISH

FIGURE 52: COMPARISON OF 2021(LEFT) AND 1% AEP (RIGHT) FLOOD EXTENTS NEAR ARMY BEACH

FIGURE 53: COMPARISON OF 2021 (LEFT) AND 1% AEP (RIGHT) FLOOD EXTENTS NEAR SWAN HAVEN

FIGURE 54: COMPARISON OF 2021 (LEFT) AND 0.5% AEP (RIGHT) FLOOD EXTENTS IN SHALLOW BAY

FIGURE 55: COMPARISON OF 2011 (LEFT) AND 0.5% AEP (RIGHT) FLOOD EXTENTS IN JACKFISH BAY

9.0 STAKEHOLDER ENGAGEMENT

KGS Group attended a series of stakeholder engagement sessions with YG and their stakeholder engagement facilitator, 3Pikas. The engagement sessions took place on:

- February 1, 2024, with representatives from TKC;
- February 5, 2024, at the Haa Shagoon Hidi;
- February 6, 2024, at the Marsh Lake Community Centre;
- February 7, 2024, at the Hootalingua Community Centre.

YG held separate meetings on February 9, 2024, with KDFN staff, and on February 13, 2024, at the Tagish Community Centre. KGS Group personnel were unavailable to attend these engagement sessions. A separate report documenting the engagement sessions was prepared by 3Pikas, but key takeaways from the engagement sessions included:

- Representatives from TKC noted that the flood extents shown in Shallow Bay were less than they recalled observing during the 2021 flood. A subsequent comparison of the flood extents to orthoimagery collected during the 2021 flood showed generally good agreement.
- Concurrence that the AEP flood extents in Carcross accurately reflected the flood-prone areas in the community;
- Concerns regarding sediment accumulation and geomorphology in Carcross;
- Concerns regarding groundwater flooding in Carcross, Marsh Lake, and Lake Laberge;
- Concerns regarding shoreline erosion were identified in Carcross and Marsh Lake;
- Some residents in Marsh Lake at Army Beach and Judas Creek expressed concern that flood protection works constructed during and/or subsequent to the 2021 flood were not accurately represented in the map;
- Other Marsh Lake residents noted that the AEP flood extents accurately represented flood-prone areas,
- Reference flood levels would be useful to ensure that any flood protection works are constructed to an adequate height;
- The community boundary lines were difficult to interpret;
- Typical flood levels would serve as a good basis for comparison on the flood hazard maps;
- Concerns were expressed regarding the potential flood level impacts associated with Lewes Dam;
- Concerns were expressed relating to boat wakes causing increased shoreline erosion.

10.0 CONCLUSIONS AND RECOMMENDATIONS

The following scope of work was completed as part of the flood mapping study for the Southern Lakes area:

- A volume routing model was developed to estimate the impacts on flood levels associated with the Lewes Dam. The high-level analysis estimated that the 1% AEP flood level on Bennett Lake, Tagish Lake, and Marsh Lake are approximately 0.2 m higher with Lewes Dam in place than without, while water levels on Lake Laberge are approximately 0.02m lower with Lewes Dam in place than without the dam in place. The magnitudes of these impacts are lower for smaller flood events.
- Statistical analyses were completed to define the statistical relationships for lake flood levels on both an annual and monthly basis, as well as for wind speeds on a directional and monthly basis. These statistical relationships were integrated into a Monte Carlo model.
- A Monte Carlo model was developed to simulate the combined effects of lake flood levels, wind setup, and wave runup. The Monte Carlo analysis was implemented at thirteen locations in Carcross, ten locations in Tagish, thirty locations on Marsh Lake, excluding the area near Tagish, and fifteen locations on Lake Laberge. Flood levels were defined for the 5%, 1%, and 0.5% AEP flood conditions at each location.
- A separate Monte Carlo model was developed considering the anticipated impacts associated with climate change. The Monte Carlo model was implemented at the same locations that were considered for current climate conditions, and was used to generate flood levels for the 5% and 0.5% AEP flood conditions.
- Flood hazard maps were developed based on available topographic data and the AEP flood levels defined by the Monte Carlo analysis. For each AEP condition, 12 map sheets were prepared for Carcross, 27 map sheets were prepared for Tagish, 56 map sheets were prepared for Marsh Lake, excluding the area near Tagish, and 34 map sheets were prepared for Lake Laberge. In total, 645 map sheets were prepared for the study.
- Stakeholder engagement sessions were organized by YG and 3Pikas for the communities of Carcross and Tagish, as well as communities throughout Marsh Lake and Lake Laberge. Separate meetings were also held with representatives from TKC and KDFN.

Over the course of this project, several recommendations were identified by KGS Group, YG, or stakeholders relating to the flood mapping study. These recommendations include:

- Future work regarding flood hazards on the Southern Lakes should consider the development and calibration of a volume routing model of the lakes, such that hydrological inflows can be defined for AEP floods of interest on the lakes. This approach would serve as an independent validation of the flood levels defined as part of this study. Furthermore, climate change impacts can more directly be integrated into the hydrological inflows to the lakes, thus providing a more robust estimation of climate change impacts on flood levels.
- As the understanding of anticipated climate change impacts improves through ongoing and future research, climate change flood levels should be revisited to integrate those improvements in understanding.

- Further analyses should be completed to better understand and refine the potential impacts of flood levels associated with the operation of Lewes Dam. This should include further investigations to better define the Marsh Lake outflow rating curve, as well as completing further hydrological analyses enhance the characterization of ungauged inflows to the lakes, which would serve to enhance the model representation of historical water levels.
- Further investigations and monitoring should be completed to confirm the potential discrepancy between WSC gauges 09AA004 (i.e. Bennett Lake at Carcross) and 09AA017 (i.e. Tagish Lake at 10 Mile Road), and identifying the source of the discrepancy, should that discrepancy be confirmed.
- Groundwater flooding was identified as a significant concern for stakeholders in Carcross, Tagish, Marsh Lake, and Lake Laberge. Future studies should be completed to better understand the ongoing changes to groundwater levels throughout the Southern Lakes, and potential mitigation measures that could be implemented to minimize flood issues.
- Considerable concern was expressed by stakeholders regarding shoreline erosion during flood events. Future studies should identify areas that are more susceptible to erosion.
- Guidance should be provided to residents regarding potential shoreline erosion protection measures, as well as different approaches to mitigating flooding due to high groundwater.
- Stakeholders in Carcross and Marsh Lake expressed concerns regarding sediment deposition on Bennett Lake and Marsh Lake. Future LiDAR surveys can serve to evaluate the ongoing geomorphological processes on Bennett Lake and Nares Lake.
- AEP flood levels from this study should be provided to residents to facilitate the construction of flood mitigation works for individual properties, as required.
- AEP flood hazard mapping and flood levels from this study should be used to facilitate community-scale flood response planning.

11.0 REFERENCES

1) Bonsal, B.R., Peters, D.L., Seglenieks, F., Rivera, A., and Berg, A. (2019). "Changes in freshwater availability across Canada," Chapter 6 in Canada's Changing Climate Report, (ed.) E. Bush and D.S. Lemmen; Government of Canada, Ottawa, Ontario, p. 261-342.
2) Canadian Climate Centre. https://climate-change.canada.ca/climate-data/#/cmip5-data . Accessed on December 6, 2023.
3) Cannon, A.J., S.R. Sobie, and T.Q. Murdock (2015). "Precipitation by Quantile Mapping: How Well Do Methods Preserve Changes in Quantiles and Extremes?" Journal of Climate, 28(17), 6938-6959, doi:10.1175/JCLI-D-14- 00754.1.
4) Cohen, S., Bush, E., Zhang, X., Gillett, N., Bonsal, B., Derksen, C., Flato, G., Greenan, B., Watson, E. (2019). "Changes in Canada's Regions in a National and Global Context," Chapter 8 in Canada's Changing Climate Report, (ed.) E. Bush and D.S. Lemmen; Government of Canada, Ottawa, Ontario, p. 424-443.
5) ClimateData.ca. Accessed on July 11, 2023.
6) Derksen, C., Burgess, D., Duguay, C., Howell, S., Mudryk, L., Smith, S., Thackeray, C. and Kirchmeier-Young, M. (2019). "Changes in snow, ice, and permafrost across Canada," Chapter 5 in Canada's Changing Climate Report, (ed.) E. Bush and D.S. Lemmen; Government of Canada, Ottawa, Ontario, p. 194-260.
7) Environmental Dynamics Inc. (2015). "Flood Frequency Relationships for Yukon Floodplain Communities." Environmental Dynamics Inc.
8) FENCO (1974). "Yukon Flood Study." FENCO.
9) Government of Yukon – Emergency Measures Organization (2021). "2021 Yukon Flood Recovery Plan." Government of Yukon.
10) Government of Yukon – Emergency Measures Organization (2022). "2022 Yukon Flood Recovery Plan." Government of Yukon.
11) Hughes, S.A. (2003a). "Wave momentum flux parameter for coastal structure design," ERDC/CHL CHETN-III-67. USACE.
12) Hughes, S.A. (2003b). "Estimating irregular wave runup on smooth impermeable slopes," ERDC/CHL CHETN-III-68. USACE.
13) Hughes, S.A. (2005). "Estimating irregular wave runup on rough, impermeable slopes," ERDC/CHL CHETN-III-70. USACE.
14) Kassambara A (2023). _ggpubr: 'ggplot2' Based Publication Ready Plots_. R package version 0.6.0, https://CRAN.R-project.org/package=ggpubr.
15) KGS Group, 2010. "Hydraulic Modelling of Yukon River: Marsh Lake to Schwatka Lake." KGS Group.
16) Kuiper, E (1965). "Water Resources Development: Planning, Engineering and Economics. Springer, New York NY.
17) McKenney, D. W., M. F. Hutchinson, P. Papadopol, K. Lawrence, J. Pedlar, K. Campbell, E. Milewska, R. F. Hopkinson, D. Price, and T. Owen (2011). "Customized Spatial Climate Models for North America." Bull. Amer. Meteor. Soc., 92 12, 1611-1622
Moriasi, D.N., Gitau, M.W., Pai, N., and Daggupati P. (2015). "Hydrologic and Water Quality Models:

Performance Measures and Evaluation Criteria." American Society of Agricultural and Biological Engineers, 58(6): 1763-1755. DOI: 10.13031/trans.58.10715.
18) Morrison Hershfield (2021). "Water Level Analysis for Yukon Communities." Morrison Hershfield.
19) Morrison Hershfield (2022). "Updated Flood Frequency Analysis for Southern Lakes." Morrison Hershfield.
20) Natural Resources Canada (2023). "Federal Hydrologic and Hydraulic Procedures for Flood Hazard Delineation, Version 2.0." Natural Resources Canada. DOI: https://doi.org/10.4095/332156.
21) Northern Climate Exchange, Yukon Research Centre, Yukon College (2012). "Projected Future Changes in Glaciers and their Contribution to Discharge of the Yukon River at Whitehorse."
22) Northern Climate Exchange (2016). "Evaluating climate change impacts on the upper Yukon River basin: projecting future conditions using glacier, climate and hydrological models."
23) Rasouli, K., Pomeroy, J.W., and Whitfield, P.H. (2019a). "Are the effects of vegetation and soil changes as important as climate change impacts on hydrological processes?" Hydrology and Earth System Sciences, 23: 4933-4954. DOI: 10.5194/hess-23-4933-2019
24) Rasouli, K., Pomeroy, J.W., and Whitfield, P.H. (2019b). "Hydrological Responses of Headwater Basins to Monthly Perturbed Climate in the North American Cordillera." Journal of Hydrometeorology, 20(5): 863-882. DOI: 10.1175/JHM-D-18-0166.1.
25) Stantec (2022). "2022 Post-Melt Dike Inspections and Flood Preparedness." Stantec.
26) Stockdon, H.F., Holman, R.A., Hownd, P.A., & Sallenger Jr., A.H. (2006). "Empirical parameterization of setup, swash and runup," Coastal Engineering, 53(7), 573-588.
27) Underwood McLellan Ltd. (1983). "Yukon River Basin Flood Risk Study." Underwood McLellan Ltd.
28) United States Army Corps of Engineers. (1984). "Shore Protection Manual." USACE.
29) United States Army Corps of Engineers. (2001). "Coastal Engineering Manual, EM 1110-2-1100". USACE.
30) Zhang, X., Flato, G., Kirchmeier-Young, M., Vincent, L., Wan, H., Wang, X., Rong, R., Fyfe, J., Li, G., Kharin, V.V. (2019). "Changes in Temperature and Precipitation Across Canada", Chapter 4 in Bush, E. and Lemmen, D.S. (Eds.) Canada's Changing Climate Report. Government of Canada, Ottawa, Ontario, pp 112-193.

APPENDIX A

Site Visit Photographs

Photo 1: 2021 High Water Mark in Carcross

Photo 2: Pedestrian Bridge in Carcross

Photo 3: Bennett Lake Shoreline in Carcross

Photo 4: High Water Mark in Carcross

Photo 5: Tagish Lake Shoreline in Tagish

Photo 6: Tagish Lake Shoreline in Tagish

Photo 7: Tagish River Shoreline in Tagish

Photo 8: Marsh Lake Shoreline near Judas Creek

Photo 9: Marsh Lake Shoreline near Judas Creek

Photo 10: Temporary Flood Protection along Marsh Lake near Judas Creek

Photo 11: Marsh Lake Shoreline near Swan Haven

Photo 12: Marsh Lake Shoreline near Swan Haven

Photo 13: Temporary Erosion Protection on Marsh Lake Shoreline near Swan Haven

Photo 14: Marsh Lake Shoreline near Army Beach

Photo 15: Marsh Lake Shoreline near Army Beach

Photo 16: Yukon River near Lewes Dam

Photo 17: Deep Creek near Lake Laberge

Photo 18: Lake Laberge Shoreline near Deep Creek

Photo 19: High Water Marks near Lake Laberge at Deep Creek

Photo 20: High Water Marks near Lake Laberge at Deep Creek

Photo 21: Lake Laberge Shoreline near Jackfish Bay

Photo 22: Lake Laberge Shoreline Near Jackfish Bay

APPENDIX B

Monthly Water Level Frequency Curves

BENNETT LAKE

BENNETT LAKE JULY FREQUENCY CURVE

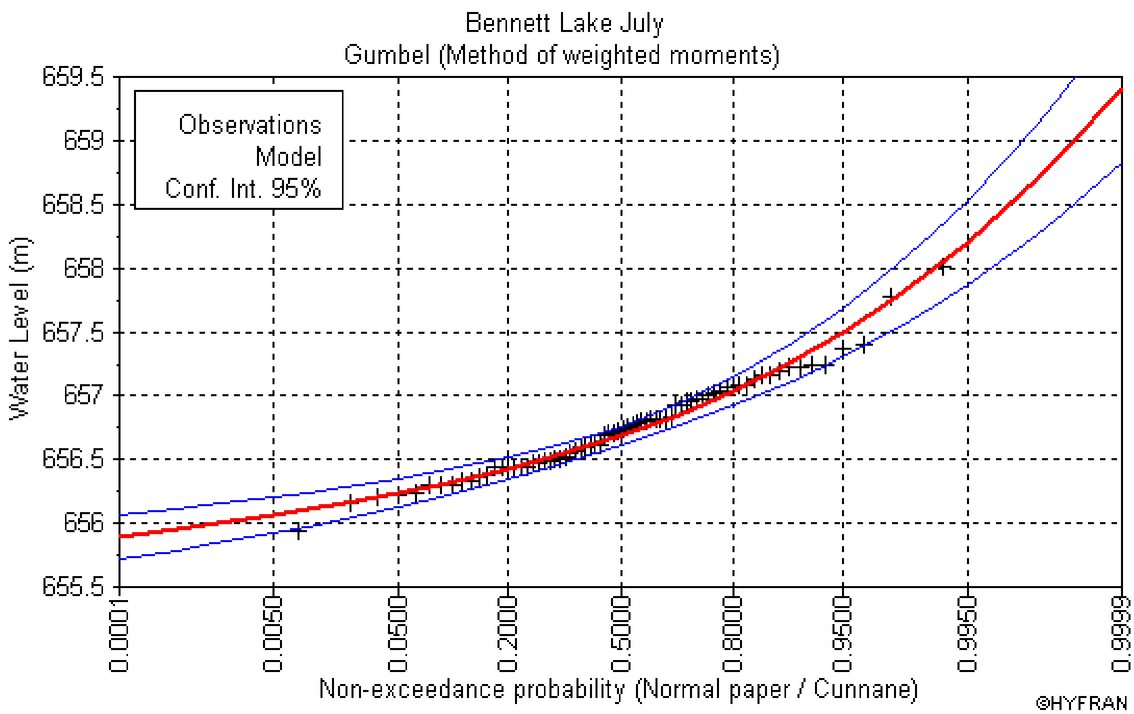

BENNETT LAKE AUGUST FREQUENCY CURVE

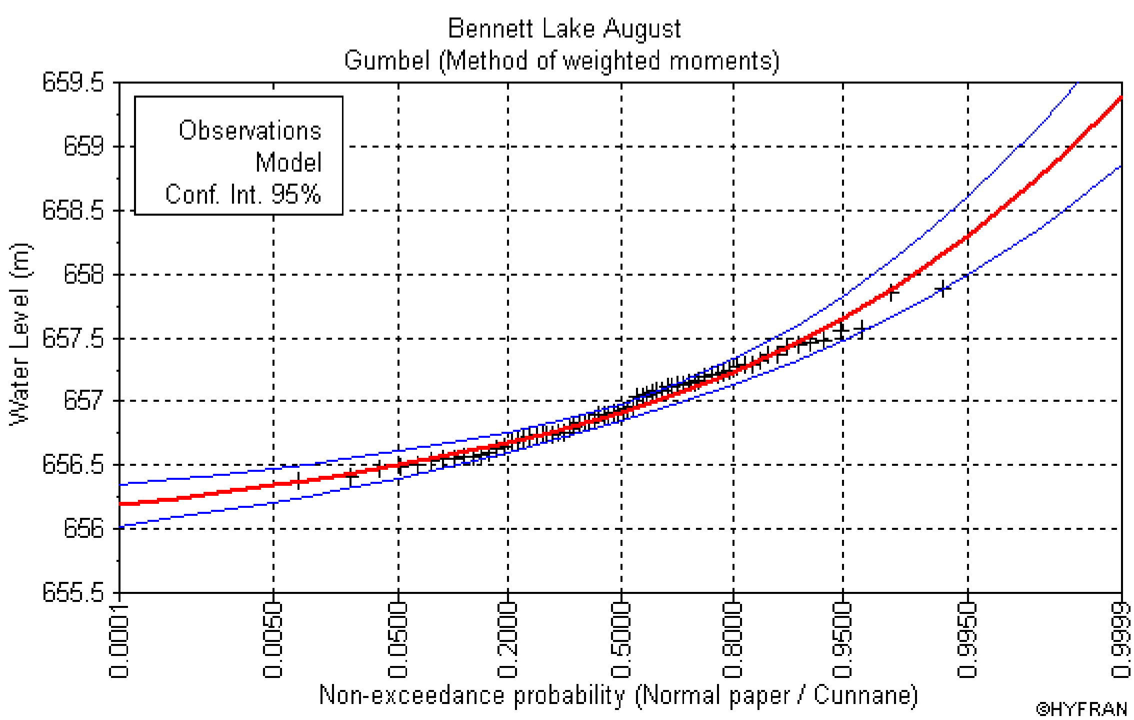

BENNETT LAKE SEPTEMBER FREQUENCY CURVE

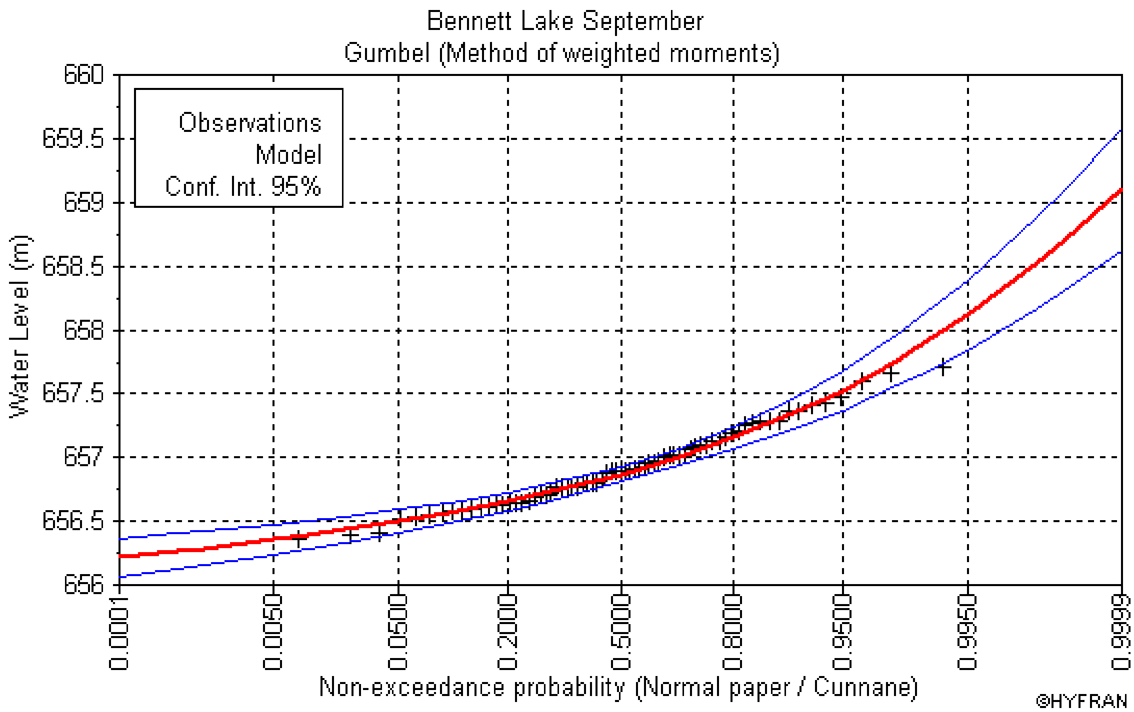

BENNETT LAKE OCTOBER FREQUENCY CURVE

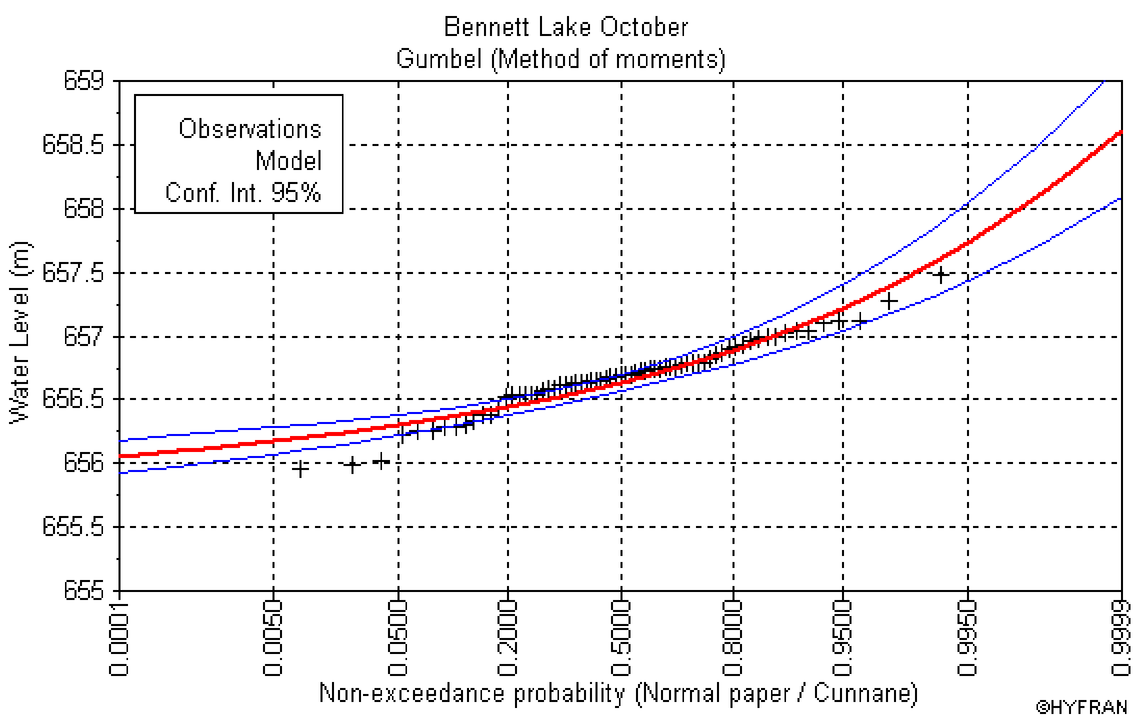

LAKE LABERGE

LAKE LABERGE JULY FREQUENCY CURVE

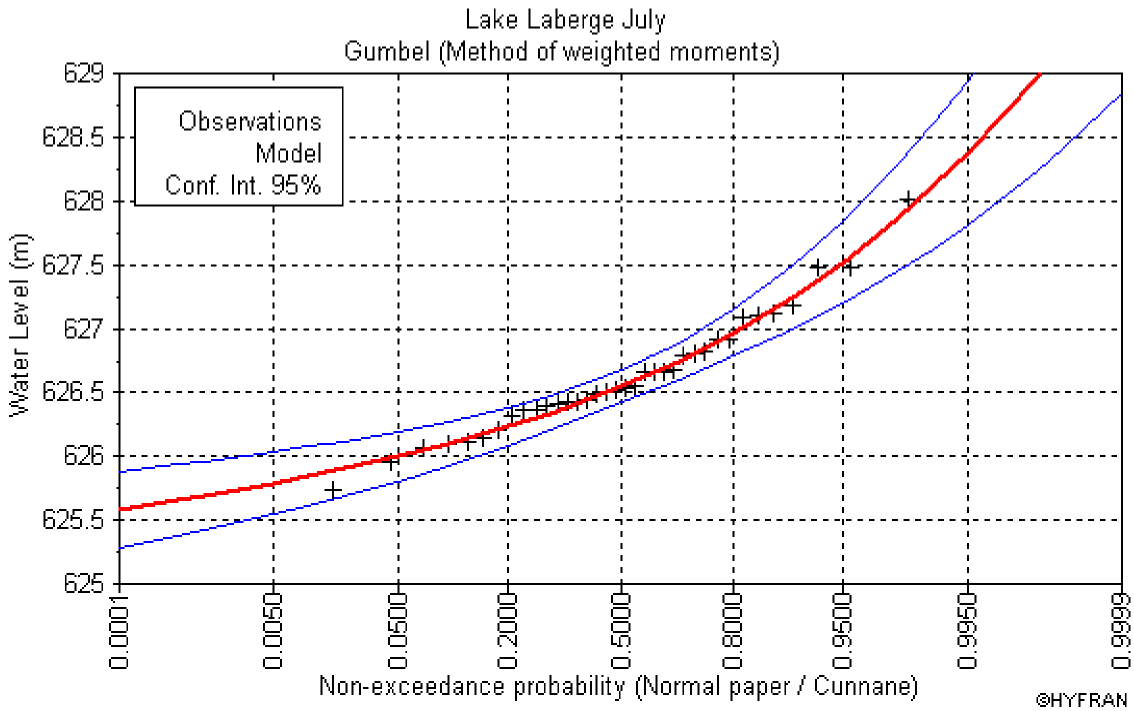

LAKE LABERGE AUGUST FREQUENCY CURVE

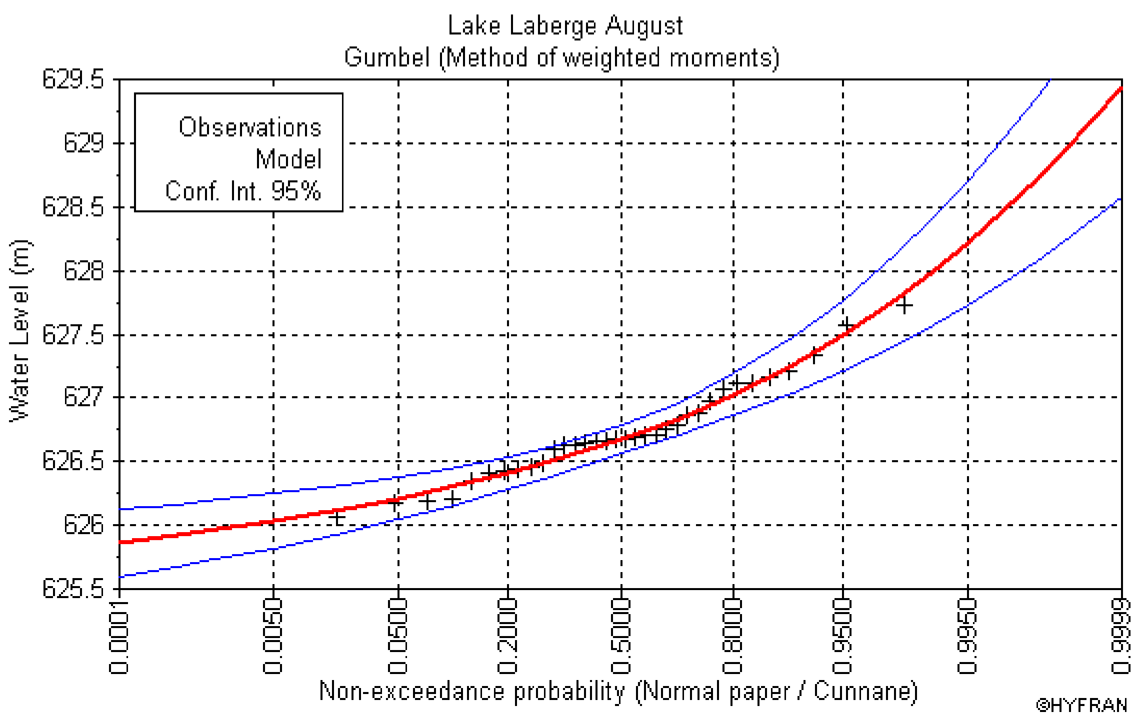

LAKE LABERGE SEPTEMBER FREQUENCY CURVE

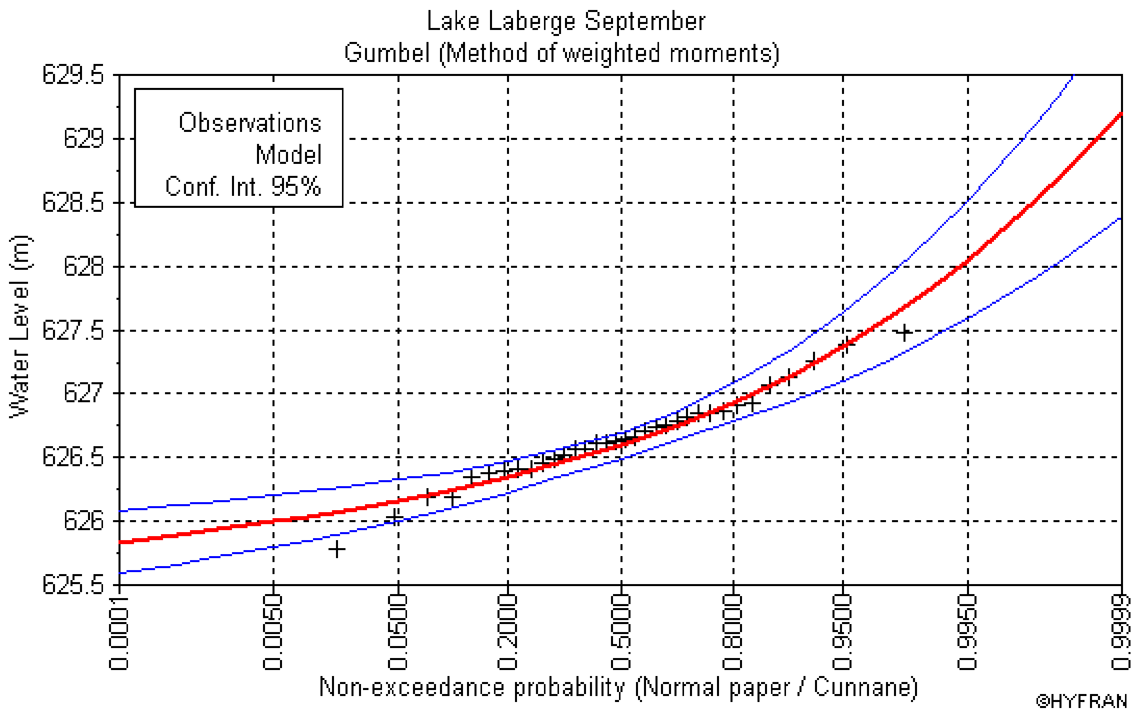

LAKE LABERGE OCTOBER FREQUENCY CURVE

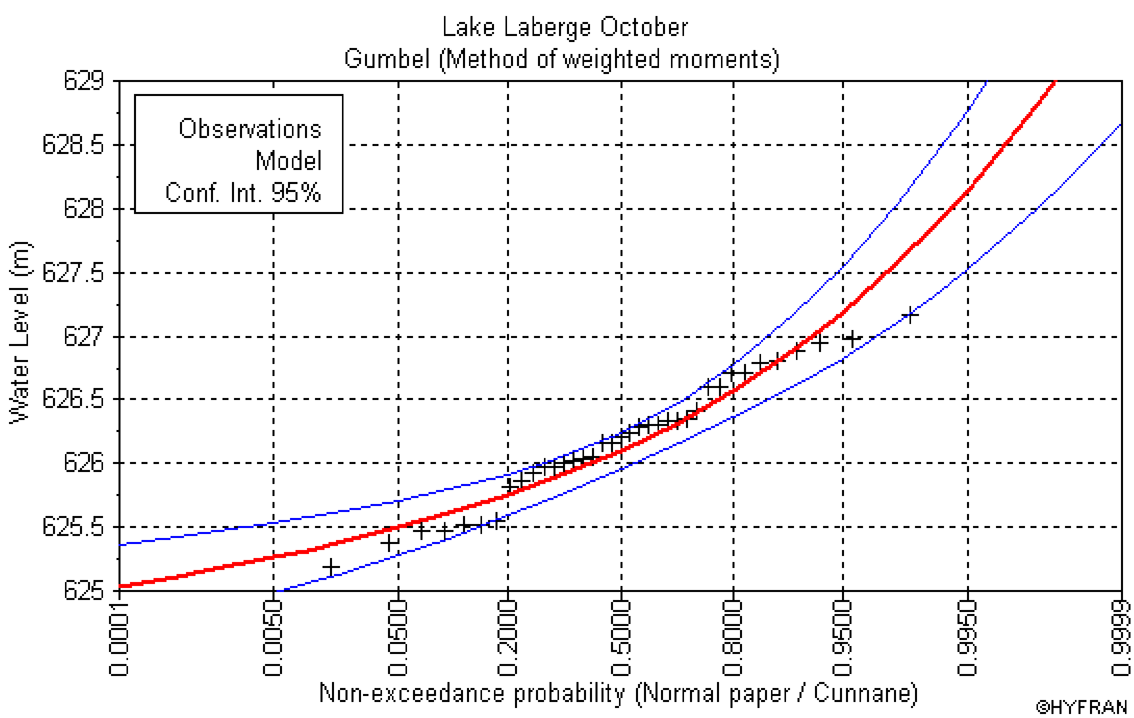

MARSH LAKE

MARSH LAKE JULY FREQUENCY CURVE

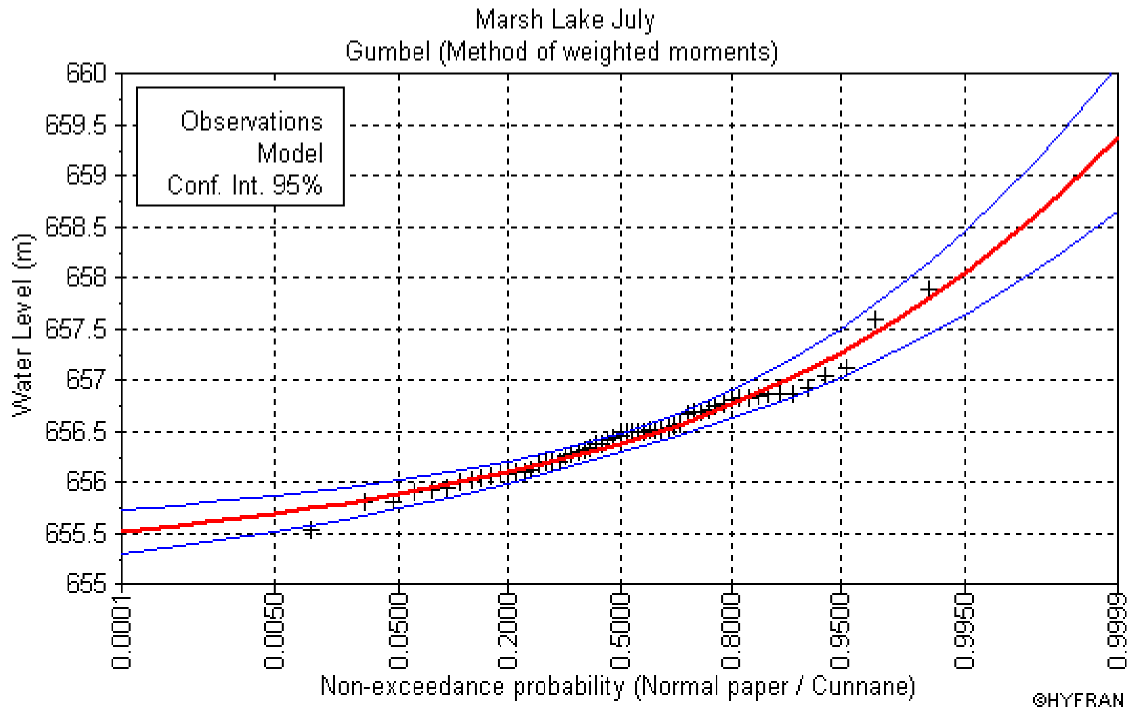

MARSH LAKE AUGUST FREQUENCY CURVE

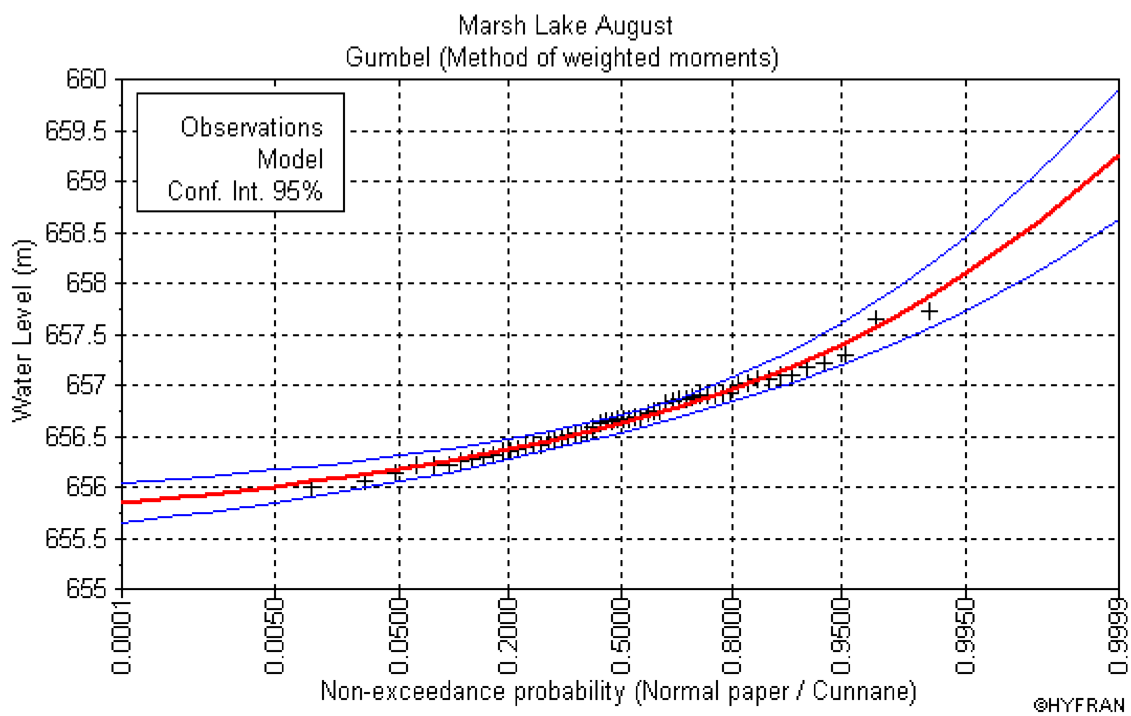

MARSH LAKE SEPTEMBER FREQUENCY CURVE

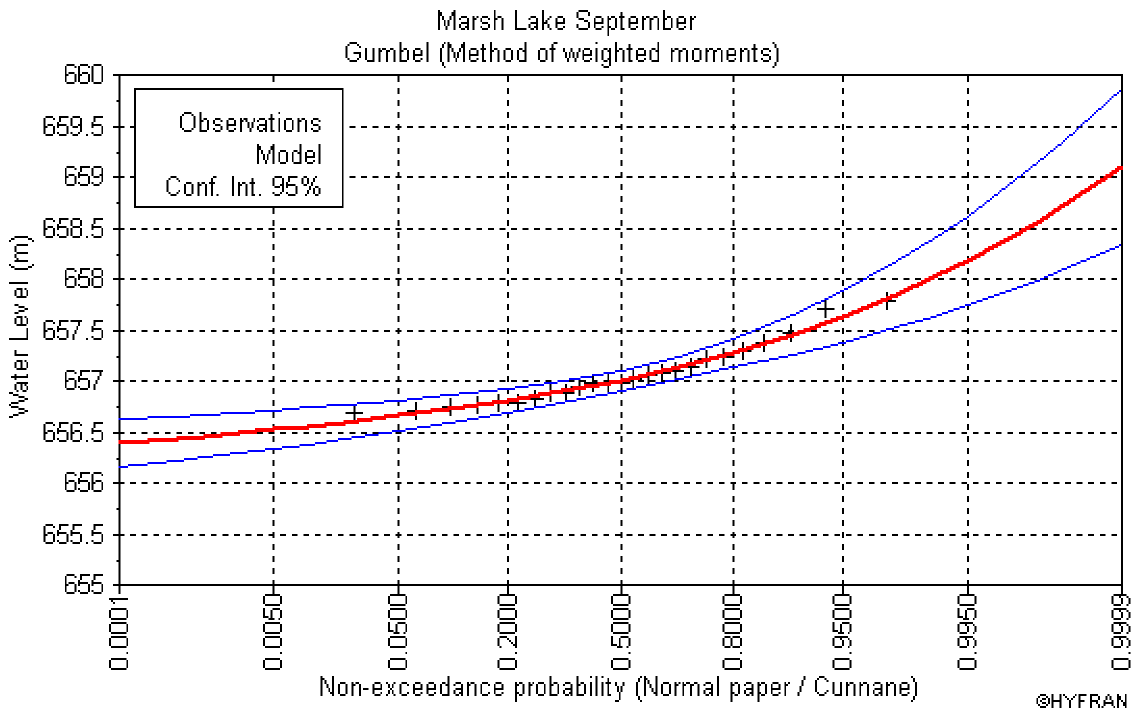

MARSH LAKE OCTOBER FREQUENCY CURVE

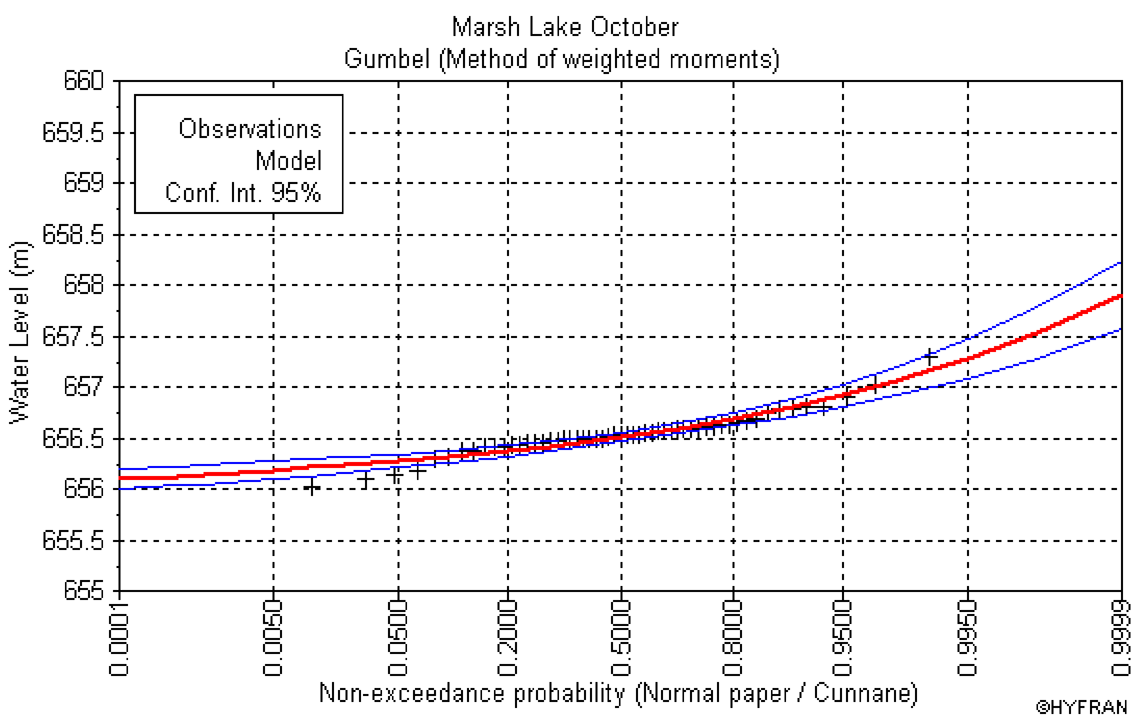

TAGISH LAKE

TAGISH LAKE JULY FREQUENCY CURVE

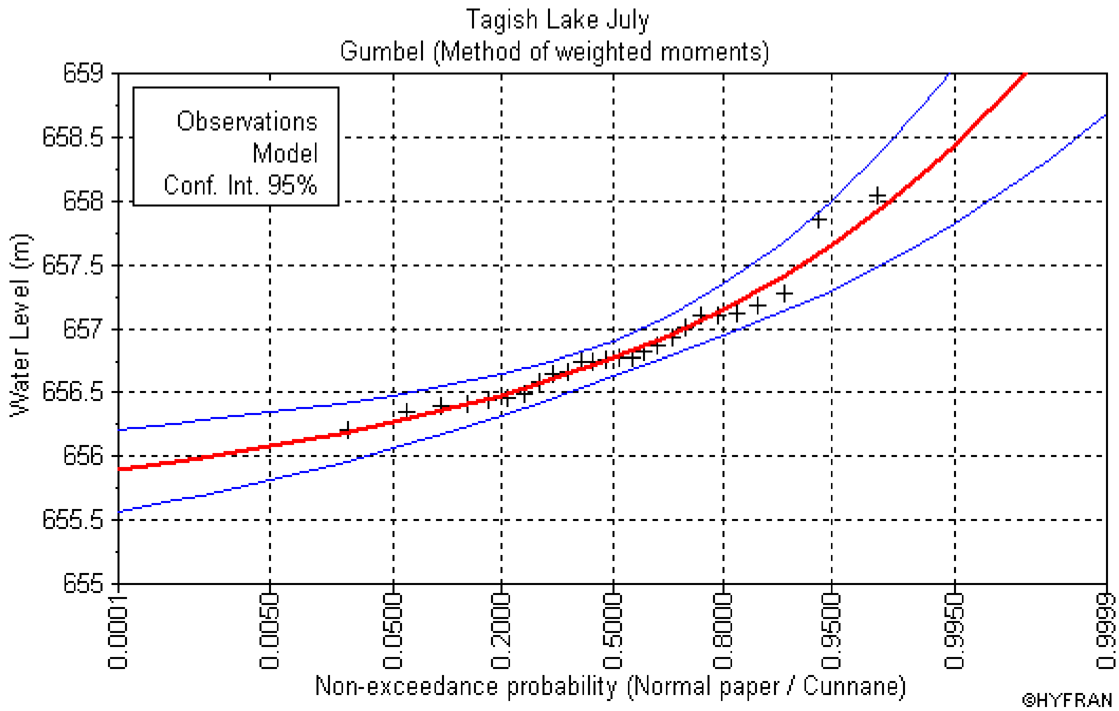

TAGISH LAKE AUGUST FREQUENCY CURVE

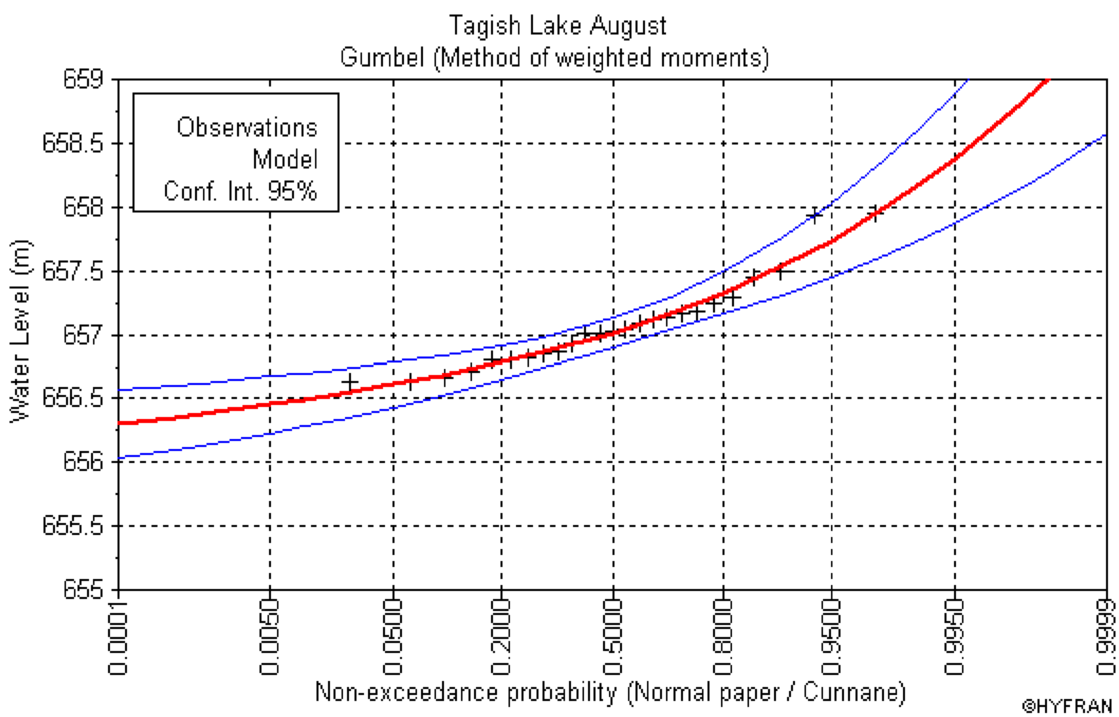

TAGISH LAKE SEPTEMBER FREQUENCY CURVE

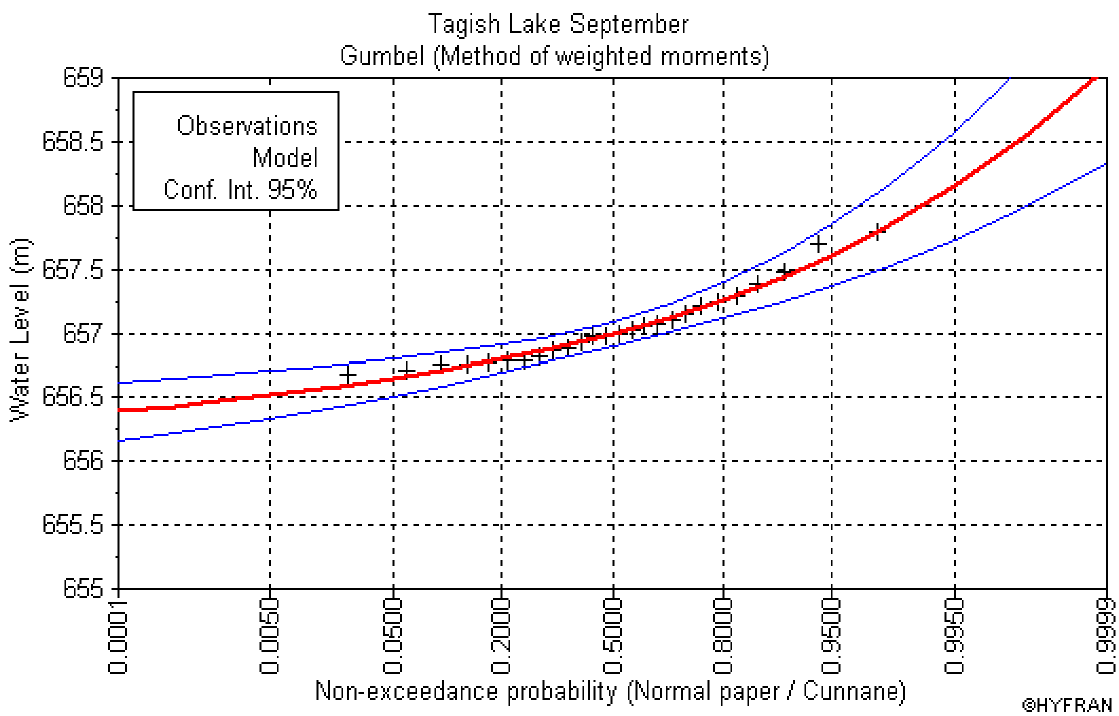

TAGISH LAKE OCTOBER FREQUENCY CURVE

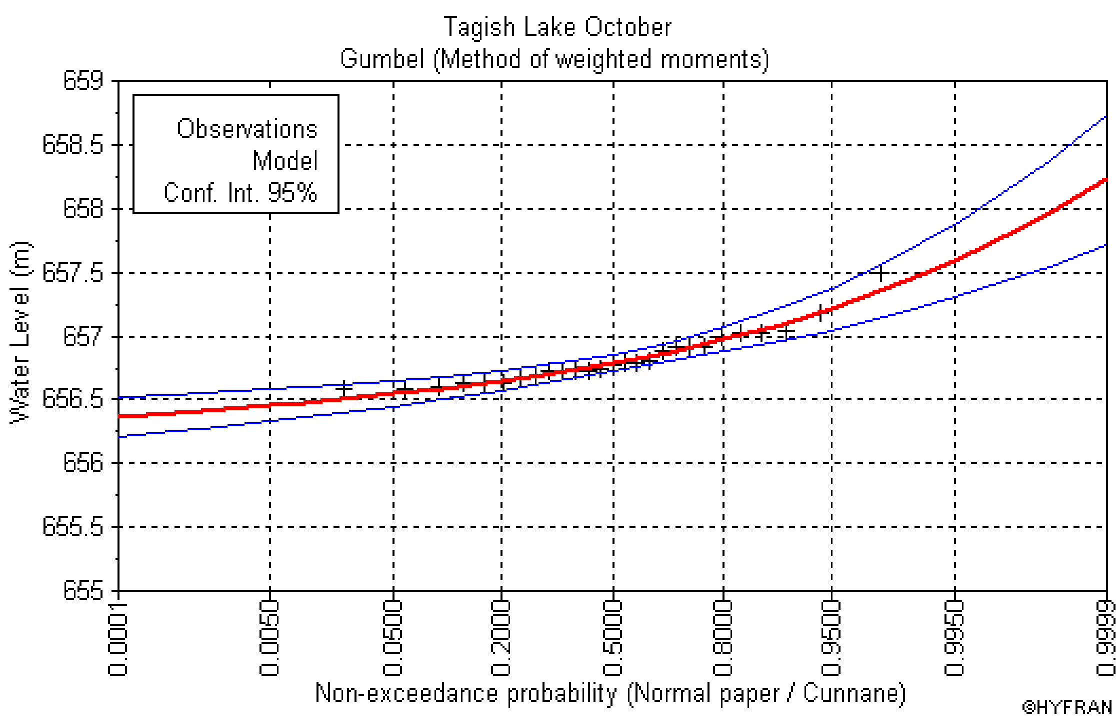

APPENDIX C

Monthly and Directional Wind Speed Frequency Curves

CARCROSS

CARCROSS NORTH MONTHLY FREQUENCY CURVES

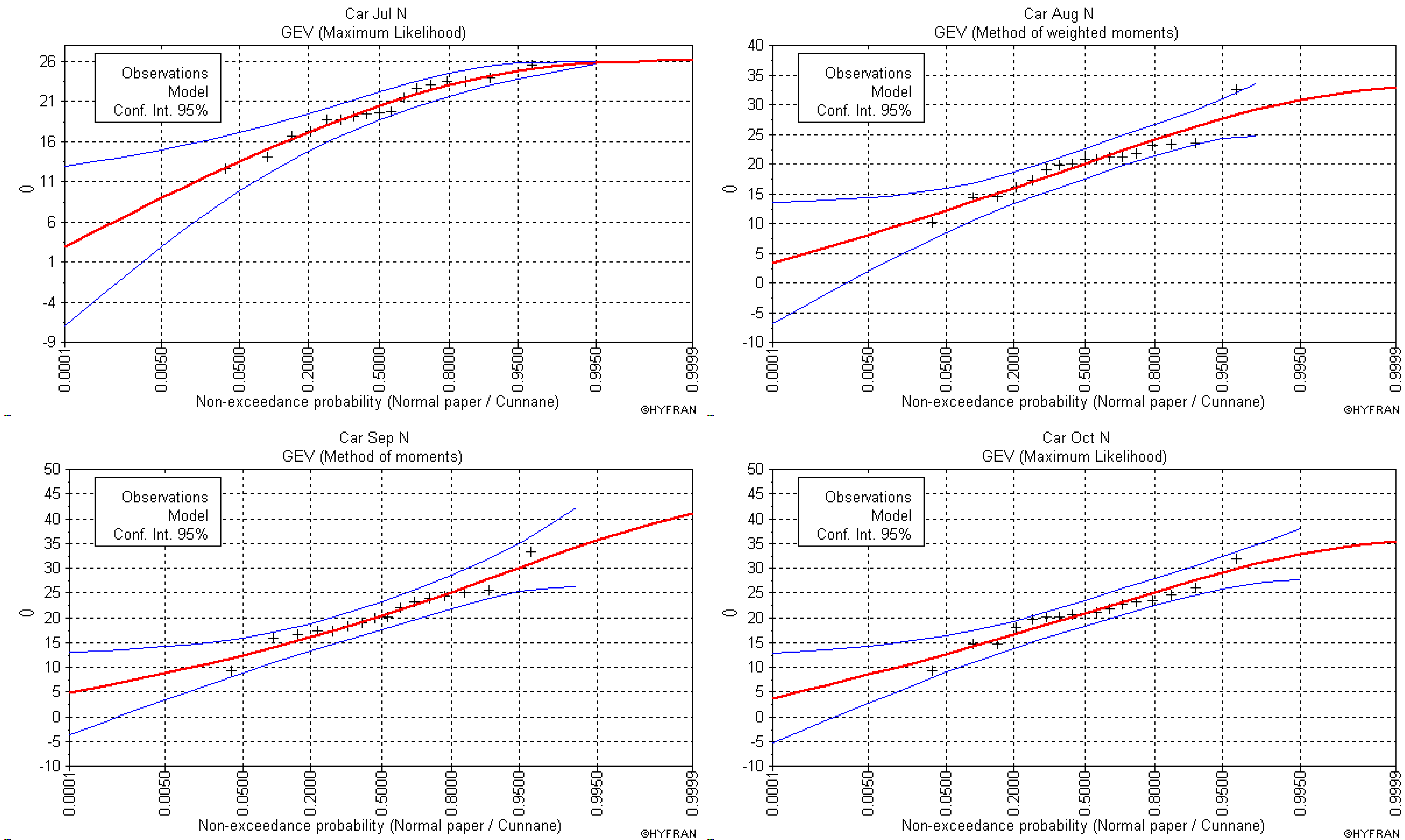

CARCROSS NORTHEAST MONTHLY FREQUENCY CURVES

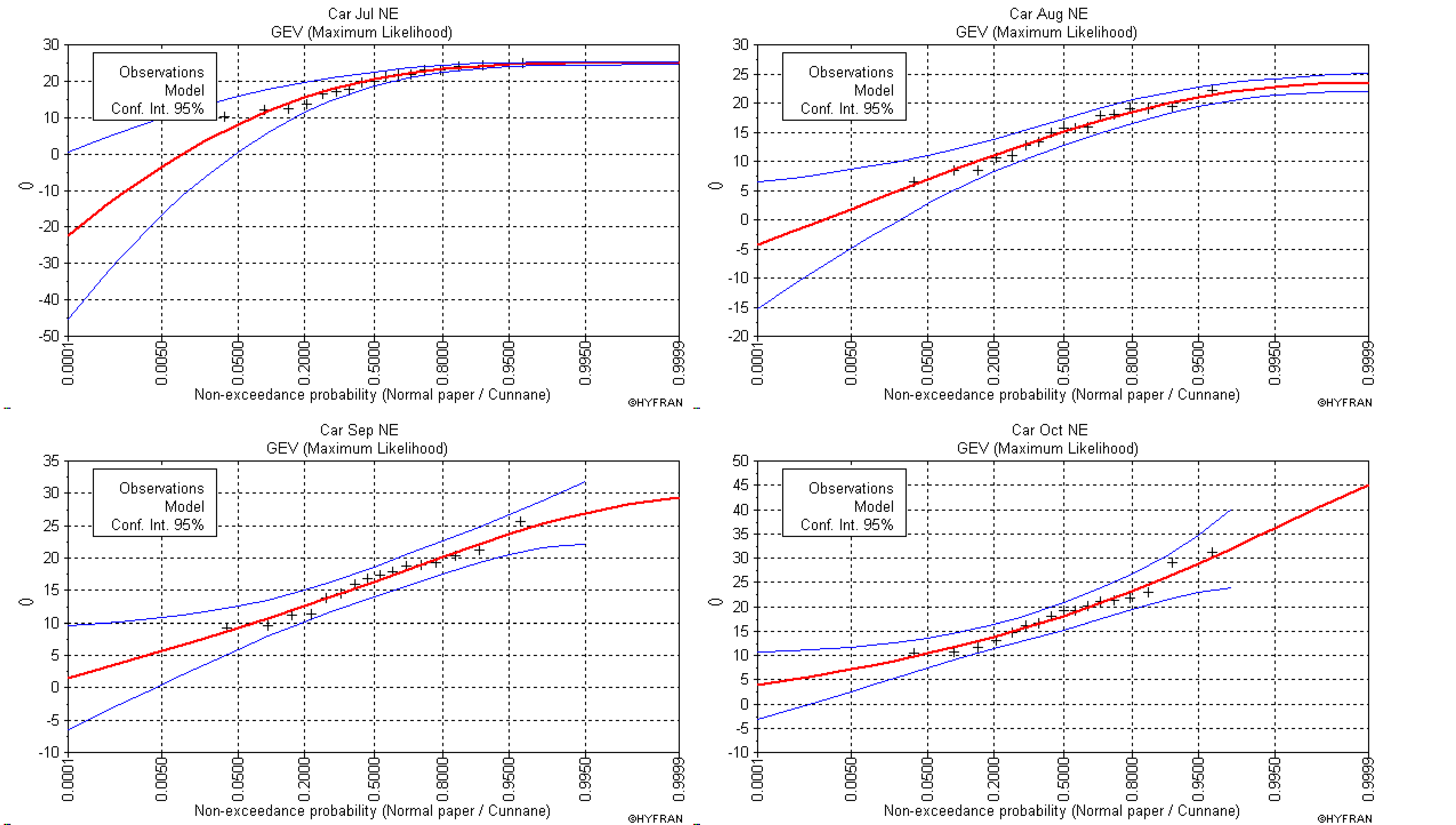

CARCROSS EAST MONTHLY FREQUENCY CURVES

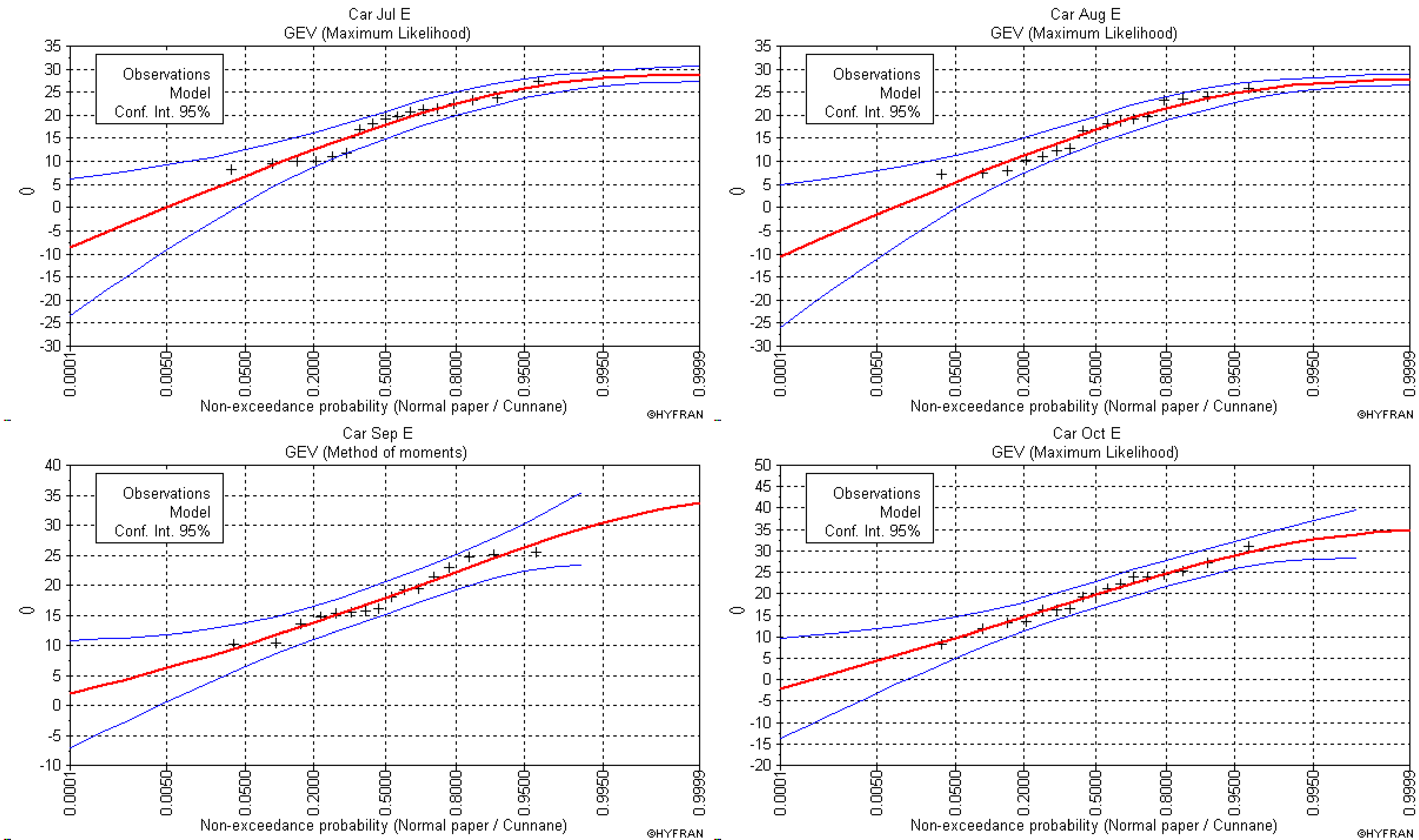

CARCROSS SOUTHEAST MONTHLY FREQUENCY CURVES

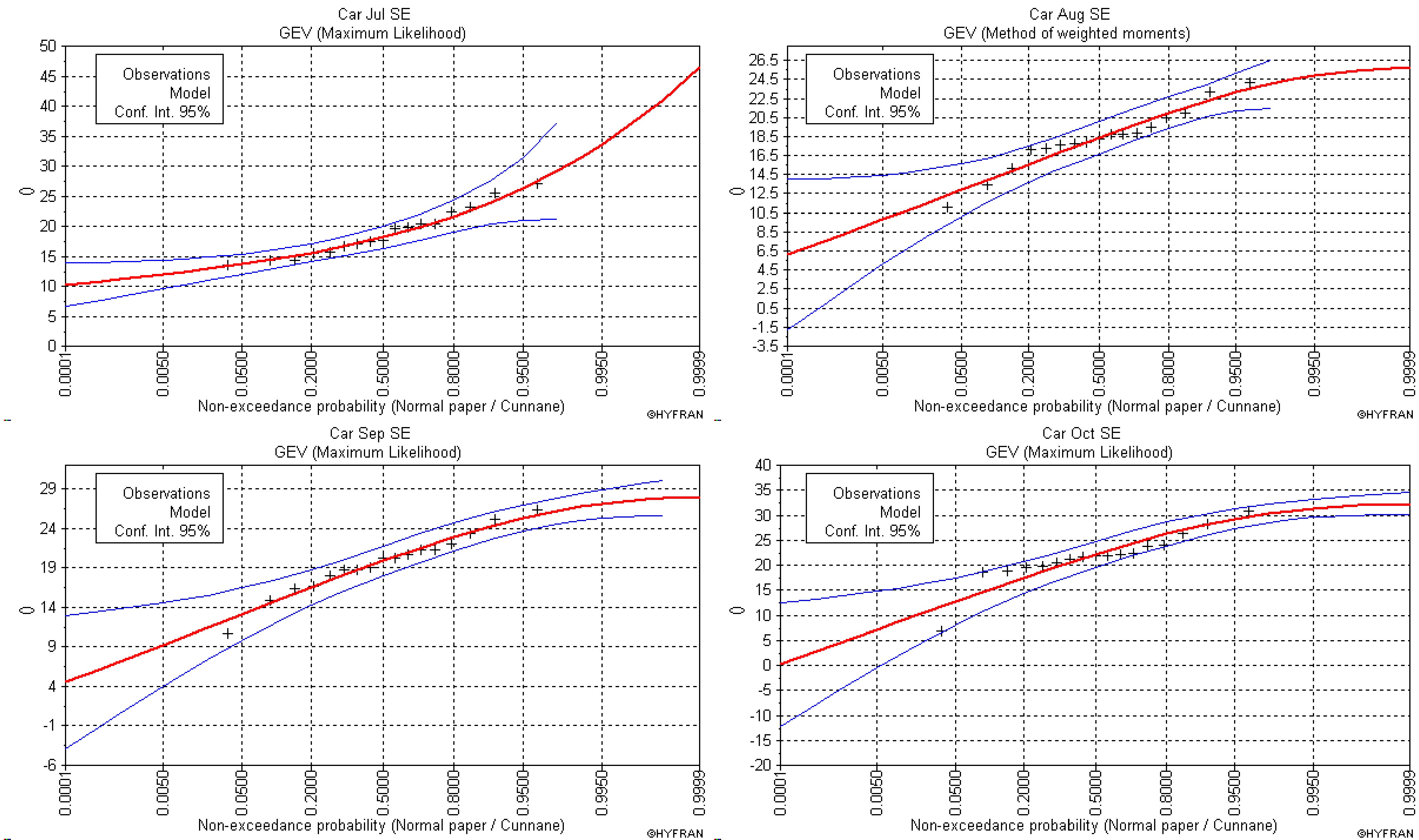

CARCROSS SOUTH MONTHLY FREQUENCY CURVES

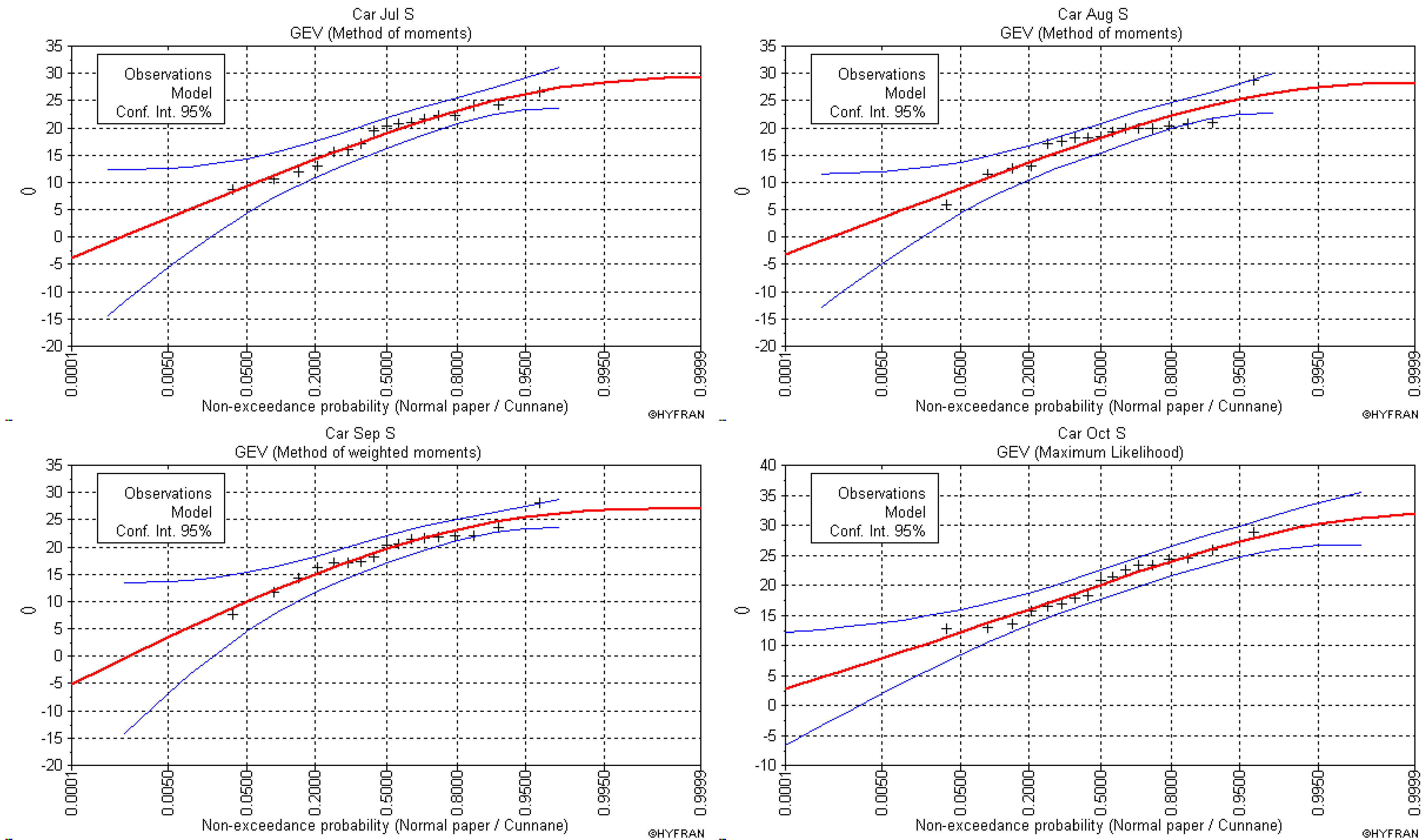

CARCROSS SOUTHWEST MONTHLY FREQUENCY CURVES

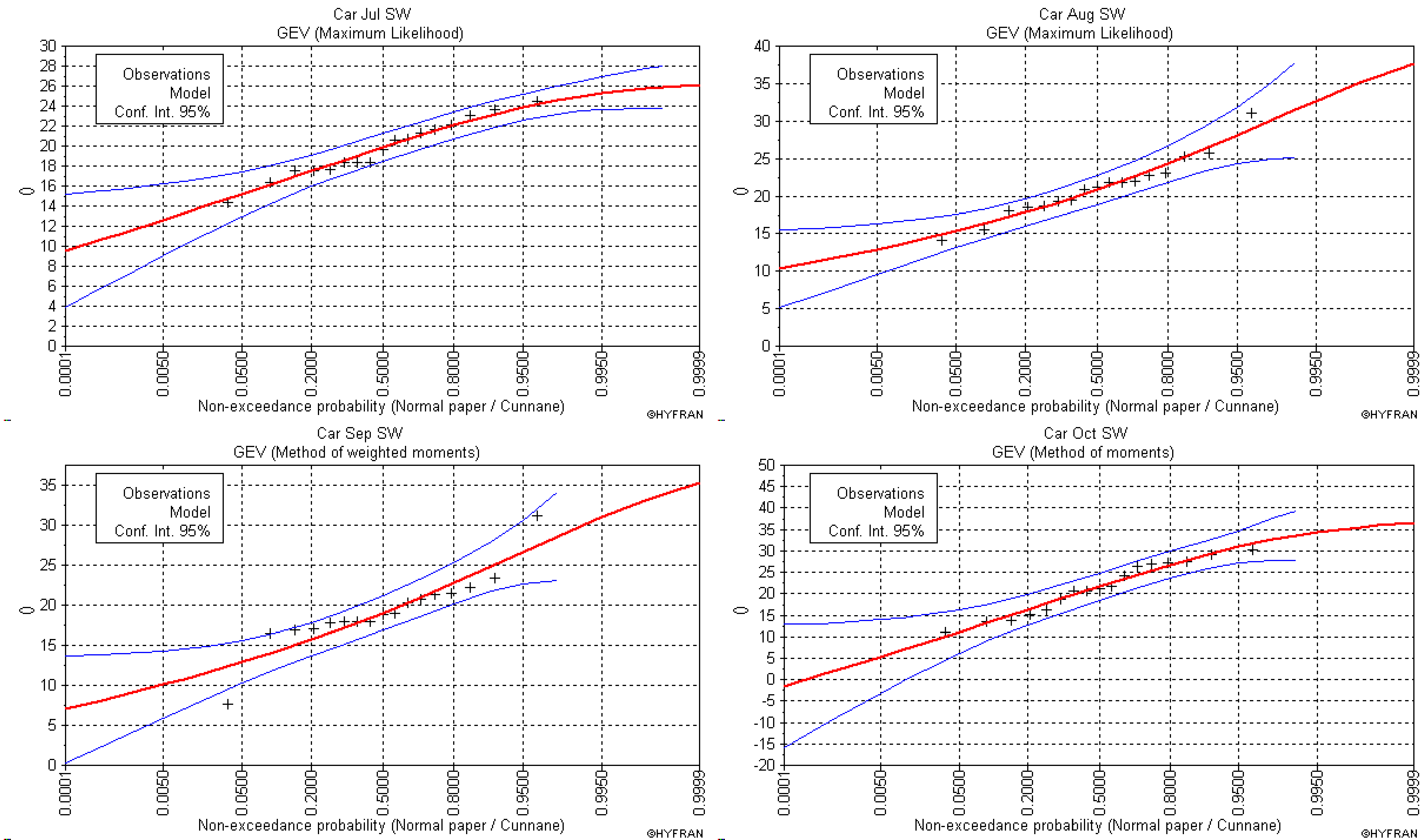

CARCROSS WEST MONTHLY FREQUENCY CURVES

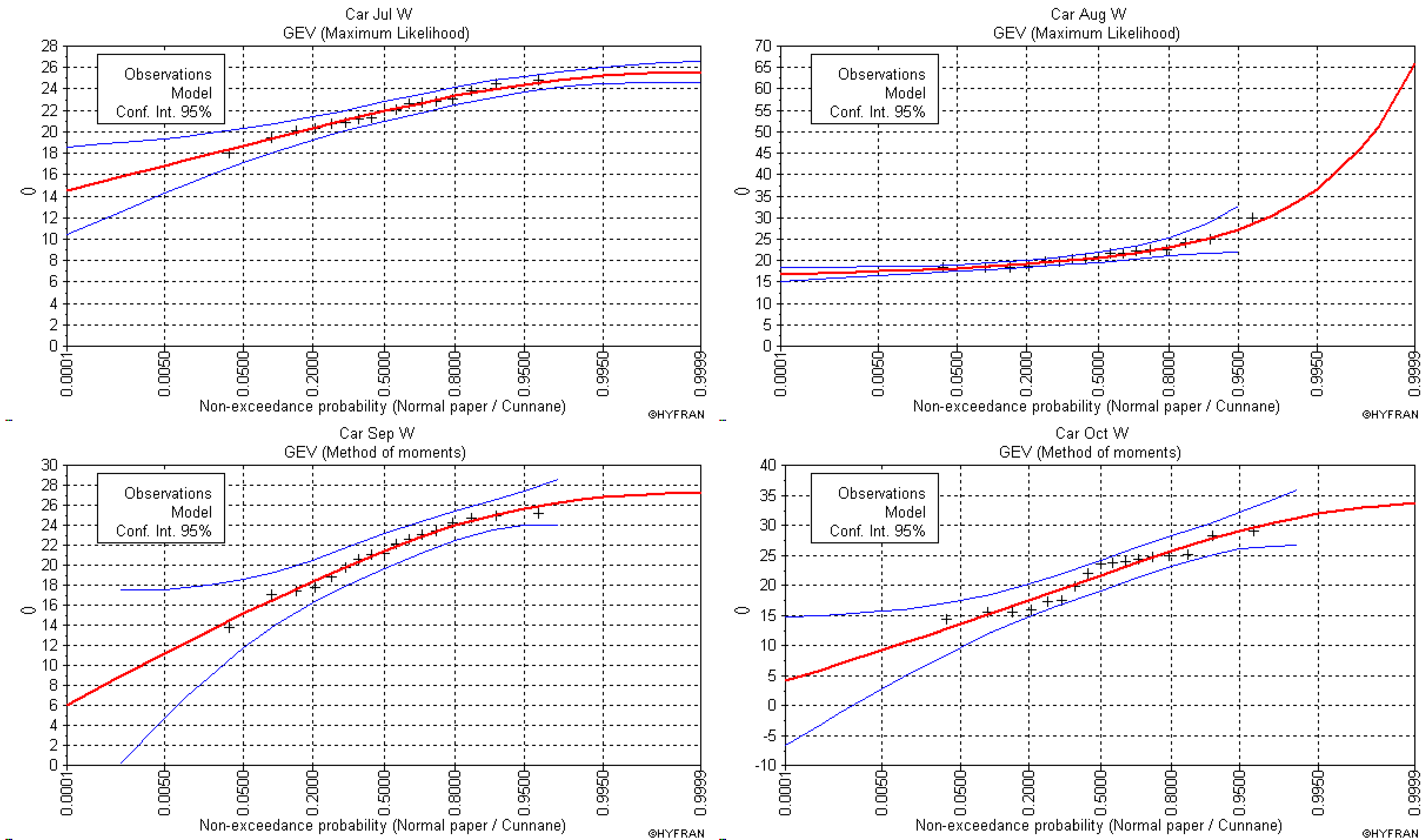

CARCROSS NORTHWEST MONTHLY FREQUENCY CURVES

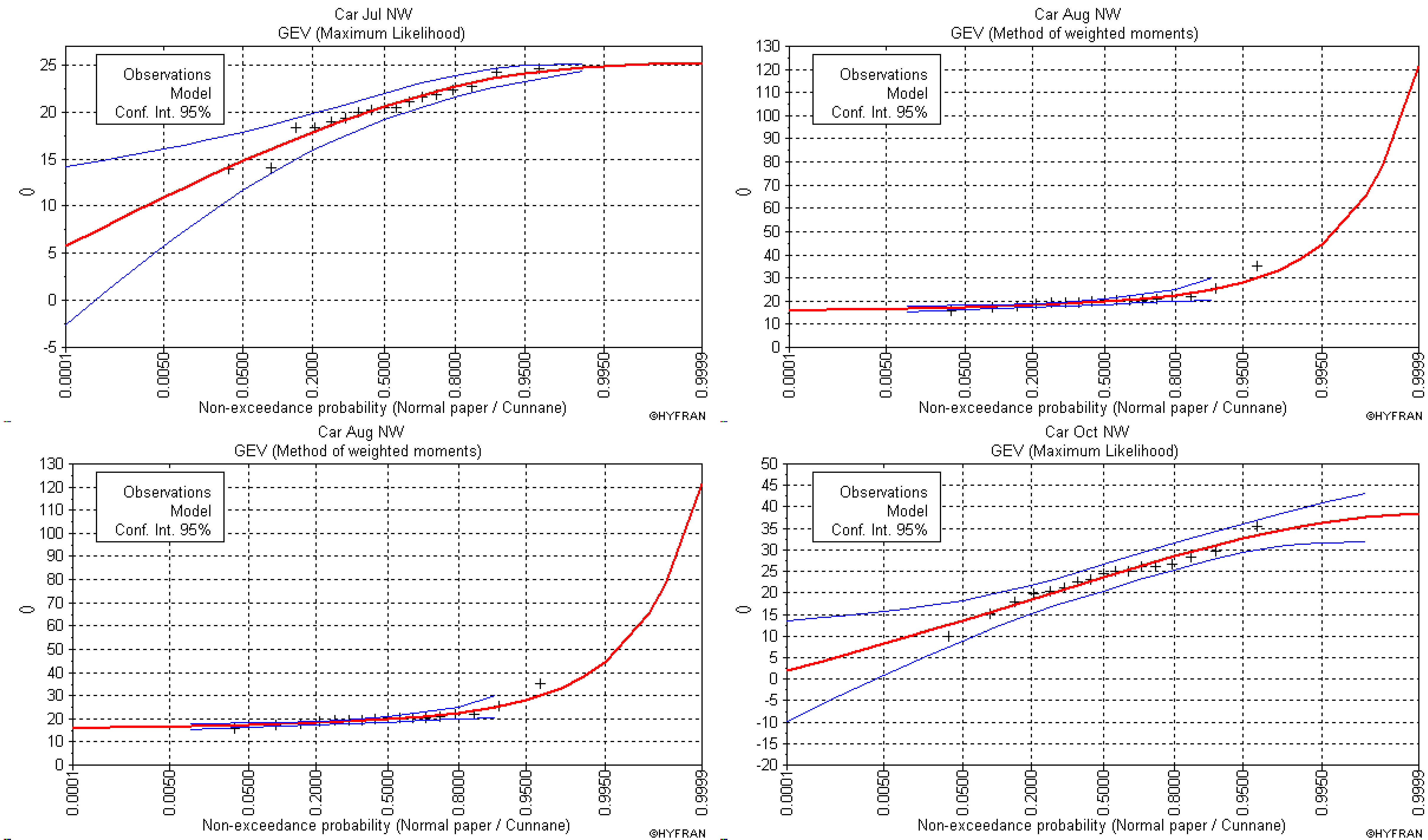

JAKE'S CORNER

JAKE'S CORNER NORTH MONTHLY FREQUENCY CURVES

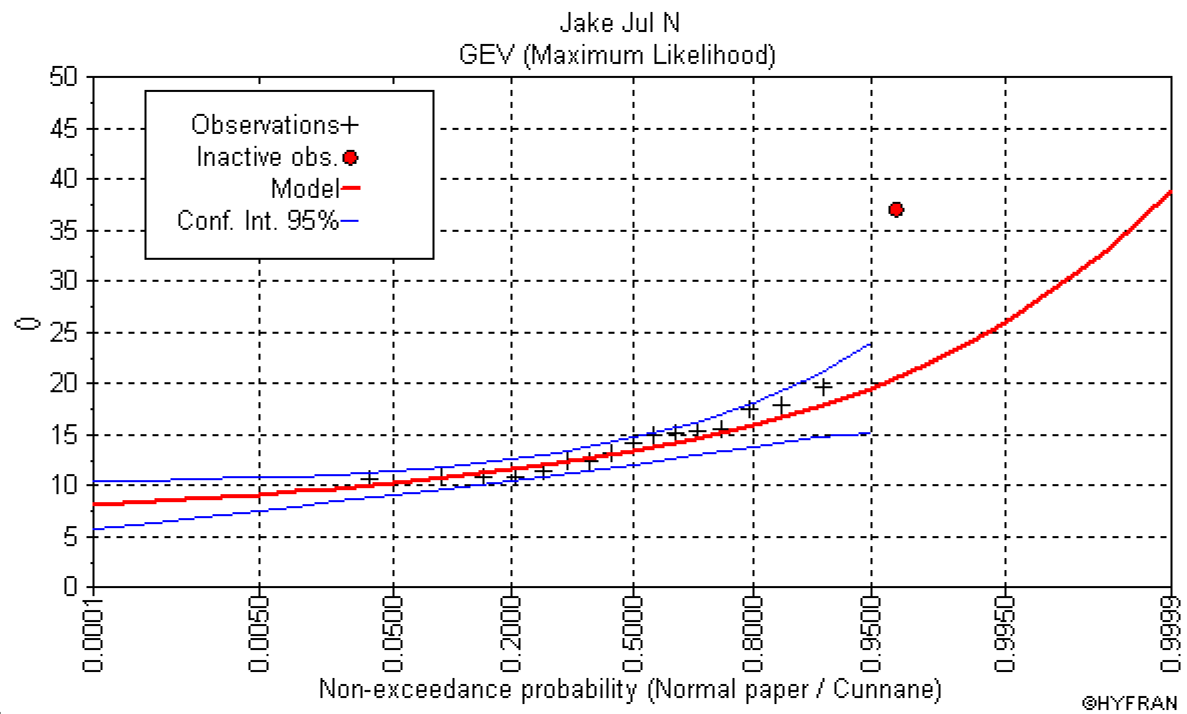

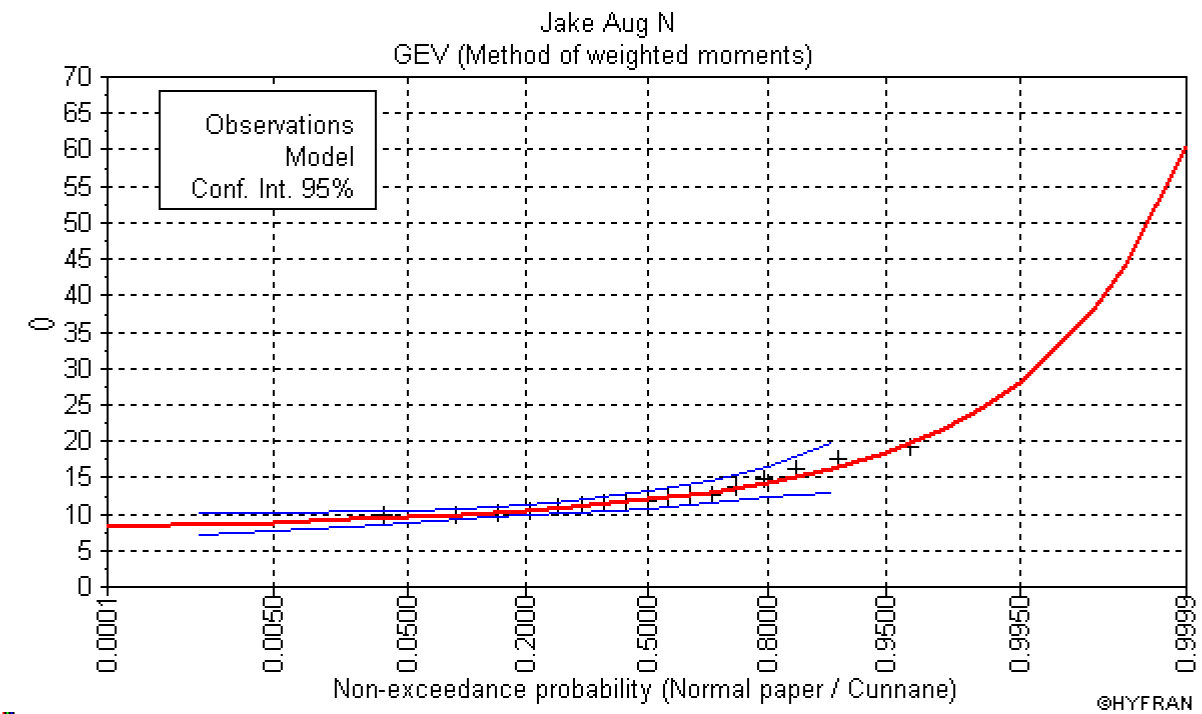

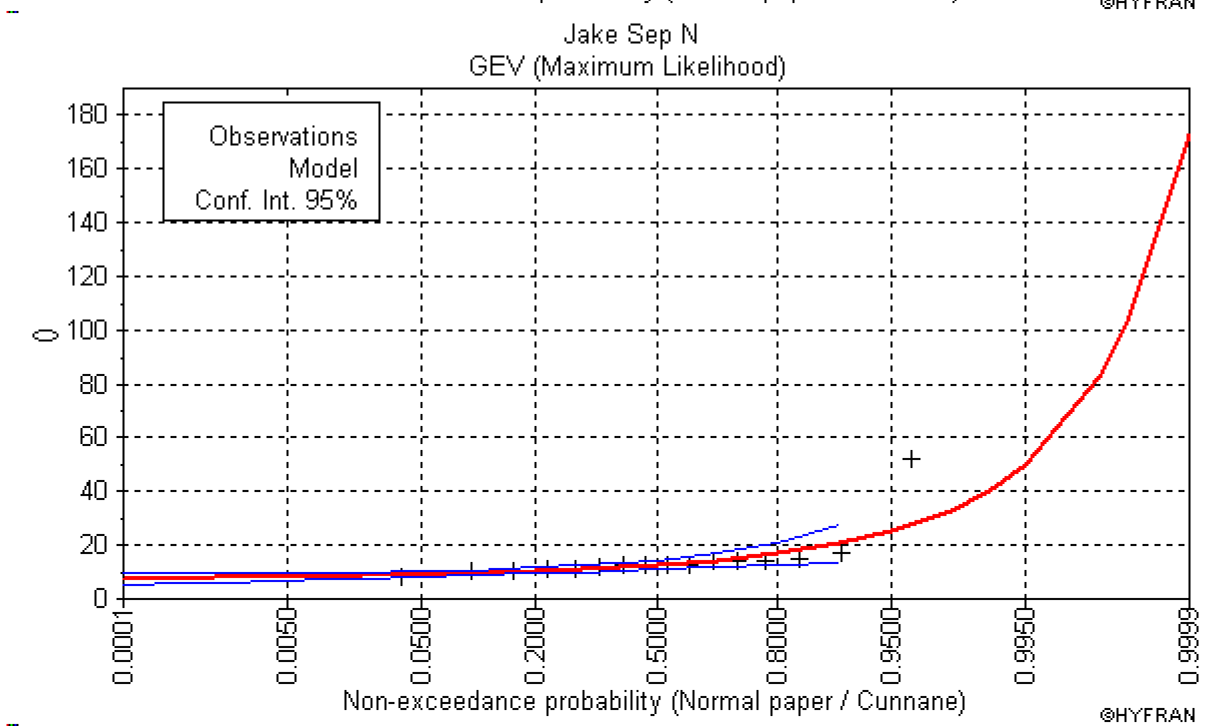

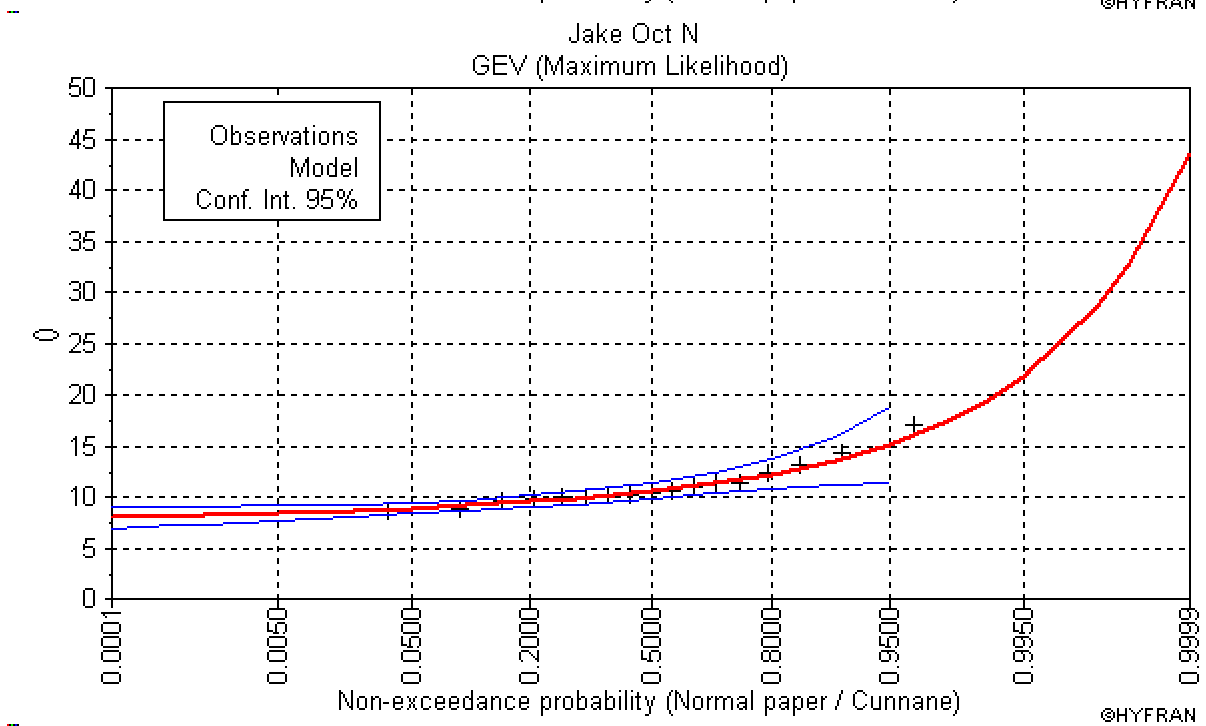

JAKE'S CORNER NORTHEAST MONTHLY FREQUENCY CURVES

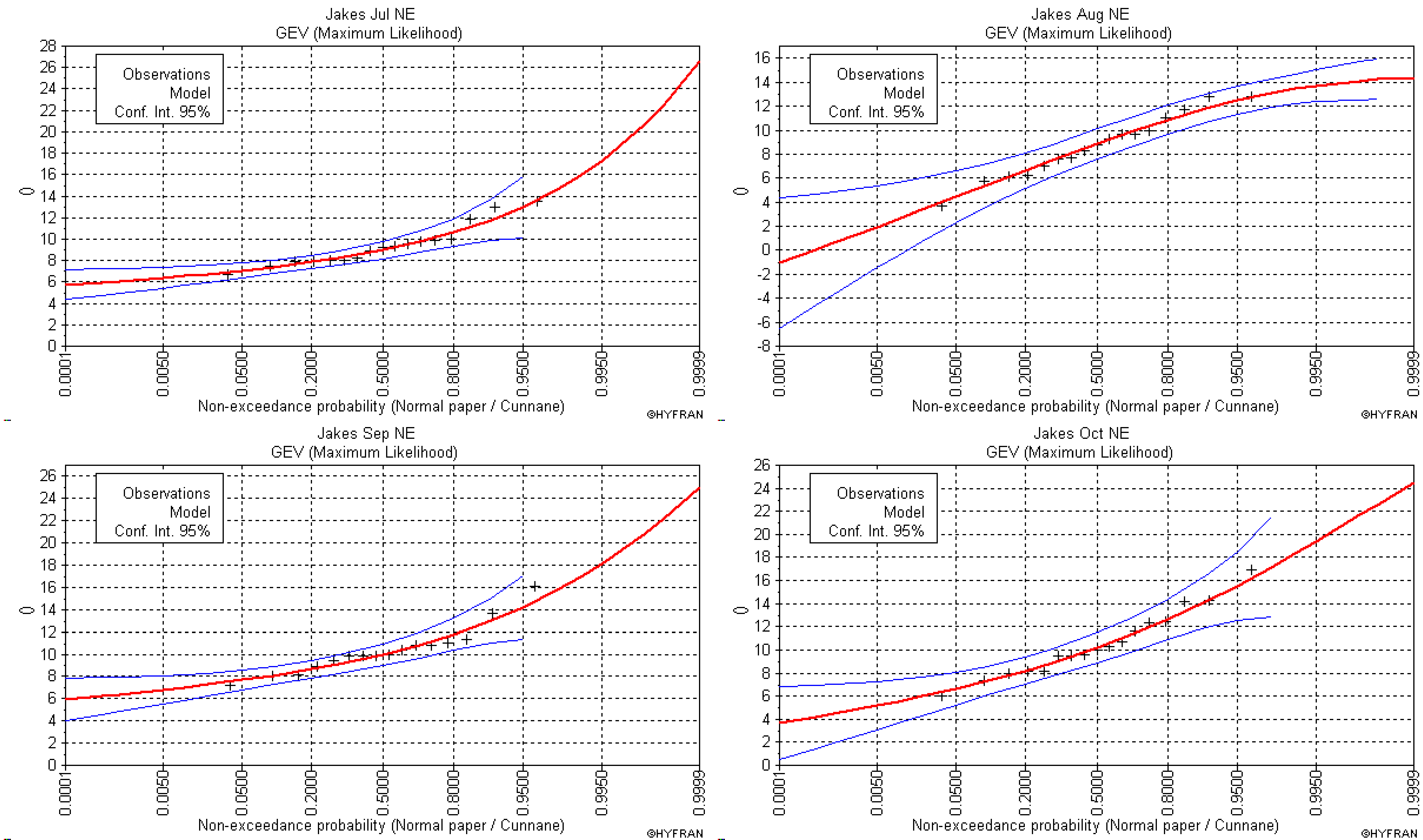

JAKE'S CORNER EAST MONTHLY FREQUENCY CURVES

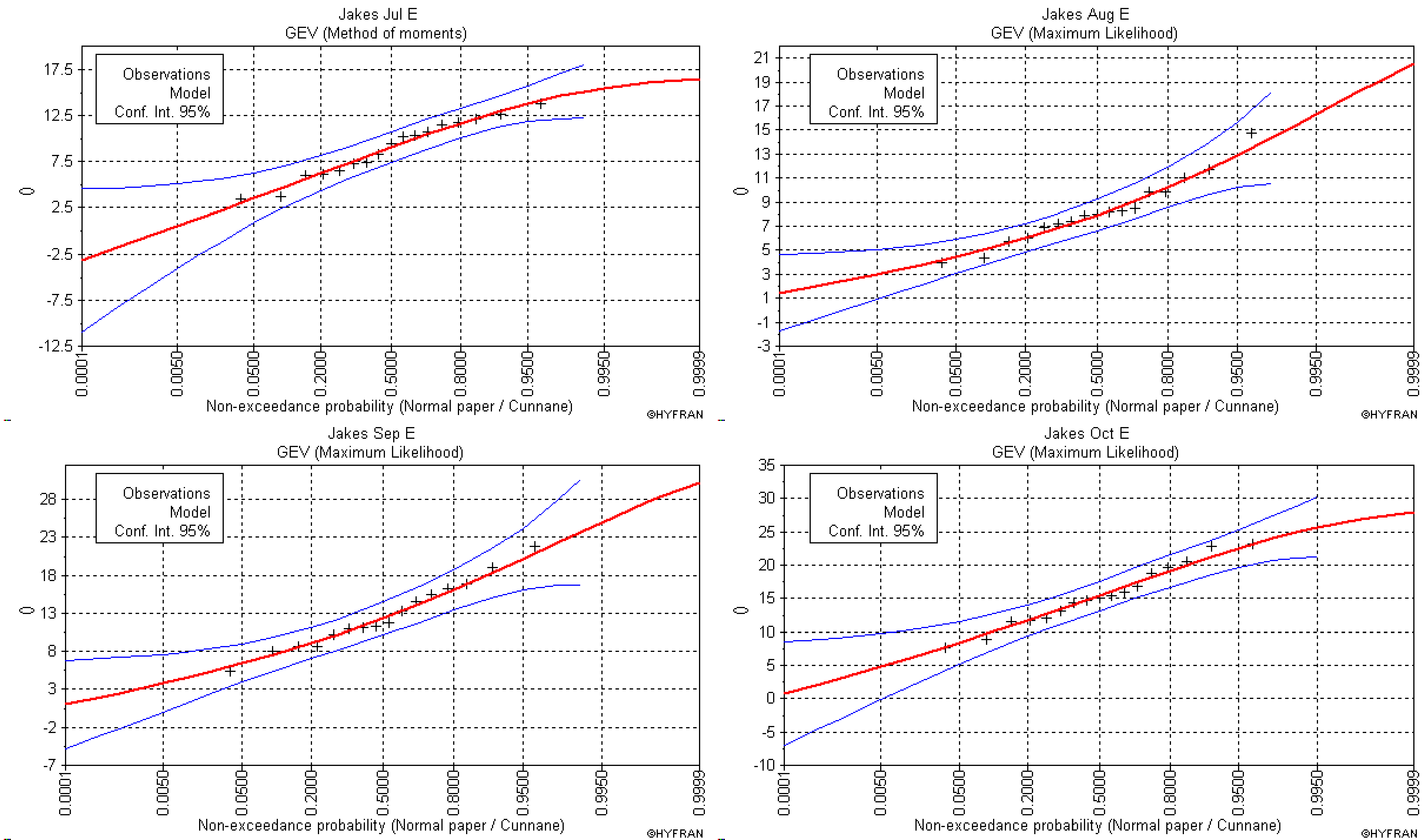

JAKE'S CORNER SOUTHEAST MONTHLY FREQUENCY CURVES

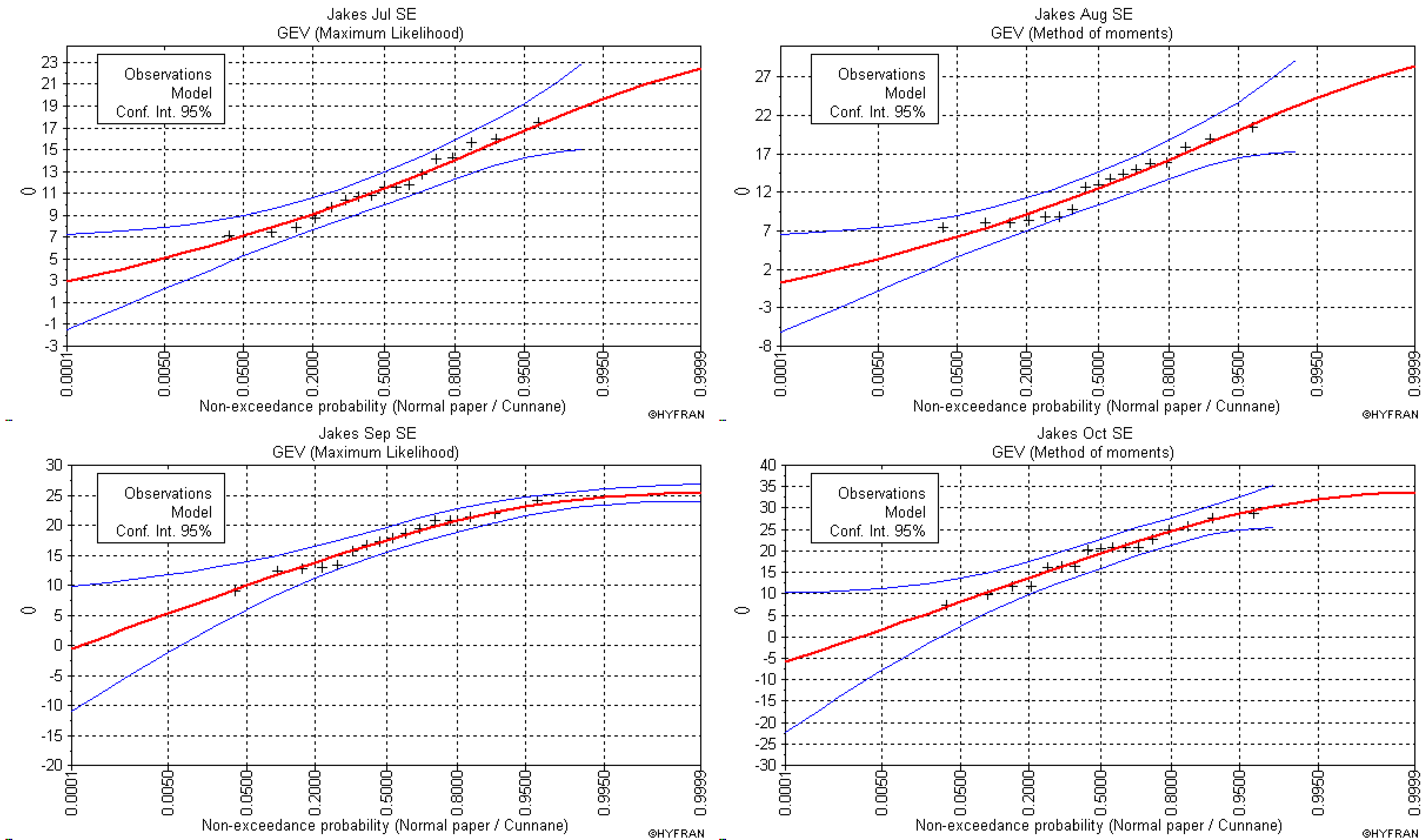

JAKE'S CORNER SOUTH MONTHLY FREQUENCY CURVES

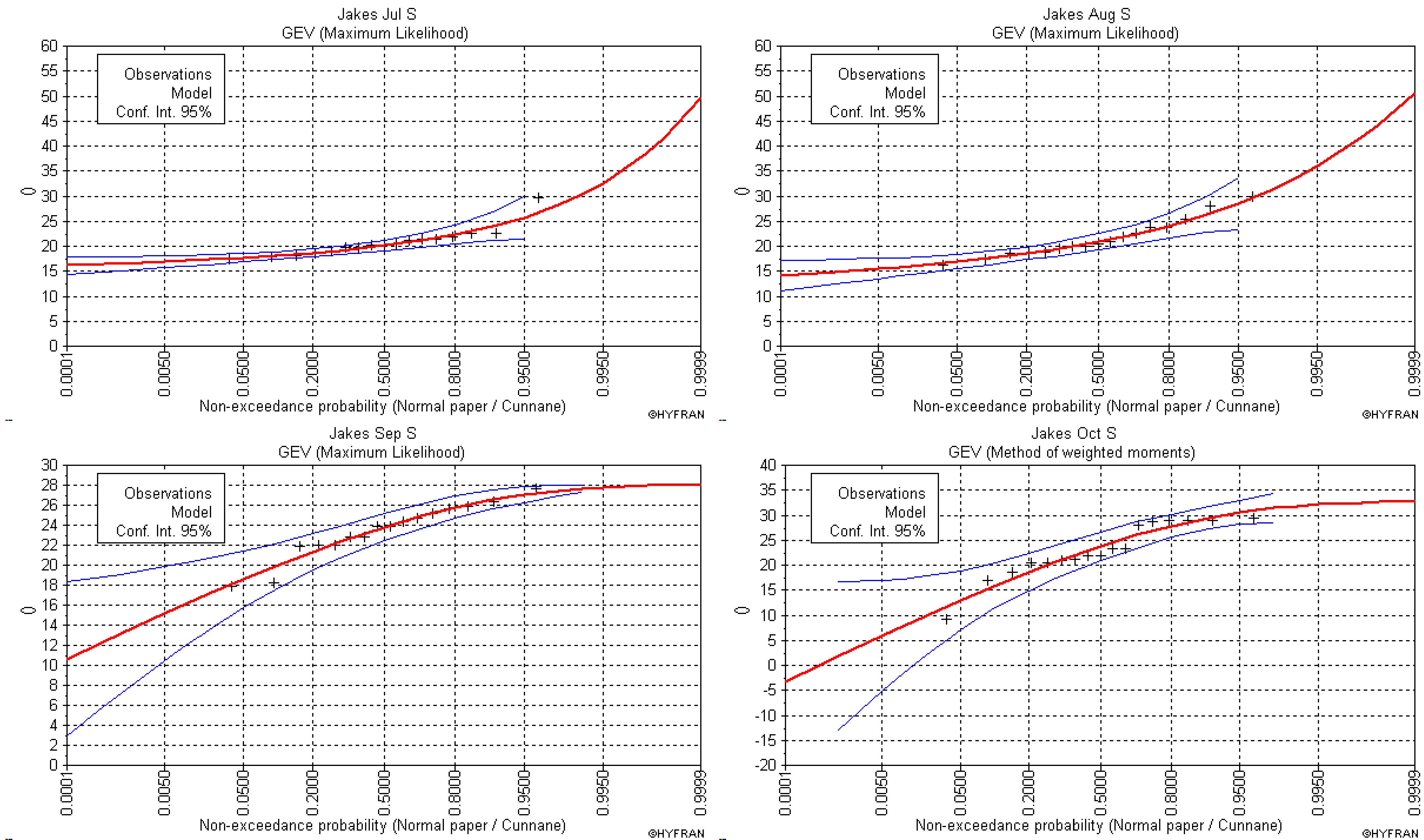

JAKE'S CORNER SOUTHWEST MONTHLY FREQUENCY CURVES

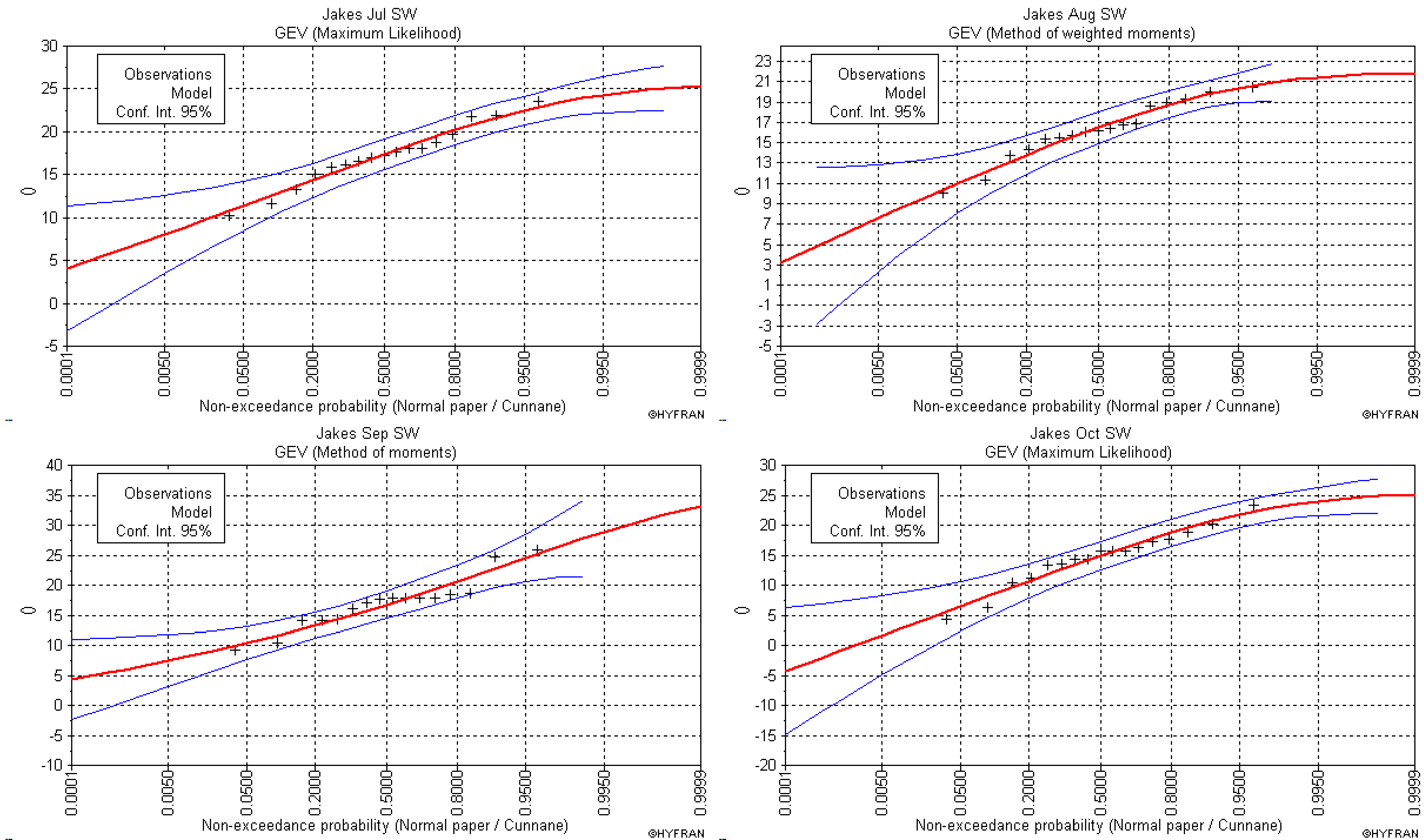

JAKE'S CORNER WEST MONTHLY FREQUENCY CURVES

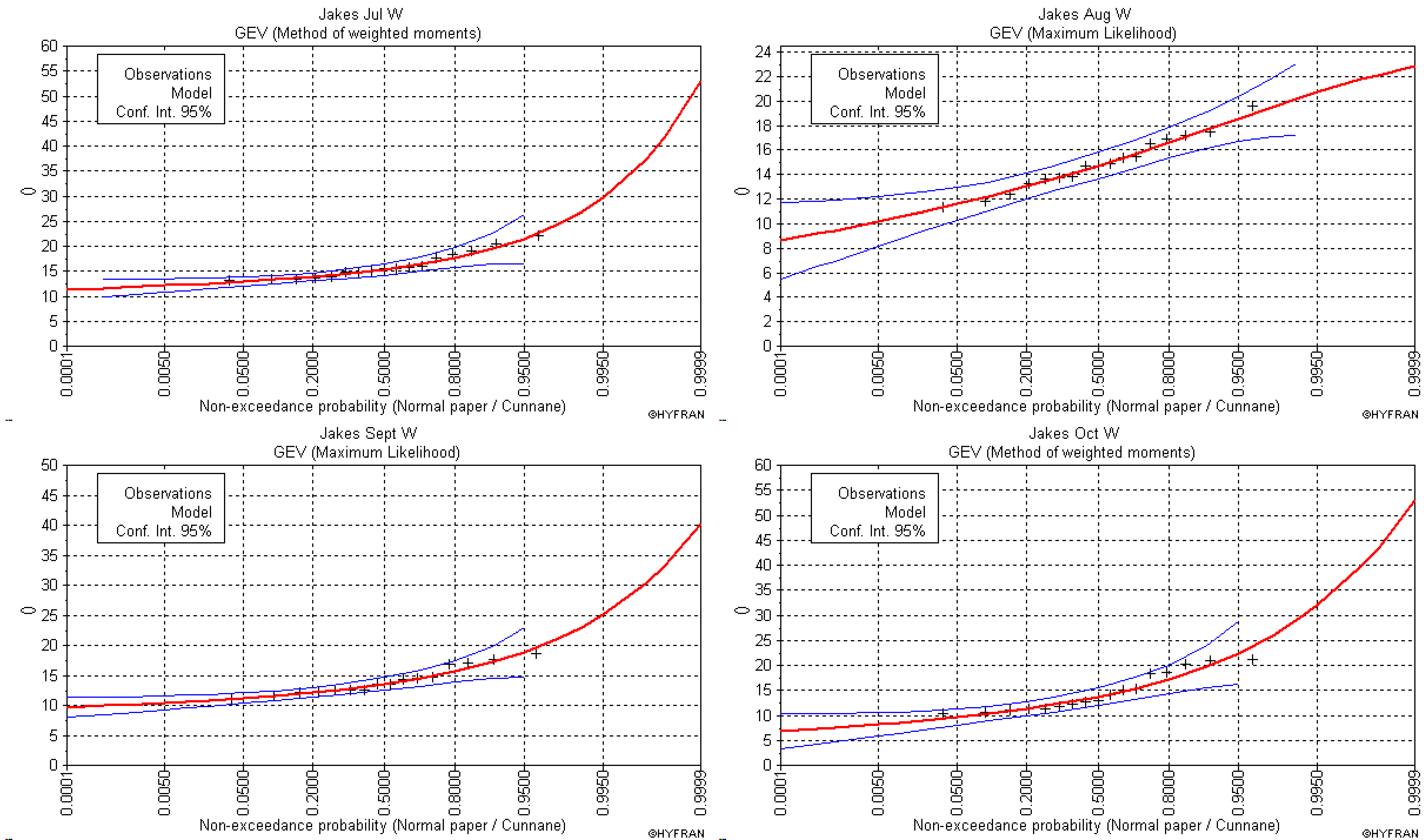

JAKE'S CORNER NORTHWEST MONTHLY FREQUENCY CURVES

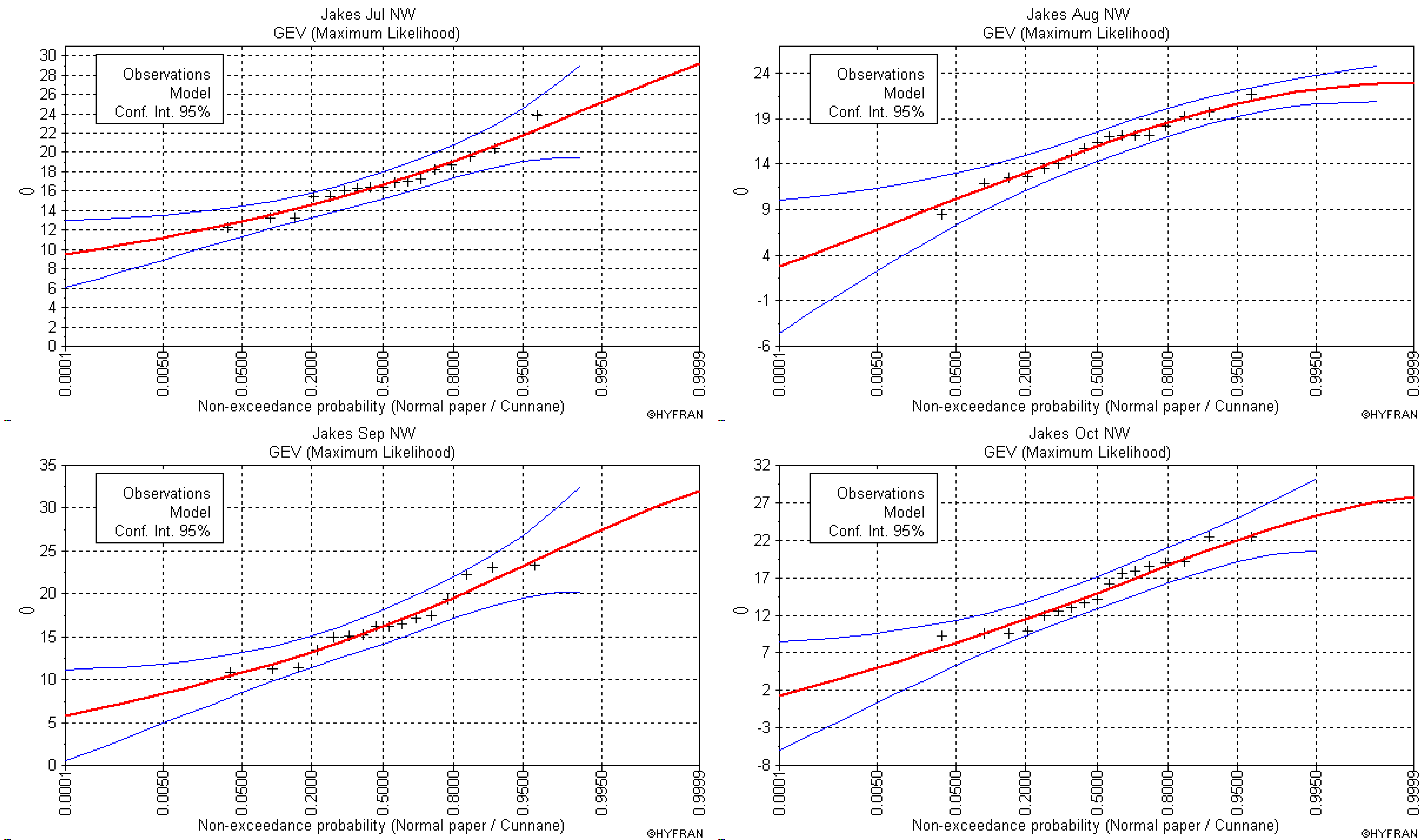

MOUNT SIMA

MOUNT SIMA NORTH MONTHLY FREQUENCY CURVES

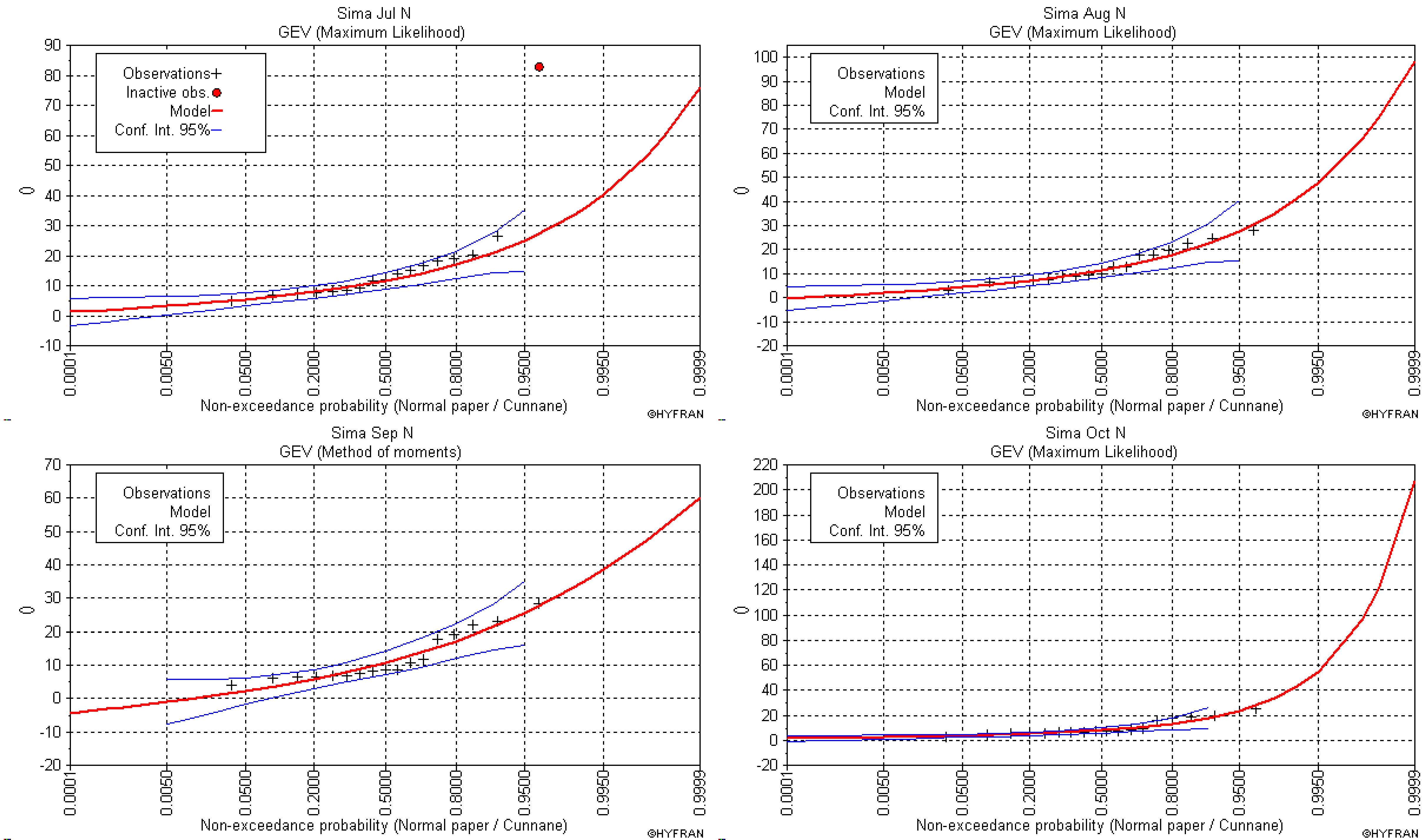

MOUNT SIMA NORTHEAST MONTHLY FREQUENCY CURVES

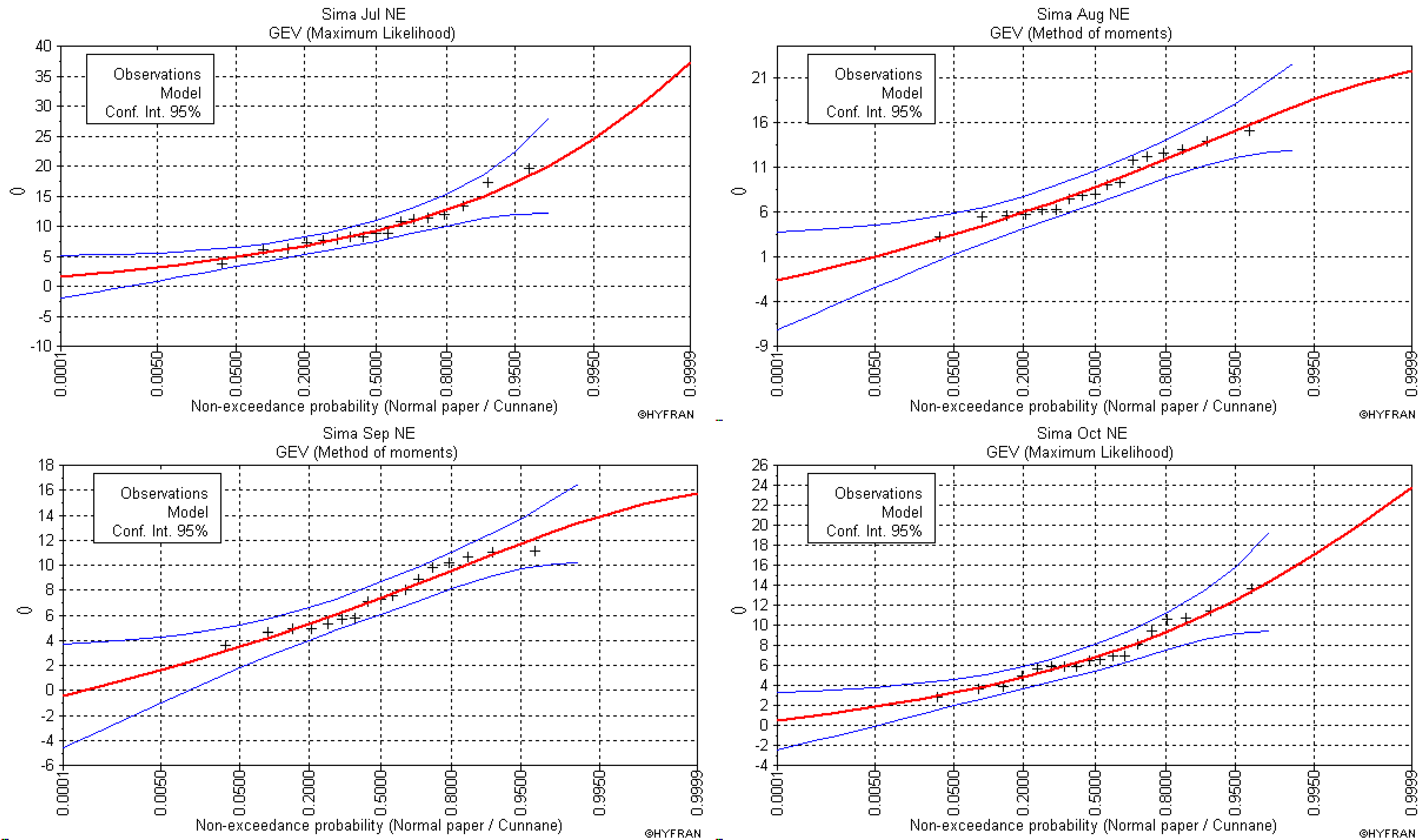

MOUNT SIMA EAST MONTHLY FREQUENCY CURVES

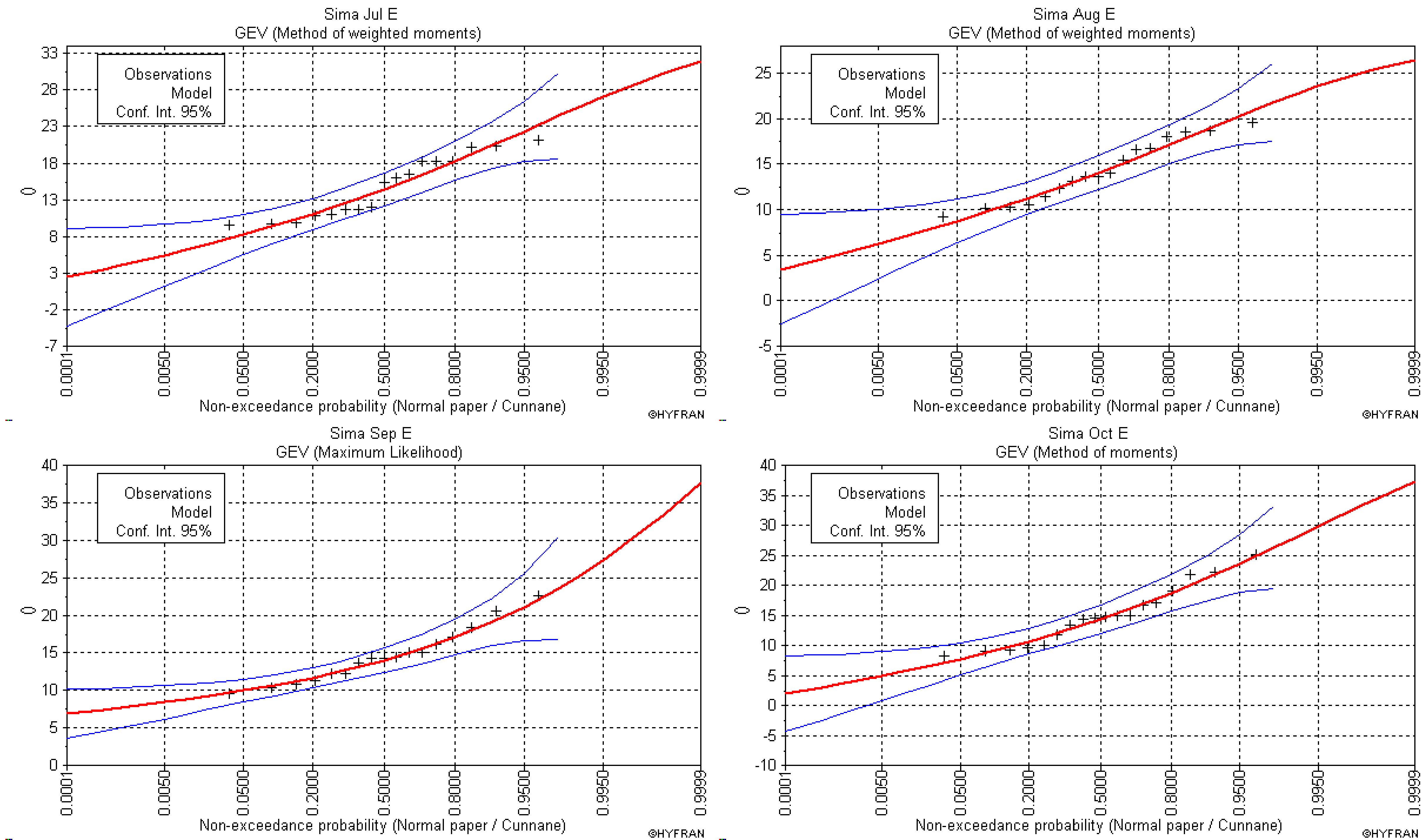

MOUNT SIMA SOUTHEAST MONTHLY FREQUENCY CURVES

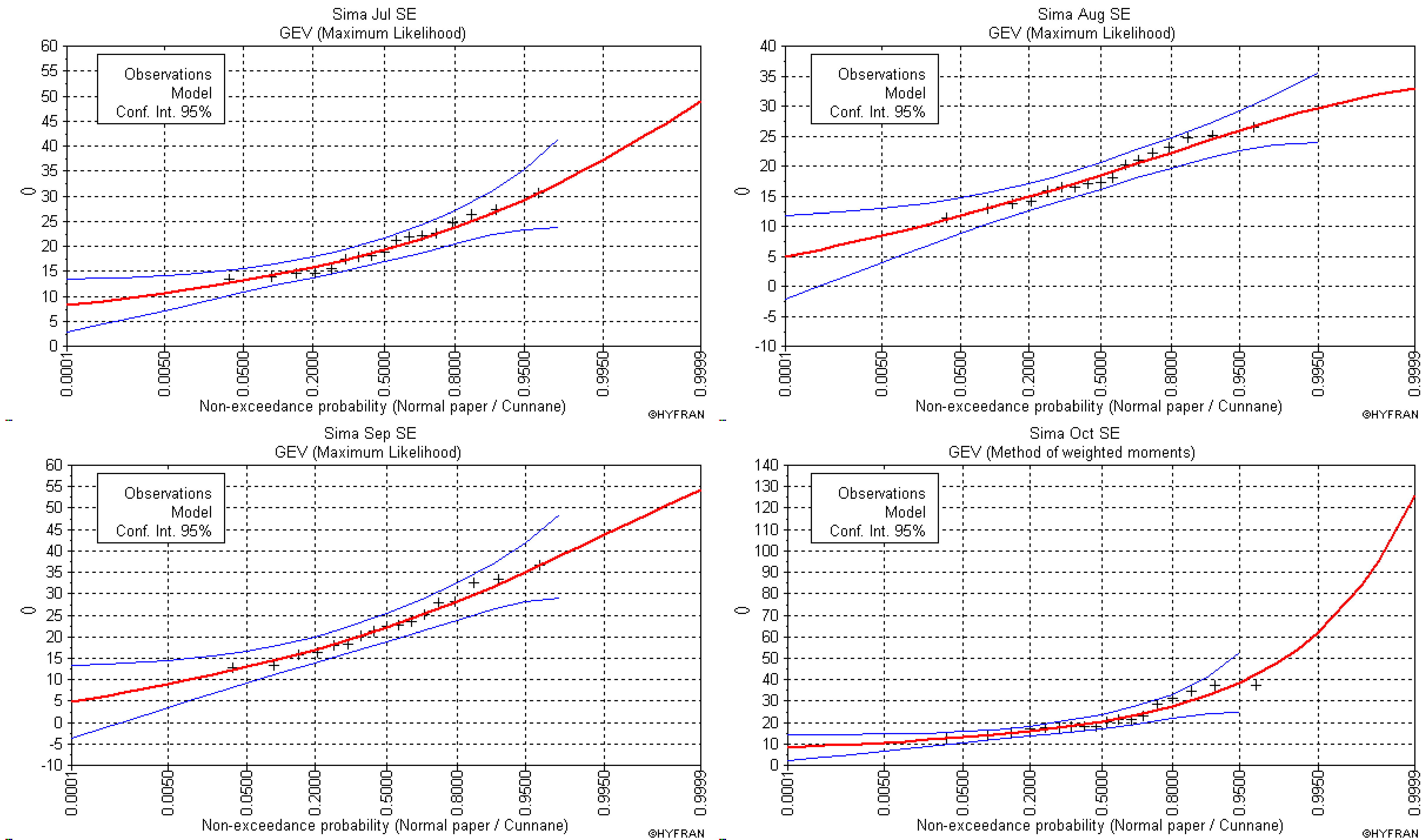

MOUNT SIMA SOUTH MONTHLY FREQUENCY CURVES

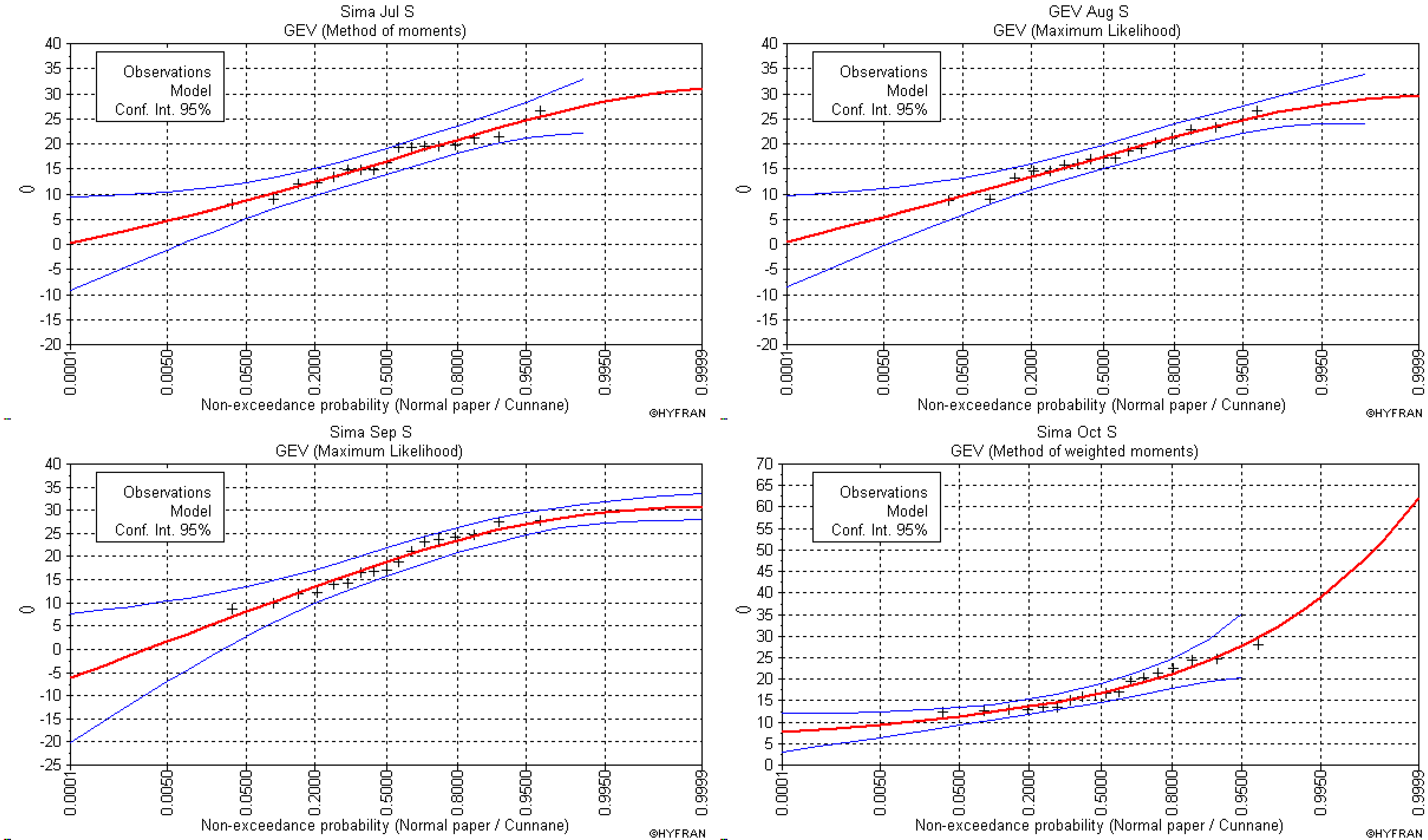

MOUNT SIMA SOUTHWEST MONTHLY FREQUENCY CURVES

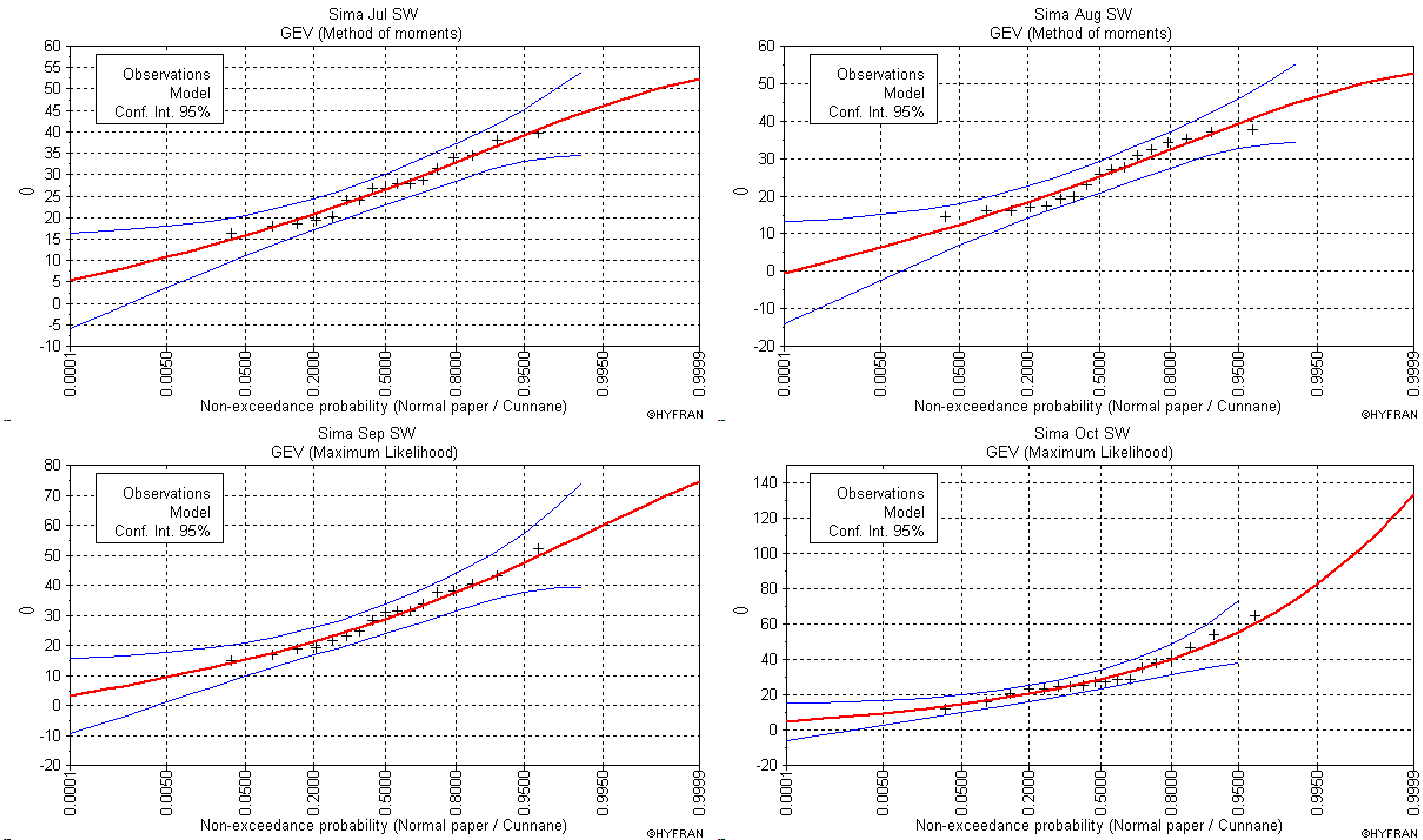

MOUNT SIMA WEST MONTHLY FREQUENCY CURVES

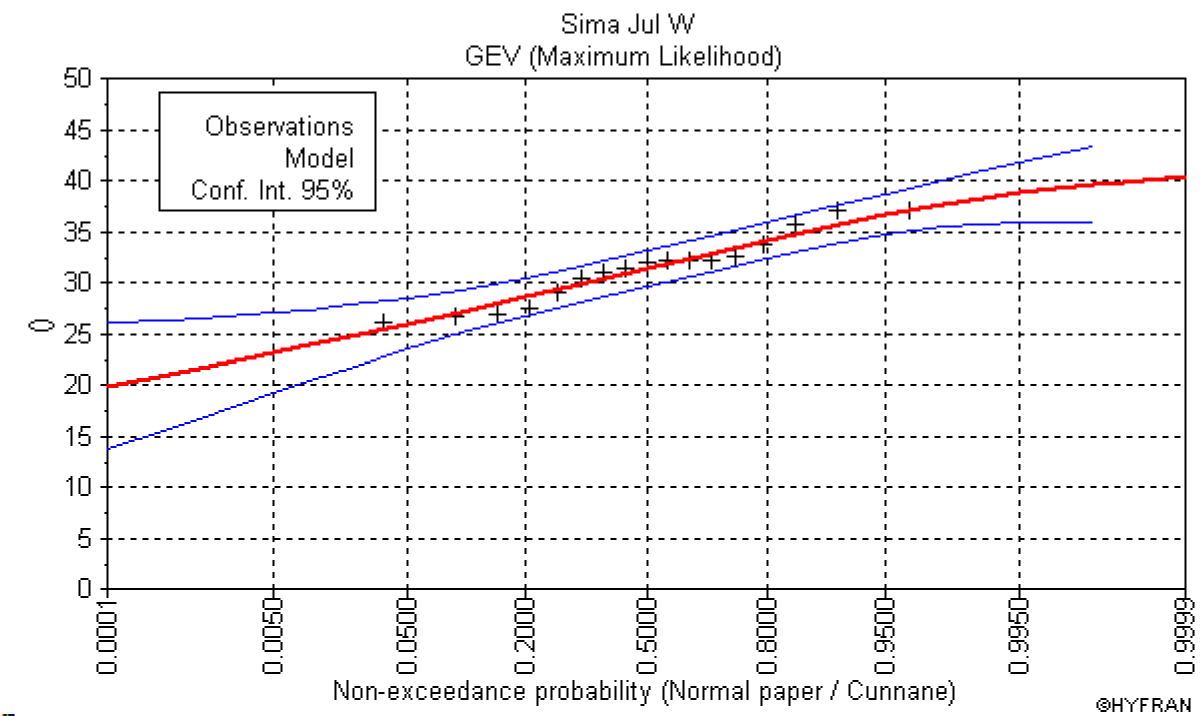

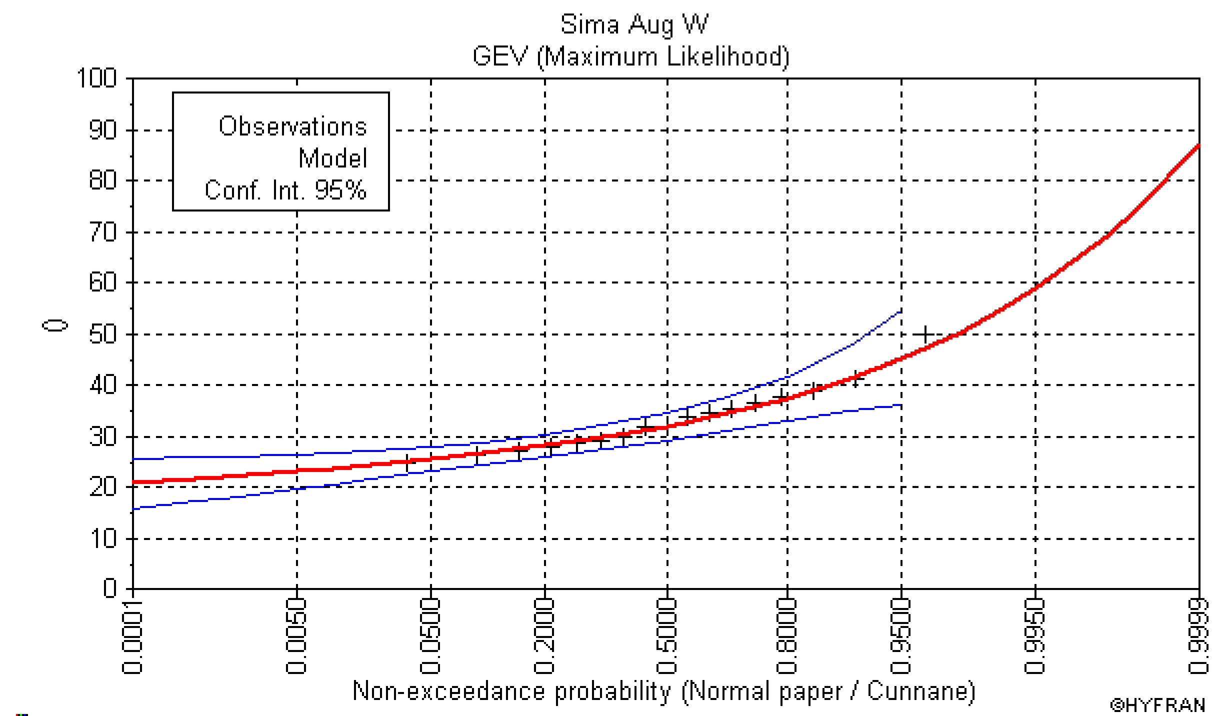

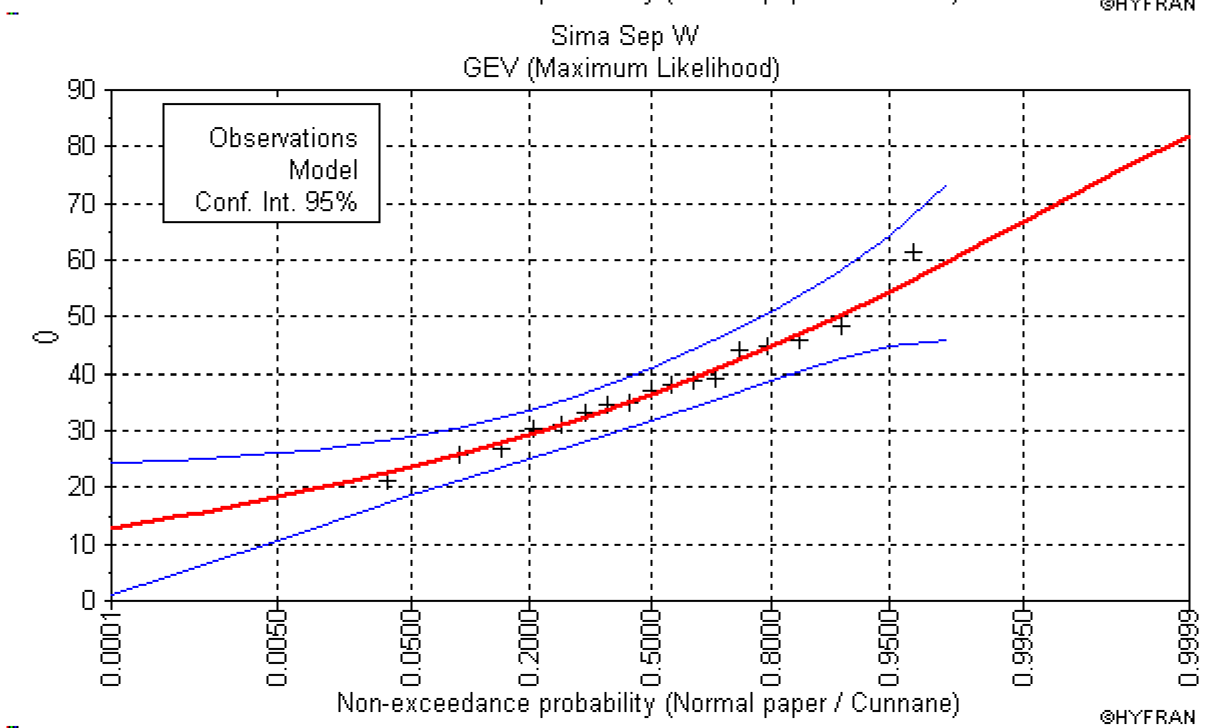

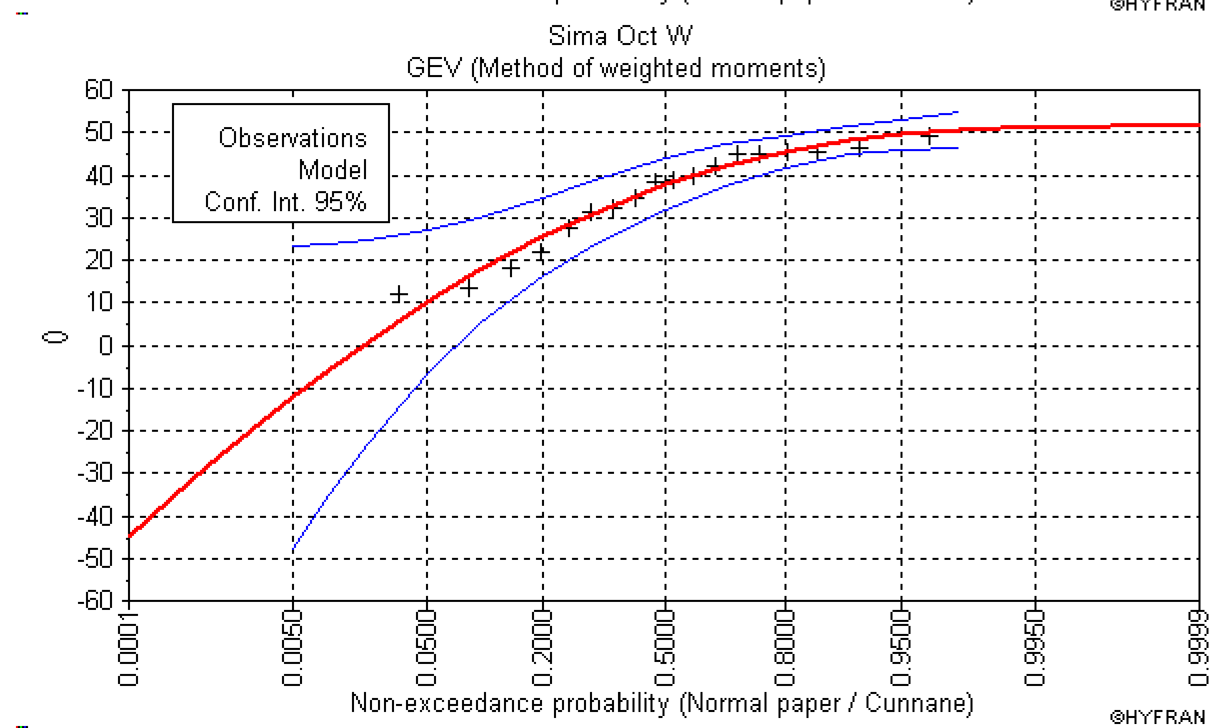

MOUNT SIMA NORTHWEST MONTHLY FREQUENCY CURVES

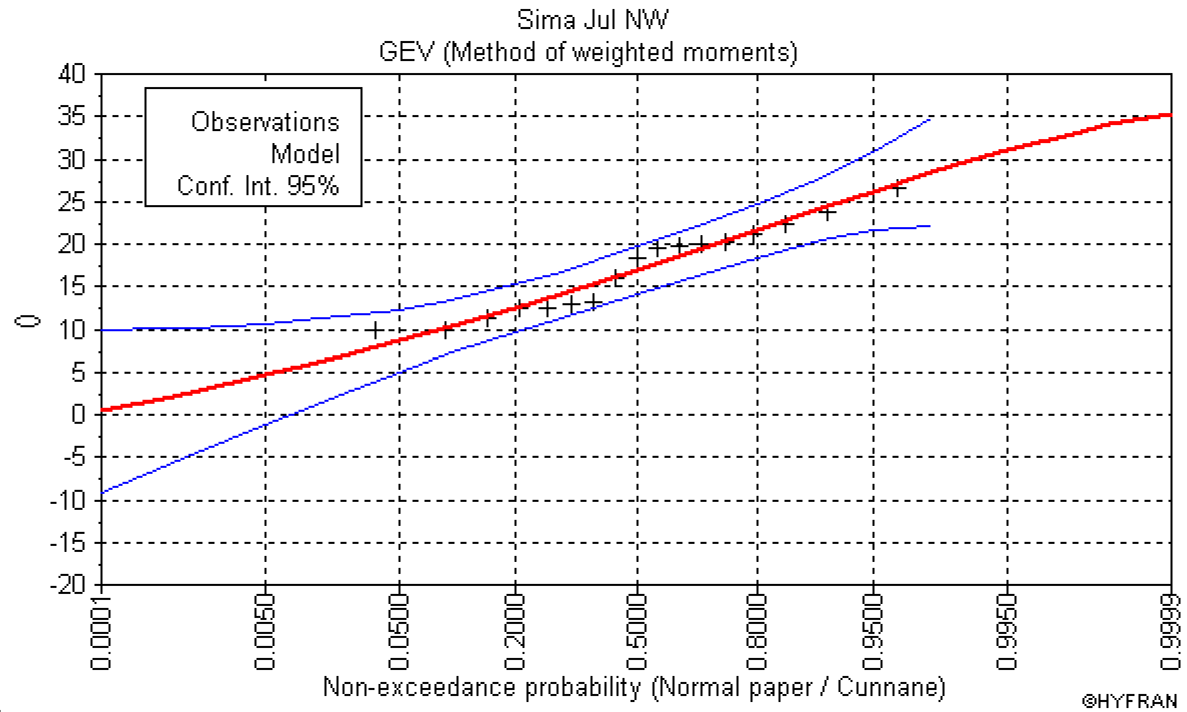

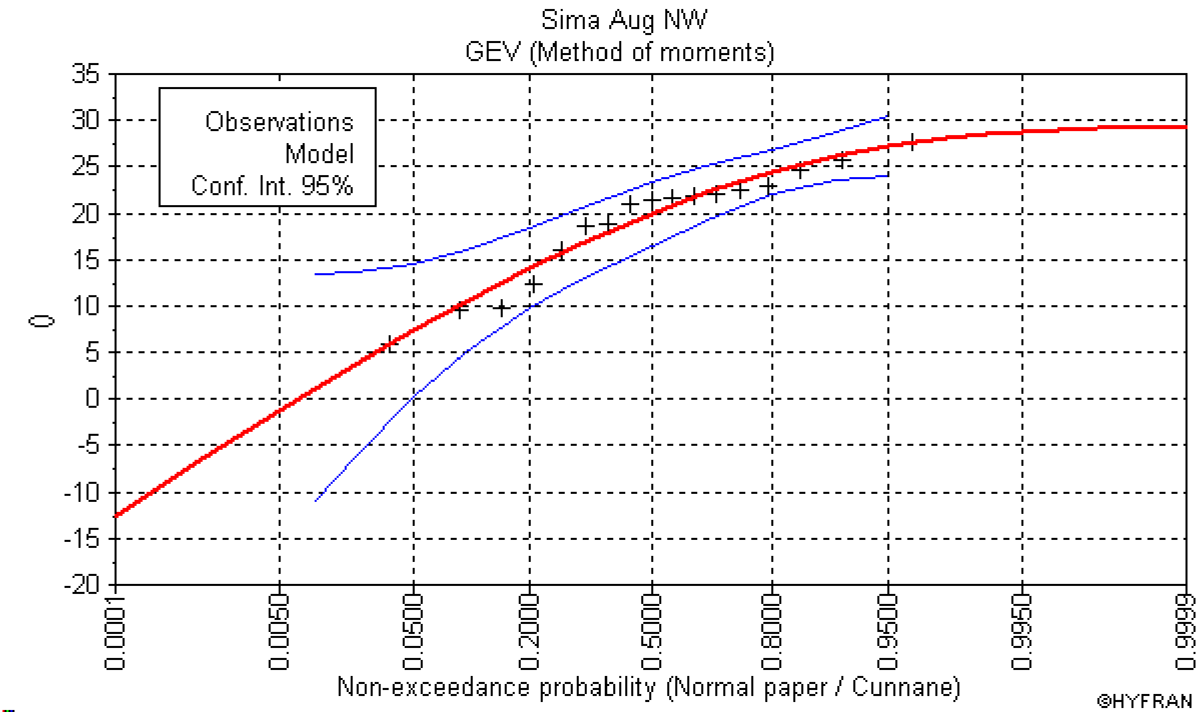

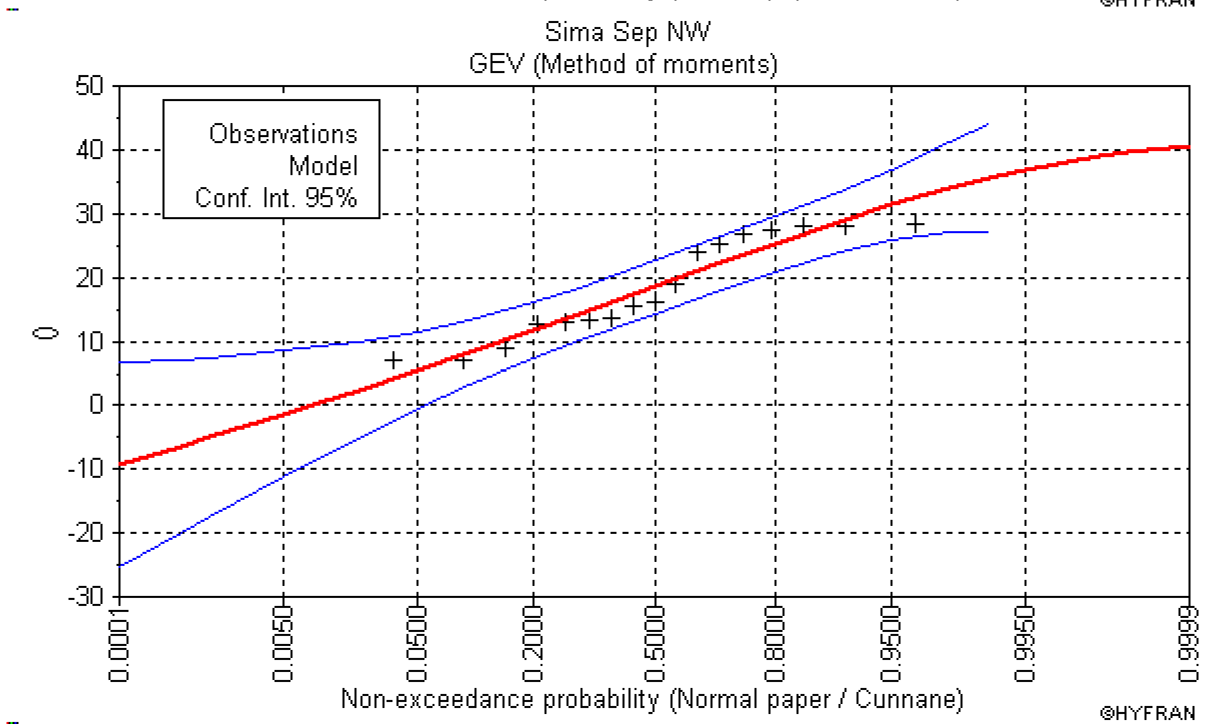

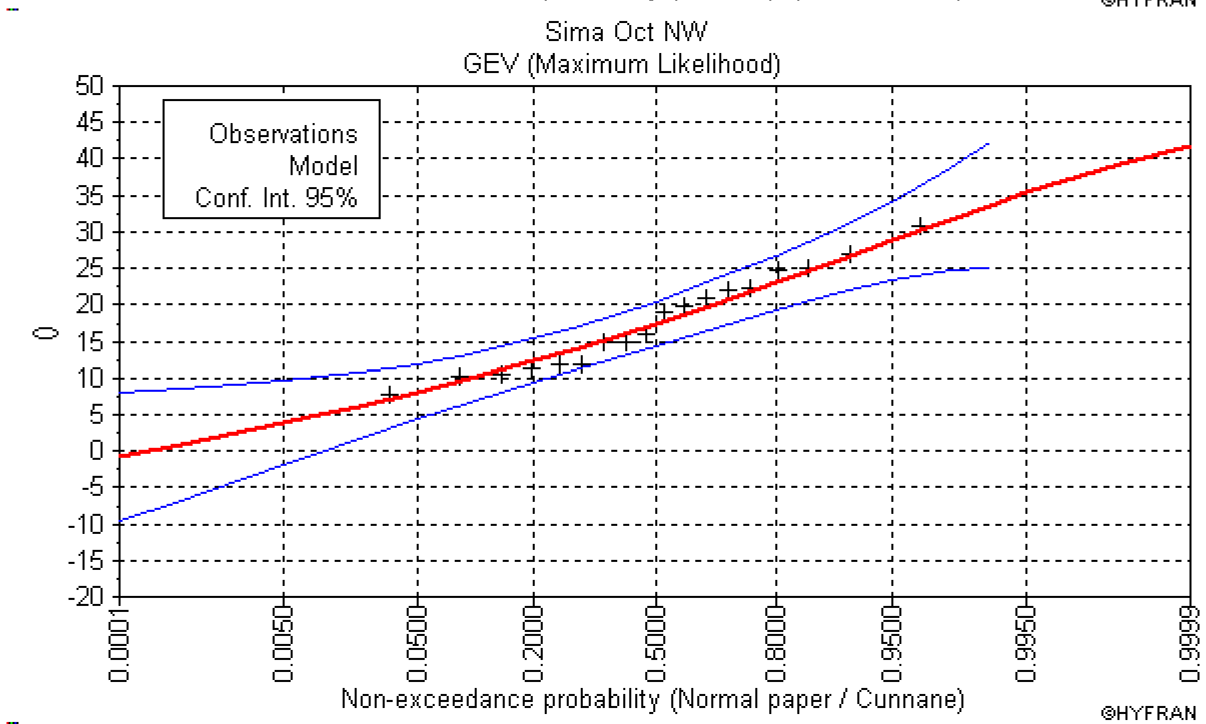

WHITEHORSE A

WHITEHORSE A NORTH MONTHLY FREQUENCY CURVES

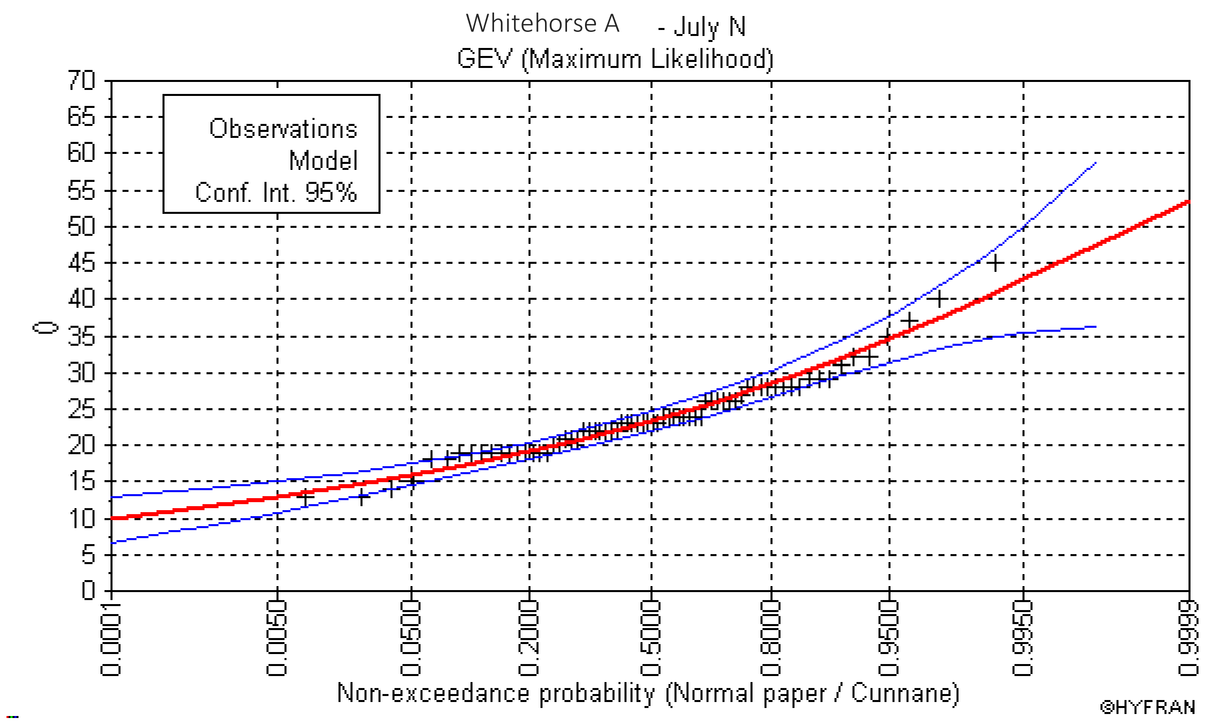

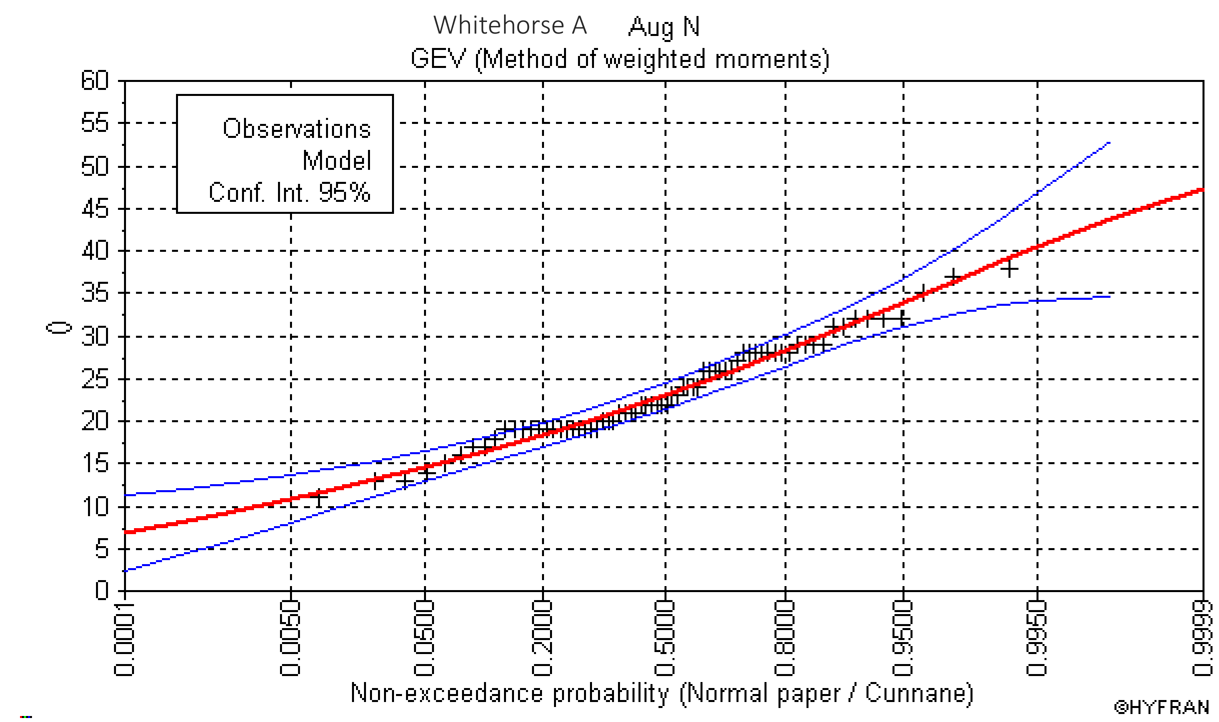

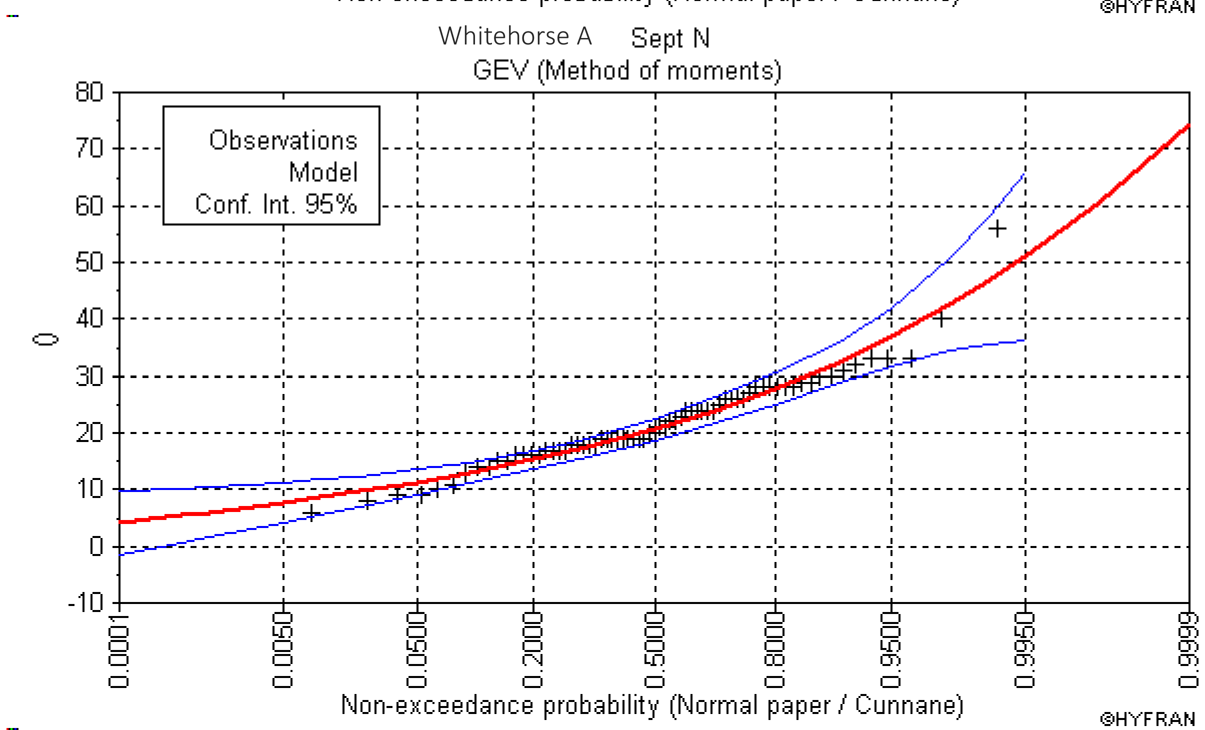

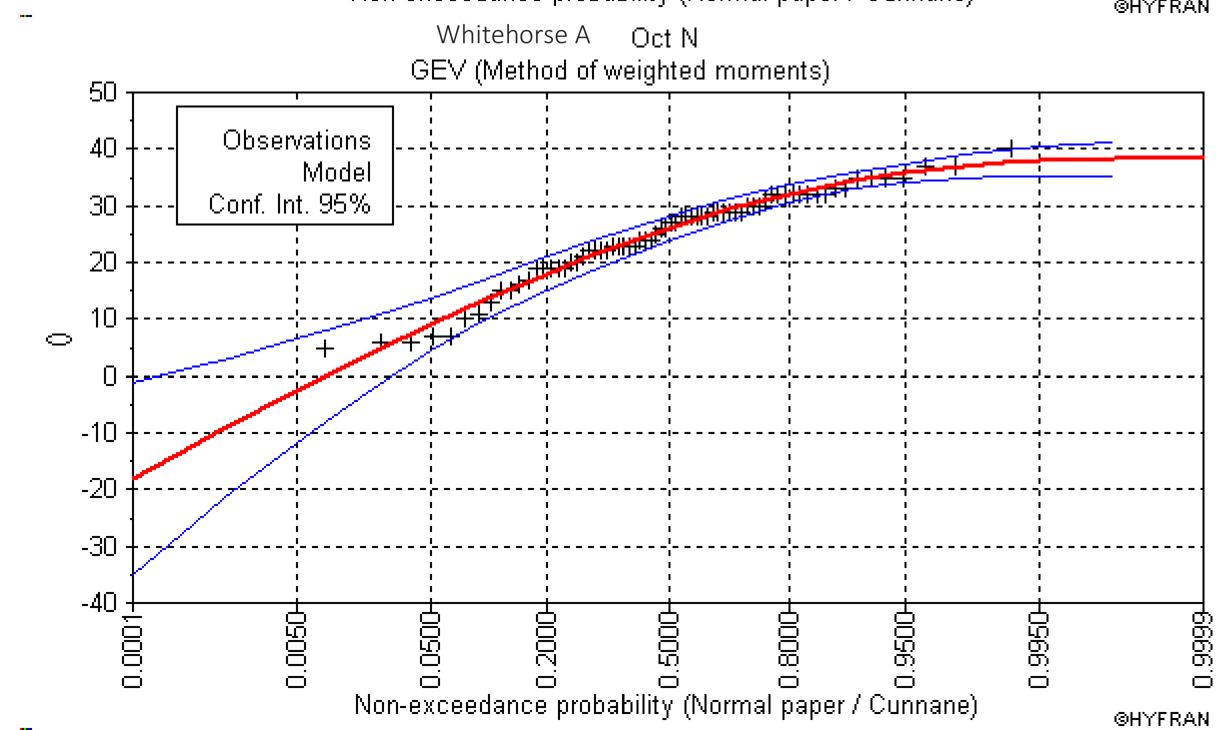

WHITEHORSE A NORTHEAST MONTHLY FREQUENCY CURVES

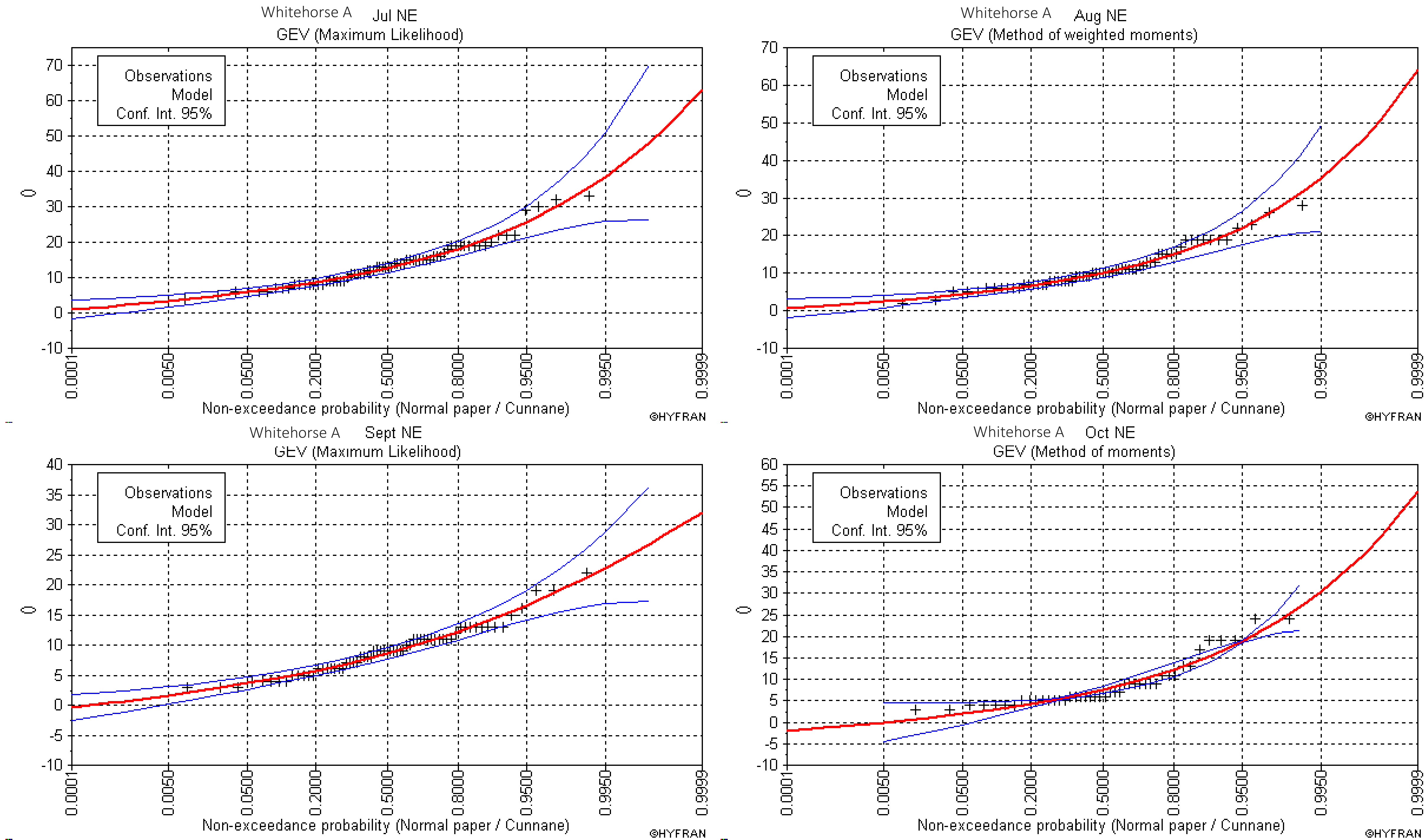

WHITEHORSE A EAST MONTHLY FREQUENCY CURVES

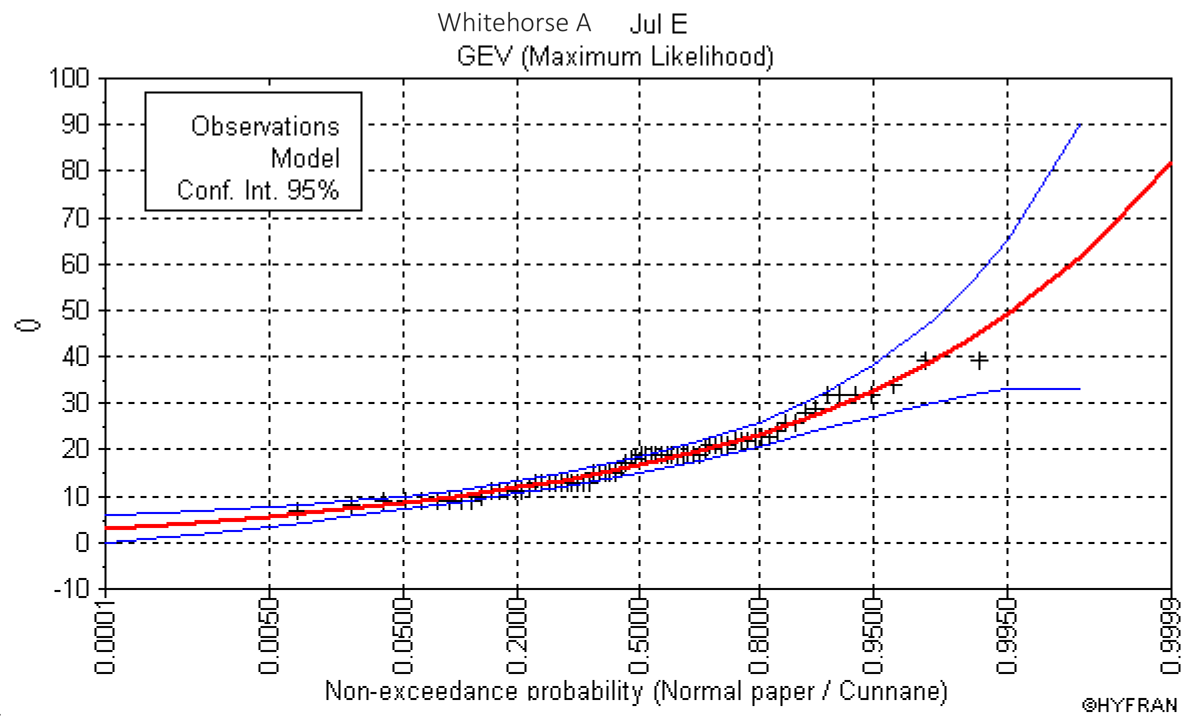

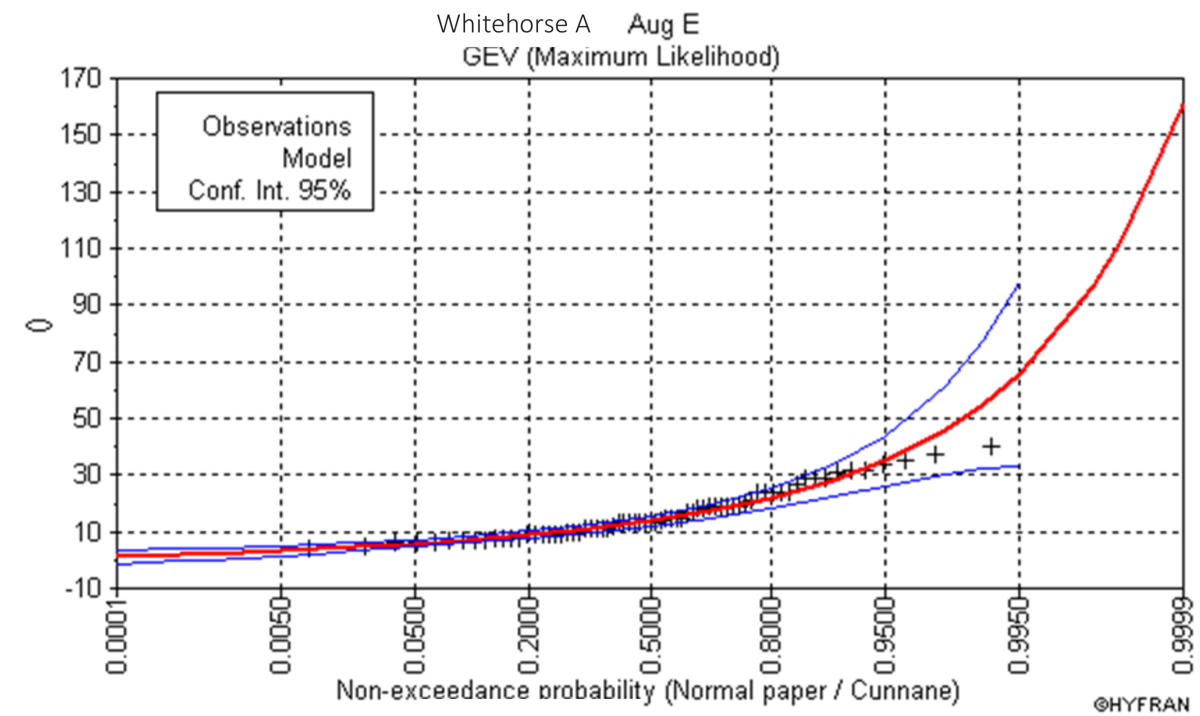

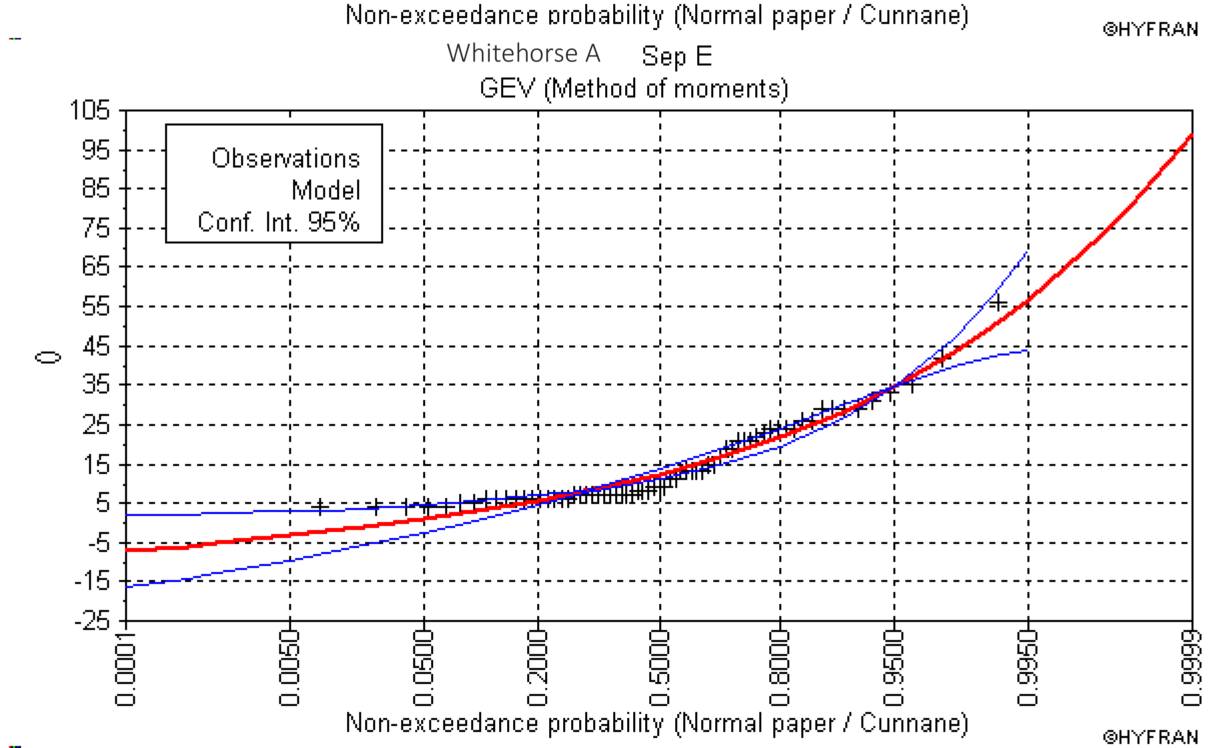

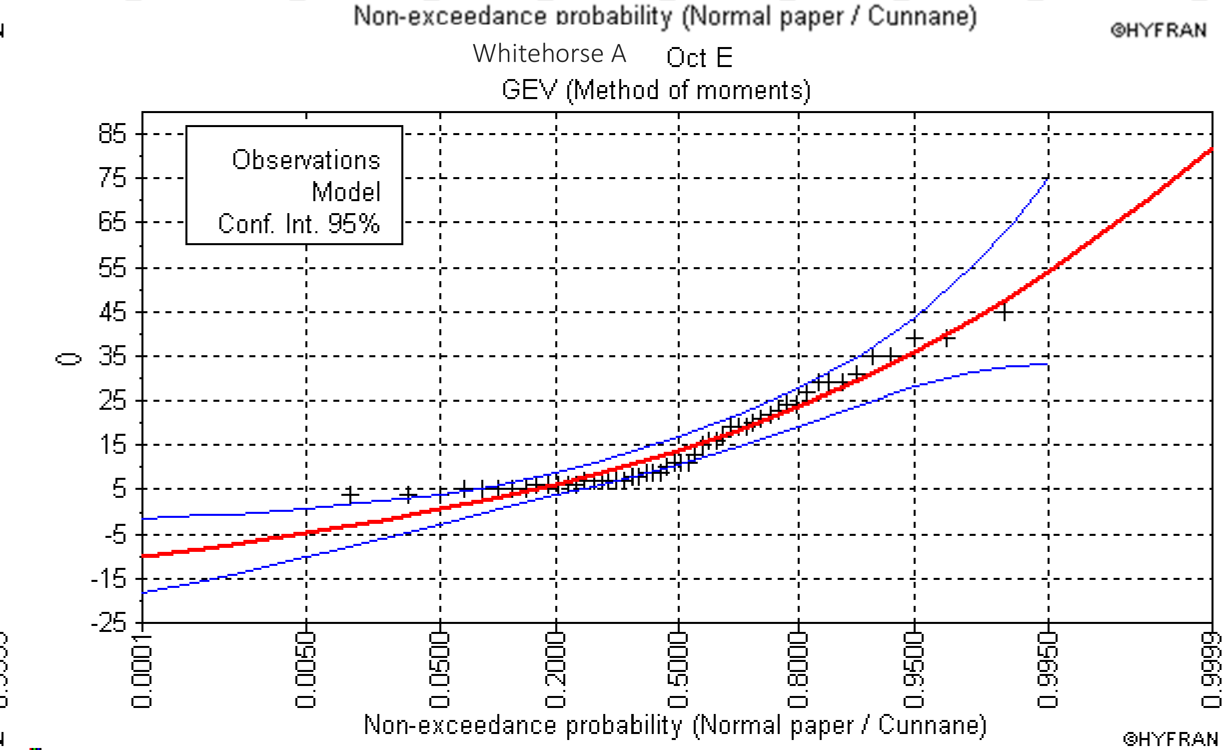

WHITEHORSE A SOUTHEAST MONTHLY FREQUENCY CURVES

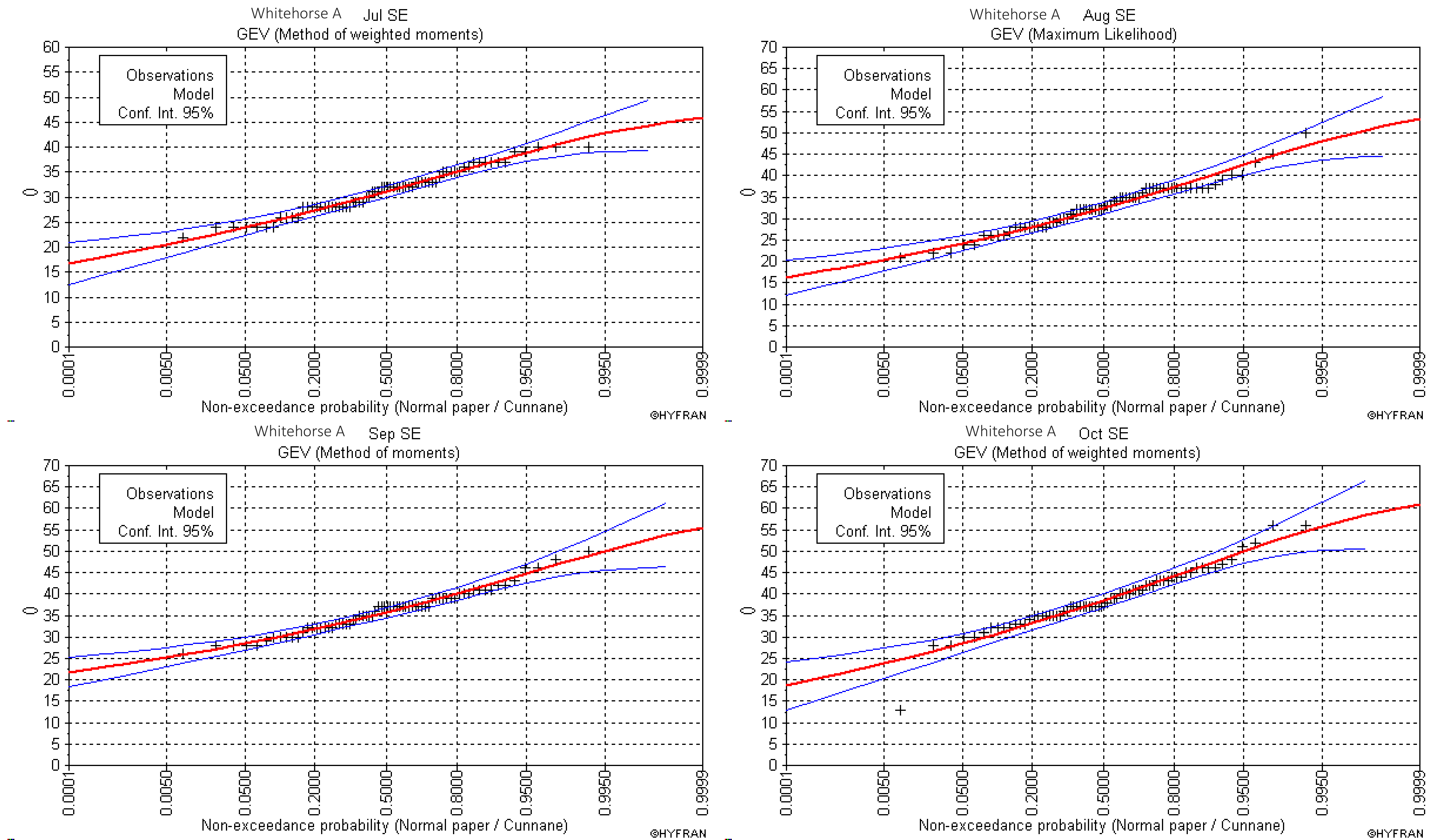

WHITEHORSE A SOUTH MONTHLY FREQUENCY CURVES

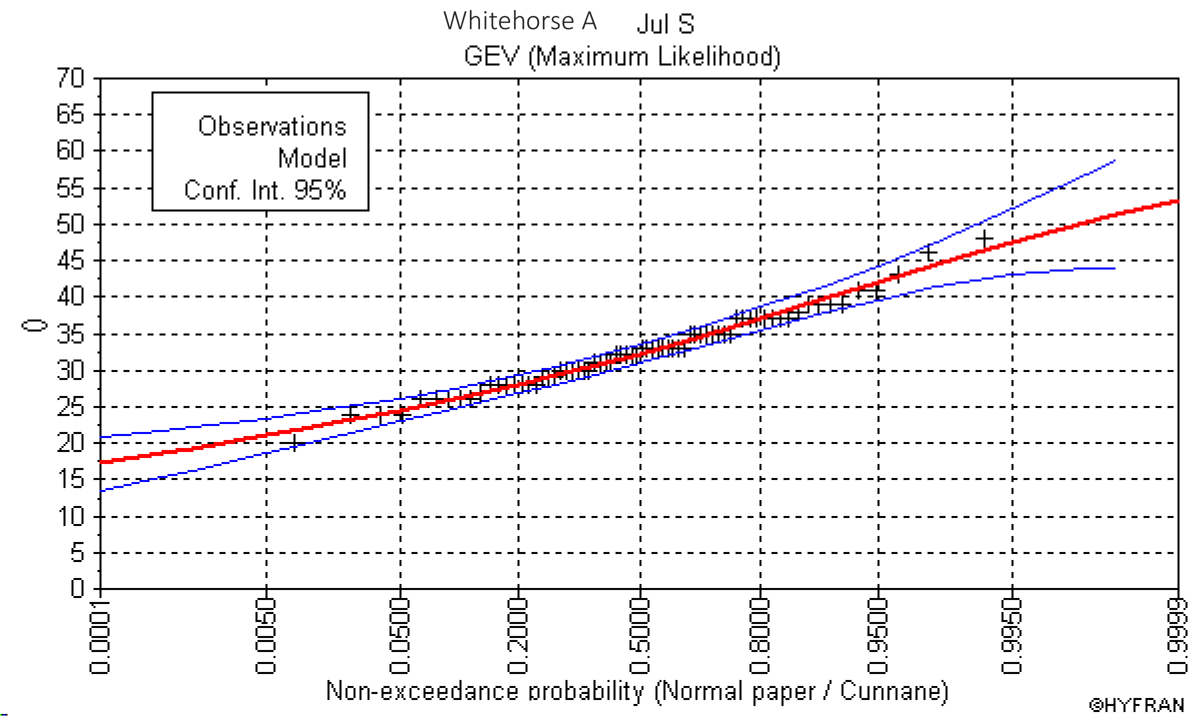

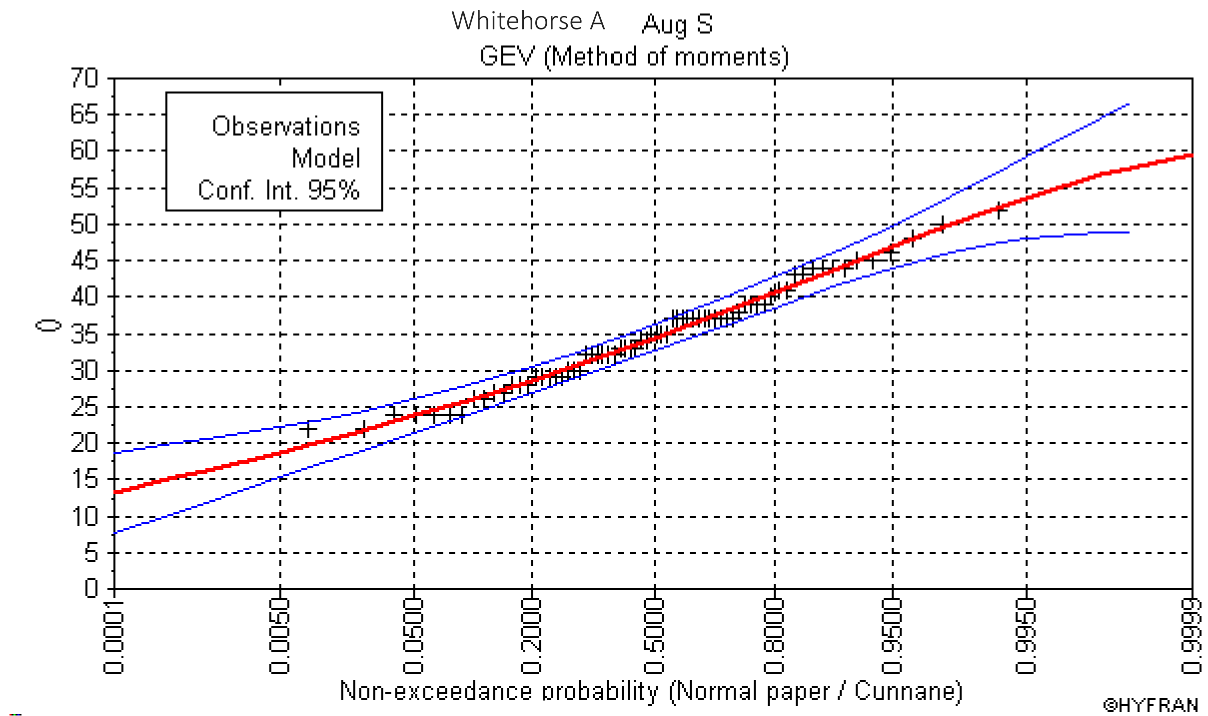

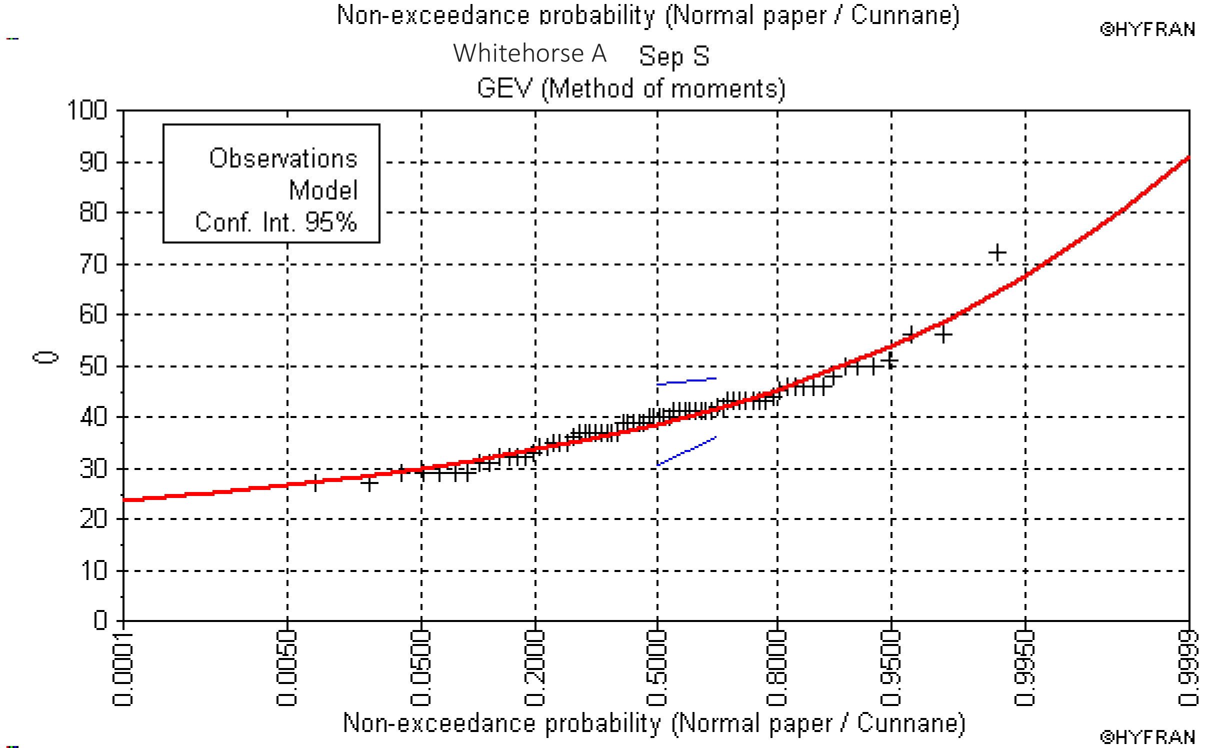

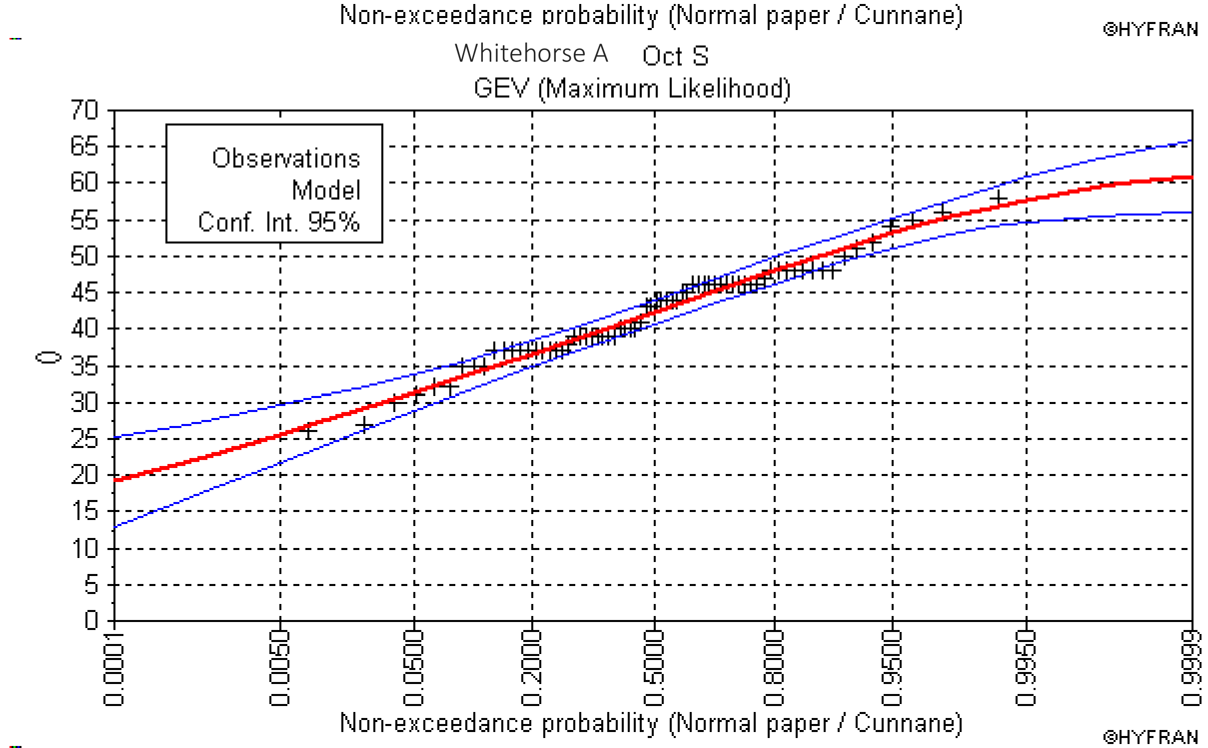

WHITEHORSE A SOUTHWEST MONTHLY FREQUENCY CURVES

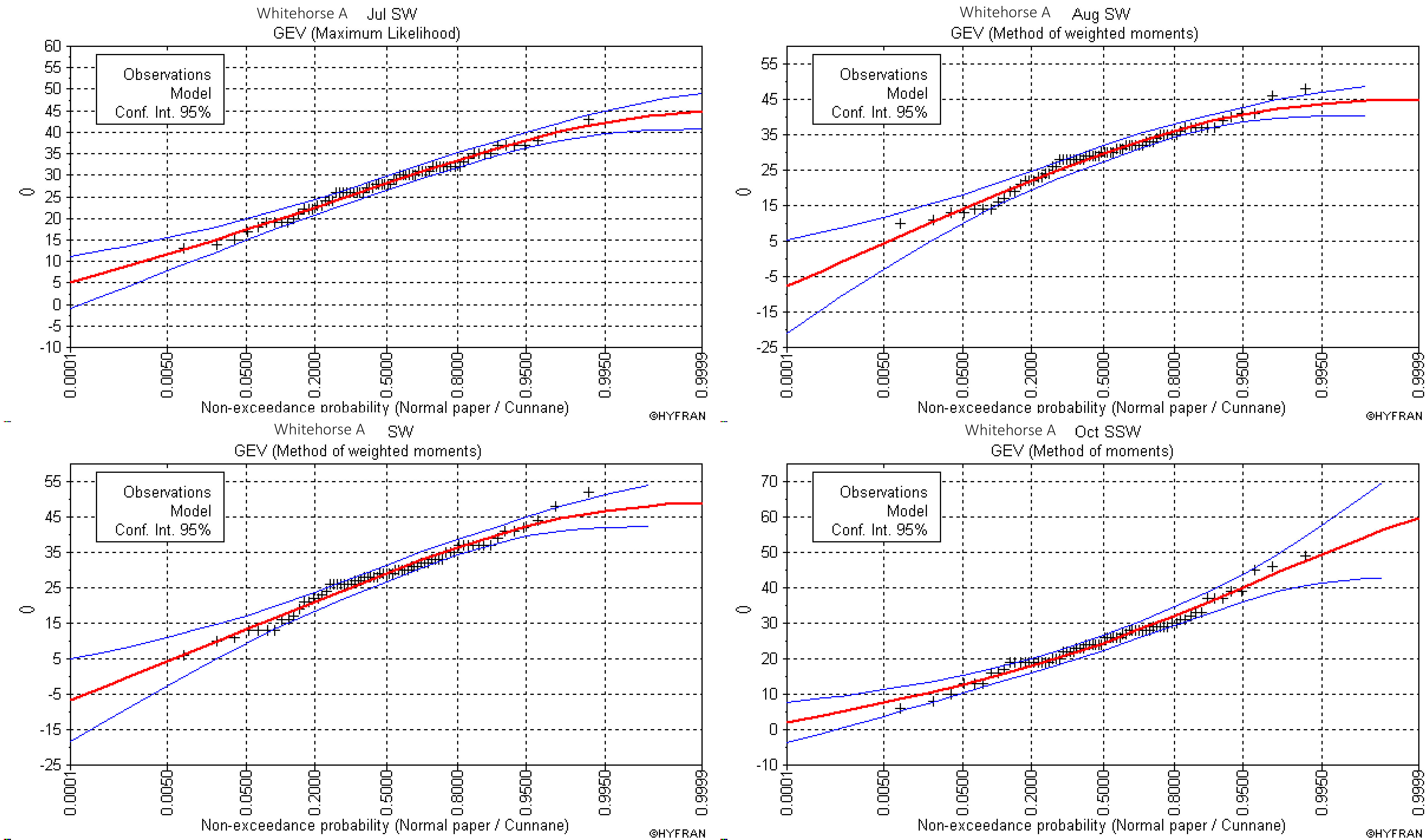

WHITEHORSE A WEST MONTHLY FREQUENCY CURVES

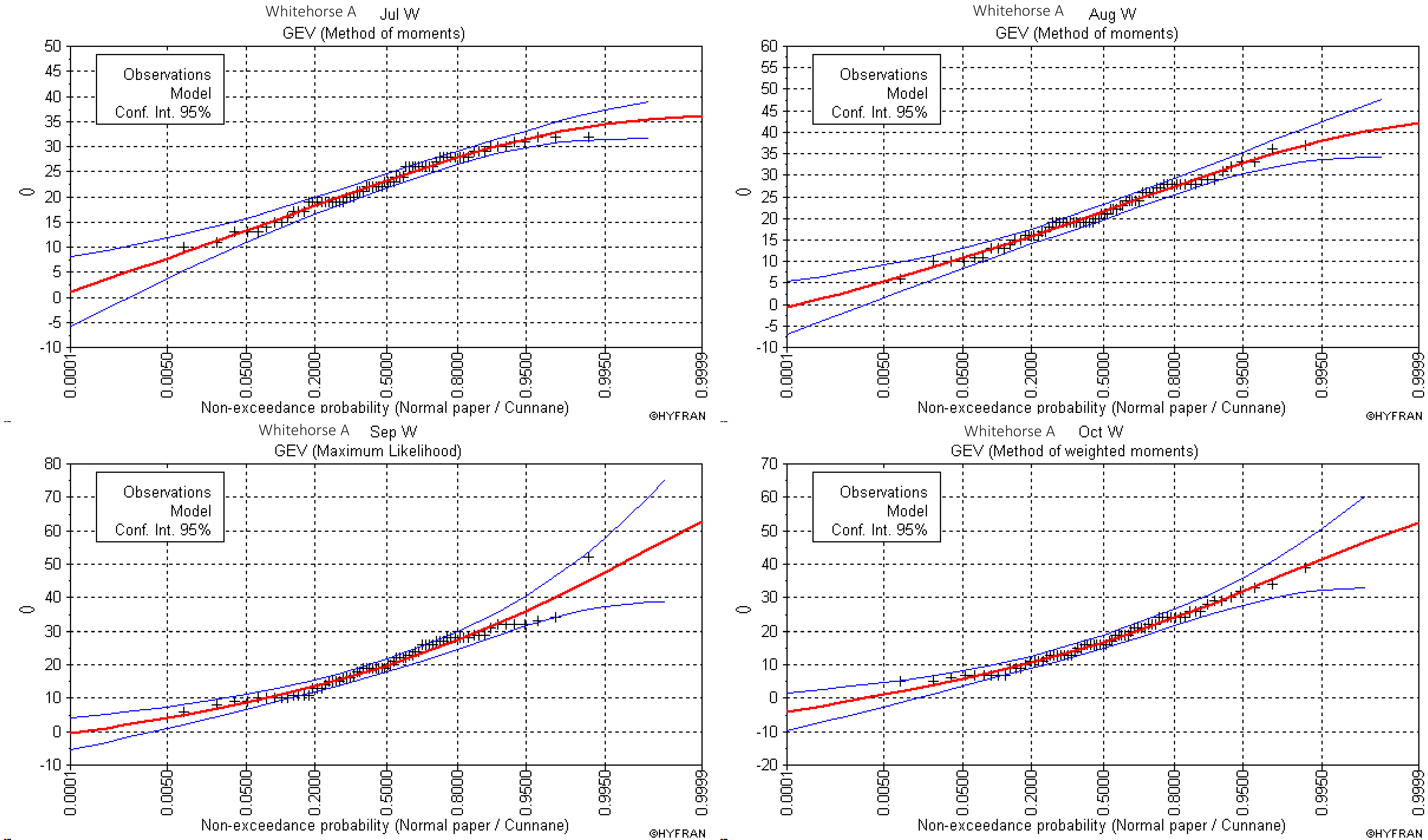

WHITEHORSE A NORTHWEST MONTHLY FREQUENCY CURVES

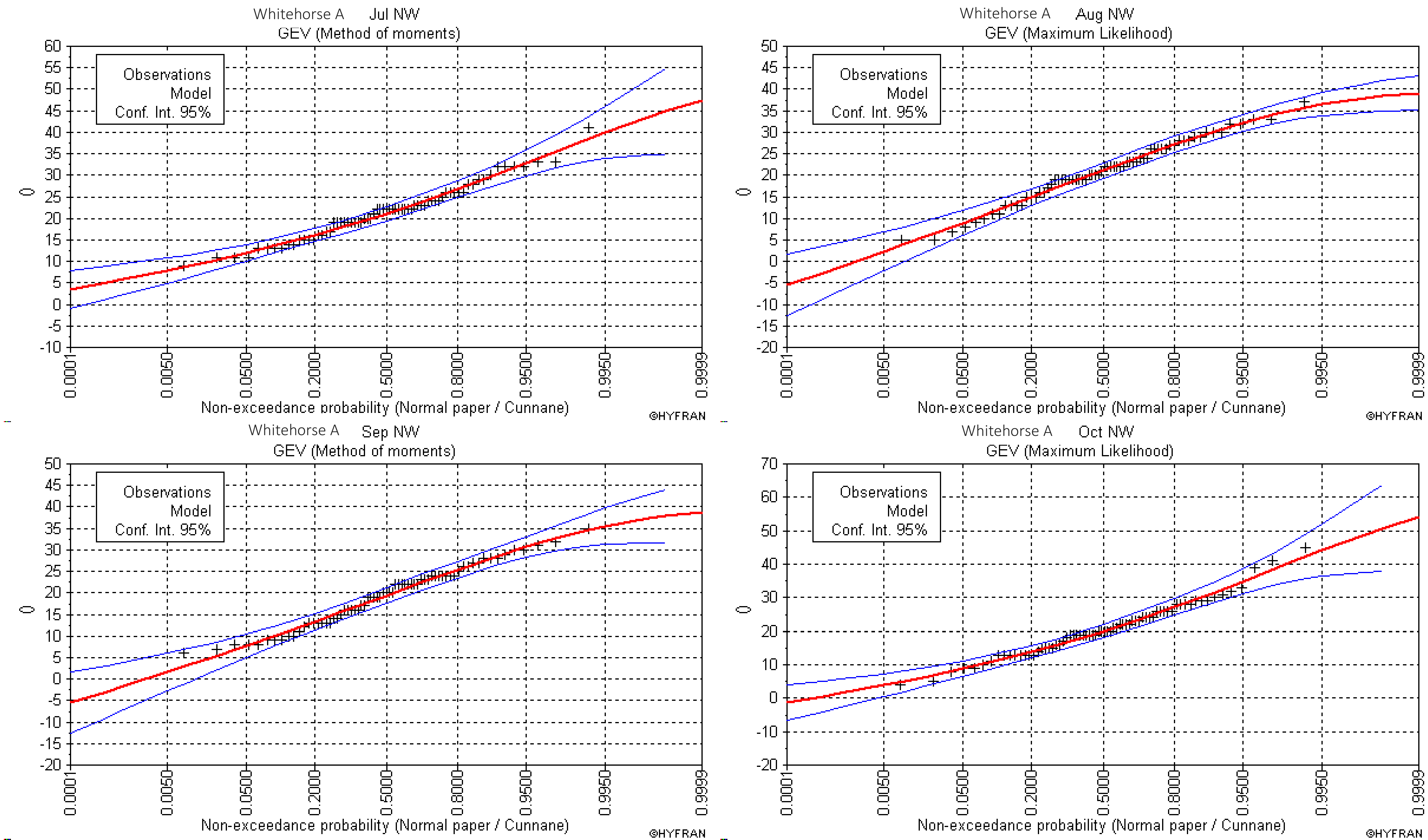

APPENDIX D

Correlation Figures

BENNETT LAKE

WATER LEVEL CORRELATION WITH WIND SPEED (10TH PERCENTILE WATER LEVEL SUBSET)

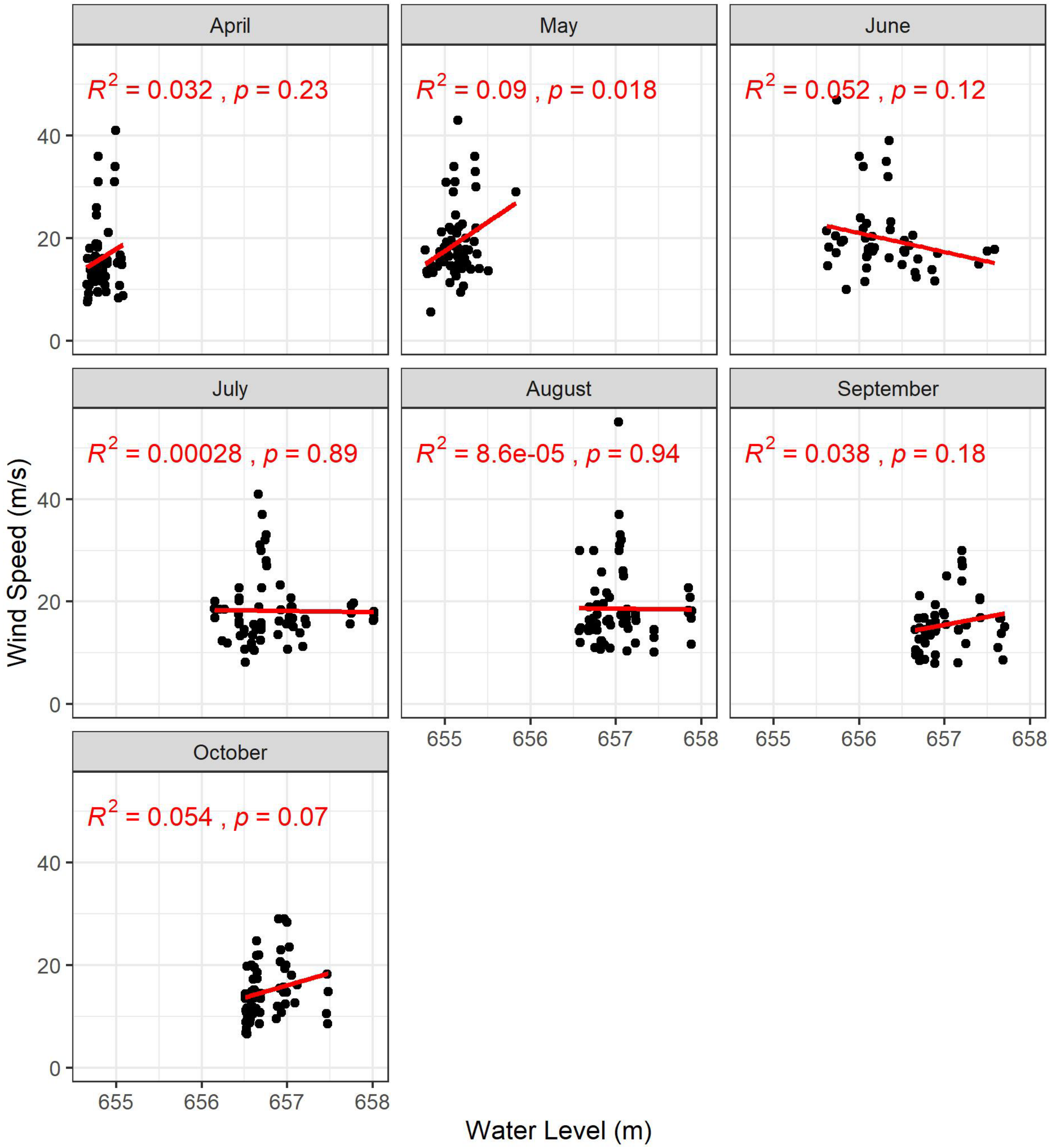

WATER LEVEL CORRELATION WITH WIND DIRECTION (10TH PERCENTILE WATER LEVEL SUBSET)

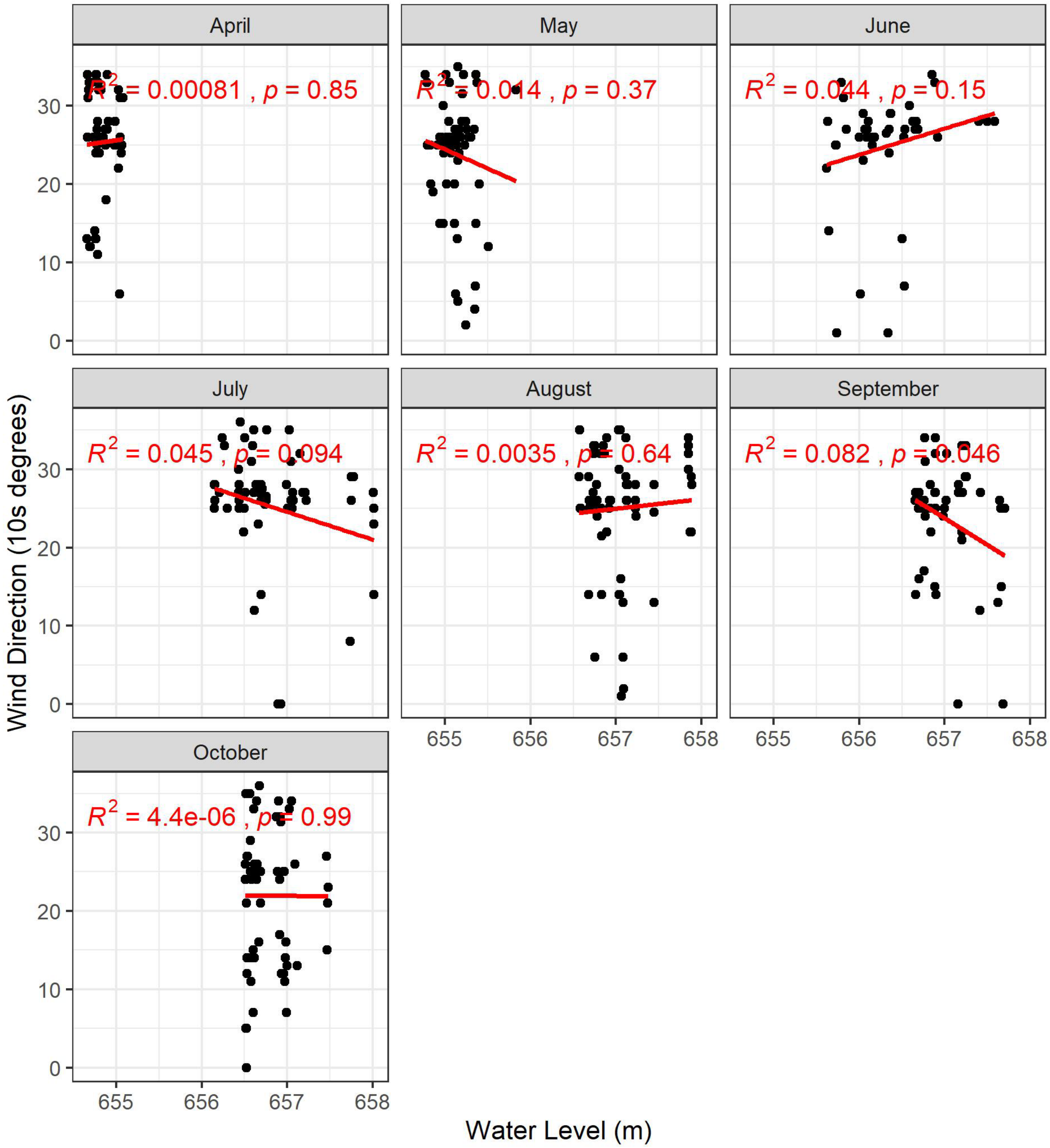

WATER LEVEL CORRELATION WITH WIND SPEED (MAXIMUM MONTHLY WATER LEVEL SUBSET)

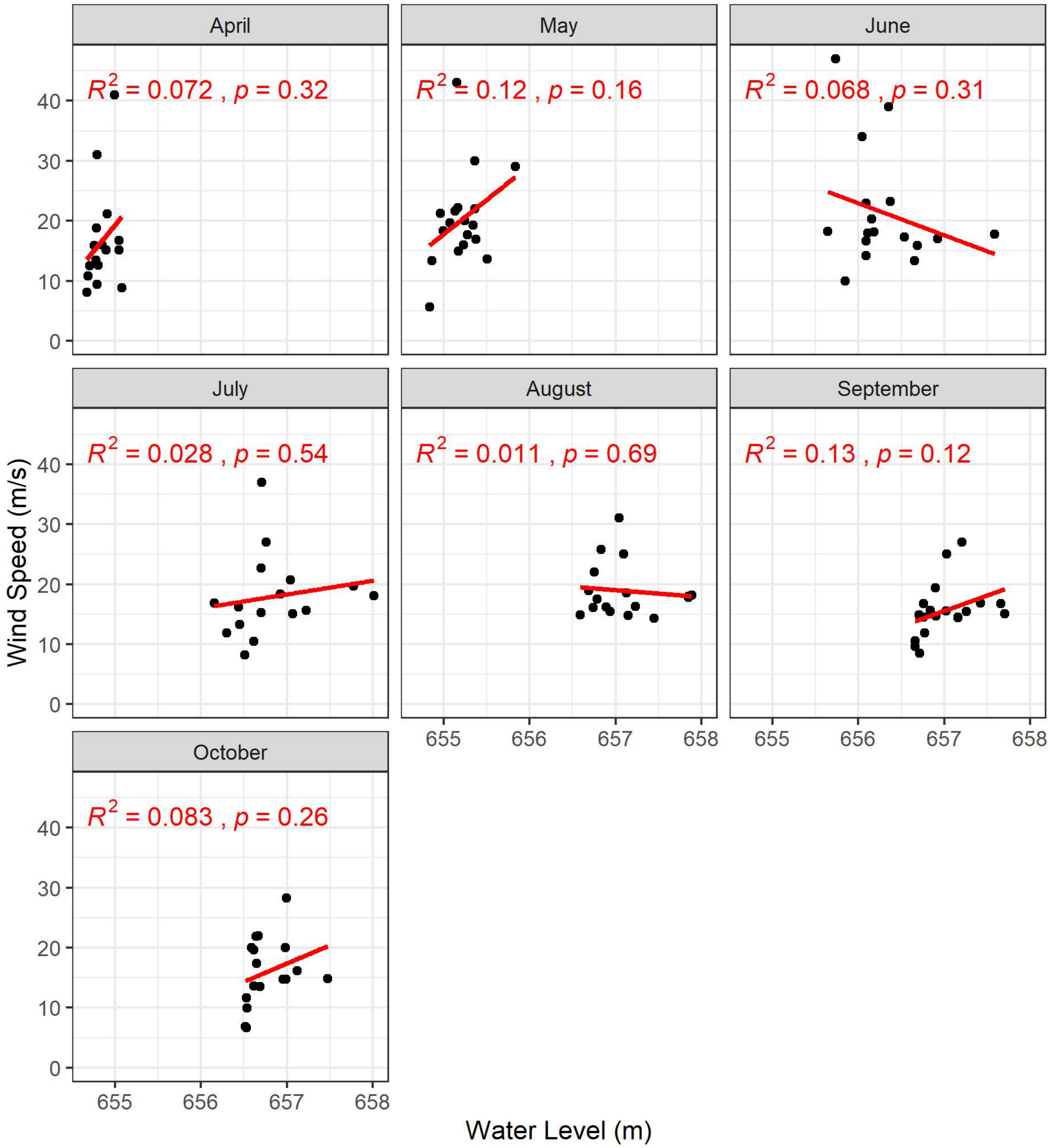

WATER LEVEL CORRELATION WITH WIND DIRECTION (MAXIMUM MONTHLY WATER LEVEL SUBSET)

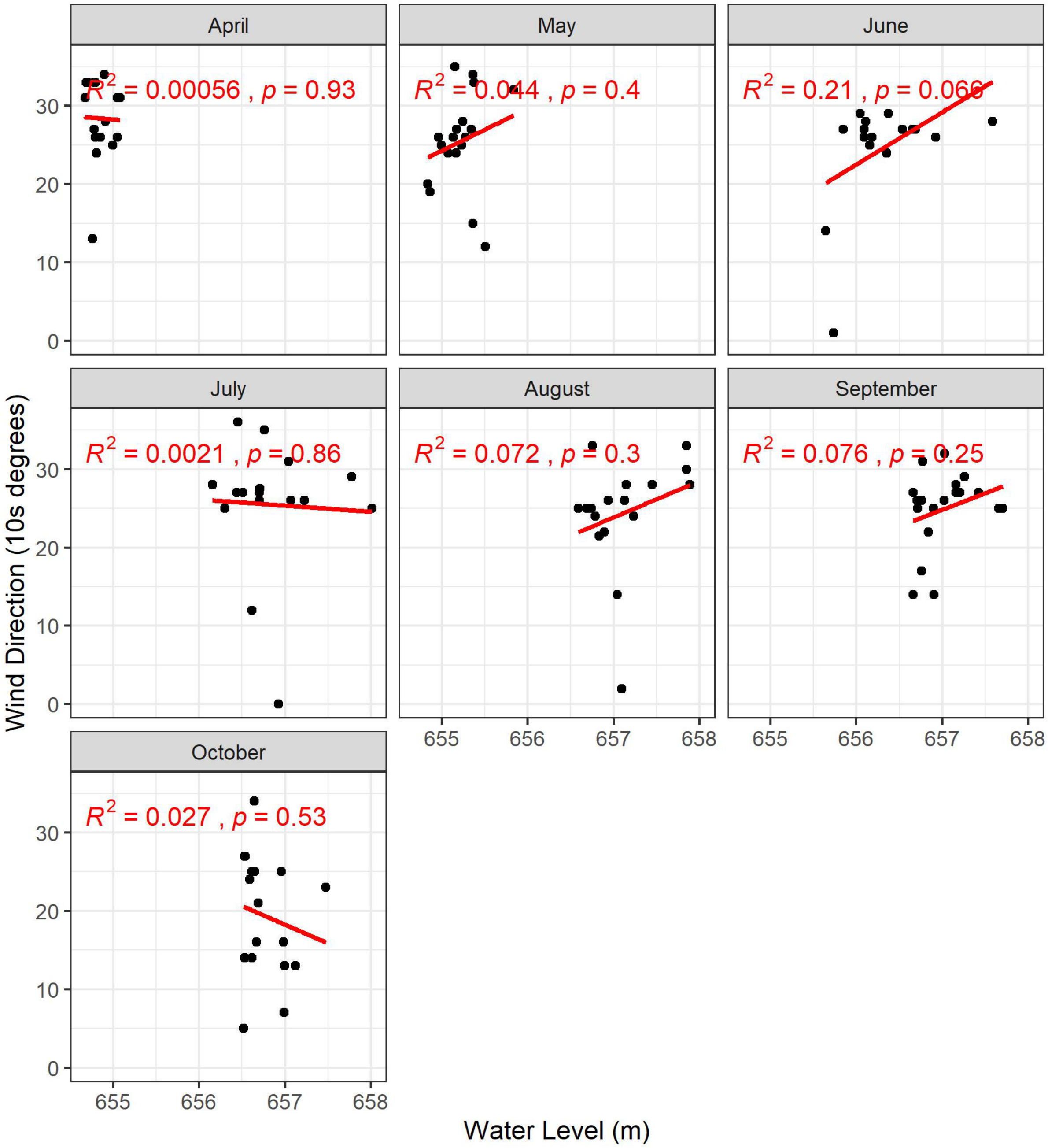

WIND SPEED CORRELATION WITH WATER LEVEL (10TH PERCENTILE WIND SPEED SUBSET)

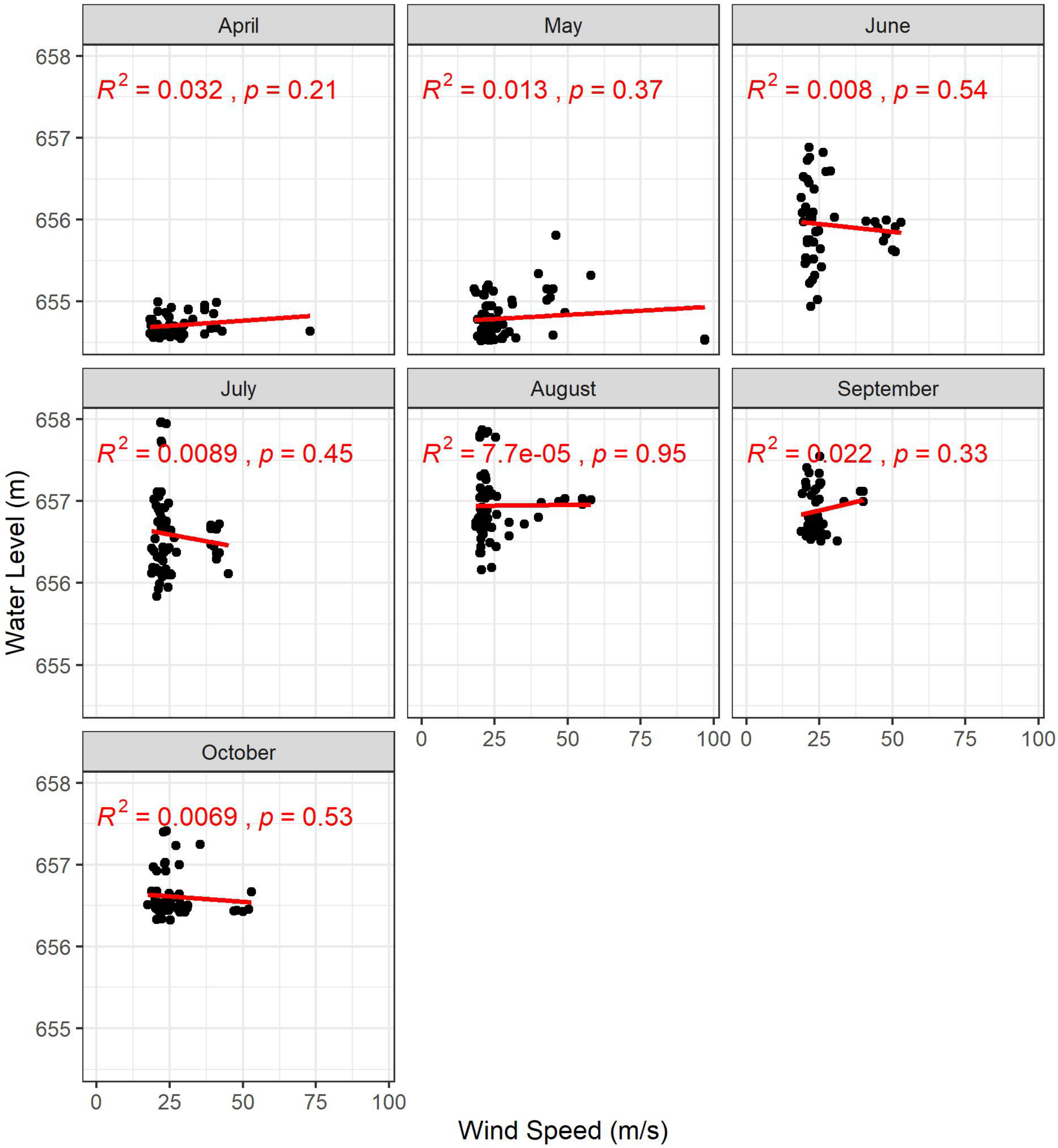

WIND SPEED CORRELATION WITH WIND DIRECTION (10TH PERCENTILE WIND SPEED SUBSET)

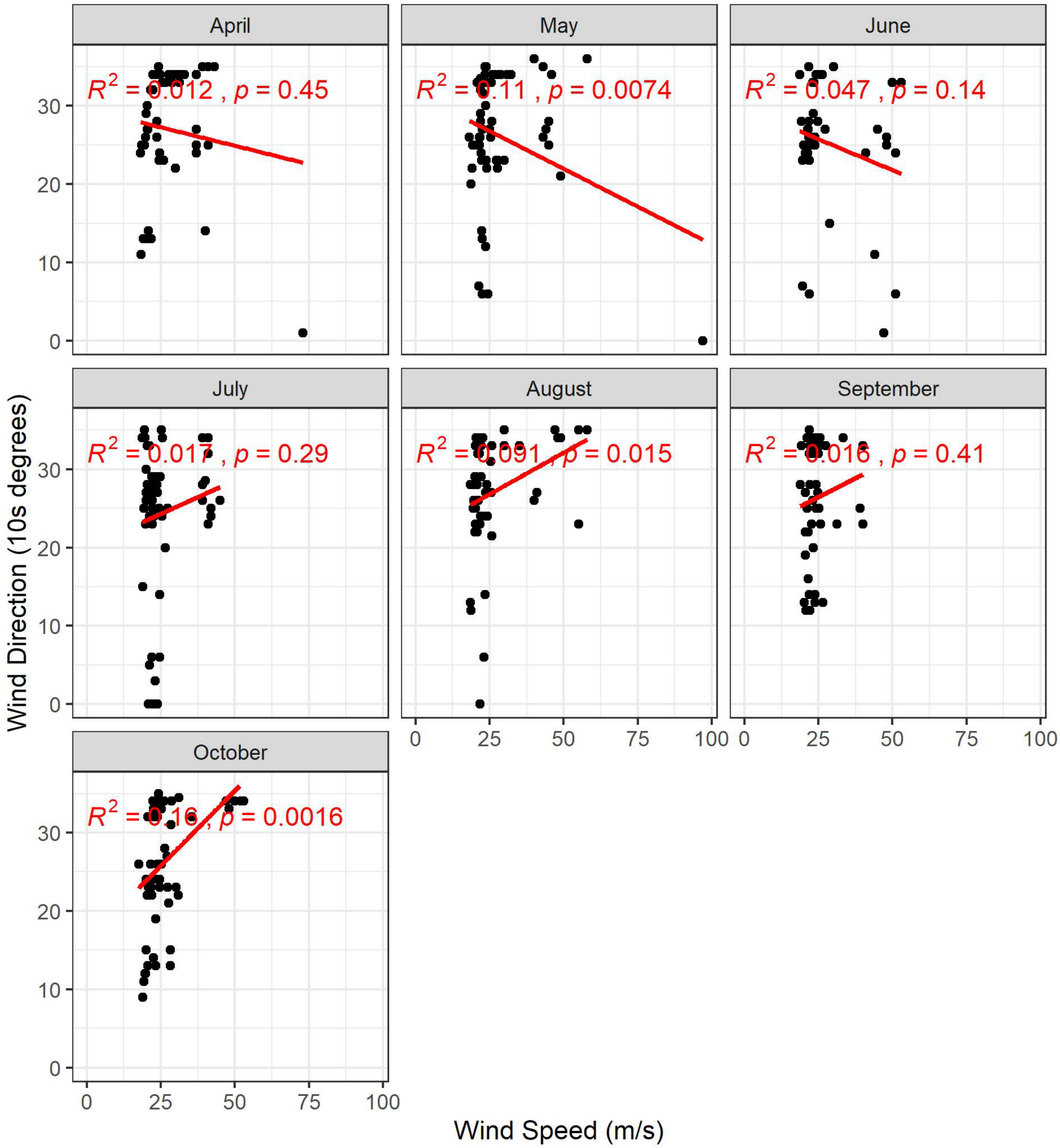

WIND SPEED CORRELATION WITH WATER LEVEL (MAXIMUM MONTHLY WIND SPEED SUBSET)

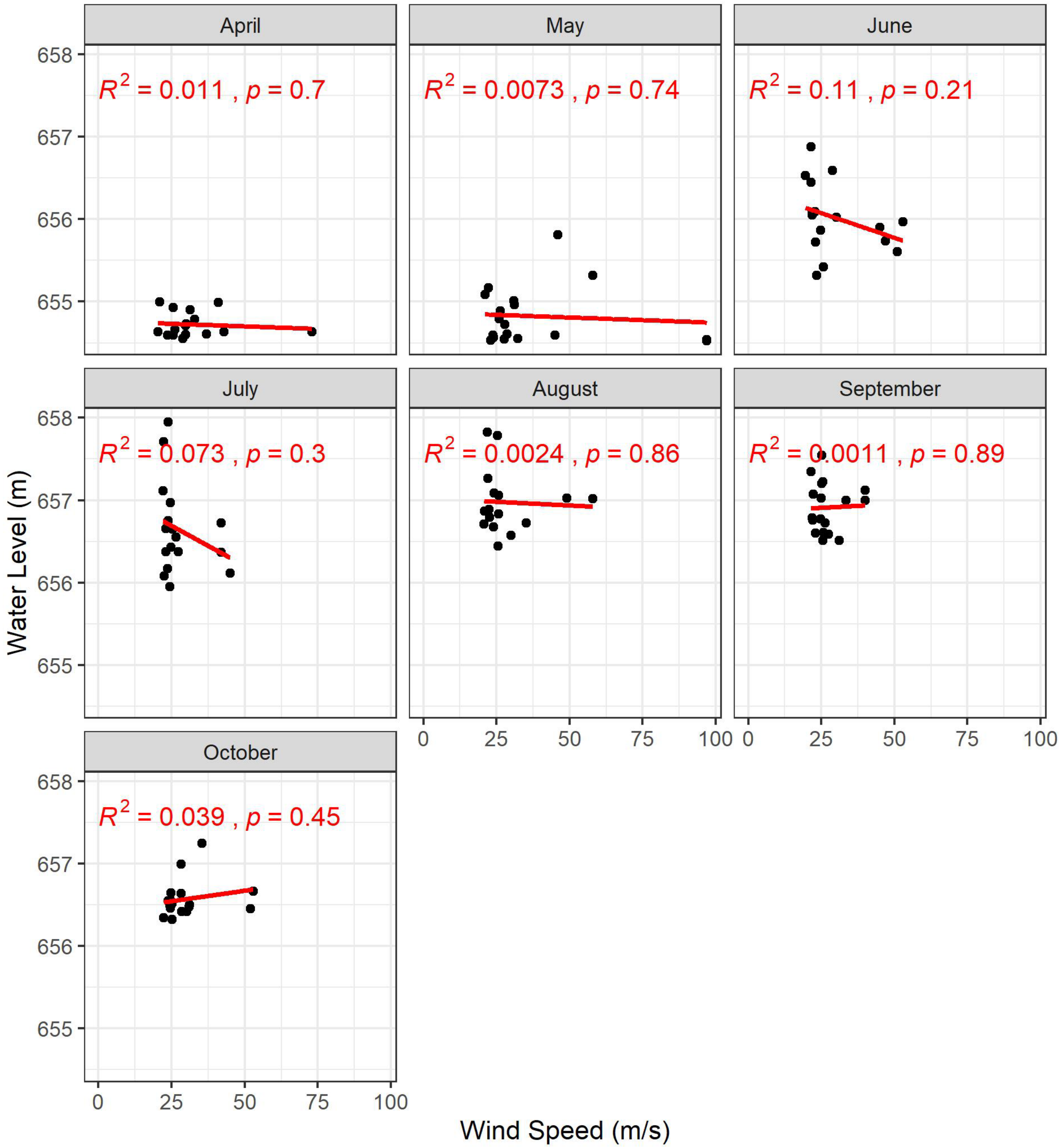

WIND SPEED CORRELATION WITH WIND DIRECTION (MAXIMUM MONTHLY WIND SPEED SUBSET)

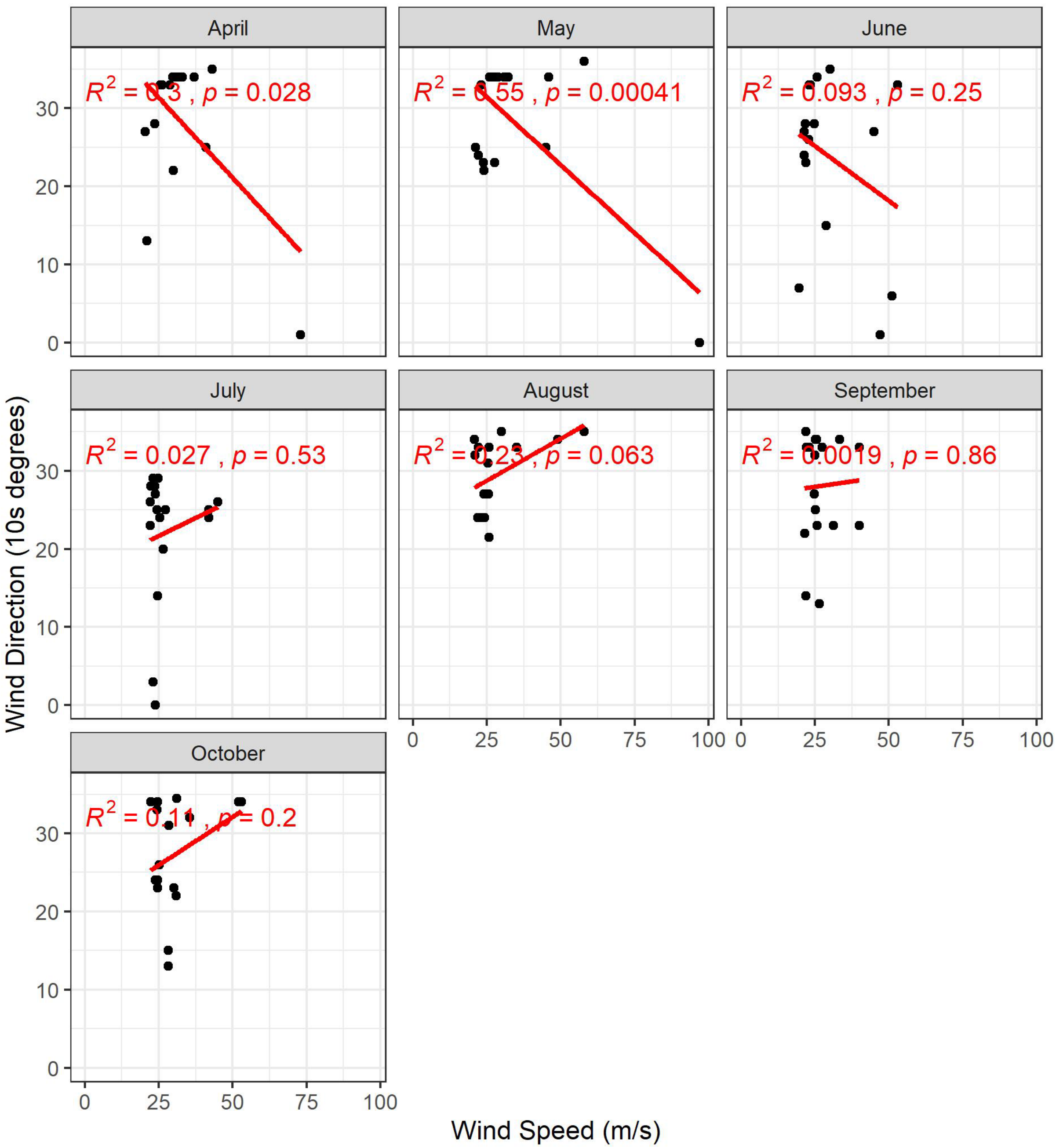

TAGISH LAKE

WATER LEVEL CORRELATION WITH WIND SPEED (10TH PERCENTILE WATER LEVEL SUBSET)

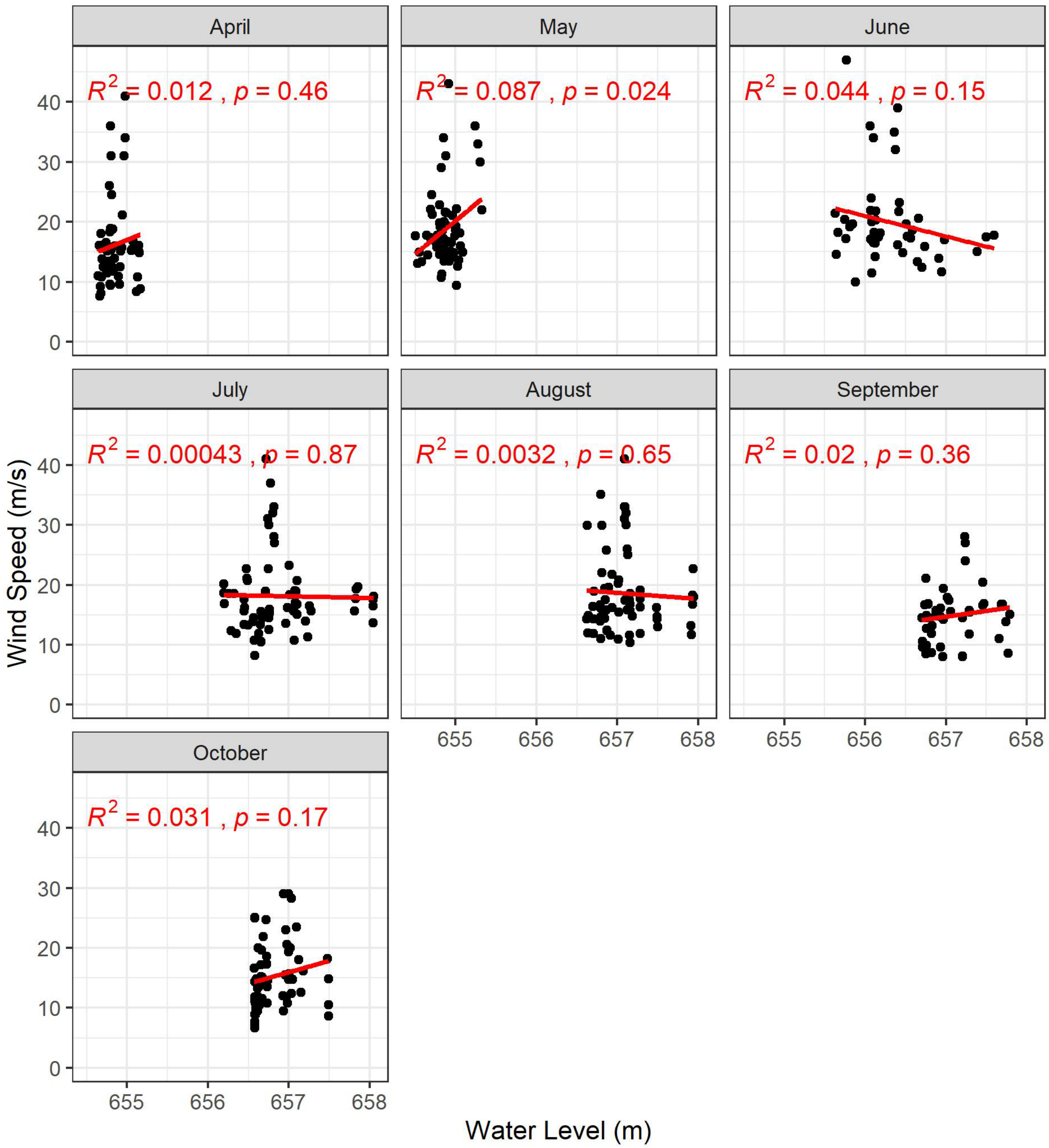

WATER LEVEL CORRELATION WITH WIND DIRECTION (10TH PERCENTILE WATER LEVEL SUBSET)

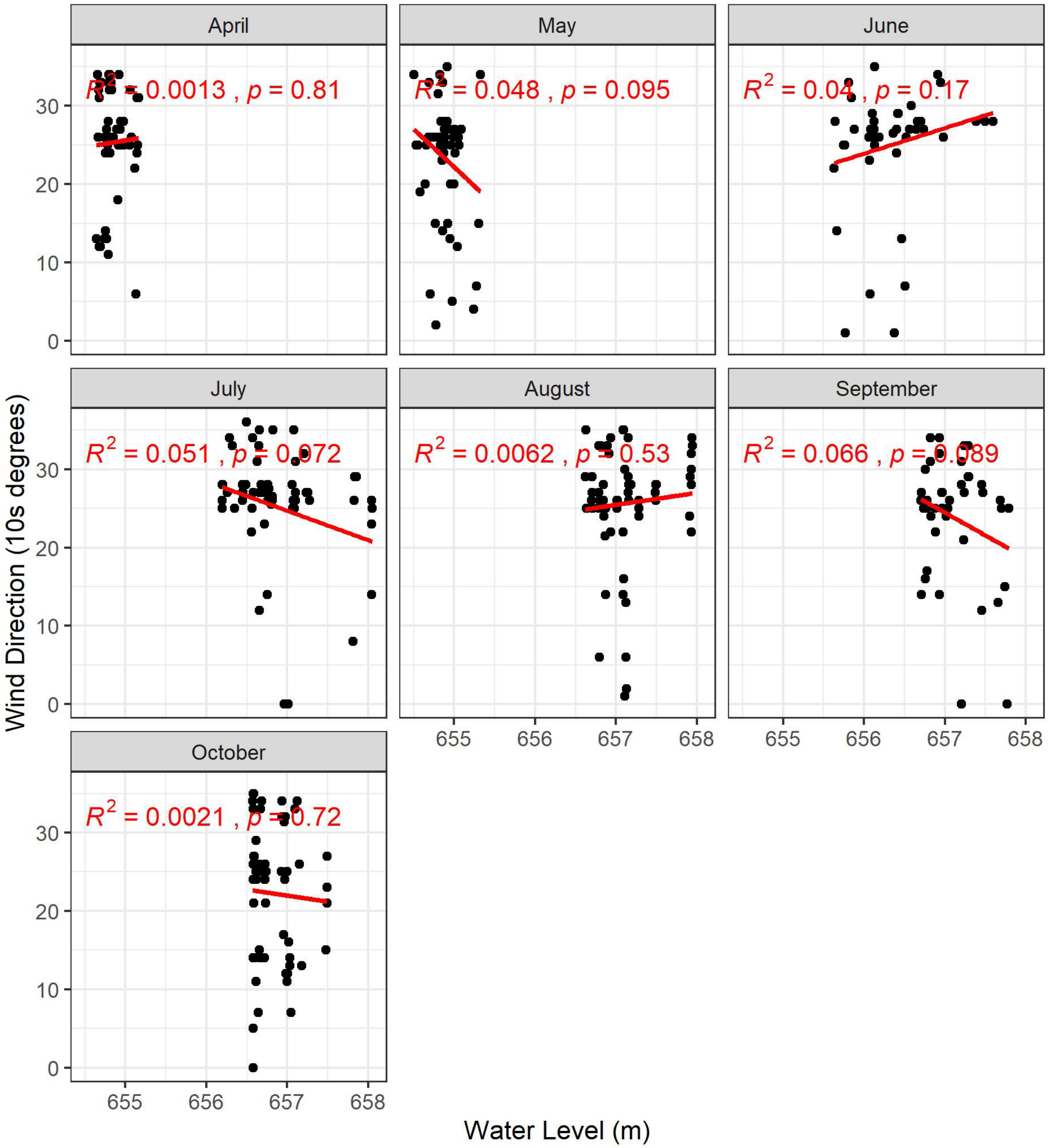

WATER LEVEL CORRELATION WITH WIND SPEED (MAXIMUM MONTHLY WATER LEVEL SUBSET)

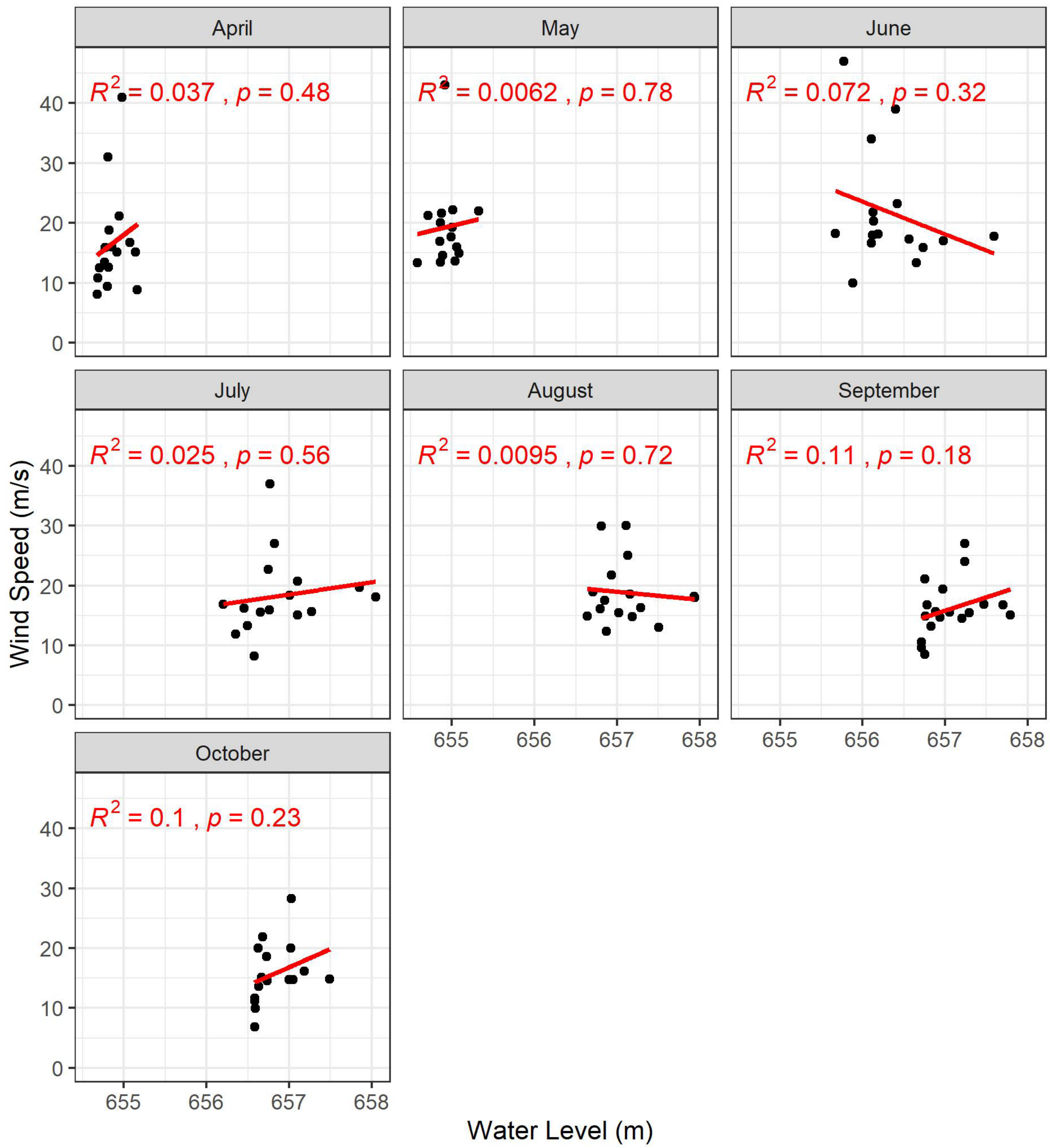

WATER LEVEL CORRELATION WITH WIND DIRECTION (MAXIMUM MONTHLY WATER LEVEL SUBSET)

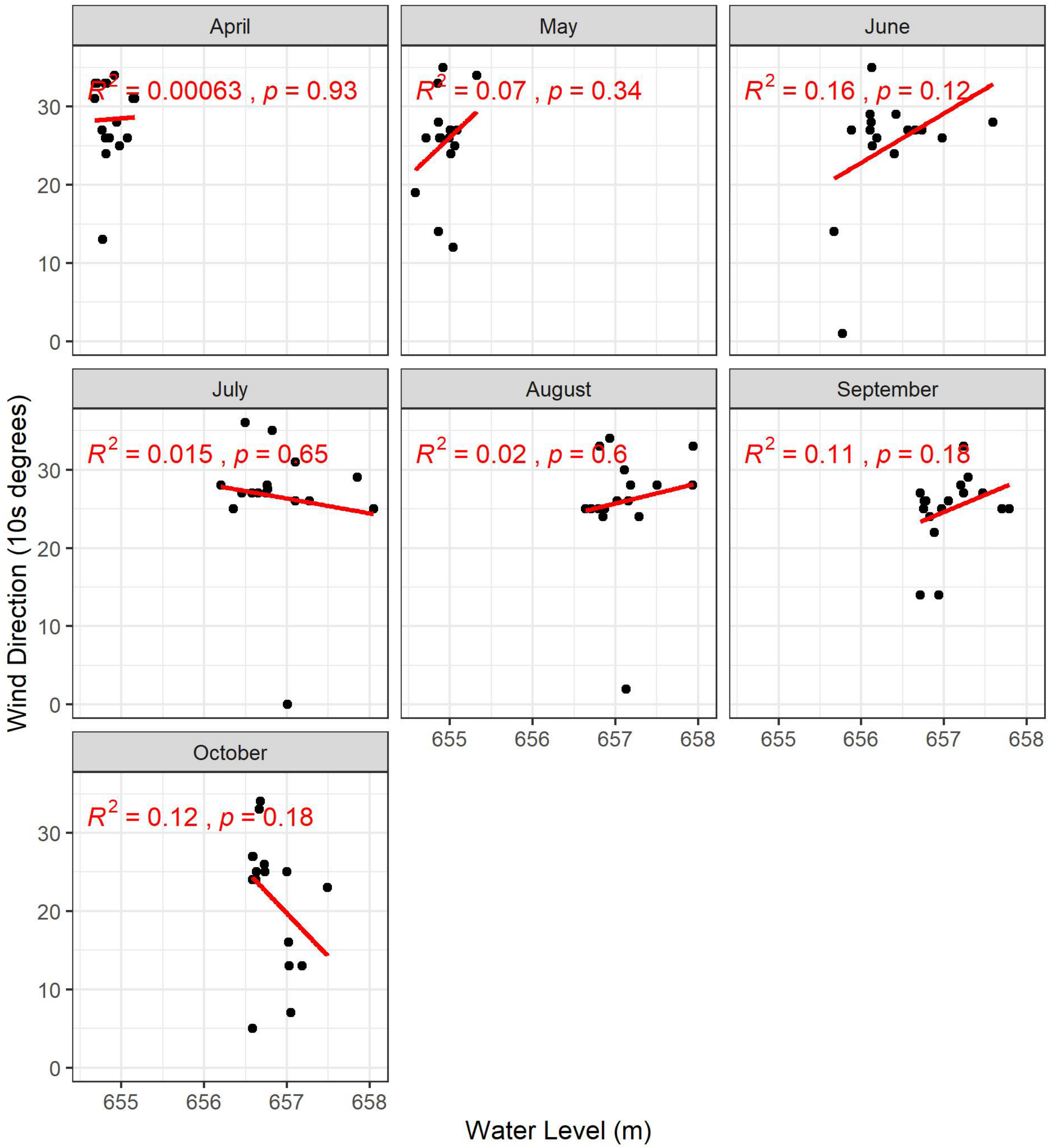

WIND SPEED CORRELATION WITH WATER LEVEL (10TH PERCENTILE WIND SPEED SUBSET)

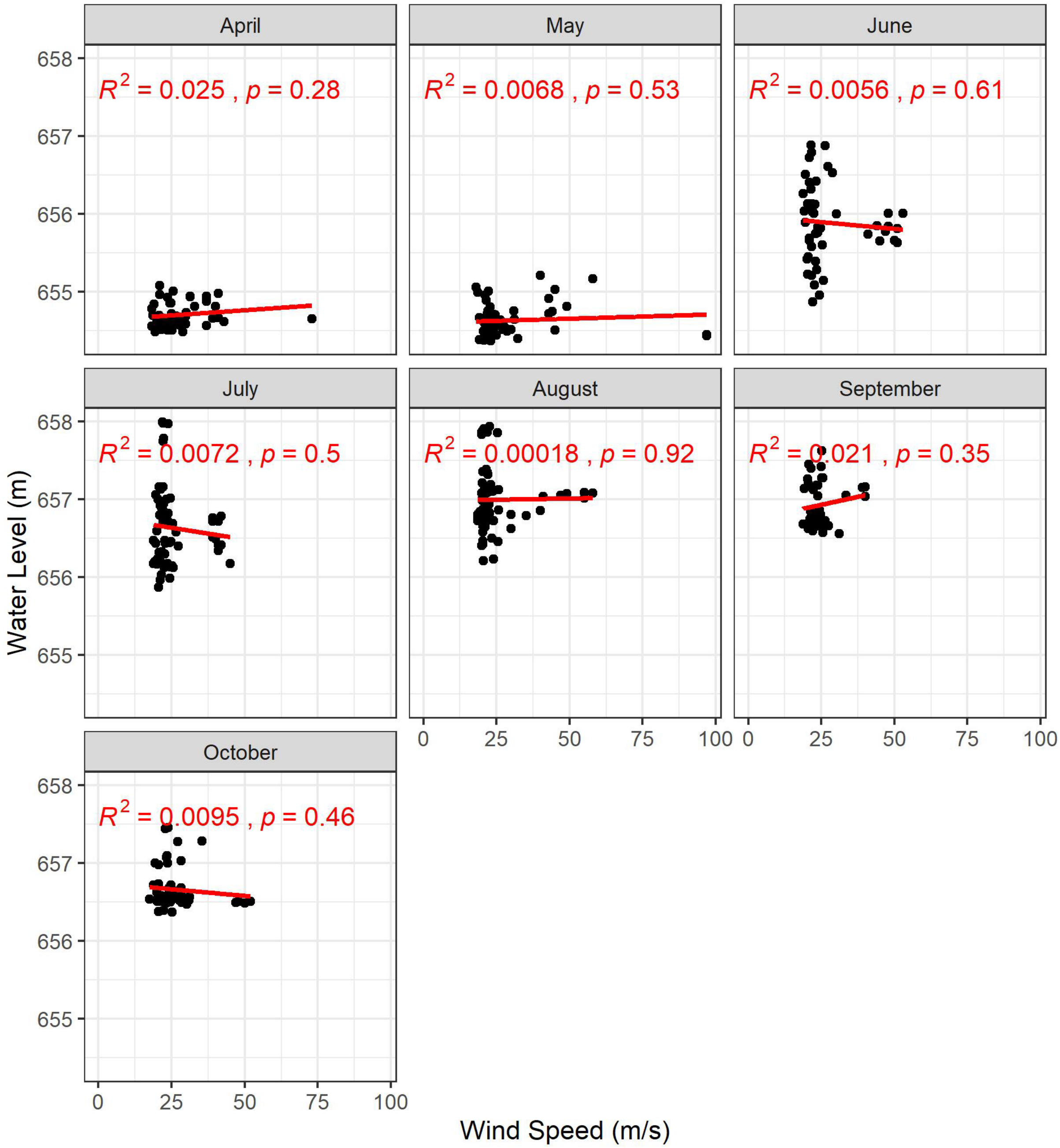

WIND SPEED CORRELATION WITH WIND DIRECTION (10TH PERCENTILE WIND SPEED SUBSET)

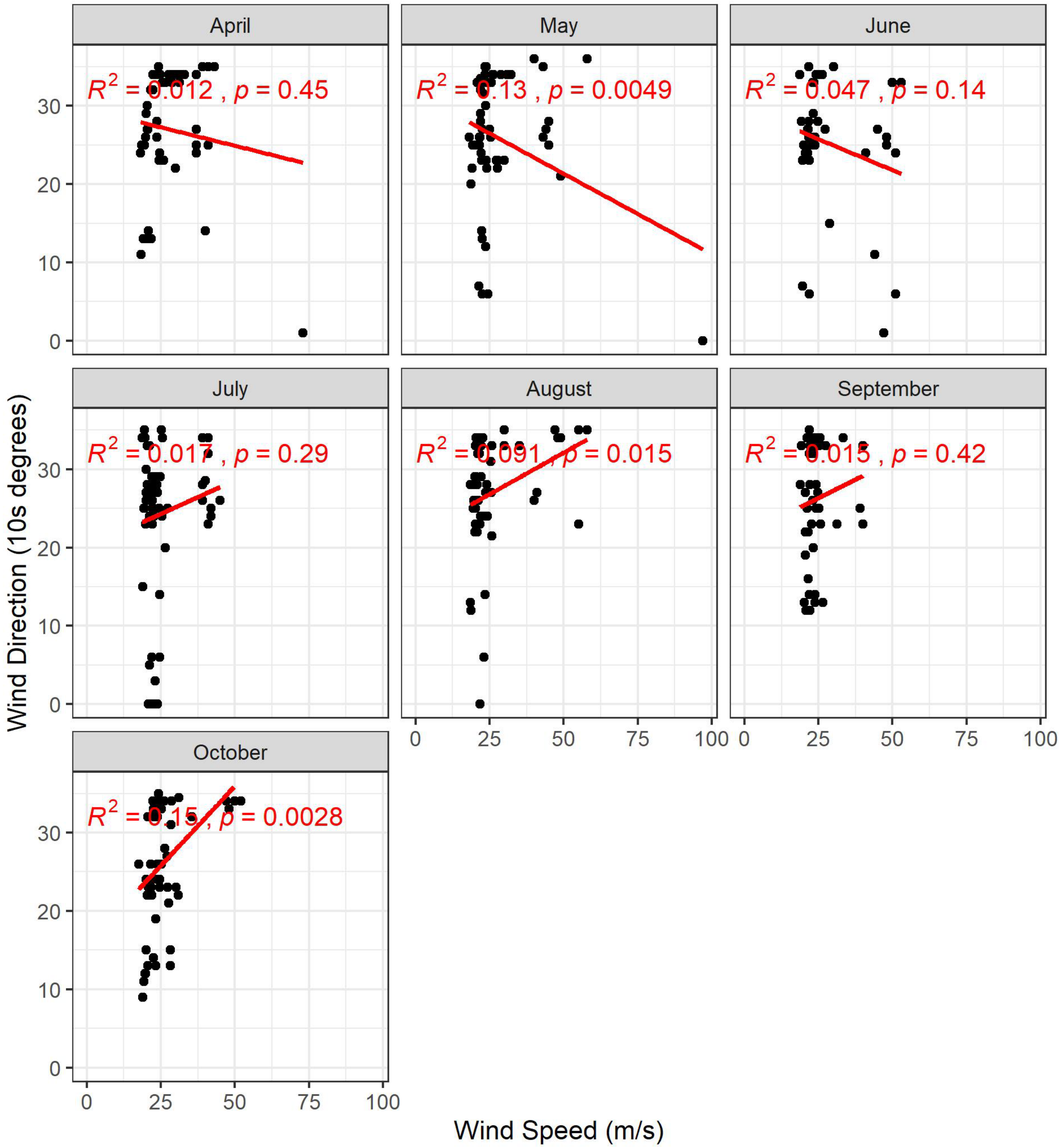

WIND SPEED CORRELATION WITH WATER LEVEL (MAXIMUM MONTHLY WIND SPEED SUBSET)

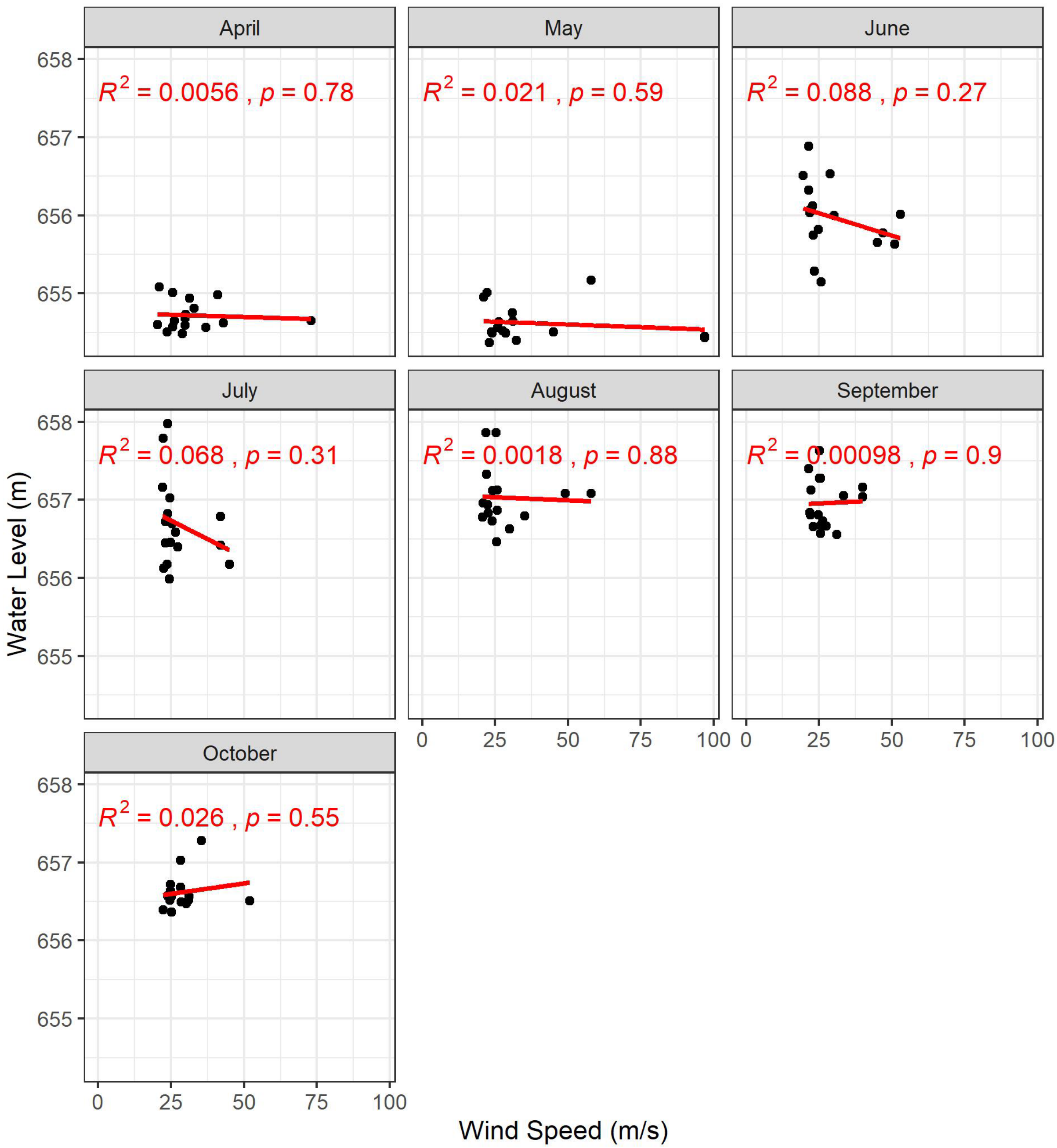

WIND SPEED CORRELATION WITH WIND DIRECTION (MAXIMUM MONTHLY WIND SPEED SUBSET)

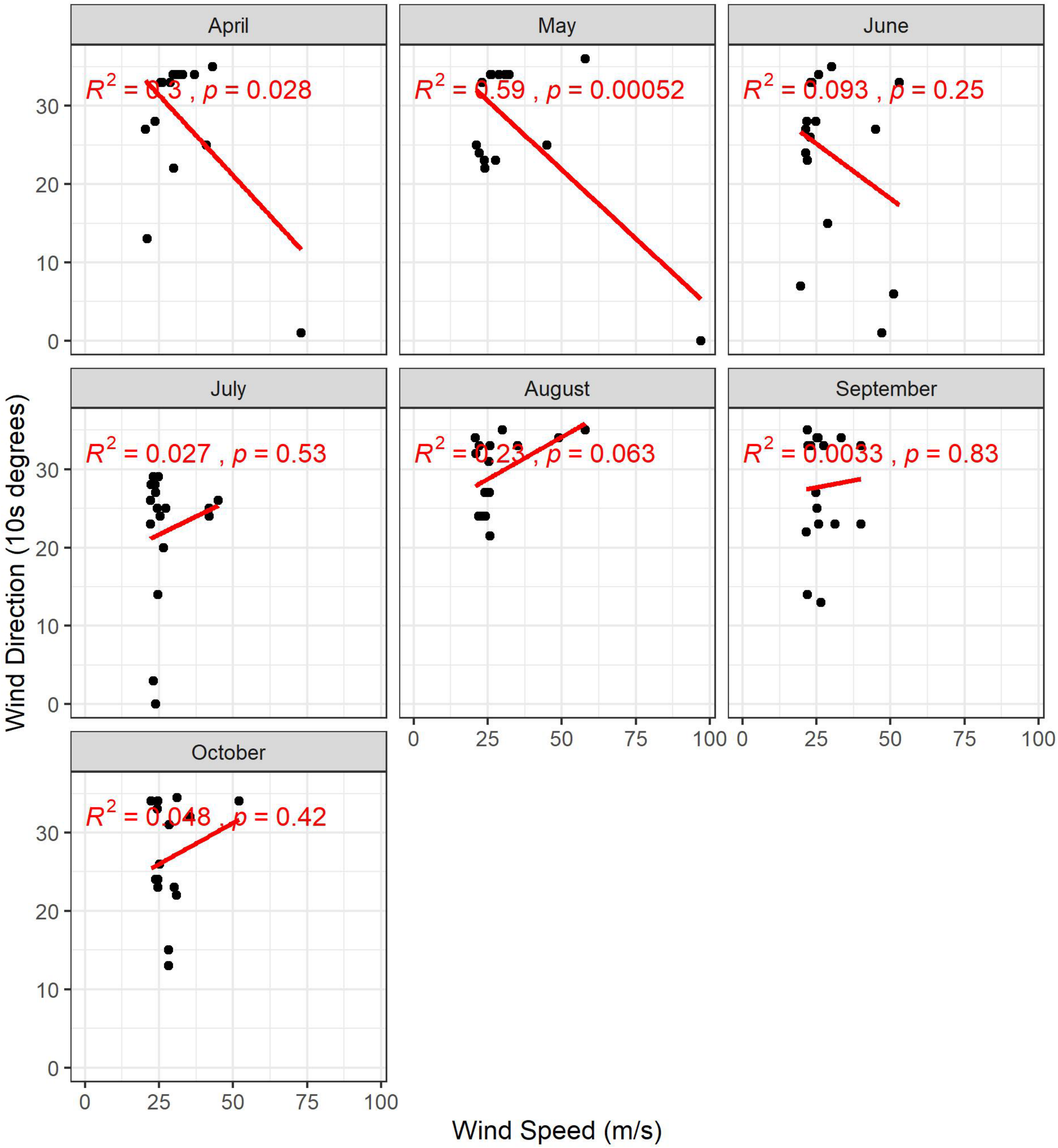

MARSH LAKE

WATER LEVEL CORRELATION WITH WIND SPEED (10TH PERCENTILE WATER LEVEL SUBSET)

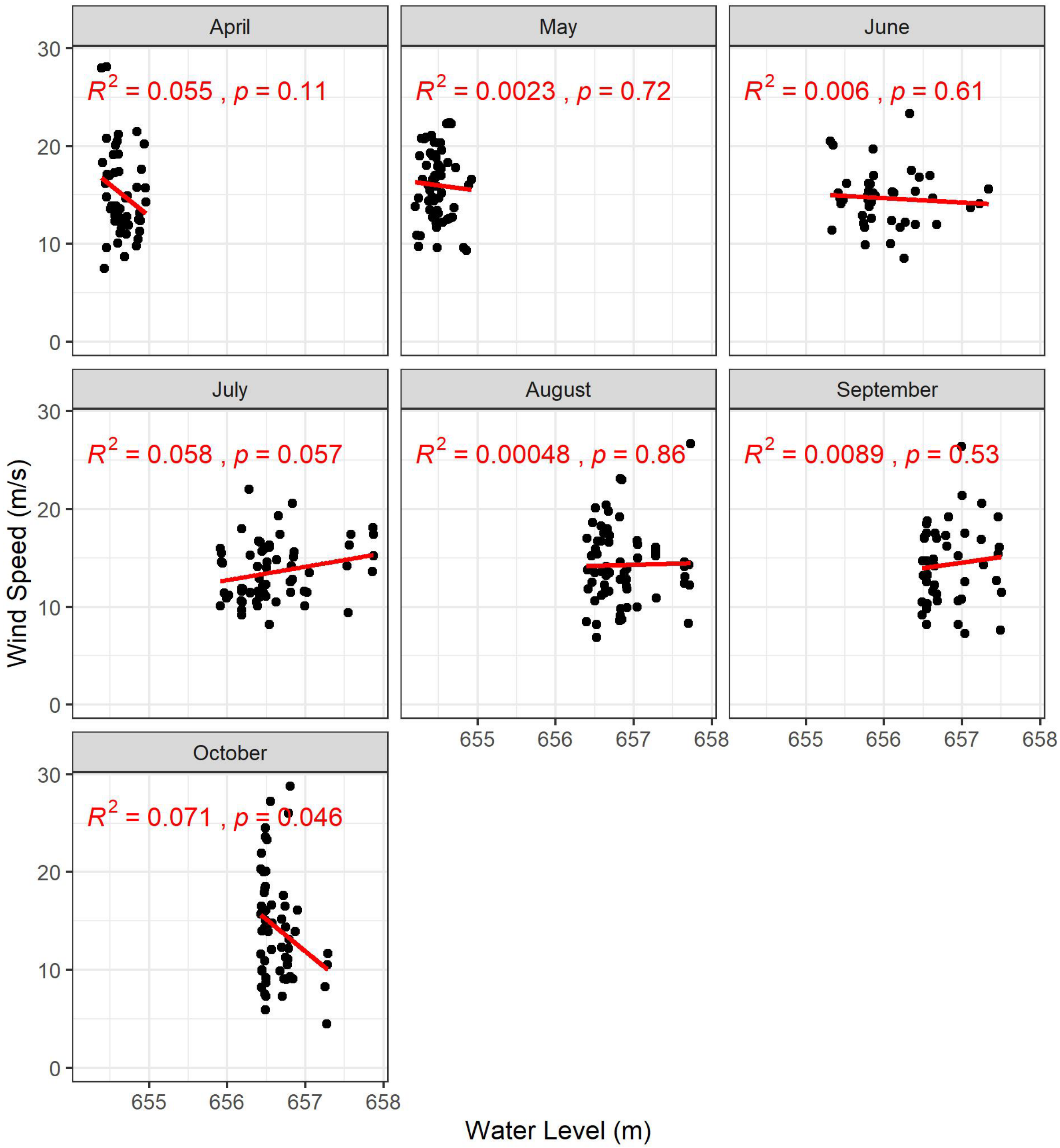

WATER LEVEL CORRELATION WITH WIND DIRECTION (10TH PERCENTILE WATER LEVEL SUBSET)

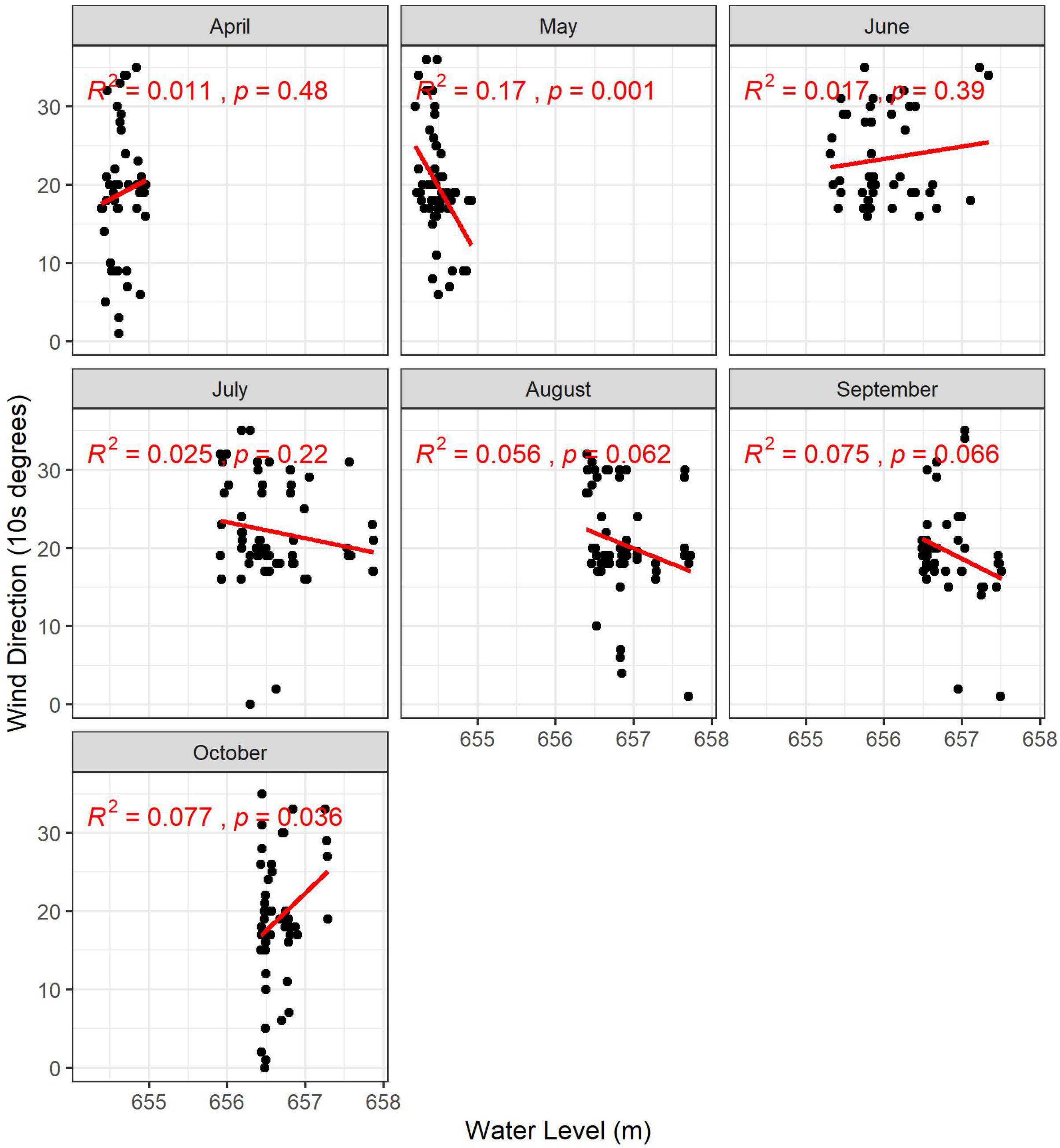

WATER LEVEL CORRELATION WITH WIND SPEED (MAXIMUM MONTHLY WATER LEVEL SUBSET)

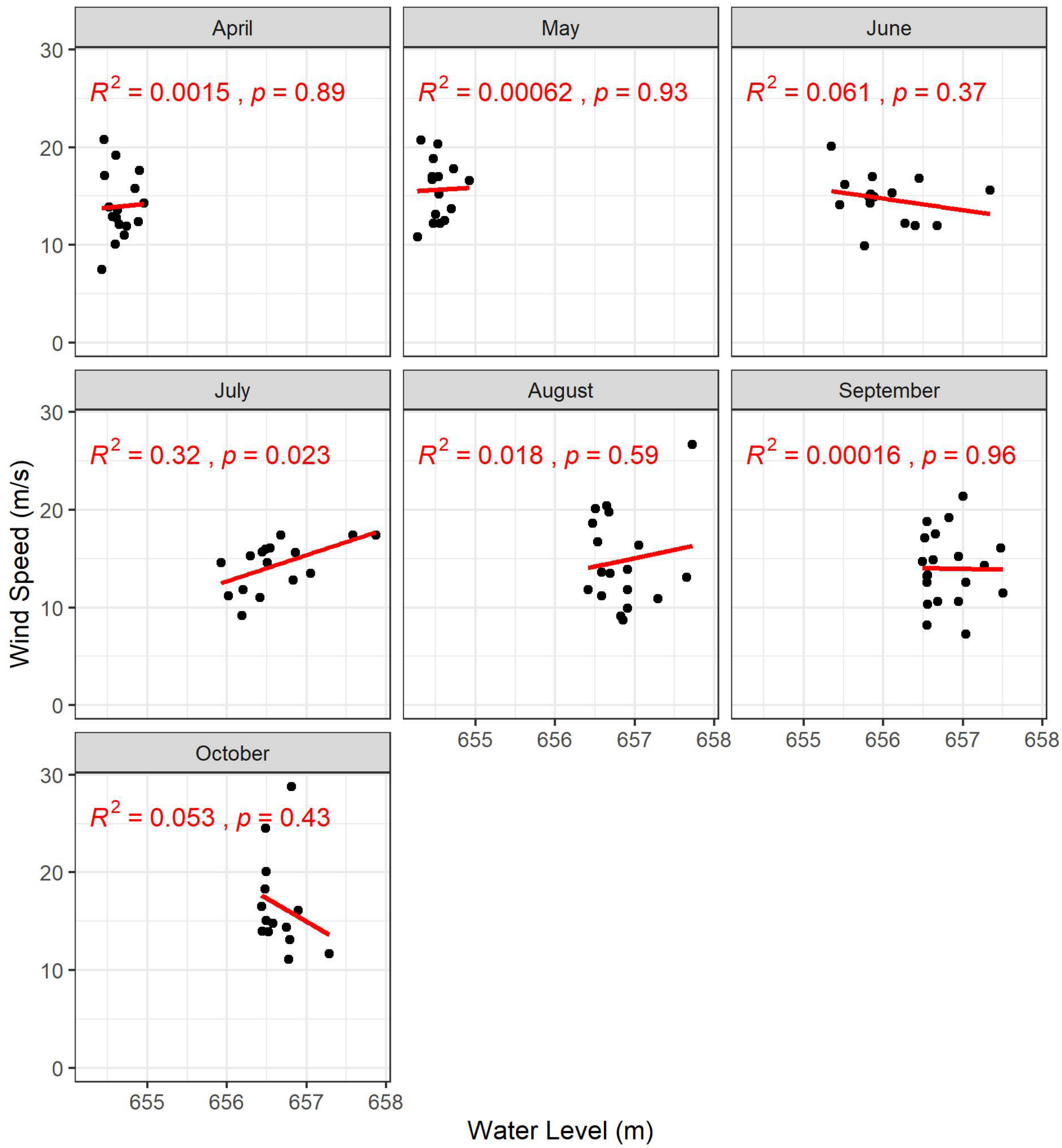

WATER LEVEL CORRELATION WITH WIND DIRECTION (MAXIMUM MONTHLY WATER LEVEL SUBSET)

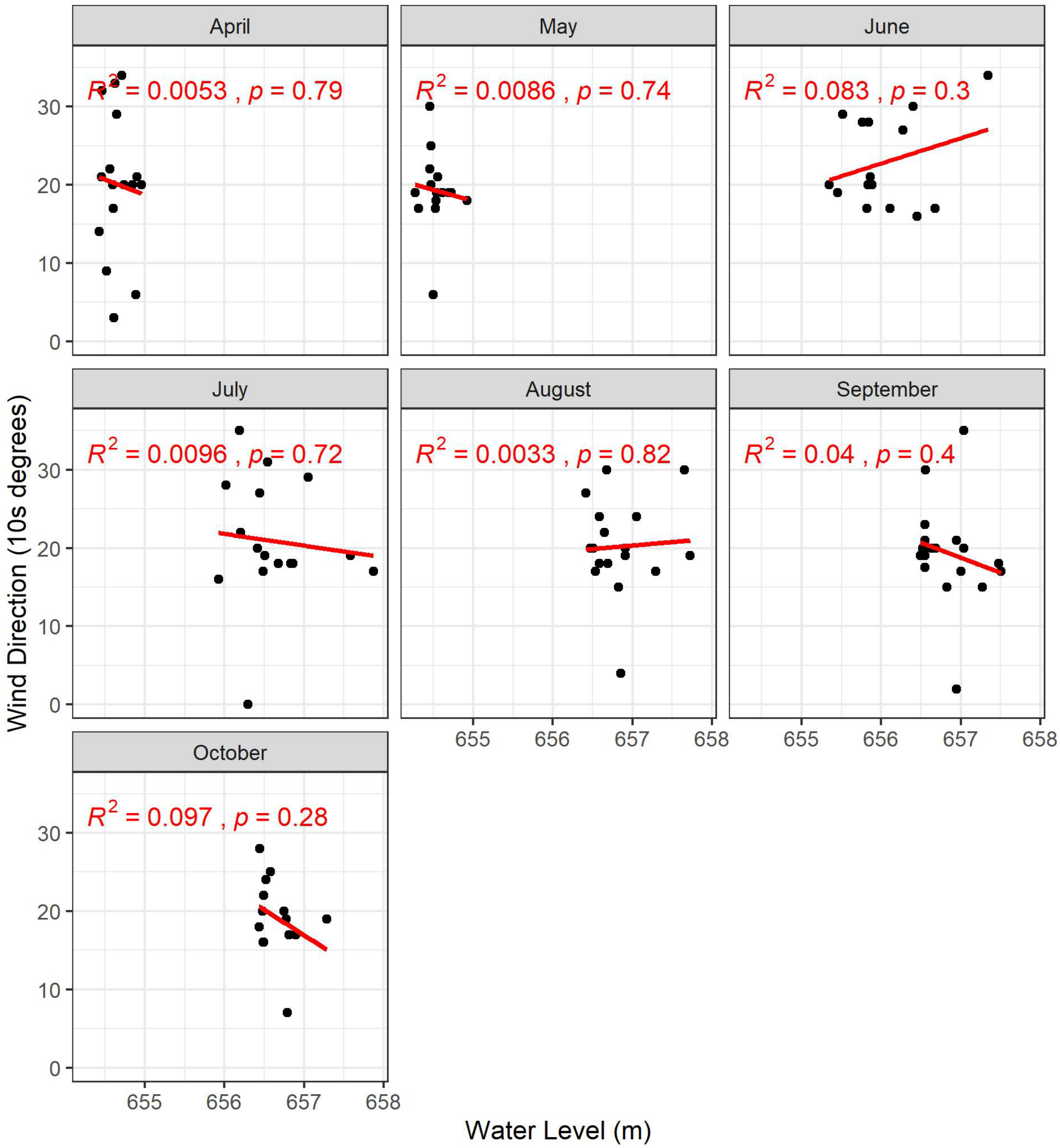

WIND SPEED CORRELATION WITH WATER LEVEL (10TH PERCENTILE WIND SPEED SUBSET)

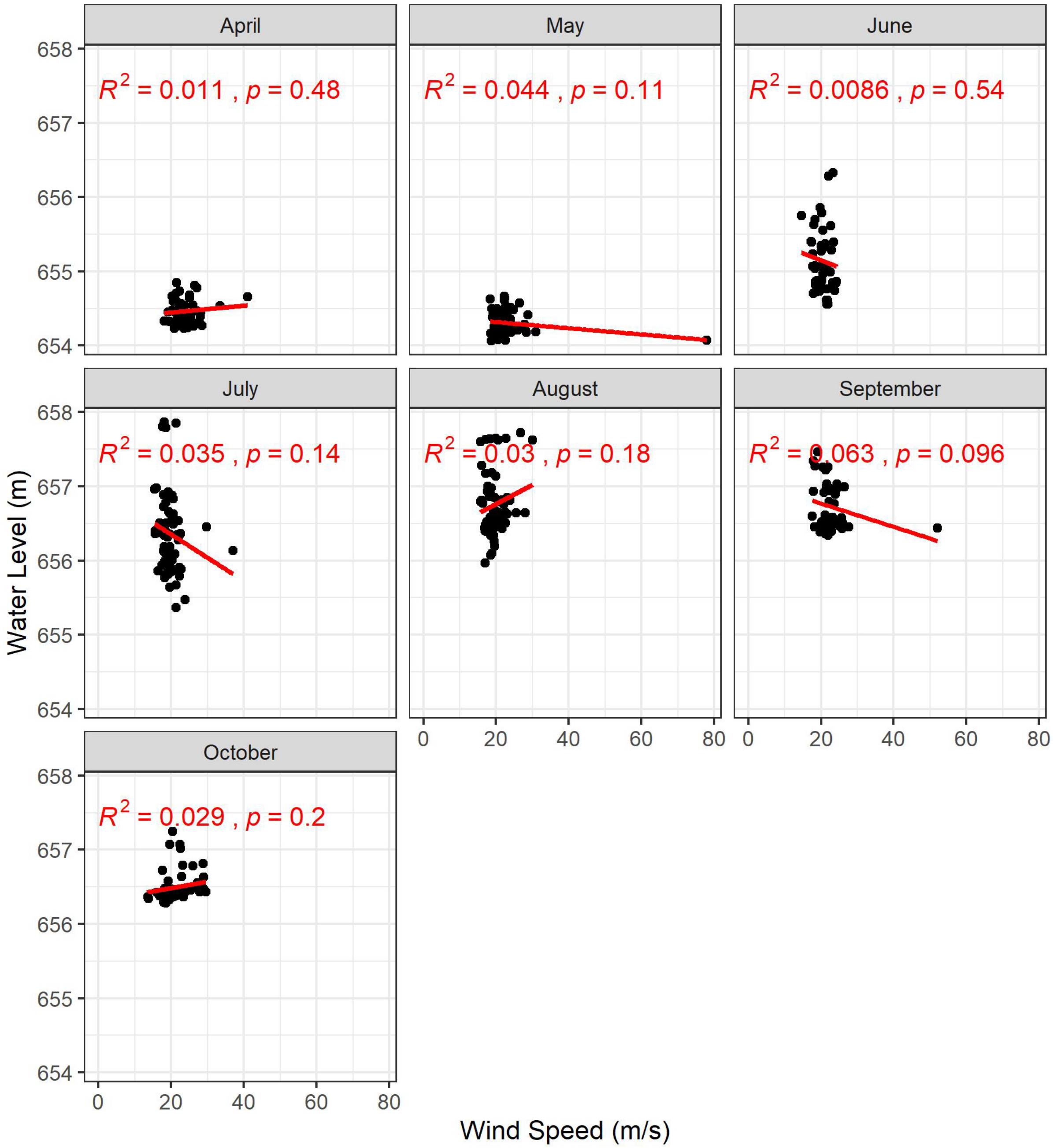

WIND SPEED CORRELATION WITH WIND DIRECTION (10TH PERCENTILE WIND SPEED SUBSET)

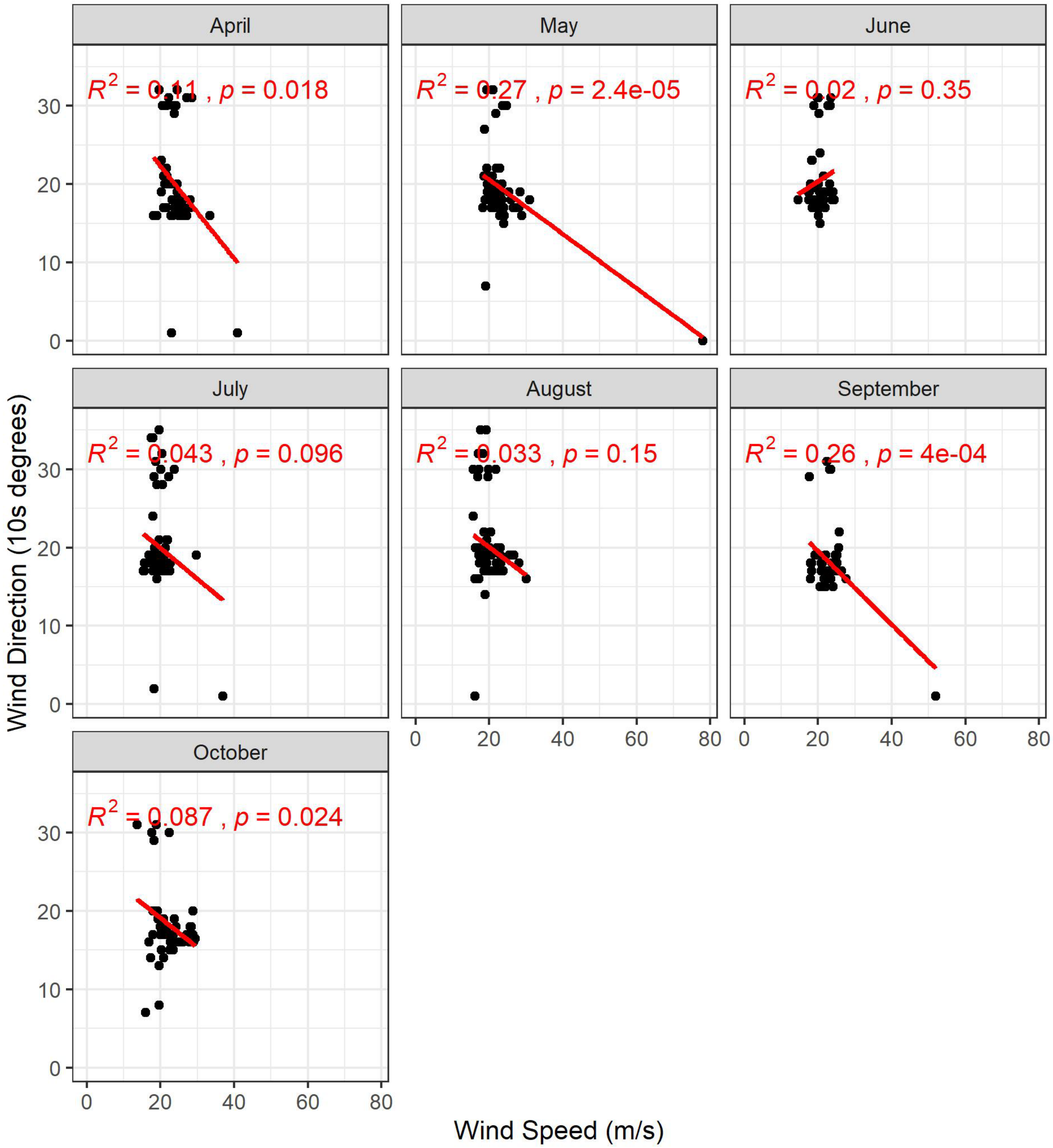

WIND SPEED CORRELATION WITH WATER LEVEL (MAXIMUM MONTHLY WIND SPEED SUBSET)

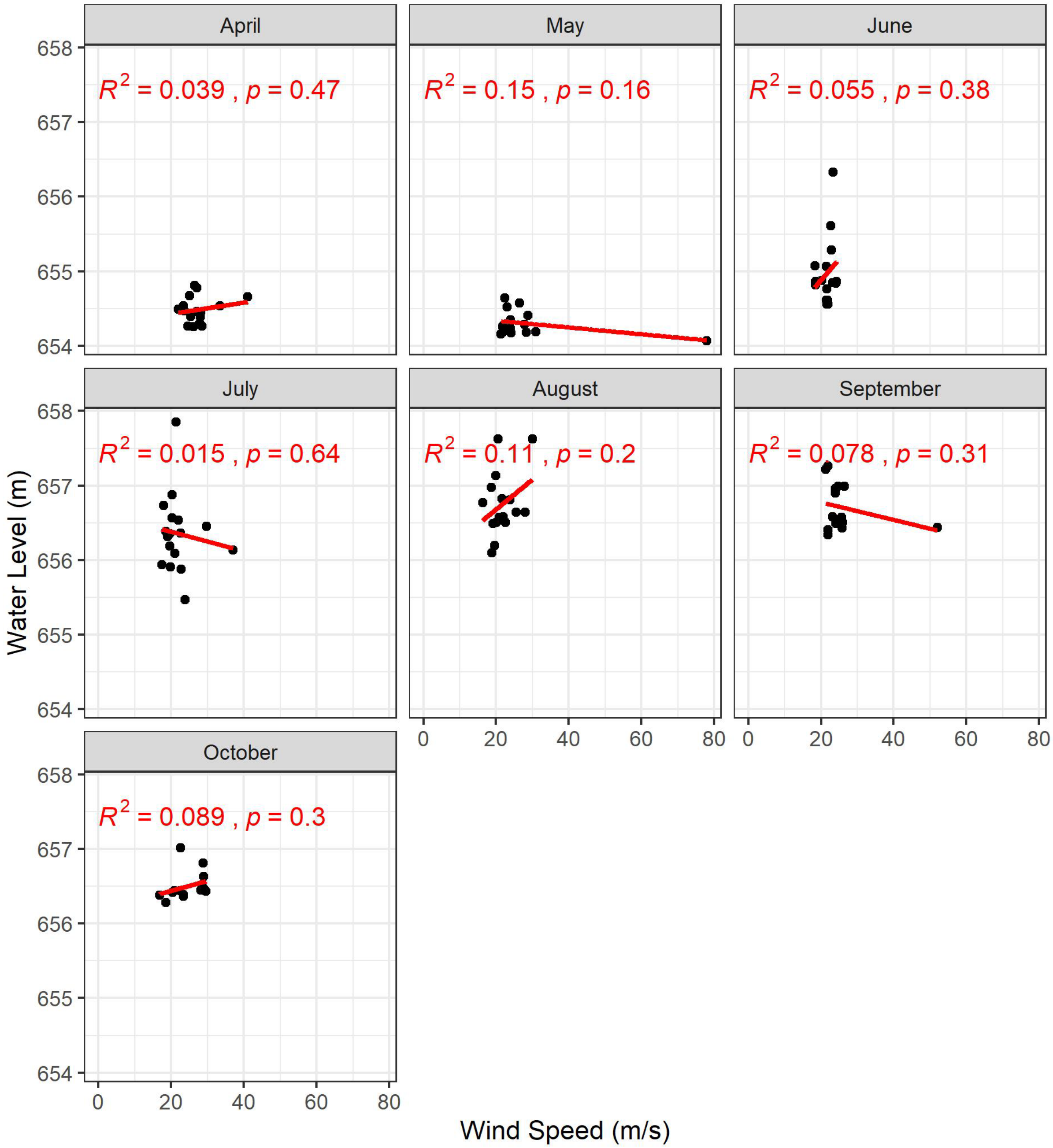

WIND SPEED CORRELATION WITH WIND DIRECTION (MAXIMUM MONTHLY WIND SPEED SUBSET)

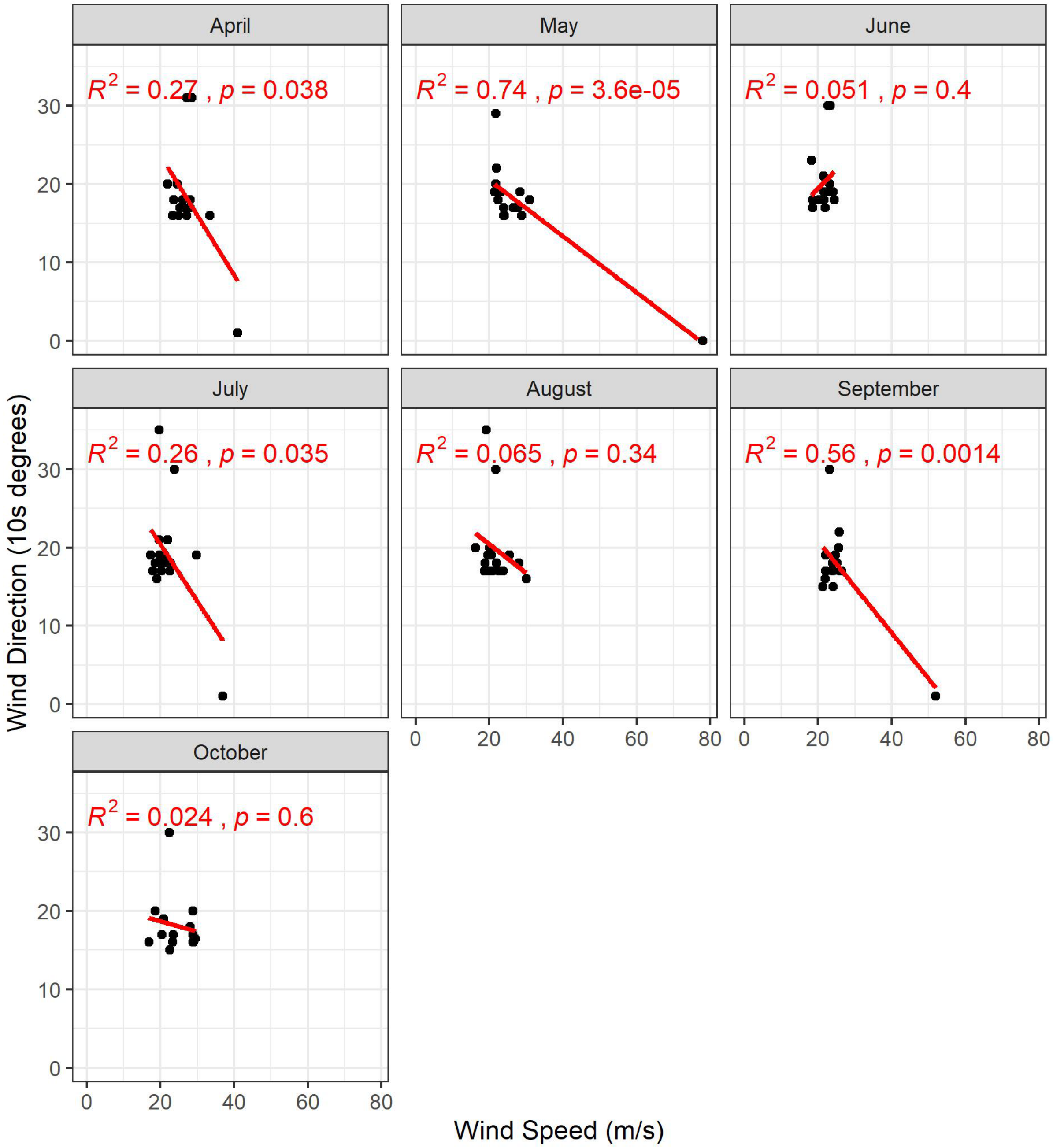

LAKE LABERGE

WATER LEVEL CORRELATION WITH WIND SPEED (10TH PERCENTILE WATER LEVEL SUBSET)

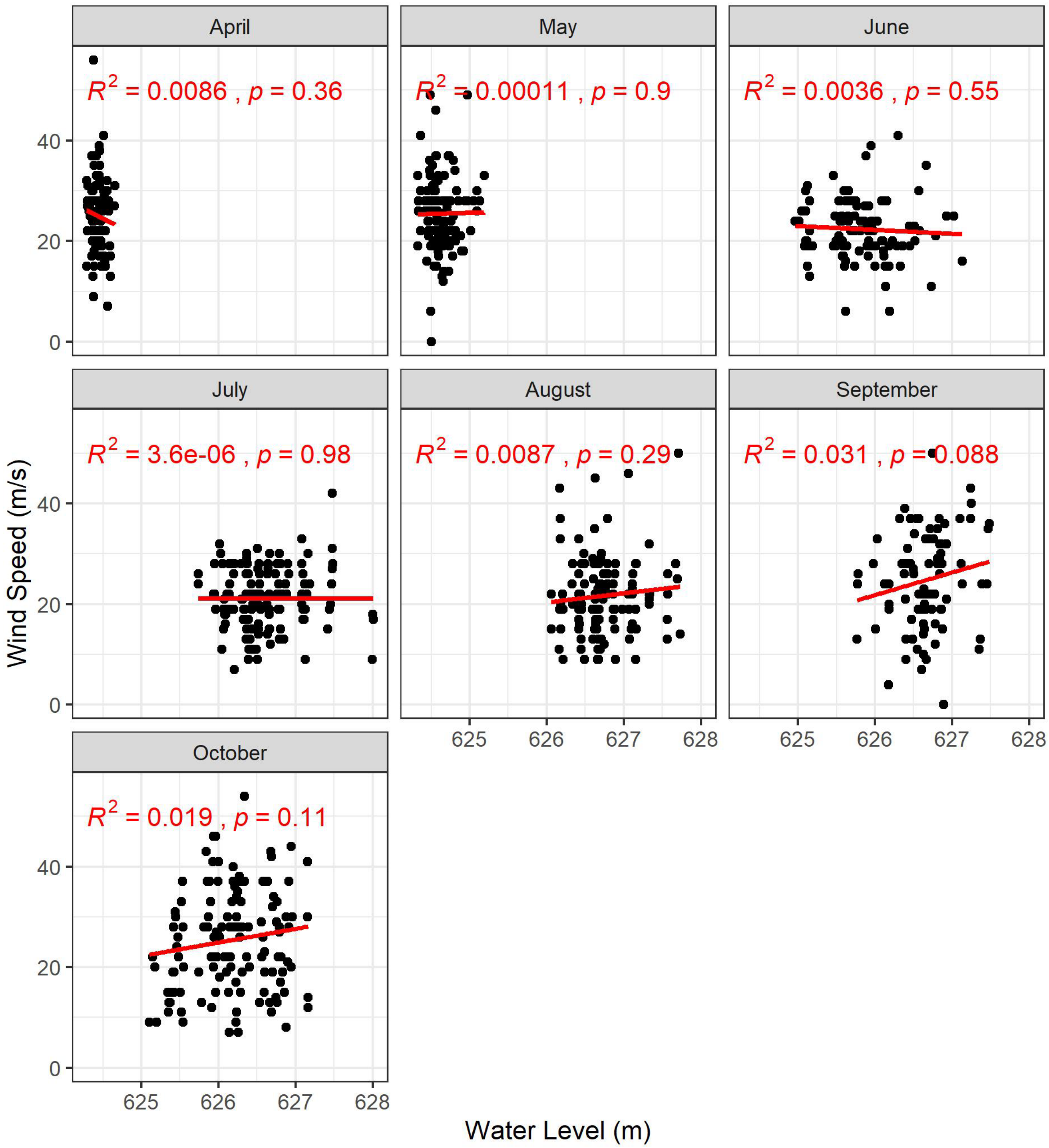

WATER LEVEL CORRELATION WITH WIND DIRECTION (10TH PERCENTILE WATER LEVEL SUBSET)

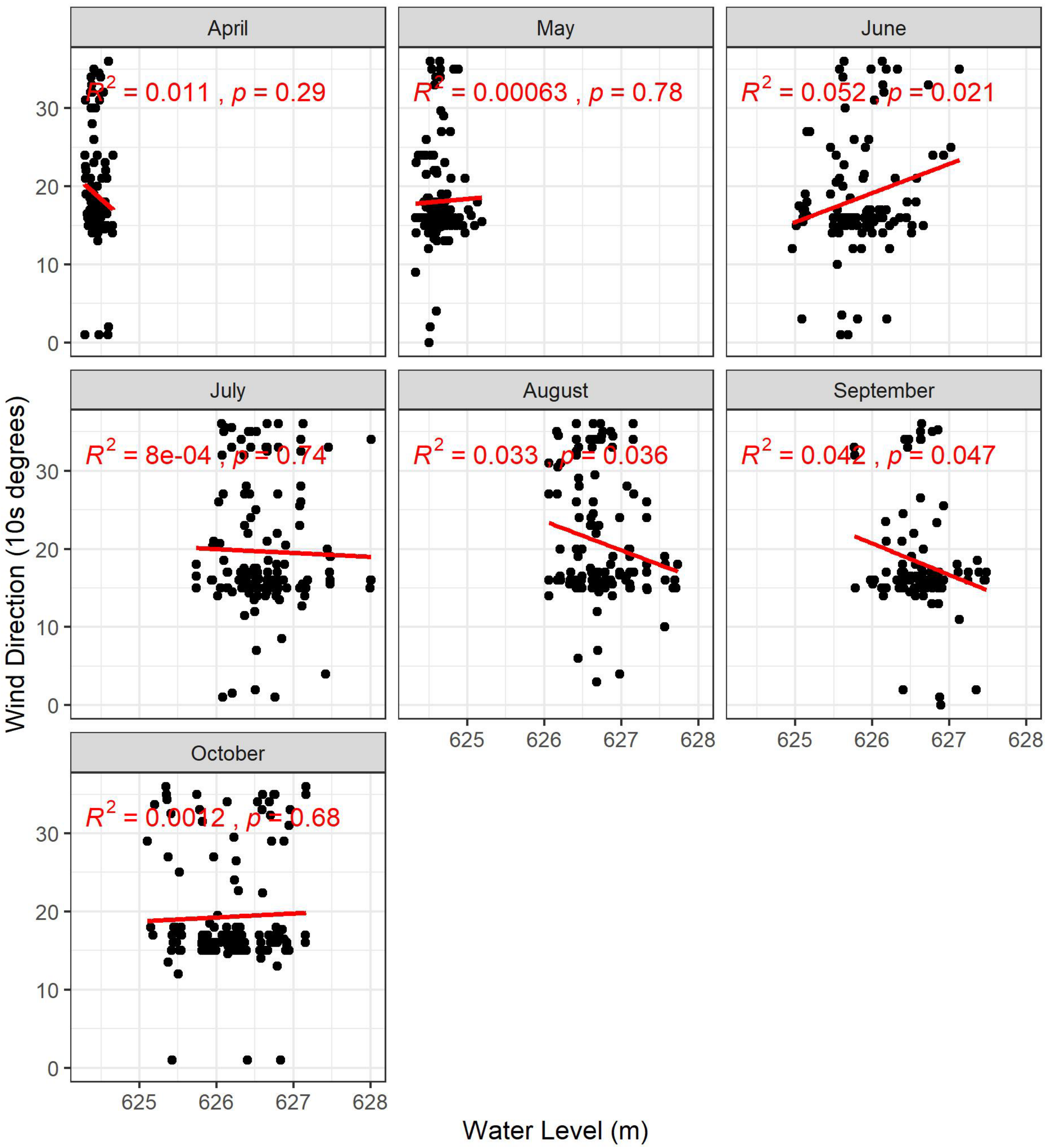

WATER LEVEL CORRELATION WITH WIND SPEED (MAXIMUM MONTHLY WATER LEVEL SUBSET)

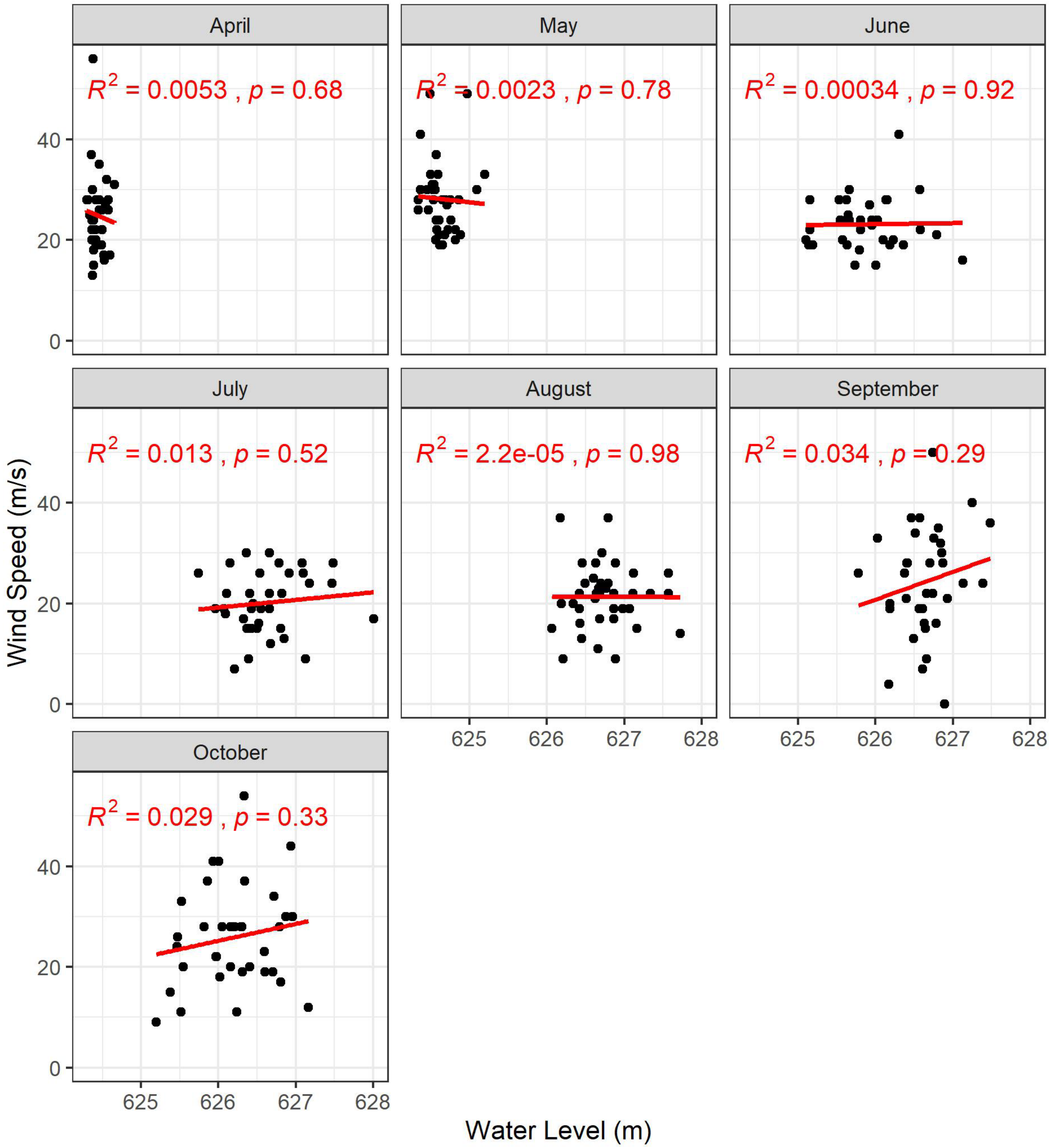

WATER LEVEL CORRELATION WITH WIND DIRECTION (MAXIMUM MONTHLY WATER LEVEL SUBSET)

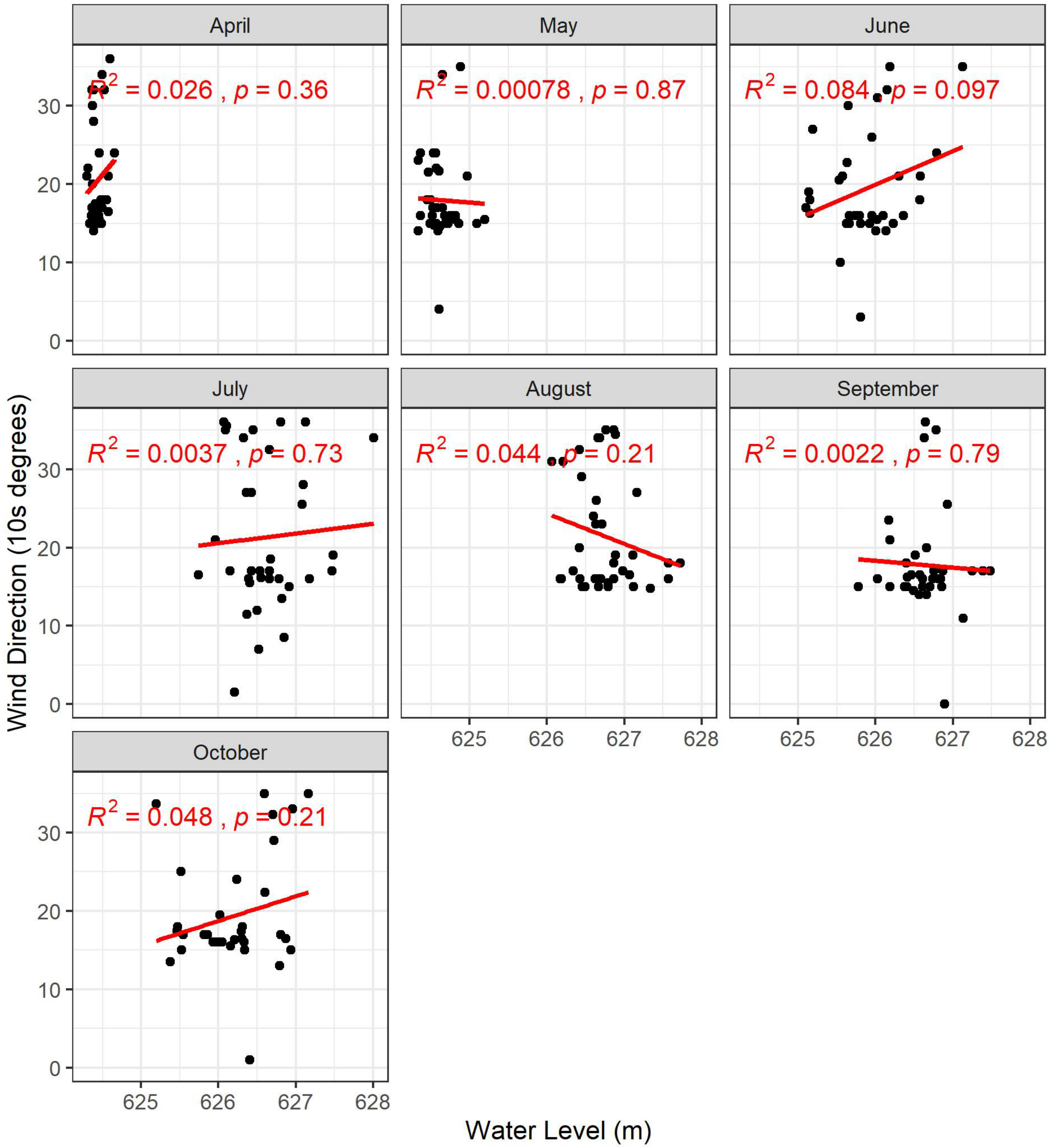

WIND SPEED CORRELATION WITH WATER LEVEL (10TH PERCENTILE WIND SPEED SUBSET)

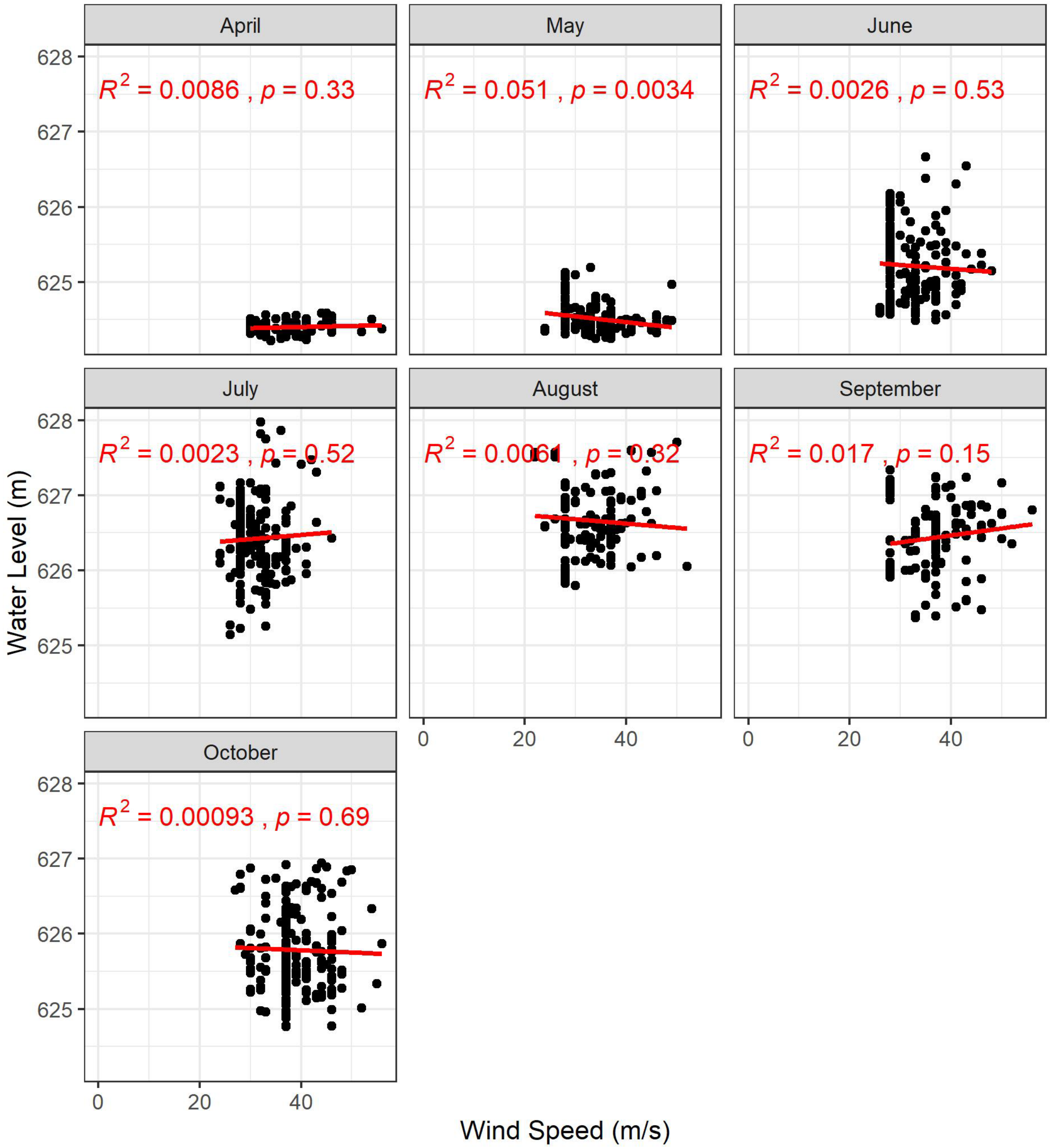

WIND SPEED CORRELATION WITH WIND DIRECTION (10TH PERCENTILE WIND SPEED SUBSET)

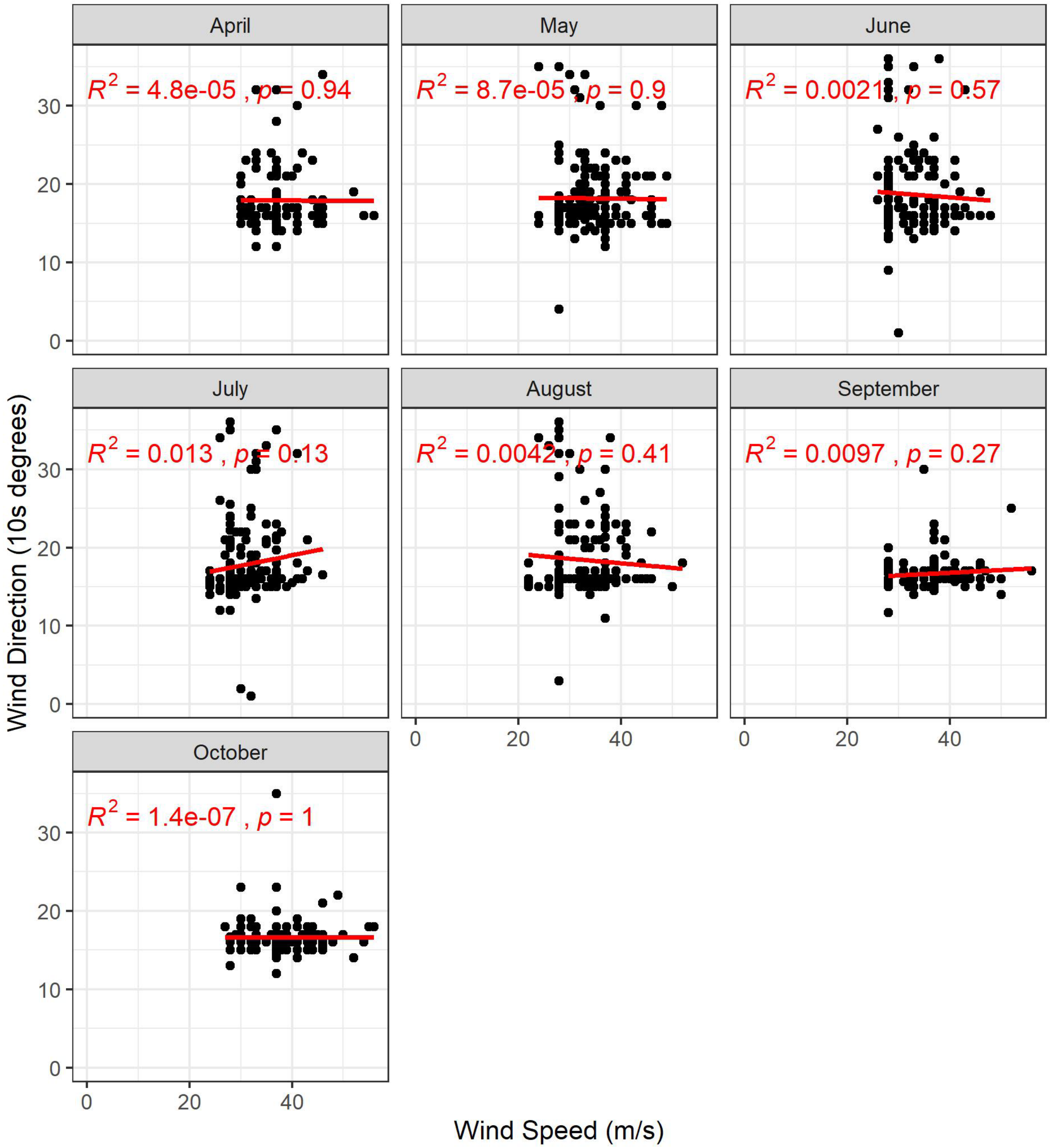

WIND SPEED CORRELATION WITH WATER LEVEL (MAXIMUM MONTHLY WIND SPEED SUBSET)

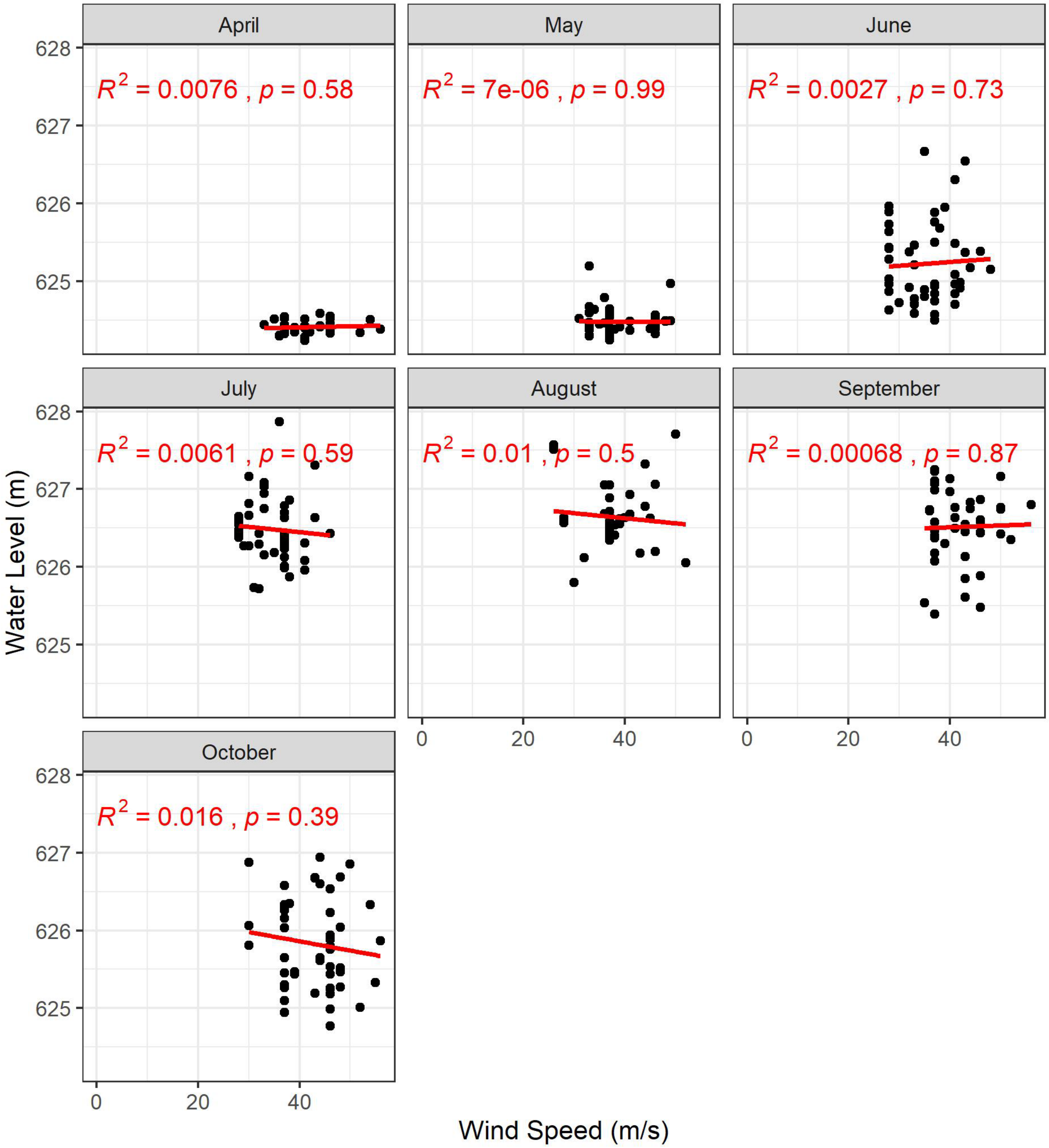

WIND SPEED CORRELATION WITH WIND DIRECTION (MAXIMUM MONTHLY WIND SPEED SUBSET)

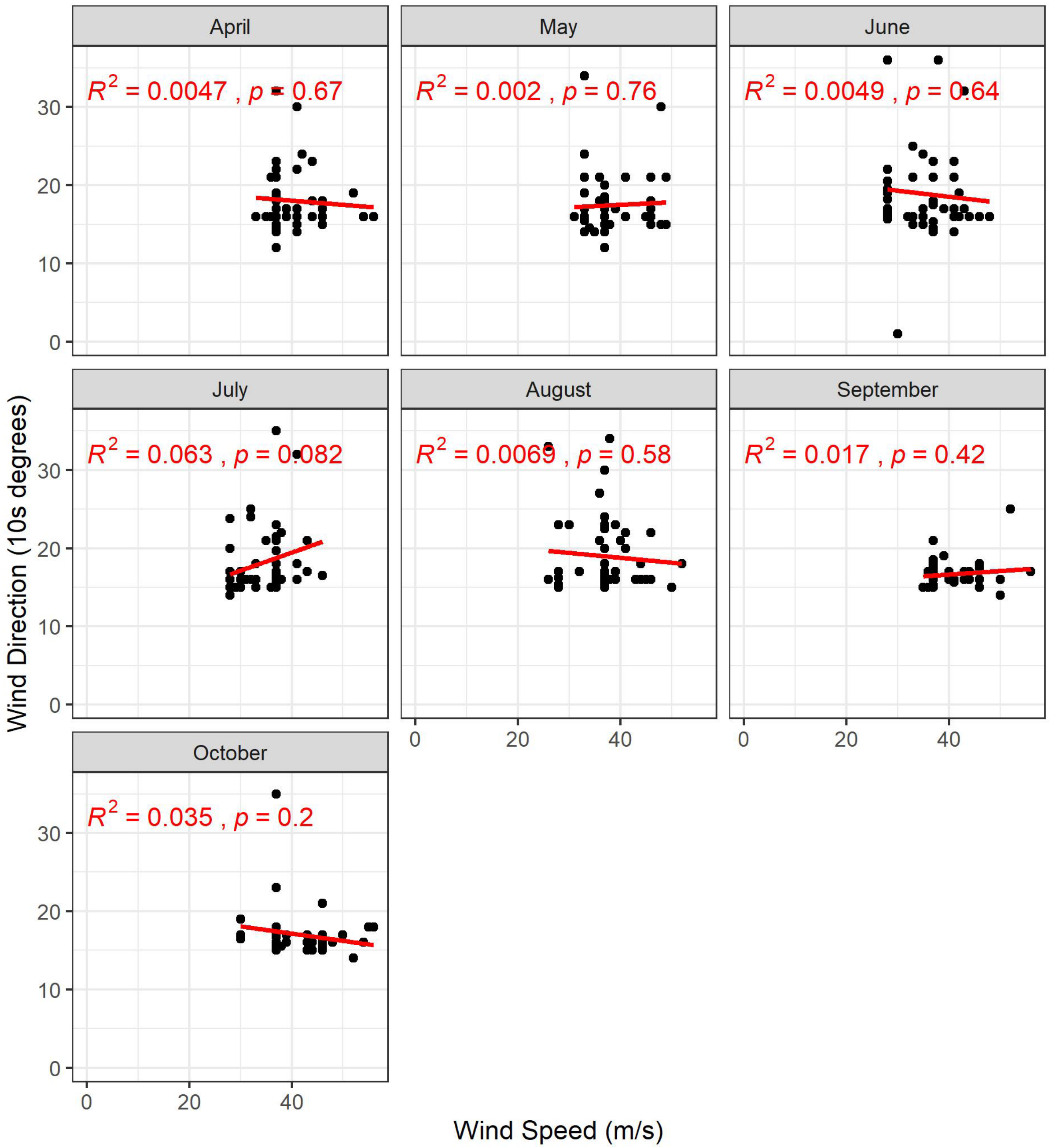

APPENDIX E

Flood Hazard Maps

KGS GROUP

Experience in Action